1989

Heat transfer to a stationary and moving sphere immersed in a fluidized bed

Chetan Jitendra Desai
Iowa State University

Order Number 8920123

Heat transfer to a stationary and moving sphere immersed in a fluidized bed

Desai, Chetan Jitendra, Ph.D.

Iowa State University, 1989

U·M·I
300 N. Zeeb Rd.
Ann Arbor, MI 48106

Heat transfer to a stationary and moving sphere immersed in a fluidized bed

by

Chetan Jitendra Desai

A Dissertation Submitted to the
Graduate Faculty in Partial Fulfillment of the
Requirements for the Degree of
DOCTOR OF PHILOSOPHY

Major: Mechanical Engineering

Approved:

Signature was redacted for privacy.

In Charge of Major Work

Signature was redacted for privacy.

For the Major Department

Signature was redacted for privacy.

For the Graduate College

Iowa State University
Ames, Iowa
1989

TABLE OF CONTENTS

LIST OF TABLES

LIST OF FIGURES

NOMENCLATURE

a	constant in the heat capacity of the copper sphere relationship, J/Kg K
a_1	radius of cylindrical heater, m
A	vibrational amplitude, m
A_1	empirical factor
A_c	area of contact of a packet with heat transfer surface
A_f	area of the float inside a rotameter
$(AK)_{eq}$	equivalent area-conductivity product for the thermocouple wire and insulation
Ar	Archimedes number, $(\frac{g d_p^3 \rho_g (\rho_p - \rho_g)}{\mu_g^2})$
A_s	vibrational amplitude of a sphere, m
A_{sph}	surface area of copper sphere, m^2
A_w	Variable area of the orifice of the rotameter
b	constant in the heat capacity of the copper sphere relationship, J/Kg K^2
Bi	Biot number, $\frac{hL_{ch}}{K_{cu}}$
C	perimeter of the outside of the hollow steel tube housing a

	thermocouple wire
C_D	drag coefficient
C_g	specific heat of fluidizing gas (J/KgK)
C_0	constant
C_{eff}	effective heat capacity of the particles, (J/KgK)
C_{m1}	Constant for heat transfer correlation-II for a moving sphere
C_{m2}	Constant for heat transfer correlation-II for a moving sphere
C_{m3}	Constant for heat transfer correlation-II for a moving sphere
C_{m4}	Constant for heat transfer correlation-II for a moving sphere
C_{m5}	Constant for heat transfer correlation-II for a moving sphere
C_{mm1}	Constant for heat transfer correlation-III for a moving sphere
C_{mm2}	Constant for heat transfer correlation-III for a moving sphere
C_{mm3}	Constant for heat transfer correlation-III for a moving sphere
C_{mm4}	Constant for heat transfer correlation-III for a moving sphere

C_p	specific heat of the glass particles, $(J/Kg\ K)$
$C_p(x)$	specific heat of emulsion phase at point x, $(J/Kg\ K)$
C_{sph}	heat capacity of the copper sphere, J/Kg K
C_{s1}	Constant for heat transfer correlation for a stationary sphere
C_{s2}	Constant for heat transfer correlation for a stationary sphere
C_{s3}	Constant for heat transfer correlation for a stationary sphere
C_{s4}	Constant for heat transfer correlation for a stationary sphere
d_c	diameter of equivalent cylinder, m
d_p	particle diameter, m
D_{probe}	heat transfer probe diameter, m
D_r	distance between two successive layers of particles, m
D_{sph}	heat transfer sphere diameter, m
D_t	fluidized bed diameter, m
f_0	fraction of time that bubbles shrouds the heat transfer surface
f_s	surface heat flux, W/m^2
F_s	frequency of sphere oscillation, Hz
g	gravitational acceleration, m/s^2
G	superficial mass velocity of gas, Kg/m^2s
h	heat transfer coefficient for sphere-bed system, W/m^2 K

h_1	heat transfer coefficient for the steel tube immersed in the fluidized bed
h_c	heat transfer coefficient through contact resistance, W/m^2 K
h_{cond}	conductive heat transfer coefficient, W/m^2 K
h_{eq}	equivalent heat transfer coefficient for the thermocouple and steel tube assembly
h_{gc}	gas convective heat transfer coefficient, W/m^2 K
h_i	instantaneous heat transfer coefficient, W/m^2 K
h_m	heat transfer coefficient for a moving sphere, W/m^2 K
h_{max}	maximum heat transfer coefficient, W/m^2 K
h_{pc}	particle convection heat transfer coefficient, W/m^2 K
h_{pr}	radiant particle heat transfer coefficient, W/m^2 K
h_r	radiation heat transfer coefficient for sphere-bed system, W/m^2 K
h_s	heat transfer coefficient for a stationary sphere, W/m^2 K
h_t	total heat transfer coefficient (radiation and convection) for sphere-bed system, W/m^2 K
h_{wil}	instantaneous local heat transfer coefficient, W/m^2 K
h_{wl}	local time averaged heat transfer coefficient, W/m^2 K
I(t)	age distribution function of emulsion packet on a surface
K_{air}	air thermal conductivity, W/m^2 K
K_{cu}	thermal conductivity of copper, W/m^2 K

K_{cn}	thermal conductivity of constantan
K_e°	thermal conductivity of packed bed, W/m^2 K
K_{eff}	effective thermal conductivity of the packet, W/m^2 K
K_{ew}	effective thermal conductivity of the contact zone near the wall, W/m^2 K
K_g	gas thermal conductivity, W/m^2 K
K_{ins}	thermal conductivity of thermocouple insulation, W/m^2 K
K_M	thermal conductivity of two phase boundary layer, W/m^2 K
K_{mf}	effective thermal conductivity of the packet at minimum fluidization condition, W/m^2 K
K_p	thermal conductivity of solid particle, W/m^2 K
K_s	thermal conductivity of steel W/m^2 K
K(x)	thermal conductivity of emulsion phase at point x, W/m^2 K
l	length of heater either flat or cylindrical, m
l_e	length of emulsion packet, m
l_{mf}	height of the bed at incipient fluidization, m
L_1	length of the thermocouple wire along with the insulation
L_2	width of the thermocouple wire along with the insulation
L_{ch}	characteristic length, m
l_H	length of a heater, m
m	constant
Nu	Nusselt number based on sphere diameter
$(Nu_l)_{conv}$	convective Nusselt number based on characteristic length

Nu_m	Nusselt number for a moving sphere
Nu_{max}	maximum Nusselt number
Nu_o	Nusselt number for an oscillating sphere
Nu_s	Nusselt number for a stationary sphere
P	bed pressure
P_b	Static pressure at fluidized bed cm of water
P_o	static pressure at operating condition at rotameter section, cm of water
Pr	Prantle number, $(\frac{C_p \mu_g}{K_g})$
P_s	standard atmospheric pressure in cm of Hg
Q_r	air flow rate at rotameter section, cc/s
Q_{rc}	air flow rate at rotameter section at calibration condition, cc/s
Q_{ro}	air flow rate at rotameter section during the operating condition, cc/s
Q_{rs}	air flow rate at rotameter section at standard condition, cc/s
Q_{wm}	air flow rate at wet testmeter section at calibration condition, cc/s
q_{cl}	heat loss due to conduction through the thermocouple wires
q_{wi}	instantaneous rate of heat flux into emulsion packet, W/m^2
R	radius of cylinder or sphere, m
R_a	thermal resistance of the packet of emulsion, m^2 K/W
Re	Reynolds number based on sphere diameter
Re_{mf}	Reynolds number at minimum fluidization, $(\frac{d_p \rho_g U_{mf}}{\mu_g})$
Re_l	Reynolds number based on characteristic length

Re_p	Reynolds number based on particle diameter
R_w	contact resistance near a wall, m^2 K/W
r	r coordinate
r_b	fluidized bed diameter, m
r_w	thermocouple wire radius, m
r_1	radius of the equivalent thermocouple wire, m
r_2	radius of the equivalent thermocouple insulation, m
r_3	inner radius of the hollow steel tube, m
r_4	outer radius of the hollow steel tube, m
s	average replacement of packet at the wall/unit time by means of side mixing
S	stirring factor
S_1	renewal frequency, s^-1
S_L	expression given by equation
t	time s
T_0	initial temperature of the copper sphere, K
T	temperature of the center of the copper sphere, K
TC	time constant of emulsion packet, sec
T_b	fluidized bed temperature, K
T_e	temperature of emulsion phase, K
T_{gc}	gas residence time, sec
T_{rc}	temperature at rotameter section at calibrating condition, K
T_s	standard temperature, K

T_{tb}	thermocouple temperature at copper sphere end, K
T_w	heat transfer wall temperature, K
T_{wm}	temperature at wet testmeter at calibrating condition, K
U	superficial gas velocity, m/s
$U_{D_{sph}}$	uncertainty in sphere diameter
U_{d_p}	uncertainty in particle diameter
U_g	gas phase velocity in r direction, m/s
U_h	uncertainty in heat transfer coefficient
U_{mb}	minimum bubbling velocity, m/s
U_{mf}	minimum fluidization velocity, m/s
U_p	particle velocity in r direction m/s
U_t	terminal velocity of glass particle velocity m/s
U_U	uncertainty in superficial air velocity
$U_{U_{mf}}$	uncertainty in minimum superficial air velocity
$U_{V_{sph}}$	uncertainty in sphere velocity
U_{X_1}	uncertainty in X_1
U_{X_2}	uncertainty in X_2
U_{X_m}	uncertainty in X_m
U_Z	uncertainty in Z
V	volume of the copper sphere, m^3
V_{avg}	equivalent average linear velocity of an oscillating sphere, m/s
V_f	volume of the float inside the rotameter, m^3

V_g	gas velocity in y direction, cm/s
V_p	particle velocity in y direction, cm/s
V_{sph}	linear velocity of sphere, cm/s
x	distance from constraining surface, m
X_1	experimental variable
X_2	experimental variable
X_m	experimental variable
x_{th}	thermal penetration distance, m
y	y coordinate

Greek

α_{eff}	thermal diffusivity of emulsion packet, $\frac{m^2}{s}$
α_M	thermal diffusivity of two phase boundary layer, $\frac{m^2}{s}$
β_r	fluid-to-particle friction coefficient in r direction
β_y	fluid-to-particle friction coefficient in y direction
γ_{bed}	mean particle concentration
δ	gas film thickness, m
δ_T	two phase boundary layer thickness around an immersed cylinder or sphere, m
δ_w	thickness of the contact resistance zone, m
ϵ	void fraction
ϵ_{mf}	void fraction at minimum fluidization

ϵ_{sph}	emissivity of the copper sphere
Θ	absolute bed temperature in K/273
Δp	pressure drop across the bed, cm of water
μ_g	viscosity of gas, Ns/m^2
ν_g	kinematic viscosity of gas, $\frac{m^2}{s}$
ρ_b	fluidized bed density, Kg/m^3
ρ_{eff}	effective density of a fluidized bed, Kg/m^3
ρ_f	density of the float inside the rotameter, Kg/m^3
ρ_g	density of fluidizing gas, Kg/m^3
ρ_{mf}	fluidized bed density at incipient condition, Kg/m^3
ρ_o	density of fluidizing gas at rotameter section under operating condition, Kg/m^3
ρ_p	density of fluidizing particle, Kg/m^3
ρ_{pb}	bulk density of packed bed, kg/m^3
ρ_{rc}	density of fluidizing gas at rotameter section under calibration condition, Kg/m^3
ρ_{sph}	density of copper sphere, kg/m^3
ρ_{std}	density of fluidizing gas at standard condition, Kg/m^3
ρ_{wm}	density of fluidizing gas at wet testmeter section under calibration condition, Kg/m^3
$\rho(x)$	density of emulsion phase at distance x, Kg/m^3
σ	Stefan-Boltzman constant, $W/m^2\ K^4$

τ	residence time of emulsion packet on a heat transfer surface, s
τ_c	time constant or response time of the copper sphere-bed system, sec
τ_{rr}	solid stress in r direction
τ_{yy}	solid stress in y direction
$\Psi(\tau)$	fraction of surface occupied by packets of age between τ and $\tau + d\tau$
ω	frequency of vibration, Hz
Φ_s	particle sphericity

1 INTRODUCTION

Fluidization is a phenomenon in which solid particles are kept in a floating state by an upward flowing gas or liquid. At a low flow rate, fluid passes through the void spaces between stationary particles. In this condition the bed remains fixed. With an increase in the flow rate, the bed expands slightly. At a critical gas flow rate the solid particles are just suspended in the upward flowing fluid. This condition is called minimum fluidization and the corresponding superficial velocity of the fluid is called minimum fluidization velocity. At this point the drag force exerted by the upward flowing fluid on the particles is just balanced by the weight of the particles. The pressure drop through any section of the fluidized bed equals the weight of the solid particles and fluid in that section. At higher flow rates, a liquid-solid fluidized bed exhibits a uniform expansion from the fixed bed to the hydraulic transport. However, with an increase in flow rate beyond minimum fluidization in the case of a gas-solid system bubbles or large voids begin to appear and movement of the solid particles becomes more vigorous. Such a bed is called bubbling fluidized bed. These bubbles form at the bottom of the bed near the distributor and rise through the bed coalescing and increasing in size. At even higher gas flow rates, the size of the bubbles can grow to the diameter of the bed column and at this stage the bed is said to be a slugging bed. At sufficiently high flow rate entrainment becomes

significant and the solid particles are carried out of the bed along with the fluid flow.

1.1 Liquid Like Behavior of a Fluidized Bed

A gas fluidized bed looks and in many ways behaves like a liquid. Light objects float on the surface of the fluidized bed and can be easily pushed under the bed surface. When a fluidized bed is disturbed, waves appear on the surface and are formed, propagated and reflected from the wall of the container and display interference just like waves on free surface of a liquid. The surface of the bed remains horizontal in a stationary vessel and becomes cylindrical when the vessel is rotated [Gelperin and Einstein 1971]. The kinetic energy of the solid particles in a fluidized bed is a function of the superficial velocity of the fluid being somewhat analogous to the case of a liquid where the kinetic energy of the molecules depends upon temperature of the liquid. Therefore, the parameter of a fluidized bed that is analogous to temperature of a liquid is the superficial velocity. The viscosity of a fluidized bed decreases with an increase in the superficial velocity just like the viscosity of liquid falls with a rise in temperature. Moreover, the viscosity of fluidized bed increases with an increase in the size of the solid particles similar to a liquid where the viscosity rises with increase in molecular size [Gelperin and Einstein 1971]. The transition of a fixed bed to a fluidized bed is similar to the melting of a solid body and entrainment of solid particles from a fluidized bed is similar to evaporation of a liquid. There are indications that near the minimum fluidization velocity, the fluidized bed behaves more like a pseudo-plastic rather than a Newtonian fluid as

occurs in certain liquids close to their melting point [Harrison and Leung 1961]. An analog to the Weissenberg effect in non-Newtonian liquids is observed by the formation of a mound on the free surface of a fluidized bed when it is mixed with a bladed mixer. These analogies between a fluidized bed and liquid exist only in the range of minimum fluidization to minimum bubbling velocity. When bubbling becomes vigorous the properties of a fluidized bed approximate those of a boiling liquid or a liquid through which gas is bubbled.

1.2 Brief History of Fluidization

The fluidization technique was first used commercially by Fritz Winkler for the gasification of coal in 1926. A number of similar units were constructed in Germany and Japan in order to supply raw gas for the synthetic chemical industry. During World War II, Standard Oil Corporation development the first fluid bed catalytic cracker (FCC) unit to produce high octane aviation gasoline. In 1944 Dorr-Oliver acquired rights to Esso's fluidization know-how for use in fields outside of the petroleum industry such as roasting of sulphide ores. Moreover, Dorr-Oliver engineers successfully developed a drying and calcination process using fluidized beds in 1950s. The Sohio process for making acrylonitrile in a fluidized bed was extremely successful in the early 1960s. In early 1970s Union Carbide developed polythylene synthesis process using fluidized bed technology. Also in the 1970s and 1980s fluidized bed combustion attracted much attention largely due to its relatively low temperature operation (800-900° C) and its ability to absorb SO_2 through the use of limestone or dolomite [Geldart 1986]. More than 2000 small atmospheric

pressure fluidized bed combustors are in use throughout the world on a variety of duties such as burning plastic waste, providing hot gases for drying grass and raising steam for process use [Highley and Kaye 1983].

1.3 Industrial Applications of Fluidized Beds

Numerous industrial processes make use of fluidized bed technology such as drying, surface coating, coating of pharmaceutical tablets, heat treatment, oil cracking, coal combustion, coal gasification, etc. Figure 1.1 shows many current industrial applications of fluidized beds arranged in five categories according to predominating mechanism [Geldart 1986].

1.4 Heat Transfer in Fluidized Beds

The most remarkable feature of the fluidized bed is its temperature uniformity produced by bubble induced solid mixing generated within the bulk of a bubbling gas fluidized bed. In practice this temperature uniformity exists in both radial and axial directions even in beds of ten meters in diameter [Kunii and Levenspiel 1969]. The heat transfer in a fluidized bed involves three modes of heat flow namely, fluid-to-particle, particle-to-particle and bed-to-surface heat transfer.

1.4.1 Particle-to-particle heat transfer

This mode of heat transfer is caused by the heat flow among particles due to the particle temperature difference. It plays an important role in many processes involving mixing of hot particles and cold particles. Particle-to-particle heat transfer

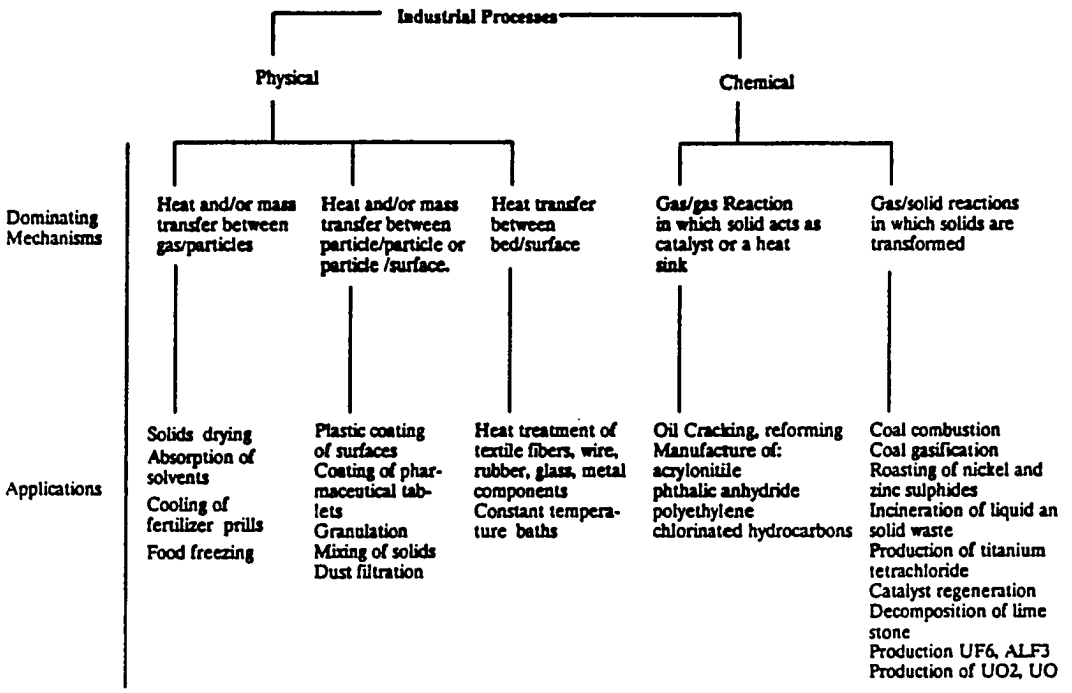

Figure 1.1: Classification of fluidized bed applications according to predominating mechanism [Geldart 1986]

may be considered as heat transfer through the following paths:

1. Radiation heat transfer.

2. Conduction through points of contacts between particles.

3. Heat absorption or release by the particles upon contacting with the gas serving as the heat transfer medium.

Radiation heat transfer is shown to be negligible below the temperature 600°C and heat conduction through the points of contacts between spherical particles and plane surfaces was experimentally found to be negligible [Botterill et al. 1975]. Therefore, heat transfer from particle-to-particle contact occurs mainly through a thin film of gas serving as the heat transfer medium.

1.4.2 Particle-to-gas heat transfer

Particle-to-gas heat transfer is due to forced convection heat transfer of the fluid to each fluidizing particle in a fluidized bed. Extremely large areas of solid particle surface are available to the fluidizing gas; e.g., a cubic meter volume of 100μm diameter particles has a surface area greater than 30,000m^2 [Geldart 1986]. Such a large surface area greatly enhances the particle-to-gas heat transfer.

1.4.3 Bed-to-surface heat transfer

The heat transfer between a surface and a fluidized bed may be consider to be composed of three additive components [Botterill, 1975].

1.4.3.1 Particle convection component The particle convection component h_{pc}, is responsible for the high bed-to-surface heat transfer coefficient due to bubble induced particle circulation and very high volumetric heat capacity of the particle (of the order of a thousand fold higher than that of the fluidizing gas). Particles usually stay in the bulk of the bed for a long time to reach to bulk bed temperature by exchanging heat with the fluidizing gas and by conduction through the gas with other particles. Therefore when a packet of particles first arrives at a heat transfer surface, it is at the bulk temperature of the fluidized bed and there exists a high local temperature difference between the packet and the heat transfer surface. This packet of particles resides on a heat transfer surface for a short time and heat is transferred by unsteady conduction [Mickley and Fairbanks 1955].

1.4.3.2 Gas convective component The interface gas convective component h_{gc}, is the heat transferred to the gas phase. This path is significant in the case of large particle fluidized beds and beds operating at high static pressure [Botterill, 1986]. As an example, for 160μm and 2500μm particles, the particle convective components were found to be 90% and 40% respectively [Baskakov and Vitt 1973]. The gas convective component was estimated experimentally by the mass transfer analogy [Baskakov and Suprun 1972].

1.4.3.3 Radiative Component The radiative heat transfer component h_{rc}, becomes significant only at temperatures above 600°C. This was experimentally observed by using a gold probe and a copper probe [Botterill 1986]. The radiative heat transfer for an immersed surface in a bubbling fluidized bed must be

considered in two parts. When the surface is in contact with particles, radiative heat transfer mainly depends upon interaction between the surface and the first layer of particles. This layer is closed to the surface temperature than the bulk temperature. Successive layers of the particle do not significantly contribute to this heat transfer mode as each layer is almost opaque to the incident radiation. It was shown that a layer of 1.7 mm particles with the thickness equal to their diameter, lets through only 6% of incident radiation [Botterill 1975]. On the other hand when the heat transfer surface is engulfed by a bubble, the radiative heat transfer takes place between the surface and the particles which are at bulk temperature.

1.5 Present Investigation

The present investigation is directed towards establishing trends useful for the purpose of industrial design in heat transfer to submerged objects in gas fluidized beds through linear and oscillating motion of the object. The general purpose of this investigation is to study the heat transfer from a hot stationary and a moving (linearly downward and oscillating) sphere immersed in a glass-particle bed fluidized by air at room temperature and pressure. First, a systematic investigation was carried out in order to understand the significance of several important variables influencing the heat transfer rate from a stationary copper sphere such as: superficial velocity, glass particle diameter, and sphere diameter. Secondly, the effect of constant vertical downward motion and oscillating motion of the copper sphere (along with previously stated variables) on the heat transfer coefficient was experimentally investigated. In the case of a linear motion, the copper sphere was moved

at a constant velocity of 0.4, 1.1, 1.9, 3.0, 4.6 and 7.5 cm/s. Whereas, in the case of oscillating motion, the copper sphere was placed about 10 cm above the distributor plate in the fluidized bed and oscillated at various amplitudes of 1.8, 4.0 and 6.9 cm and at 1.1, 2.0 and 2.85 Hz frequencies. For all of the heat transfer studies, 5-44, 126-147 and 355-420 μm size glass particles and 1.0, 1.4 and 2.0 cm diameter copper spheres were used in various combinations.

The transient temperature of the hot copper sphere as it is cooled in the fluidized bed was recorded by a computer controlled data acquisition system using a thermocouple embedded at the center of the sphere. A sufficiently small Biot number observed for all the cases enabled the use of lumped heat capacity theory for cooling of the sphere. A transient temperature record was used to obtained heat transfer coefficient. The heat transfer coefficients obtained for the case of a stationary sphere immersed in the glass bead fluidized bed were correlated to glass particle size, superficial air velocity and copper sphere diameter. However, the primary goal of this study was to correlate the enhanced heat transfer coefficient with the bed parameters as described previously for linear and oscillating motion of the copper sphere.

A theoretical model proposed by Gelperin and Einstein [1971] was used to predict the heat transfer coefficient in the case of linearly moving sphere in a fluidized bed at minimum fluidization condition.

1.6 Significance of Present Investigation

The superior heat transfer characteristics as well as safer, cleaner and cheaper operational performance have made fluidized beds an alternative to conventional salt and lead baths that are used for heat treatment purposes. The use of fluidized beds for heat treatment of metal parts such as: hardening, annealing, carburizing, nitrocarburizing, bright tempering, etc. is a relatively new but well established industry in the United States, Canada and Europe. For example, for ferrous materials, neutral hardening involves first heating the metal to its austenitic state in an inert atmosphere, then rapidly cooling it to produce a martensitic structure. Conventional quenching is accomplished with oil, water, brine, air, salt or lead baths. Salt and lead baths contain cyanide poison in the molten salt, which must be properly handled and disposed off. Whereas, the fluidized bed bath uses inert sand like bed material, such as aluminum oxide along with inert gases such as nitrogen or argon gas. Furthermore, the fluidized bed can be turned off during shutdown periods to reduce running and maintenance cost. Quenching and heat transfer rates are an important part of these heat treatment processes. The present study provides new information into the heat transfer rate and the enhancement through controlled motion of a submerged sphere motion in a fluidized bed. Furthermore, the knowledge of heat transfer from such a moving object in a fluidized bed could be beneficial to controlling processes such as, freezing of food grains, physical operation involving particle coating, drying and gasification, and burning of a single particle in a fluidized bed combustor. The effect of controlled motion of a heat transfer surface immersed into a fluidized bed on heat transfer rates has been reported in only a

limited number of studies [Reed and Fenske, 1955].

1.7 Literature Survey

Heat transfer from an immersed object to a fluidized bed greatly depends on the hydrodynamics of solid particles in the vicinity of the object. Glass and Harrison [1964] visually observed the flow pattern near a horizontal tube in a two dimensional bed. The vertical component of gas velocity increases in the region close to the immersed object and exceeds the minimum fluidization velocity U_{mf}, even though the superficial gas velocity is less than U_{mf}. This phenomenon produces local fluidization near the immersed object. At higher superficial velocities, unstable gas voids forms underneath the obstacle, which acts as a source of small bubbles which are periodically detached [Ginoux et al. 1974 and Colver 1985]. However, there exists a defluidized region above the immersed object.

Several industrial processes utilize the high surface-to-bed heat transfer coefficient which have been found to be 20 to 40 times that of gases alone [Kunii and Levenspiel 1969]. The mechanism of heat transfer between a surface and a fluidized bed is complicated because of the large number of variables such as those of gas properties (density, viscosity, specific heat, thermal conductivity), properties of solid particles (diameter, density, sphericity, specific heat, thermal conductivity), conditions at minimum fluidization (superficial velocity, void fraction), geometrical properties (diameter of bed, geometry and orientation of heat transfer surface, spacing, static bed height, position of heat transfer surface in the fluidized bed) and mechanical action (vibration of fluidized bed, motion of the heat transfer surface).

The influence of various parameters on heat transfer coefficient as determined from the various observations can be summarized as follows:

1.7.1 Superficial gas velocity

The common findings from heat transfer in fluidized bed studies suggests that the average heat transfer increases rapidly near fluidization and either levels off [Yamazaki and Jimbo 1970], or drops as the average size of the bubbles increased at higher superficial gas velocities [Richardson and Shakiri 1979, Kharchenko and Makhorin 1964]. As early as 1949, Cibrowski [Zabrodsky 1966] studied heat transfer characteristics between walls of a deep air fluidized bed of alumina particles (44-55, 74-149 and 149-210 μm). The tube wall was electrically heated over a length of 1 meter. He found that the heat transfer coefficient increased with material concentration in the tube which depended on the superficial gas velocity. Mickley and Trilling [1949] studied the effect of solid concentration, glass particle diameter and superficial air velocity on heat transfer coefficient for an externally heated and an internally heated fluidized bed. Glass particles ranging in size from 50 to 5000 μm were suspended in an upward flowing air stream at superficial velocities varying between 24.4 cm/s to 457.2 cm/s. The empirical correlation for an externally heated fluidized bed was given by,

$$h = 0.0118[\frac{\gamma_{bed} G}{d_p^3}]^{0.263} \tag{1.1}$$

and for an internally heated fluidized bed,

$$h = 0.0433[\frac{\gamma_{bed}^2}{d_p^3}]^{0.233} \tag{1.2}$$

They noted that the air velocity exerts a direct influence on the heat transfer coefficient in the case of an externally heated fluidized bed. While in case of the internally heated system, the gas velocity does not exert any such effect on heat transfer coefficient and is independent of the solid concentration. Shirai et al. [1966] experimentally investigated heat and mass transfer from the surface of solid spheres fixed within a fluidized bed. They used active carbon, alumina, silica gel and sand particles and 8, 15, 28 cm diameter fluidized beds. The minimum fluidizing velocities ranged from 0.8 to 10.5 cm/s. Five different sizes of brass and stell spheres were used ranging in size from 0.45 to 5 cm in diameter, with and without an internal heater, The heat transfer coefficient was determined from the transient cooling curve of a sphere in case of a sphere without the internal heater. When the sphere had an inside heater, the electrical power consumption and the surface temperature of the sphere and the bed temperature where measured and used to calculate the heat transfer coefficient. Their results indicated that heat transfer coefficient was proportional to $(U/U_{mf})^{0.36}$ considering different materials of fluidizing particles. Whereas, Dow and Jacob's data [1951] showed that h $\alpha U^{0.8}$ and Van Heerden et al. [1953] obtained h $\alpha U^{0.45}$.

1.7.2 Particle diameter

The common results of most of the experimental studies suggests that the heat transfer coefficient decreases with an increase in particle diameter. In 1950 Baerg et al. [Zabrodsky 1966] carried out detailed experimental work on the maximum heat transfer coefficient between a heated wall and fluidized beds of iron filings, round

sand, molding sand, crushed silica gel, glass beads, cracking catalyst and alumina with particle sizes ranging from 60 to 878μm, over a wide range of fluidizing air velocities. They proposed the following empirical correlation for h_{max},

$$h_{max} = 239.5 log_e(7.05 \times 10^{-6} \frac{\rho_b}{d_p}) \tag{1.3}$$

Yamazaki and Jimbo [1970] investigated the heat transfer between a hot 1.2 cm steel sphere immersed in a fluidized bed of 8.1 cm inner diameter and 80 cm height. They used limestone, molding sand and fused alumina of 68 to 310μm size. Heat transfer coefficients were calculated using the Heissler chart. It was shown that the heat transfer coefficient increased more rapidly for larger particles and maximum heat transfer coefficient was approximately proportional to the $d_p^{-0.5}$, without considering the effect of porosity. Richardson and Shakiri [1979] found that the maximum heat transfer coefficient was proportional to the $d_p^{-0.4}$. Gelperin and Einstein [1971] reported an initial decrease in the heat transfer coeficient with increasing particle diameter, then leveled off and increased slightly once again for very large particle diameter of 4.8 mm.

1.7.3 Size of the heat transfer surface

The heat transfer coefficient increases with a decrease in the immersed heater diameter while the heat transfer rate diminishes as the diameter of the heater is increased. Shirai et al. [1966] found that an increase in sphere diameter resulted in a decrease in the heat transfer coefficient at minimum fluidizing condition and heat transfer coefficient was found to be proportional only to the -0.06 power of the sphere diameter. They correlated their data in the following equation where h is in

kcal/m^2hr°C and d_p and D_t are in cm, within 30% deviation,

$$h = 74(\frac{U}{U_{mf}})^{0.36}(D_{sph})^{-0.06}(D_t)^{0.27} \tag{1.4}$$

Vreedenberg [1952] found no regular relationship between heat transfer coefficient and the height of the heat transfer surface because of the considerable nonuniformity of the bed which was investigated.

Wicke and Fetting [Zabrodsky 1966] published their data on heat transfer between a wall and fluidized beds of carborundum, sand, aluminum, lead and glass particles. The particle size was varied from 65 to 3000μm. They found that the heat transfer coefficient decreased with increase in height of the heating surface due to the heating of the stream of particles moving along its surface.

More recently, Botterill et al. [1984] measured heat transfer coefficient between spherical probes of different sizes and gas fluidized bed of alumina and sand in the size range 250 to 400 μm with operating condition extended up to 980°C. In the case of low Biot number probes (copper probe, 0.64, 0.87 cm diameter; phosphor bronze 0.89 and 0.95 cm diameter and gold 1.11 cm diameter) the lumped heat capacity method was used to determine the heat transfer coefficient. They also used large spherical probes of 3.16 cm in diameter the heat transfer coefficient was determined by numerically solving the unsteady conduction equation in spherical coordinates. They noted that for small spherical calorimeter probes, at lower values of the ratio of probe to particle heat capacity, enhancement in heat transfer was observed compared to the larger probes.

1.7.4 Static pressure of the bed

Vreedenberg [1952] investigated the effect of air pressure, position and height of the water cooled tubes on heat transfer coefficient in a large fluidized bed of 0.565 m diameter and 1.2 to 1.7 m in height. Sand was used as the fluidized material. the heat transfer coefficient was measured between the fluidized bed and water cooled horizontal and vertical tubes of 1.18 m in height and 34 mm diameter. He found that the heat transfer coefficient was independent of air pressure at a constant superficial air velocity.

Richardson and Shakiri [1979] carried out an experimental investigation of heat transfer from a small electrically heated element of 2.5 cm square teflon sheet wound with 78 turns of tungston wire to a gas fluidized bed. Glass, diakon, synclyst and aluminum particles were used in the size range of 25 to 450 μm. It was observed that in most cases that the heat transfer coefficient improved as the static pressure of the bed increased in the range of 0.03 to .148 MN/m^2. The gas properties other than density varied only slightly over the range of pressure used. The increase in heat transfer coefficient with pressure was attributed to an improvement in the quality of fluidization [Botterill and Desai 1972] resulting from the formulation of smaller bubbles. This was also observed experimentally by the instantaneous temperature traces. They correlated the maximum heat transfer coefficient by the following equation;

$$Nu_{max} = 0.30.4r^{0.20}Pr^{0.40} \tag{1.5}$$

Zabrodsky et al. [1976] cited an experiment which showed that a 7.5 fold reduction of pressure below atmospheric pressure diminished the maximum heat transfer

coefficient by 16% for fluidized beds of 200μm sized particles. This experimental finding was attributed to the gas film between the wall and contacting particle is important for bed-to-wall heat transfer and at low pressure the property of this thin gas film changes in such a way that reduction in heat transfer coefficient is resulted.

Recently, Saxena and Ghanza [1985] studied the effect of pressure on heat transfer coefficient for immersed surfaces in fluidized beds by examining the various correlations and theories developed. They proposed a new classification scheme utilizing the concept of Archimedes number. They summarized their conclusions as follows:

1. For particle system characterized by $Re_{mf} < 40$ and $Ar < 130,000$, minimum fluidizing velocity and heat transfer coefficient are almost independent of pressure.

2. For particle system characterized by $40 < Re_{mf} < 200$ and $130,000 < Ar < 1.6 \times 10^6$, U_{mf} and h are dependent on pressure.

3. For particle system characterized by $Re_{mf} > 200$ and $Ar > 1.6 \times 10^6$, U_{mf} and h becomes proportional to the static pressure of the gas to the 0.5 and h is dependent on pressure.

1.7.5 Particle sphericity

The heat transfer characteristics for irregular shaped aluminum dust particles fluidized by air were studied by Richardson and Shakiri [1979]. They found that the heat transfer coefficient was very low near and above $U/U_{mf} = 2$ because of

channelling. Kharchenko and Makhorin [1964] noted that sharp edged clay particles gave lower values of maximum heat transfer coefficients compared to sand particles under similar conditions.

1.7.6 Position of the heat transfer surface

Shirai et al. [1966] showed that heat transfer coefficient remained almost constant in the bed except in the part where the influence of the perforated plate predominates. Whereas above the settled height of the bed, the heat transfer coefficient reduces abruptly as the bed becomes dilute. In the radial direction, there was no change in heat transfer coefficient except very near to the wall. A short critical review of many experimental studies was reported by Zabrodsky et al. [1976]. They commented that heat transfer coefficient for an internal surface is higher than the external wall at low gas flow rates. They attributed this behavior to the amount of gas collected at the bottom of a body and deflected along its sides causing additional local aeration. This aeration promotes solid motion which in turn increases the heat transfer coefficient. Vreedenberg [1952] found no effect of the position of the heat transfer surface in the bed because of the considerable nonuniformity of the bed which was investigated.

1.7.7 Gas conductivity

The effect of gas thermal conductivity on the heat transfer coefficient was studied by Jackob and Osberg [1957]. They investigated heat transfer between a submerged electrically heated horizontal wire and a fluidized bed of glass particles

ranging in size from 30 to 290μm. The wire diameter (0.132 mm) was of the same order of magnitude as the particle diameter. Eight different gases were used ranging in thermal conductivities from 0.00715 to 0.15 Kcal/m hr$^{\circ}$C. The results showed a direct proportionality between heat transfer coefficient and the gas thermal conductivity. Richardson and Shakiri [1979] conducted heat transfer experiments using air, hydrogen, carbon dioxide and freon-12. The results showed that, the heat transfer coefficients for hydrogen in both fixed and fluidized beds were considerably higher than for the other gases because of its high thermal conductivity.

1.7.8 Baffled fluidized bed

An interesting study of heat transfer in free beds and beds divided into ten sections thermally insulated from each other by horizontal screens was carried out by Massimilla and Bracale [Zabrodsky 1966]. They observed that at lower superficial air velocities the heat transfer coefficient in the free bed was higher than that of a restricted bed, while at higher superficial air velocities, the opposite was true. On the basis of their results, they concluded that, in the region of high flow rates where the particle velocities are quite high, the screen prevented an increase in the bed voidage and that in turn improved the heat transfer.

1.7.9 Bed diameter

Heat transfer coefficients were measured between a hot silver sphere of 2 cm diameter and a fluidized beds of 82.5 and 157 mm diameter by Varygin and Martyushin [Zabrodsky 1966]. Various fluidized particles were used such as: ferrosilicon,

hermatite, carborundum, quartz sand and glass particles ranging in size from 82.5 μm to 1160μm. They found no observable effect of bed diameter on the heat transfer coefficient. Shirai et al. [1966] conducted heat transfer experiments using 8, 15 and 28 cm diameter beds and found that heat transfer coefficient increased with increase in fluidized bed diameter. The heat transfer coefficient was approximately proportional to the $D_t^{0.27}$.

1.7.10 Bed temperature

Dow and Jacob [1951] carried out an experimental investigation of heat transfer between a fluidized bed and a steam jacketed wall. They found the presence of a core in which the radial temperature remained almost constant and a thermal boundary layer of gas and particles along the wall which was responsible for the main thermal resistance to heat transfer between the wall and the bed. An experimental investigation of heat transfer between a spherical copper alpha calorimeter 6 cm in diameter and a high temperature (300 to 1050°C) beds of quartz sand and fire clay fluidized by flue gases was carried out by Kharchenko and Makhorin [1964]. The bed diameter was 22 cm and unexpanded height of the fluidized bed was kept at 10 cm. They determined the heat transfer coefficient from the transient heating curve of the copper sphere. Their results showed that the heat transfer coefficient increased with the bed temperature and the maximum heat transfer coefficient was approximately linear with the bed temperature. This was caused by the change in physical properties of the gas. They concluded that since the heat transfer coefficient varied linearly with the bed temperature, the radiant component of heat

transfer was unimportant. Botterill et al. [1984] found that a higher heat transfer coefficient was obtained when a hot probe at 800°C was immersed in the bed at 350°C, compared with the case of a cool probe at room temperature.

1.7.11 Heat transfer surface temperature

Botterill et al. [1984] showed that increasing the surface temperature of the heat transfer probe with a constant bed temperature increased the bed-to-surface heat transfer coefficient because of the change in the gas thermal conductivity adjacent to the surface. Whereas, Abuaf and Gutfinger [1974] concluded that, within experimental uncertainty, the heat transfer coefficient was independent of the initial temperature of the object over a initial temperature range of 175 $^{\circ}C$ and 50 $^{\circ}$ C.

1.7.12 Particle thermophysical properties

Ziegler et al. [1964] measured the heat transfer coefficient from a sphere and a cylinder to a bed of solids fluidized in an air stream. Copper, nickel and solder (50% Pb and 50% Sn), whose densities were nearly the same but the thermal properties that varied over a reasonable range were used as fluidizing materials. The celite sphere was electrically heated with a thermocouple soldered to the surface of the sphere. From the heat input and the temperature difference between the heat transfer surface and the bed, the heat transfer coefficients were obtained. The heat transfer coefficient was found to increase with solid heat capacity and was independent of solid thermal conductivity. Copper and nickel bed particles whose thermal conductivities vary widely, but has similar heat capacities, produced almost

the same heat transfer coefficient. However, increasing heat capacity of the particles, the heat transfer coefficient increased by 50 to 100%.

Regarding the effect of particle thermal conductivity, Zabrodsky et al. [1976] noted that for short residence time of the packet of particles on the heat transfer surface that the heat wave penetrates only the particles next to the wall and a change in the thermal conductivity of particle could be important for heat transfer. However if the first row of the particles are separated by a gap of 0.1 d_p from the wall, there was no influence of the particle conductivity.

1.7.13 Local heat transfer coefficient on a tube or sphere perimeter

Samson [1974] experimentally studied the variation in the local surface heat transfer coefficient on a large horizontal cylinder, a vertical cylinder and a sphere immersed in a correspondingly large fluidized bed using small heat transfer plugs. The cylinder measured 11.5 cm in diameter by 11.5 cm long and the sphere 11.5 cm in diameter and were made up of bronze. The fluidized bed 46 cm in diameter by 65 cm length was used with sand particles of 141μm mean diameter fluidized by air. He plotted heat transfer coefficient on polar coordinate graphs, showed the detrimental effects of a defluidized zone formed above the objects and a gas film adjacent to the underside of the objects. In the case of the horizontal cylinder the maximum local surface heat transfer coefficient was observed to occur at 72° from the underside or bottom for both low and high gas flow rates. However, this angle was found to be 90° in a separate study conducted by Gelperin et al. [1963]. This discrepancy can be explained by the presence of a considerably wider defluidized zone in the latter

studies since the diameter of the cylinder used was six times smaller in size. The variation in local radial heat transfer coefficient was observed to be significant along the radial angle at the low fluidizing rate for a vertical cylinder. This was attributed to the lack of uniformity in the fluidization over the bed cross section. However at higher superficial air velocities, the variation in the radial heat transfer coefficient became less marked. In the case of the immersed sphere, the general pattern of the variation in the heat transfer coefficient was found to be similar to that for the horizontal cylinder. The maximum local heat transfer coefficient occurred at 70° from the base. The heat transfer coefficient at the base of the sphere was found to be lower than for the cylinder owing to the presence of gas pockets collected at the base of the object before moving upwards. Since the collecting surface is smaller for a sphere than a cylinder, resulted in thickening of the gas film. The photographs obtained by him of the defluidizing and gas void zones are shown in Figure 1.2.

Baskakov et al. [1972] measured the temperature field on the surface of a sphere submerged in a fluidized bed. This temperature distribution was used for calculating the local heat transfer coefficient. They used 4.0 cm and 8.2 cm diameter spheres and 60 and 320μm corundum particles. They observed the maximum local heat transfer coefficient at the equatorial zones of the sphere and the heat transfer coefficient at the lower portion of the sphere was found to be higher than for the upper portion.

Figure 1.2: Defluidized and gas film zone, Gelperin et al. [1963]

1.7.14 Orientation of heat transfer surface

Baskakov et al. [1973] carried out experiments to measure the heat transfer coefficient for an inclined plate with the heated surface up and heated surface down immersed in the same fluidized bed. The heat transfer coefficients for the top surface of an inclined plate were lower from those obtained with a vertical plate because of a defluidized layer formed above the plate. Furthermore, heat transfer coefficients to vertical tubes are usually 5 to 15 % higher than to horizontal tubes as the latter have inferior conditions of contact with the fluidized bed [Gelperin and Einstein 1971].

1.7.15 Moisture

The effect of particle moisture content was studies by Baskakov et al. [1973]. In the case of a bed of nonabsorbent corundum particles, heat transfer coefficient first increased with increased moisture content because of the reduction in inter particle electrostatic effects within the bed. With a further increase in the moisture, the air became saturated and the flow properties of the bed changed sharply and the heat transfer coefficient was reduced. For porous charcoal particles, particle heat capacity increased as moisture was absorbed and for 13% absorption of moisture by weight, the heat transfer coefficient increased by 26%.

1.7.16 Mixed particle size

The effect of mixed particle size distribution on heat transfer in a gas fluidized bed was studied by Figliola et al. [1986]. They used an electrically heated cylinder

(5 cm diameter by 25.4 cm length) immersed in a fluidized bed of 200 cm height and 30.5 cm×30.5 cm cross section of glass particles. They found that the heat transfer coefficient was augmented by 25% at G=0.23 Kg/m^2s to 40% at G=0.30 Kg/m^2s with the addition of fine particles to 453μm particles reduced the mean particle size by about 11%. However beyond 340μm mixture heat transfer coefficient practically remained constant even though the mixture mean particle size was decrease by 33% further.

1.7.17 Packed bed height

Pillai [1976] investigated heat transfer to a sphere immersed in a shallow fluidized bed. He recorded the transient temperature of a sphere of low Biot number when immersed into heated air fluidized beds. Heat transfer coefficient were measured at bed temperatures of up to 1100°C. Particles of silica sand, zircon sand and silicon carbide ranging in size from 200μm to 800μm were investigated. The heat transfer coefficient was found to be somewhat higher than those reported for deeper beds. He noted major features of shallow beds as the violent coalescence of bubbles, thermal entry region, and a jetting region next to the distributor plate which occupied most of the shallow bed. He suggested that solids motion within a shallow bed might be significantly greater than in a deep bed reducing the residence time of the particles at the immersed surface. He also concluded without any physical explanation that the bed temperature dependence of the maximum heat transfer coefficient was very much stronger in a shallow bed which he expressed in

an empirical correlation;

$$Nu_{max} = 0.365 Ar^{0.22} \Theta^{0.82} \tag{1.6}$$

Kharchenko and Makhorin [1964] carried out experiments to establish the relation between the height of the unexpanded bed and the heat transfer coefficient for quartz sand particles of 340μm mean diameter and superficial air velocities ranging from 65 to 70 cm/s at a bed temperature of 800 $^{\circ}C$. It was found that as the bed height was changed, the heat transfer coefficient reached an optimum value at an initial bed height approximately equal to the bed diameter. While at other values of bed height, the heat transfer coefficients were lower than the optimum values.

1.7.18 Gas convective component

Botterill et al. [1981] performed experiments with spherical probes of low Biot number immersed in a hot 18.8 cm diameter stainless steel fluidized bed operating at temperatures ranging from 250°C to 700°C. Sand, coal and alumina particles of mean diameter size range from 380μm to 2320μm were used. They observed that bed-to-surface heat transfer coefficients were sensitive to the superficial velocity with group 'B' materials. Whereas for group 'D' materials, gas convective heat transfer was more important and there was less influence of gas velocity. They also observed a transition in behavior between the characteristics of a bed of group 'D' to 'B' type material as the operating temperature increased.

Shirai et al. [1966] estimated the amount of heat transferred to the particles, by subtracting the amount of heat transferred by the gas phase from the experimental heat transfer coefficient. The heat transfer coefficient for the gas phase was

estimated using the Ranz and Marshall [1952] correlation. From this estimation, they concluded that about 88% of heat is transferred by the particles. Similar results were obtained by Ziegler and Brazelton [1964]. They performed experiments in which simultaneous heat and mass transfer from a 1.27 cm diameter sphere of clay like material was studied in a gas fluidized beds of copper, glass and alundum particles. The systems were chosen so that the fluidized particles had a capacity for heat transport but not mass transport. O'Brien et al. [1985] measured mass and heat transfer coefficients for a horizontal tube submerged in a fluidized bed of glass particles ranging in size from 215μm to 3400μm. The gas convection component was determined by measurements of the rate of mass loss from a submerged naphthalene cylinder and utilizing the heat and mass transfer analogy. Total heat transfer coefficients were measured under identical conditions using an instrumented and electrically heated copper cylinder. They found that the gas convective coefficient increased significantly with particle size and demonstrated an increased dependence on superficial gas velocity for the large particles. The relative contribution of the gas convection to total heat transfer ranged from 6.8% for the smallest particles at optimum heat transfer to 100 % for the largest particles.

1.7.19 Vibrated bed

In recent years, the vibrated fluidized bed has gained significant attention for its ability to overcome certain drawbacks associated with the conventional fluidized bed such as, gas bypassing, attrition and entrainment of particles. It has been found that vibrated fluidized beds offer higher heat and mass transfer rates than

conventional fluidized beds at lower operating pressure drops. Moreover, suspending the equipment on a well-designed resonating spring assembly, the electrical energy for vibration can be maintained to a minimum [Mujumdar 1983]. A vibrated fluidized bed is particularly useful for heat transfer of immersed objects in a bed of hard to fluidized and sticky granular solids. Some of the vibrated fluidized bed applications include the drying of granulated fertilizers, polymer chips, inorganic and organic chemicals, pharmaceuticals, food products (e.g., sugar, cocoa, coffee), asbestos fibers, clay, etc.

Recently Malhotra and Mujumdar [1987] presented results of an experimental study of heat transfer from an immersed electrically heated copper cylinder to a vertically vibrated fluidized bed of glass particles ranging in size from 325μm to 2360μm. A two dimensional fluidized bed of rectangular cross section was vibrated by means of an eccentric mechanism at frequencies varying from 0 to 105 rad/s and amplitudes up to 0.425 cm. An interesting result was reported, the heat transfer coefficient increased by more than 20 times for a packed bed vibrating at accelerations, $\frac{A\omega^2}{g}$ near 2. This enhancement was attributed to vigorous particle mixing. Similar heat transfer enhancement was obtained for aluminum oxide, kaoline and zinc particles when vibrated moderately in nonaerated beds. For fluidized beds, as the superficial velocity increased, the maximum heat transfer coefficient occurred at lower values of vibrational acceleration due to improved particle mixing induced by air flow rate. Malhotra and Mujumdar [1987] also studied the effect of surface stickiness by adding controlled amount of glycerine into the glass particles. The heat transfer coefficients were found to be about 40 to 50% higher for those sticky

particle beds as compared to the dry beds for vibrational accelerations below 4. However for a vibrational acceleration above 4, the difference between heat transfer coefficient for sticky bed and dry bed vanished. In fact, for glass particles of 1017 μm, the dry bed produced a slightly higher heat transfer coefficient than the sticky bed at vibrational acceleration above 2 and $U/U_{mf} = 0.9$.

Lu et al. [1976] conducted an experimental study of heat transfer between a stationary sphere and a vibrated fluidized bed. Also the particle motion by using tracer technique was investigated. Polystyrene beads of 1840 μm size were used as fluidizing particles. The test spheres were made up of aluminum of 1.3 and 3.1 cm diameters, which were inserted into the hot bed and the transient temperature of the center of the sphere was recorded. The heat transfer coefficient was determined using the lumped heat capacity method. The results of the pressure drop across the vibrated fluidized bed suggested that the bed could be fluidized at a lower gas flow rate than that of a unvibrated system. Heat transfer experiments were carried out in two sets. In one set, the amplitude was kept constant at 1.0 cm and frequencies were varied as: 65, 120, 210, 260, 480, 840 rpm. In an another set of experiments, the frequency was kept constant at 65 rpm and the amplitude was varied from 1 to 0.3 cm. The heat transfer coefficient was found to increase with amplitude as well as frequency compared to the stationary bed at lower superficial gas velocities. However, for Reynolds number based on fluidized bed diameter and superficial velocity greater than 1000, the effect of vibration of the heat transfer coefficient was negligible. Their results also showed that additional gas flow rate did not increase the heat transfer coefficient of the system if its vibrational acceleration was greater

than 3. Furthermore, they estimated the residence time of the packet of particles by measuring the particle velocities. Mickley and Fairbanks' [1955] packet model was used to predict the heat transfer coefficients from these residence time data. The agreement between the theoretical and experimental heat transfer coefficients were very reasonable in the higher vibrational acceleration region and was poor in the lower vibrational acceleration region.

Abuaf and Gutfinger [1974] performed an experimental study of the heat transfer and coating in a vibrated fluidized bed. Nylon particles of mean diameter of 125μm size were used in a 11.4 cm diameter and 25.6 cm high (packed bed height=15.5 cm) fluidized bed. The heat transfer experiments were performed with copper plate of dimensions 6.4 $\times$5.4$\times$0.3 cm^3 with attached thermocouples and heat transfer coefficients were determined by the cooling temperature-time history record. This work showed the spread about 15 to 22% in heat transfer coefficient at a constant superficial gas velocity. This result confirmed an important aspect of fluidized bed heat transfer regarding the the difficulties in obtaining reproducible heat transfer data. They attributed this spread to the dynamic conditions of the fluidized bed.

1.7.20 Vibrating plate

Reed and Fenske [1955] in an effort to attain higher heat transfer rate conducted an experimental study of measuring the heat transfer rate from a vibrating plate immersed in a gas fluidized bed. Nickel powder, lead powder and carbon granules of 26, 38, 880 and 550 μm average particle diameters were used. They found that

below 1 ft/s superficial air velocity and at an amplitude of 0.313 in. with vibrational frequencies up to 2000 cycles/min, the vibrating motion of the plate was effective in enhancing the heat transfer rate. This enhancement was more pronounced for the nickel particles, somewhat less for the lead particles, and still less for the large carbon granules. At the high gas flow rates of 3.8 and 7.5 ft/s used to fluidize the steel shot, the vibrating motion of the plate, had practically no effect on heat transfer coefficient. The results of the horizontal vibrating plate immersed in a fluidized bed of 100 μm granular material showed that as the amplitude of the vibration increased from 0.158 cm to 0.795 cm, the heat transfer coefficient increased rapidly with the frequency of oscillation. They plotted the product of frequency and amplitude vs heat transfer coefficient between a vibrated plate and bed of aerated nickel powder and showed that at 0.2 ft/s superficial velocities, the data for 0.0625 and 0.125 inch stroke length coincided. However, the 0.313 inch stroke line fell below the curve obtained at the lower strokes. This was attributed to bed density at the plate region being lower than the average in the bed and at such a large stroke and high frequencies, the plate probably sweeps out a volume sufficiently large and rapidly so that the particles do not immediately fill the space left by the motion of the plate.

1.7.21 Freely moving sphere

In recent years, studies of heat transfer from a freely moving object in a fluidized bed has gained special attention. Knowledge of such heat transfer data is essential in some physical operations such as; drying, gasification and combustion of fossil fuels.

Prins et al. [1986] evaluated heat transfer coefficient for a freely moving sphere in a gas fluidized beds of glass particles of 1000μm size and alumina particles of 631μm size at elevated temperatures of 300°C, 600°C and 900°C. Silver and graphite spheres of 0.4 to 2.0 cm in diameter were used as heat transfer probes, which were connected to very thin long and flexible thermocouples so that they could move almost freely through the entire bed. The fluidized bed used had 10.3 cm internal diameter and 12 cm of packed bed height. The bed was maintained at 300°C using hot air for glass particles bed and at 600°C and 900°C for fused alumina particles bed. The cold sphere was immersed in the hot fluidized bed and the transient temperature of the center of the sphere was recorded to determine the heat transfer coefficient utilizing the low Biot number aspect of the system. It was shown that the difference in the heat transfer coefficient between a fixed silver sphere and a freely moving graphite sphere was relatively small and tended to become less for beds of large sized particles. For smaller sized particles the heat transfer coefficient for a freely moving graphite sphere was smaller than that of a fixed silver sphere for the fluidized bed of glass particles. They correlated their final results within 15% accuracy, within the range; $10 < Ar < 2000$ and $3 < D_{sph}/d_p < 200$. For a fixed sphere;

$$Nu_{max} Ar^{-m} = 4.175(\frac{D_{sph}}{d_p})^{-0.278} \tag{1.7}$$

where,

$$m = 0.087((\frac{D_{sph}}{d_p})^{0.128} \tag{1.8}$$

For a freely moving sphere;

$$Nu_{max} Ar^{-n} = 3.539(\frac{D_{sph}}{d_p})^{-0.257} \tag{1.9}$$

Where,

$$n = 0.105(\frac{D_{sph}}{d_p})^{0.082} \tag{1.10}$$

Rios and Gibert [1984] studied heat transfer from a fixed object, a light object freely floating and circulating in the entire layer, and a light object only allowed to move in a restricted zone in an air fluidized bed of glass particles ranging in size from 315-400 μm. Light plastic spheres of different sizes 0.8 to 3.5 cm in diameter were used as large freely moving objects. In some cases they were allowed to circulate throughout the bed in others they were permitted to move in the upper part of the bed delimited by inserting a large mesh wire lattice 4 cm below the upper surface. Heat transfer coefficients were determined from the heat stored from several cold spheres that were plunged into the hot fluidized bed during a given time. Experimental determination of this stored heat was carried out using a calorimeter. Their results showed that for 0.8 and 2 cm diameter plastic spheres, without a wire lattice within the layer, the heat transfer coefficient increased continually over the gas velocity range from the minimum fluidizing velocity U_{mf} to $2U_{mf}$ and then become independent of superficial air velocity. They also compared heat transfer coefficients for stationary, freely moving and hindered moving spheres at $U = 2.3U_{mf}$ for various sphere sizes. One unexpected result obtained was that the heat transfer coefficient for a stationary sphere were independent of sphere diameter at U_{mf} to $2U_{mf}$. The heat transfer coefficients for fixed and freely moving 0.8 cm diameter spheres were quite different. The heat transfer was enhanced by 68% for a freely moving 0.8 cm diameter plastic sphere and 32% for hindered moving plastic sphere. This result was quite contrary to that of Prins et al. [1986]. However, for larger

plastic spheres, e.g., 3.5 cm diameter the heat transfer coefficient for stationary, freely moving and hindered moving plastic spheres were found to be very similar.

1.8 Theoretical Models

Three basic trends has been observed in modeling the heat transfer phenomena in fluidized beds.

1.8.1 Conductive heat transfer through the gas boundary layer

In this model heat is conducted through the gas boundary layer near the heat transfer surface. This gas layer was assumed to be scoured by solids moving along the heat transfer surface decreasing the boundary layer thickness near the wall and increasing the heat transfer coefficient. Such a model has been developed by Leva [1959], Dow and Jacob [1951] and Levenspiel and Walton [1954].

Levenspiel and Walton [1954] developed a model where the resistance to the heat flow in due to a laminar gas layer which is destroyed by the scouring action of solid particles passing through it. The average thickness of the laminar gas layer is much thinner than that of a tube without solid particles. They assumed stationary particles of uniform diameter d_p arranged in equally spaced horizontal layers. As shown in the Figure 3, the boundary layer is destroyed at the points of contact with the stationary solid and develops again. The distance between two successive layers of solid particles is given as;

$$D_r = \frac{\pi d_p}{6(1-\epsilon)} \tag{1.11}$$

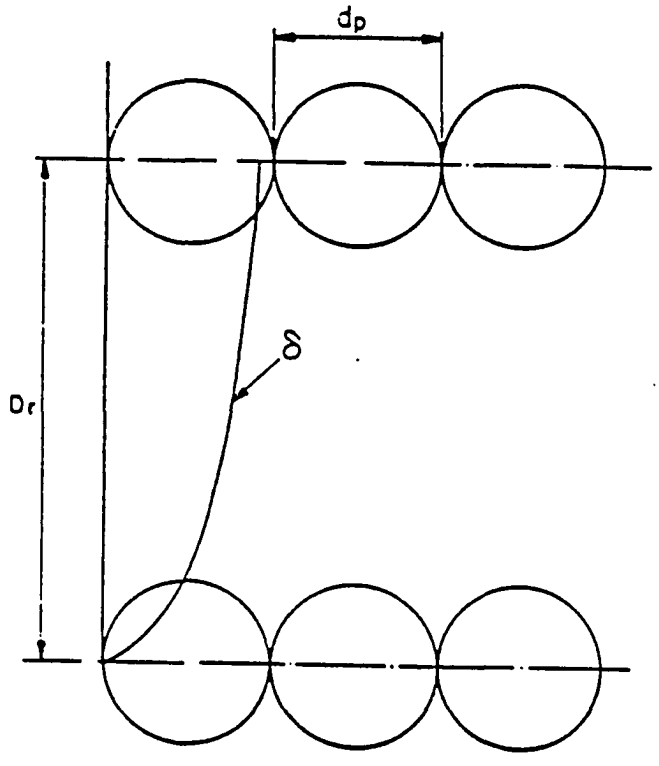

Figure 1.3: Laminar boundary layer thickness between two layers of particles close to the heat transfer wall [Levenspiel and Walton 1954]

The heat transfer coefficient for an average boundary layer thickness;

$$h = \frac{K_g}{\delta} \tag{1.12}$$

The boundary layer thickness can be given by;

$$\delta = 3.333\left(\frac{\mu_g D_r}{U\rho_g}\right)^{0.5}\gamma \tag{1.13}$$

were

$$\gamma = \left[\left(1+\beta^2\right)^{1.5} - \beta^2\right] \tag{1.14}$$

and

$$\beta = 0.041(1-\epsilon)\left(\frac{D_r U \rho_g}{\mu_g}\right)^{0.5} \tag{1.15}$$

Though this model agreed well with the experimental data for air fluidized beds of coal, glass and silica catalyst. This model does not take into account the influence of the solid particles on the heat transfer and hence the mechanism can not be considered complete.

1.8.2 Unsteady heat conduction by particles

Photographic observations show that solid particles tend to associate in groups and remain in contact with the heat transfer surface for a certain amount of time [Botterill et al. 1962]. They considered an isolated solid particle in contact with the heat transfer surface. By neglecting conduction through the points of contacts, radiation effects, and thermal convection through the surrounding fluid, the unsteady heat conduction between a plane surface and an insulated spherical particle surrounded by a static gas was addressed. The system of Laplace equations for

heat transfer within the two homogeneous phases, namely fluid and solid particles with residence times up to 70μs was solved numerically. Because of the low thermal conductivity of the gas, the rise in the temperature of the particles was very small throughout the residence time of the particle. The calculated spacing of the isotherms showed that significant heat transfer is confined to the region around the point of contact between the particle and surface, where the paths are very short. However, heat entering the particle is rapidly conducted because of high thermal conductivity of the solid phase. The average rate of heat transfer to a single particle during a given residence time was calculated by integration of the instantaneous rate. The overall heat transfer rate was estimated from the average rates taking into account the number of particles in contact per unit area of the heat exchange surface and scaling to unit temperature difference. The experimental results, obtained by varying the residence time of the particles at the surface by stirring the bed compared well with this model for short residence times. In the case of long residence time, the heat penetrates further into the bulk of the bed and the second row of particles also play an important role in the heat transfer mechanism. Botterill [1975] extended this model to the case of heat transfer into two adjacent particles touching the surface in order to compare the experimental results obtained at large residence times.

Gabor [1970b] proposed two unsteady state heat transfer models relating residence time to the rate of the heat transfer based on a string of particles normal to the heater surface and characteristic length functionally dependent on the depth of heat penetration from the heater surface. The first model was based on a string

of spheres of indefinite length normal to the heater wall when viewed from the side and in an hexagonal pattern when viewed from the heater surface. He made the following assumptions in this model:

1. An orthorhombic array is a reasonable approximation of the array of the particulate phase of both fluidized beds and packed beds. The void fraction for such an array is 0.395.

2. As the volumetric heat capacity of solid particles is many orders of magnitude greater than the volumetric heat capacity of gases, the heat removal by gas convection can be neglected.

3. The radial heat transfer between particles is neglected.

The system of heat conduction equations was solved numerically for air-glass and air-copper systems. A grid of five divisions per particle radius and incremental time interval of $t/{d_p}^2$ of 1.455×10^{-3} and 3.89×10^{-4} hr/ft^2 was used. The heat transfer flux was determined by weight averaging the temperature of each particle and then multiplying this temperature by the particle heat capacity and dividing by the total time. The heat transfer coefficients calculated from this model agreed well with the experimental data for glass and copper particles in air with the assumption that the gas gap between particles is $0.015d_p$ and $0.0075d_p$ between the wall and the first layer of particles. The second model was based on heat transfer through a series of alternating gas and solid slabs. The thickness of the solid slab was taken as $0.66d_p$ and the thickness of the gas phase between the particles was taken as $0.1d_p$ and $0.05d_p$ respectively as suggested by Kunii and Smith [1960]. These values of

gas slab thicknesses gave a good agreement with published experimental data. The main drawback of this model is that it cannot be applied to a fluidized bed with strong agitation and bubbles.

More recently, Ganzha et al. [1982] developed a mechanistic theory for the heat transfer between an immersed surface and a fluidized bed of large particles in the absence of radiation. The conduction heat transfer coefficient was computed by considering a composite of infinite layers of gas and solid. For a large particle system, it was assumed in this model that all of the resistance to heat transfer is confined to the first row of particles near the heat transfer surface only. The heat is transferred by conduction through the gas film between the surface and the particle with a uniform thickness of δ. Particles were replaced by equivalent cylinders having the same volume as the actual particles and of equal height and diameter. The transient one dimensional heat conduction equations for each phase were solved using appropriate initial and boundary conditions. The approximate (within 30 %) solution valid for all the gases except helium and hydrogen in the temperature range of 273 *to* $1100K$ and pressure range 0.1-10 MPa was given as:

$$h_{cond} = 1.06\frac{K_g}{\delta} \tag{1.16}$$

They modified this equation to account for the bed voidage and developed a equation for the thickness of the gas-film for a curved heat transfer surface as the gas film thickness is larger for the case of a curved surface. The final equation was given as:

$$Nu_{cond} = 1.02\frac{(1-\epsilon)^{0.666}}{(0.114+\frac{h_c}{d_p})} \tag{1.17}$$

The convection heat transfer coefficient was calculated recognizing the fact that for

beds of large particles, the Reynolds number is invariably larger than 100 and the flow around the particle is turbulent [Leva 1959]. The turbulent boundary layer formed on the immersed surface is continuously disturbed by the front half of the bed of particles and formed again in their wake [Levenspiel and Walton 1954]. The heat transfer surface was regarded as being covered with a continuous arrangement of unit orthorhombic cells which in time keeps reforming as new particles arrive at the surface. The heat transfer from the surface through the turbulent boundary layer was considered similar to that of a flat plate immersed in a turbulent gas stream. The heat transfer from a plate placed in a turbulent fluid flow is given by:

$$(Nu_l)_{conv} = C Re_l^{0.8} Pr^{0.43} \tag{1.18}$$

For a unit orthorhombic particle arrangement they [Levenspiel and Walton 1954] obtained an expression for l as;

$$l = 0.451 d_p (1.0 - \epsilon)^{2/3} \tag{1.19}$$

$$(Nu_l)_{conv} = C_o Re^{0.8} Pr^{0.43} \left[\frac{(1-\epsilon)^{0.133}}{\epsilon^{0.8}} \right] \tag{1.20}$$

The constant C_o was obtained by simultaneous measurement of total heat transfer coefficient and void fraction. Ganzha et al. [1982], performed an experiment with a single 1.3 cm diameter vertical tube and staggered bundles in a restricted bed at superficial gas velocities. This experiment gave a mean value of C_o as 0.12.

1.8.3 Packet theory

Mickley and Fairbanks [1955] developed this model which is generally known as packet theory. They introduced a picture of a packet of particles at the bulk bed

temperature is swept into close proximity with the heat transfer surface under the bubble induced circulation pattern occurring within the bed. The packet of particles remain in contact with the heat transfer surface for a certain period of time called the residence time of the packet only to be swept away from the surface and replaced by a fresh packet of emulsion. When this packet first arrives close to heat transfer surface, there is a high local temperature difference between the packet and the surface, consequently heat transfer is rapid. The longer the residence time, the more closely the surface and local bed temperatures approach and this decreases the heat transfer rates. Their reasoning for this packet theory was based upon the experimental evidence that the dense phase bubbling beds retained a constant void fraction independent of superficial gas velocity and that this void fraction was essentially that of quiescent beds. In a dense fluidized bed each particle may be expected to be in contact with several neighbors most of the time. The packets are not permanent; they have finite persistence in time. Their void fraction, density, heat conductivity and heat capacity are assumed to be the same as those of the quiescent bed. The main features of the packet theory as shown in Figure 1.4. Consider a packet of particles at bed temperature T_b, swept into contact with a flat surface of temperature T_w. Unsteady conduction will commence on contact. If A_c is the contact area between the packet and the wall and considering a homogeneous packet, the instantaneous heat flux after time τ is given by:

$$q_{wi} = A_c \left(\frac{K_{eff} \rho_{mf} C_p}{\pi \tau} \right)^{1/2} (T_w - T_b) \qquad (1.21)$$

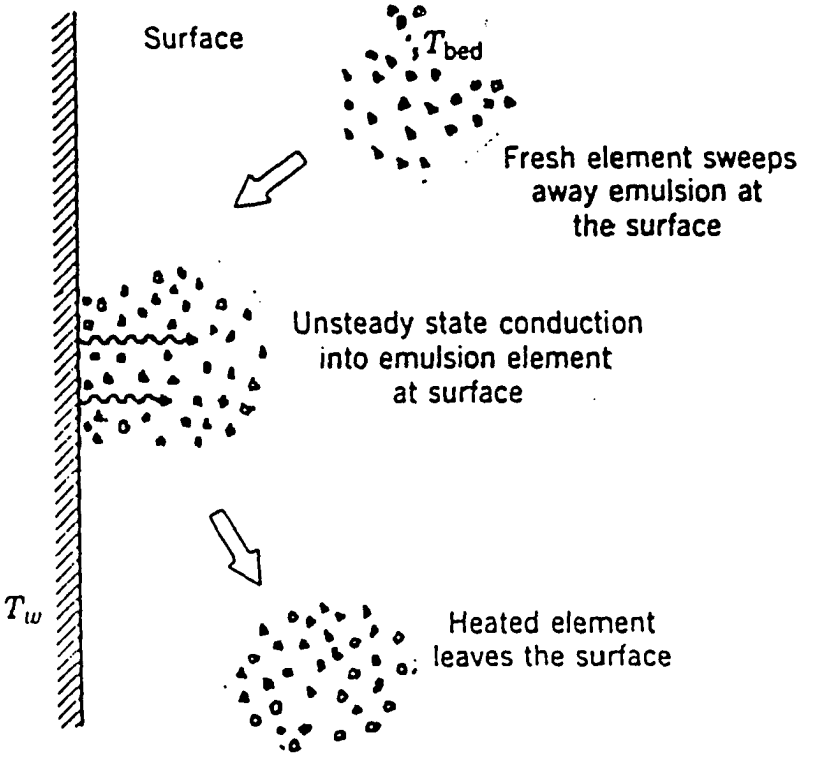

Figure 1.4: Packet theory model

The local instantaneous heat transfer coefficient is given by,

$$h_{wil} = \left(\frac{K_{eff}\rho_{mf}C_p}{\pi\tau}\right)^{1/2} \tag{1.22}$$

If $\psi(\tau)$ is the fraction of the surface occupied by packets of age between τ and $\tau + d\tau$, then the local time averaged heat transfer coefficient;

$$h_{wl} = \int_0^\infty h_{wil}(\tau)\psi(\tau)d\tau \tag{1.23}$$

$$h_{wl} = \left(K_{eff}\rho_{mf}C_pS_L\right)^{\frac{1}{2}} \tag{1.24}$$

where,

$$S_L = \pi^{-1}\left[\int_0^{infty} \tau^{-1/2}\psi(\tau)d\tau\right]^2 \tag{1.25}$$

and the average heat transfer coefficient over an entire isothermal area is,

$$h = \frac{1}{A}\int_A h_{wl}dA$$
$$\left(K_{eff}\rho_{mf}C_pS\right)^{1/2} \tag{1.26}$$

$$S^{1/2} = \frac{1}{A}\int_A S_L^{1/2}dA \tag{1.27}$$

Here S is a stirring factor representative of the frequency of particle replacement at the surface. Mickley and Fairbanks [1955] applied this derivation to two idealized bed models.

1. **Slug flow of solids past the surface** In a bed which is operating at low superficial gas velocities, there is not much turbulence, and solid particles are observed to move upward at the center and downward along the outside walls. If the solids move downward with a constant velocity u_p, the residence time

of the packet τ is given by;

$$\tau = \frac{L_H}{u_p} \tag{1.28}$$

where, L_H is the length of the heater. For this condition, the heat transfer coefficient is;

$$h = \left[\frac{4K_{eff}\rho_{mf}C_p}{\pi}\left(\frac{u_p}{L_H}\right)\right]^{1/2} \tag{1.29}$$

2. **Side mixing** With a large surface and highly turbulent beds, side wise transfer of the packet of particles occurs. The packet is flowing down while some of the surface is exchanged with solid brought in sideways from the core of the fluidized bed. When the side mixing is predominant, the heat transfer coefficient is given by;

$$h_{wl} = \left(K_{eff}\rho_{mf}C_p\right)^{1/2} \tag{1.30}$$

where s is the average replacement of packets at the wall per unit time by means of side mixing, and $S_L = s$.

Mickley et al. [1961] experimentally measured instantaneous and time averaged heat transfer coefficient in a fluidized bed. The low values of instantaneous heat transfer coefficient were attributed to gas bubbles, and high values to the sudden contact with a fresh packet of emulsion. One essential deficiency of this model is that the instantaneous heat transfer coefficient is inversely proportional to the square root of the residence time of the packet. Hence at very low values of residence time the heat transfer coefficient becomes extremely high.

1.8.4 Packet model including contact resistance

Baskakov [1964] extended the packet model with an added contact resistance to heat transfer located at the wall. This prevented the heat transfer coefficient for small residence times from becoming infinite. The expression for an added contact resistance was given as;

$$\frac{1}{h_c} = \frac{d_p}{\pi K_g \left[\ln(\frac{K_p}{0.1K_g} - 1)\right]} \tag{1.31}$$

Baskakov [Gelperin and Einstein 1971] assumed this contact resistance to be independent of time and in series with the thermal resistance of the packet itself R_a. The wall resistance R_w was given by;

$$R_w = \frac{\delta_w}{K_{ew}} \tag{1.32}$$

δ_w is the extent of the zone near the wall and it is of the order of dp/2. Experimental results showed that the surface-to-bed heat transfer is influenced by gas thermal conductivity and the particle diameter. This dependence can be accounted for by expressing the contact resistance as,

$$R_w = \frac{d_p}{mK_g} \tag{1.33}$$

For a cubic packing of the particles at the surface, Koppel et al. [1970] obtained m=2π. Zabrodsky et al. [1981] predicted from their work m to be of the order of 7.2. Baskakov and Vitt [1973] obtained from their data m=8, and Botterill et al. [1962] used m=10 to make their two particle model agree with experimental predictions. Catipovic et al. [1980] also used m=6, and Xavier and Davidson [1985]

found that m=4 was more appropriate for a horizontal surface. Thus in general $4 \leq m \leq 10$ has been suggested. The contact resistance has been assumed to be in series with the actual thermal resistance in the packet of particles, hence,

$$h_i = \frac{1}{R_w + R_a} \tag{1.34}$$

where,

$$R_a = \left(\frac{\pi \tau}{K_{eff} \rho_{mf} C_p} \right)^{1/2}. \tag{1.35}$$

The average heat transfer coefficient can be given by,

$$h = \frac{2}{R_a} \left[1 - \frac{R_w}{R_a} \ln(1 + \frac{R_a}{R_w}) \right] \tag{1.36}$$

Patel [1967] presented two surface renewal models, which included both contact resistance and finite characteristic length.

1. **Model I** A packet with the same properties as the bed at the minimum fluidization condition, initially at T_b comes in contact with the heat transfer surface to receive heat from the wall through a contact resistance. Heat penetrates up to a certain distance during the residence time.

2. **Model II** In this model it is assumed that heat from the heat transfer surface is transferred first to the single spherical particle near the wall and the particle near the wall also loses heat by conduction to a packet of particles of certain thickness situated between the wall particle and the bulk of the bed. Patel[1967] obtained asymptotic values for the heat transfer coefficients for zero and infinite residence time.

These various penetration models can be categorized as: having no contact resistance but a finite characteristic length [Toor and Marchellow 1958]; having no contact resistance and infinite characteristic length [Mickley and Fairbanks 1955]; having finite contact resistance but infinite characteristic length [Baskakov 1964]; with contact resistance and a finite characteristic length [Gutfinger and Abuaf 1974]. Furthermore in all these penetration type models, the residence time of the packet is to be estimated by experimentation. This can be achieved by: measuring the temperature fluctuations in the heater [Baskakov et al. 1973]; using a stirrer as heat transfer surface [Botterill et al. 1962]; by tracing the particle movements [Wei-Ming Lu et al. 1976] or by moving the packed bed at various speeds. Moreover, the measurement of the fraction of time bubbles shroud the heat transfer surface has been used to correct the heat transfer coefficient.

The resistance near the wall region has been assumed as a first approximation to be independent of time. More recently, this resistance has been associated with the surface roughness [Decker and Glicksman 1981]. They assumed a representative model of surface roughness of the particle to properly deal with the conduction resistance. Furthermore, the heat transfer surface was assumed to be smooth as compared to the particle roughness. The region of possible solid contacts extended to the point on the particle where the average distance between the particle and the surface is equal to the surface roughness. With this assumption, the overall particle-to-surface heat transfer was found to be only modestly influenced by the magnitude of the roughness. Due to the limited number of contact points due to microscopic roughness elements, small size and limited heat capacity of the roughness asperities,

very high heat transfer rates occur for only the first 10 to 20 ms of the residence time. During this time the contact zone of the asperities approaches a mean temperature between that of the surface and the bed. This is followed by a longer period of slower heat transfer rate until the average temperature of the entire particle changes appreciably. This initial period of high heat transfer rate occurs so rapidly that its influence on the time averaged heat transfer is negligible.

Gloski et al. [1984] developed an experimental apparatus to measure the heat transfer rate for periods as short as 10 to 20 ms. A thin tin foil heater, which was rapidly heated to initiate the transient heat transfer from the heater to a fluidized bed of glass particles ranged in size from 1000μm to 645μm. From the transient record of the heater temperature, heat transfer coefficients were determined for discrete times (10, 20, 40, 60, 80, 100, 120 and 140 ms). For gas flow conditions slightly above and below the minimum fluidization, large heat transfer coefficients were obtained for glass particles with diameter between 650 to 1000μm in the initial 10 ms, followed by a rapid decrease in the heat transfer coefficient during the first 10 to 20 ms. At longer times, the instantaneous heat transfer coefficient remained constant within the level of experimental uncertainty. From these results, they concluded that the elevated heat transfer coefficients at short times were due to the conduction heat transfer between the surface asperities on the particle which were in contact with the heat transfer surface, and that no gas layer existed separating the particles from the surface in fluidized beds. The constant heat transfer coefficient found after the initial 20 ms was attributed to the greater local resistance due to the greater local voidage.

These penetration models considered a packet of particles having constant voidage and constant thermophysical properties. Kubie and Broughton [1975] extended the packet theory to include the property variations described in terms of the voidage variations in the vicinity of a constraining surface. Most of the assumptions in their model are similar to those introduced by Mickley and Fairbanks [1955] except for the consideration of the variation of voidage normal to the wall and the influence of the surface on the local packing and hence alteration of the local thermophysical properties. They considered the heat transfer to be in the direction normal to the wall in the packet of emulsion and applied the semi infinite layer approximation. The conduction equation in one dimension was given as;

$$\rho(x)C_p(x)\frac{\partial T_e}{\partial t} = \frac{\partial}{\partial x}(K(x)\frac{\partial T_e}{\partial x}) \tag{1.37}$$

With boundary conditions;

$$t \geq 0, \quad x = 0, \quad -K(x)\frac{\partial T_e}{\partial x} = f_s \quad t = 0, \quad x \geq 0, \quad T = 0$$

The voidage variation with distance from the constraining surface takes the form of a damped oscillation curve having a minimum voidage at about one particle radius from the surface. In the case of fluidized beds the oscillations of the voidage appears to be damped much more rapidly and the voidage minimum is shifted further from the constaining surface [Korolev et al. 1971]. Kubie and Broughton [1975] utilized this observation and expressed voidage variation in terms of distance from the constraining surface from simple geometrical considerations. They further assumed that at a distance of one particle diameter away from the constraining surface the void fraction is equal to that of bulk void fraction. The heat capacity of the gas was

neglected and the local effective thermal conductivity of a packet was expressed in terms of the particle conductivity, the local void fraction and the gas conductivity using the method proposed by Kunii and Smith [1960]. They solved the unsteady equation numerically using the voidage distribution and thermophysical property distribution. The results obtained with this model agreed well with controlled residence time data [Kubie and Broughton 1975]. This property boundary layer model required no physically unjustified concepts in order to produce general agreement with experimental data.

Recently, Chen and Pei [1985] developed a theoretical model of heat transfer between a fluidized bed and an immersed sphere and a cylindrical surface based on two-phase boundary layer and surface renewal theory. The following assumptions were made in this model:

1. A spherical or cylindrical heating surface has an average constant temperature and has radius R.

2. There is a concentric two-phase boundary layer of constant average thickness δ_T surrounding the heat transfer surface.

3. The radial temperature derivative is zero at the outer boundary of the layer.

4. The thermophysical properties are constant.

5. Radiant heat transfer is negligible.

6. The two-phase thermal boundary layer is renewed from time to time by the moving particles and fluidizing gas.

The transient heat transfer problem described by the differential equation and boundary conditions in cylindrical and spherical coordinates, assuming azimuthal symmetry were solved by taking laplace transform. The solutions were simplified utilizing the fact that in a fully developed fluidized bed the particle velocity is large and $R > d_p$ as,

$$Nu = \frac{K_M}{K_g} d_p \left(\frac{S_1}{\alpha_M} \right)^{1/2} \tag{1.38}$$

Based on their model, a correlation for predicting the maximum heat transfer coefficient was obtained which correlated experimental data well.

Yoshida et al. [1969] proposed a model for mechanisms of heat transfer between a fluidized bed and the wall surface, following the film penetration theory. They considered a finite characteristics length of emulsion packet l_e, which suddenly contacts a heat transfer surface and after certain time it is replaced by a fresh packet of emulsion from the core portion of the bed. They represented this phenomenon by,

$$\frac{\partial T_e}{\partial t} = \alpha_{eff} \frac{\partial T_e^2}{\partial x^2} \tag{1.39}$$

with the boundary conditions;

$$T_e = T_b \; att = 0 \;\; T = t_w \;\; atx = 0 \; T = T_b \;\; atx = l_e$$

From the solution of above equation, the instantaneous local heat transfer coefficient h_i was found to be,

$$h_i = \left[\frac{K_{eff} \rho_{eff} C_p}{\pi \tau} \right]^{1/2} \left[1 + 2 \sum_{i=1}^{\infty} \exp\left(\frac{-i^2 l_e^2}{\alpha_{eff} \tau} \right) \right] \tag{1.40}$$

which converges rapidly and is useful for short residence times. Whereas for long residence time, the following equation is useful;

$$h_i = \frac{K_{eff}}{l_e}\left[1 + 2\sum_{i=1}^{\infty}\exp(\frac{i^2\pi^2\alpha_{eff}\tau}{l_e^2})\right] \tag{1.41}$$

The time averaged value of heat transfer coefficient was obtained from;

$$h_w = \int_0^{\infty} h_i I(\tau)d\tau \tag{1.42}$$

where $I(\tau)$ is the age distribution function of emulsion packet on the surface. They used two types of age distribution functions.

1. **Random surface renewal** This is most representative of a surface in the main body of the bed continually contacted by rising bubbles. The age distribution of emulsion packet was is given by;

$$I(t) = \frac{1}{\tau}e^{\frac{-t}{\tau}} \tag{1.43}$$

Using this, for rapid replacement, $\alpha_{eff}\tau/l_e < 0.8$ within 20% error,

$$h_w = \left[\frac{K_{eff}\rho_{eff}C_p}{\tau}\right]^{\frac{1}{2}} \tag{1.44}$$

for slow replacement, $\alpha_{eff}\tau/l_e > 1.2$, within 20% error,

$$h_w = \frac{K_{eff}}{l_e} \tag{1.45}$$

2. **Uniform surface renewal** This model is most representative of an emulsion flowing smoothly past the heating surface and the age distribution function was given by, for $0 < t < \tau$

$$I(t) = \frac{1}{\tau} \tag{1.46}$$

For $t > \tau$

$$I(t) = 0 \tag{1.47}$$

For short contact times,

$$h_w = \frac{2}{\pi^{0.5}} \left(\frac{K_{eff} \rho_{eff} C_p}{\tau} \right)^{\frac{1}{2}} \tag{1.48}$$

For long contact times or steady state heat transfer,

$$h_w = \frac{K_{eff}}{l_e} \tag{1.49}$$

Gabor [1970a] developed a model predicting the rate of heat transfer from a flat plate and a cylinder immersed in a packed and fluidized bed at incipient fluidization. He solved steady state conduction equation for both the cases. The heat transfer coefficient for the flat plate,

$$h = \left(\frac{4 K_{eff} C_p G}{\pi l} \right)^{0.5} \tag{1.50}$$

and for cylindrical heater,

$$h = \left(\frac{4 K_{eff} C_p G}{\pi l} \right)^{0.5} + \frac{K_{eff}}{2al} \tag{1.51}$$

For K_{eff}, the following expression was used,

$$K_{eff} = K_e^{\circ} + 0.1 (C_p d_p G) \tag{1.52}$$

where K° is the conductivity term without gas flow, predicted for an orthorhombic packing. The theoretical predictions for both the cylinder and flat plate heaters were in good agreement with his experimental data.

1.8.5 Residence time study

Baskakov et al. [1973] conducted an experimental study of heat transfer from a cylindrical probe (made up of a 5 micron platinum strip glued to the side of 1.5 and 3 cm diameter vertical rubber cylinder) immersed in a fluidized bed of corundum particles of mean diameter of 120, 320 and 500μm. The beds used were 9.8 and 9.2 cm diameter and the fluidizing gases were carbon dioxide, helium and air at temperatures from 20°C to 550°C. They determined the bubble contact time, packet contact time, bubble frequency and the fraction of the time that bubbles shrouded the heat transfer surface f_0 from the the foil temperature fluctuations of the platinum strips mounted on the vertical tubes.

The contact resistance R_w, taken as an inverse of the values of the instantaneous heat transfer coefficient was determined from the platinum foil probe. The contact resistance decreased almost linearly with the particle diameter. The gas resistance was found to be independent of the fluidizing velocity and height at which the probe was located within the bed. They obtained the empirical correlations for τ and f_0 as follows;

$$\tau = 0.44[\frac{d_{pg}}{U_{mf}^2(\frac{U}{U_{mf}} - A1)^2}]^{0.14}(\frac{d_p}{D_{probe}})^{0.225} \tag{1.53}$$

$$f_0 = 0.33[\frac{U_{mf}^2(\frac{U}{U_{mf}} - A1)^2}{d_{pg}}]^{0.14} \tag{1.54}$$

The empirical factor A1, made allowance for the effects of probe diameter and particle shape. From the frequency and amplitude of the temperature fluctuation of the heating element, Richardson and Shakiri [1979] estimated the mean residence

time of the solids at the surface and applied Mickley's packet theory to estimate heat transfer coefficients. These predicted heat transfer coefficients compared well with their experimental values.

2 EXPERIMENTAL SET UP AND PROCEDURE

2.1 Introduction

The aim of this investigation was to evaluate the heat transfer coefficients for a stationary and a moving (linearly and oscillating) sphere immersed in an air fluidized bed of glass particles for various superficial air velocities. The following measurements were required as part of the experiment: air flow rate, temperature history of the center of the copper sphere, air pressure at the inlet of the rotameter, pressure drop across the bed, linear velocity of the sphere, and frequency and amplitude of the oscillating sphere. A experimental rig was designed in order to acquire these parameters.

2.2 Experimental Setup

The schematic diagram and the actual photograph of the experimental set up are shown in Figures 2.1 and 2.2. The main components of the system are: the fluidized bed; the rotameters for air flow measurements; the linear and oscillating mechanisms for controlling the motion of the sphere; various manometers for measuring rotameter pressure and pressure drop across the bed; the copper sphere; a heating cup used to preheat the copper sphere and a computer controlled data

acquisition system.

2.2.1 Fluidized bed

The fluidized bed is shown in Figure 2.3. This bed was designed by the Chemical Engineering Department at Iowa State University to study the fluidization characteristics of fly ash. The bed consisted of 0.3175 cm thick plexiglas column with an inside diameter of 9.5 cm which served as a container for the bed of glass particles. There were three separate column sections of the same diameter which could be fastened together tightly by bolts and sealed with o-rings. The bottom two sections were both 20.3 cm high to allow convenient loading or unloading of the bed materials. The longest column section available was 3 feet high which could be use for deep bed fluidization experiments which serve as a transport disengagement section to keep particle elutriation to a minimum. However, this section was not used for the heat transfer study as the required length of the hollow steel pipe (surrounding the copper sphere and thermocouple) was too long for a sturdy system. The fluidization column was fitted with a porous disc at the base to act as an air distributor. The porous gas distributor plate employed in this work was half inch thick Alundum porous disc (mixture P236, 240 μm porosity), manufactured by ceramic division of the Norton Company. After the plexiglas column was set up with rubber gaskets in place, an attempt was made to check the uniformity of the air distribution within the column. Using glass particles in a very shallow bed, it was observed that the flow was initiated first around the inside wall at very low flow rates while particle movement was also observed simultaneously in the center region

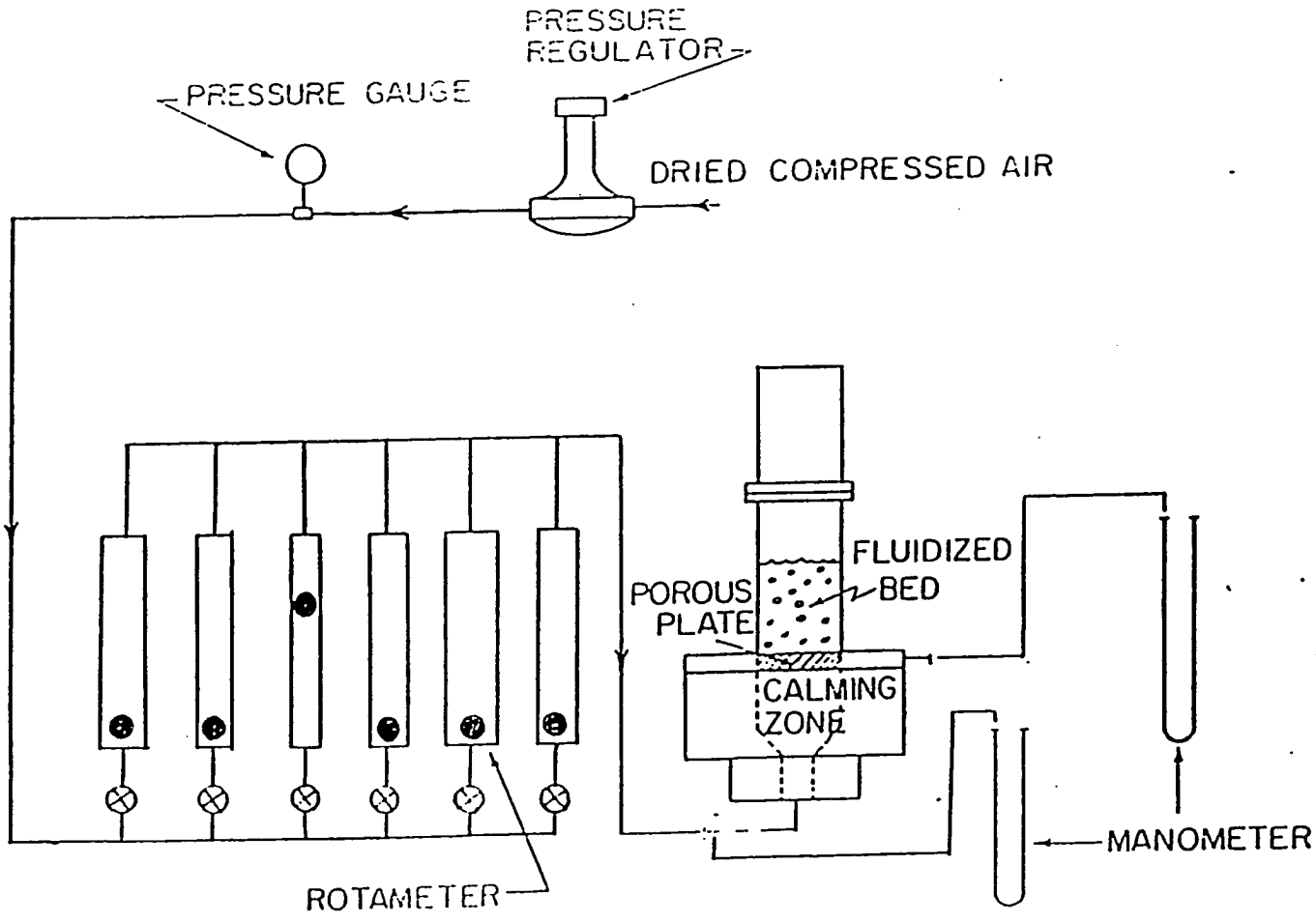

Figure 2.1: Schematic of the experimental setup

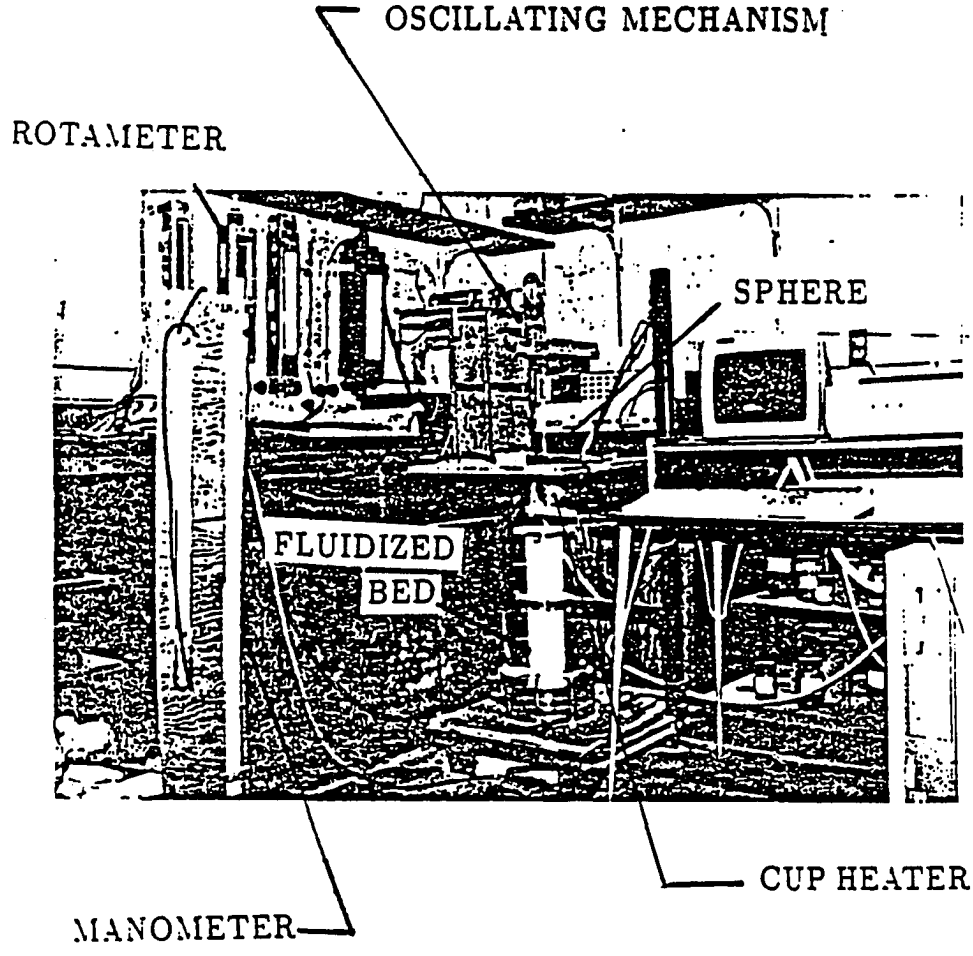

Figure 2.2: Photograph of the experimental set up

of the column. This was considered satisfactory fluidization in terms of a uniform air distribution. In order to check the leakage of air through the gasket and other joints, the fluidized bed was immersed in a large water tank and air was allowed to pass through the fluidized bed. In this way leaks were found near the bottom flange. A closer inspection of the rubber gasket revealed that it was not effectively sealing off the air bypass above the porous plate. To remedy this problem, a high vacuum grease manufactured by Dow Corning was used to seal the gaps at the gasket joints. Pressure taps were located along the column sections to measure the pressure drop across various sections of the fluidized bed. Fiberglass plugs were used to prevent particles from entering the manometer lines.

2.2.2 Flowmeters

Six rotameters of different ranges were used to measure the air flow rate. Appendix A describes the rotameter calibration equations and lists all the rotameters along with their range. All rotameters except rotameter number 6 were calibrated using wet test meters of appropriate range. The higher capacity rotameter number 6 was calibrated using the flow meter calibration rig located in the Chemical Engineering Department at Iowa State University.

2.2.3 Heater Cup

A metal heating cup connected to an A. C. rheostat was used to heat the copper spheres. This heater cup was placed on a swinging platform for easy removal of the heater cup after heating the sphere to a required temperature.

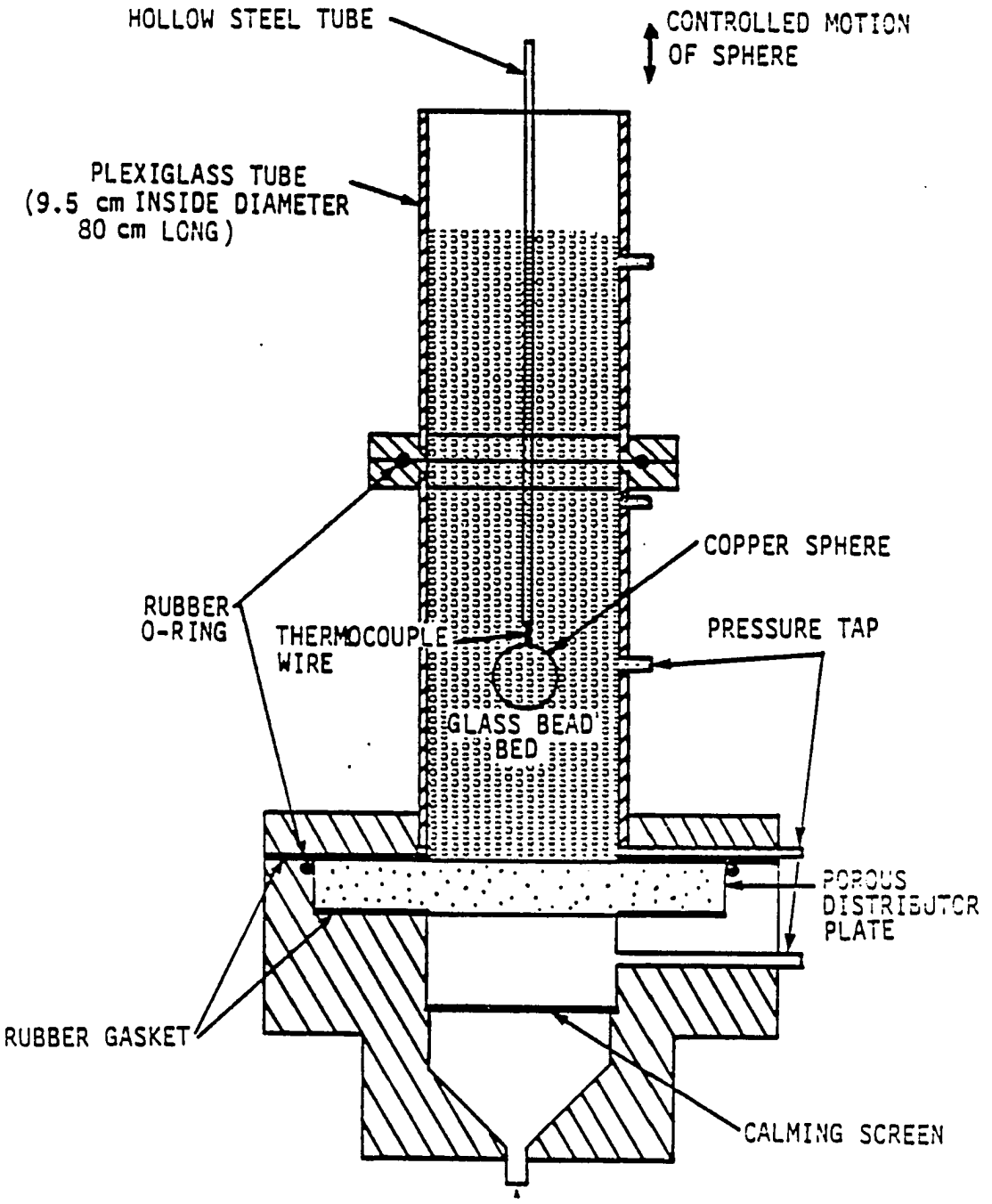

Figure 2.3: Schematic of the fluidized bed

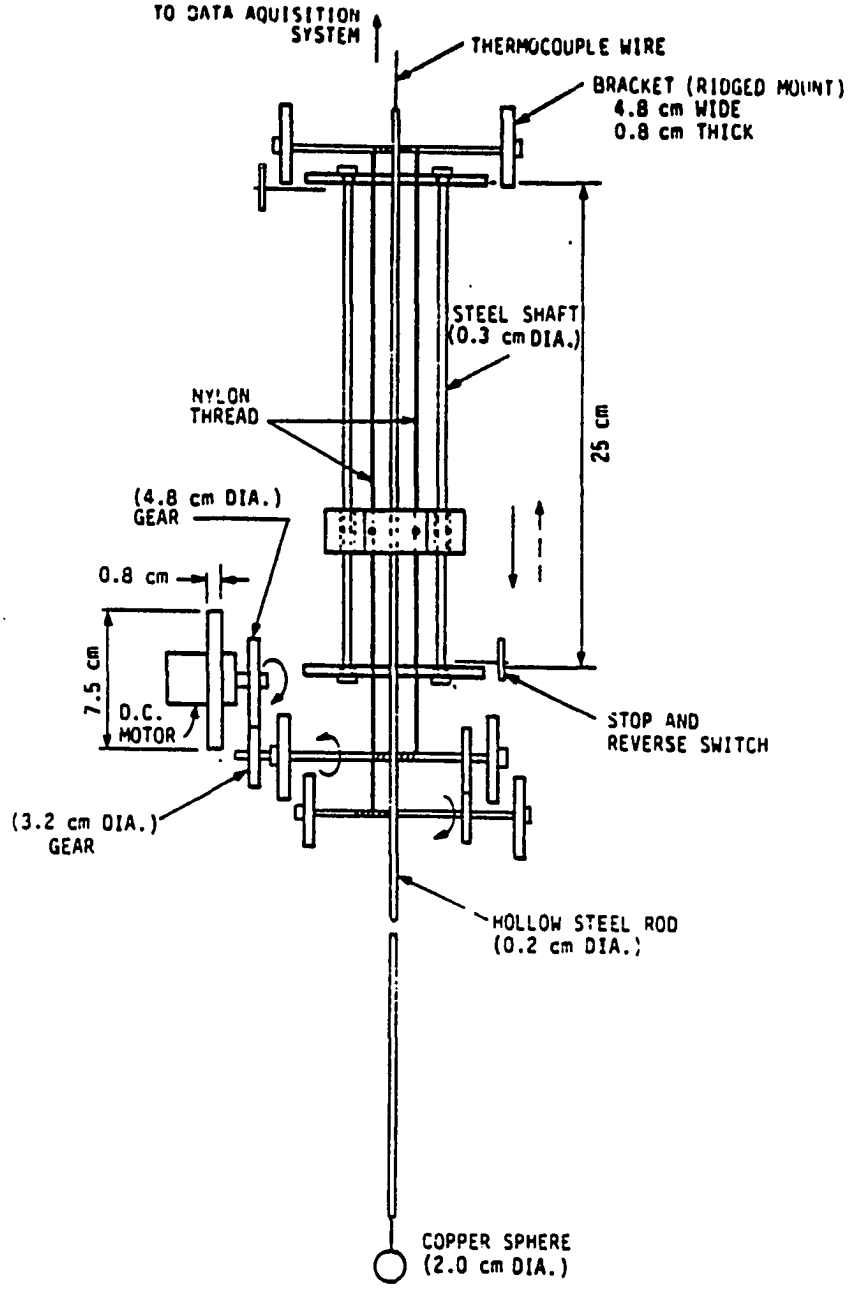

Figure 2.4: Schematic of a motor driven gear mechanism for controlling sphere motion in linear direction inside the fluidized bed

2.2.4 Sphere Driving Mechanisms

The schematic of the motor and gear drive assembly for controlling the linear vertical motion of the sphere is shown in Figure 2.4. This mechanism was designed to move the copper sphere in a vertically linear direction inside the fluidized bed. A sliding aluminum block, holding hollow steel rod and the thermocouple and copper sphere assembly firmly and was allowed to slide freely over a set of two parallel polished shafts with the help of a nylon thread attached to the sliding block. This nylon thread was wounded around two driving shafts and an idle shaft as shown in Figure 2.4. This driving shafts were driven by a reversible D.C. variable speed motor connected through a gear train. The motor was driven by a dual D.C. power supply (Hewlett-Packard, 0-24 V). Various linear speeds of the sphere were obtained by varying the speed of the D. C. motor or changing the gear ratio so as to obtain the required torque. With this arrangement it was possible to move a sphere in the vertical downward direction for about 22 cm in the fluidized bed. Two stop and reverse switches were installed at the top and bottom end of the steel shafts to prevent any sudden impact of the sliding block with the brackets housing the steel shafts. Moreover a stop and reverse manual switch was also connected in between the D. C. power supply and the D. C. motor.

The schematic diagram of the mechanism used to oscillate the copper spheres is shown in Figures 2.5. As in the case of the linear motion in this arrangement, a sliding block made of aluminum was allowed to slide freely over a set of two polished steel shafts. This sliding block carried the hollow steel rod, thermocouple and sphere assembly, and was also connected to an aluminum wheel 8 cm in diameter

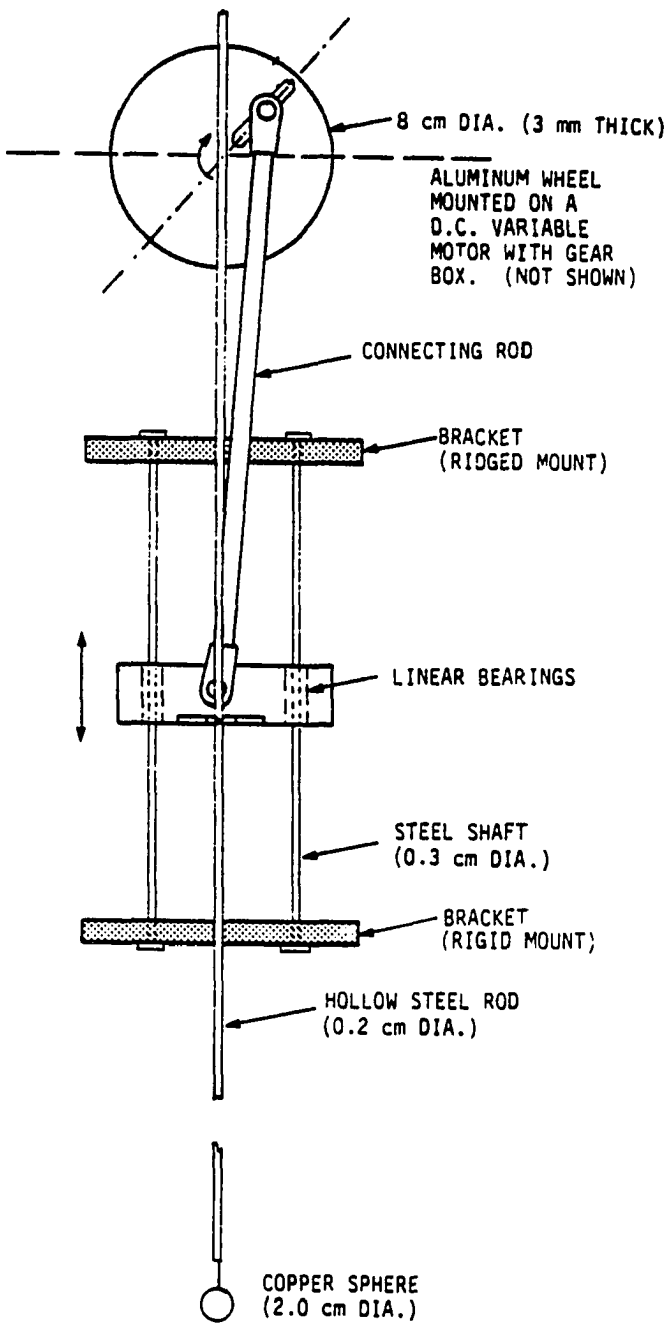

Figure 2.5: Schematic of a sliding mechanism for controlling oscillatory sphere motion within the fluidized bed

and 3 mm in thickness. The aluminum wheel was mounted on a shaft of a gear train driven by a 0-24 volts D.C. motor (Electro Craft Corporation, Hopkins, MN). The wheel and the sliding block were connected by an adjustable connecting rod. This arrangement was similar in principle to that of a piston oscillating inside a cylinder with a connecting rod. The amplitude of the oscillating motion was varied by placing the connecting rod at various positions inside the wheel groove. The frequency of oscillation was changed by varying the speed of the D. C. motor with an appropriate gear ratio was selected for required torque.

2.2.5 Copper sphere

Three copper spheres 1.0, 1.4 and 2.0 cm in diameters were used for the heat transfer studies. Precision copper spheres (99.9 % purity) used in this study were obtained from Industrial Tectonics Inc., Dextor, MI. Copper was selected because of its high thermal conductivity, availability and its low cost. A small thermocouple wire (copper-constantan, 0.254 mm wire diameter) was passed through a long hollow steel tube having a 1.7 mm outside diameter and were soldered into a 0.6 mm hole extending all the way to the center of the copper sphere. The soldering procedure adopted here was one in which, an extremely small amount of silver solder was inserted into the hole of the copper sphere. Then the sphere was heated from the outside with a propane torch and as soon as the soldered appeared to have melted, the clean thermocouple bead was inserted inside the hole and very quickly the copper sphere along with the thermocouple wire was quenched in a water bath. The continuity of the thermocouple connection was checked by a multimeter. During

the experiments, frequent breakage of the thermocouple wire would occur because of fatigue. In this case, the soldering process was repeated using a clean hole and new clean thermocouple. The copper sphere was insulated but held rigidly to the end of the steel tube using epoxy.

2.2.6 Fluidized bed material

Glass microbeads (density=2.5 gms/cc, conductivity=0.0025 cal/sec/sq. cm, specific heat= 0.27 cal/gm/°C) were used as the fluidized bed material obtained from the Microbead Division of Cataphote Corporation, Jackson, Mississippi. These glass particles were sized by sieving with a mechanical shaker in three size groups; 5-44, 126-147 and 355-420 μm. This size range was also examined by taking the photographs of these glass particles as shown in Figures 2.6, 2.7, 2.8. From the measurement of the size of the glass particle in the photograph and knowing the magnification factor, the actual size of the glass particles were determined. The size range obtained this way was very close to the size range determined from sieving.

2.2.7 Data acquisition system

A computer controlled data acquisition system was designed and developed for this experimental work. It consisted of PRO 380 computer, an LA50 printer, an analog to digital module (Digital Corporation), a digital multimeter (Hewlett-Packard) and a reference junction compensator (Omega) as shown in Figure 2.9. In a somewhat different setting thermocouple readings were recorded directly by the ADM unit alone without a digital voltmeter using a modified interactive analog

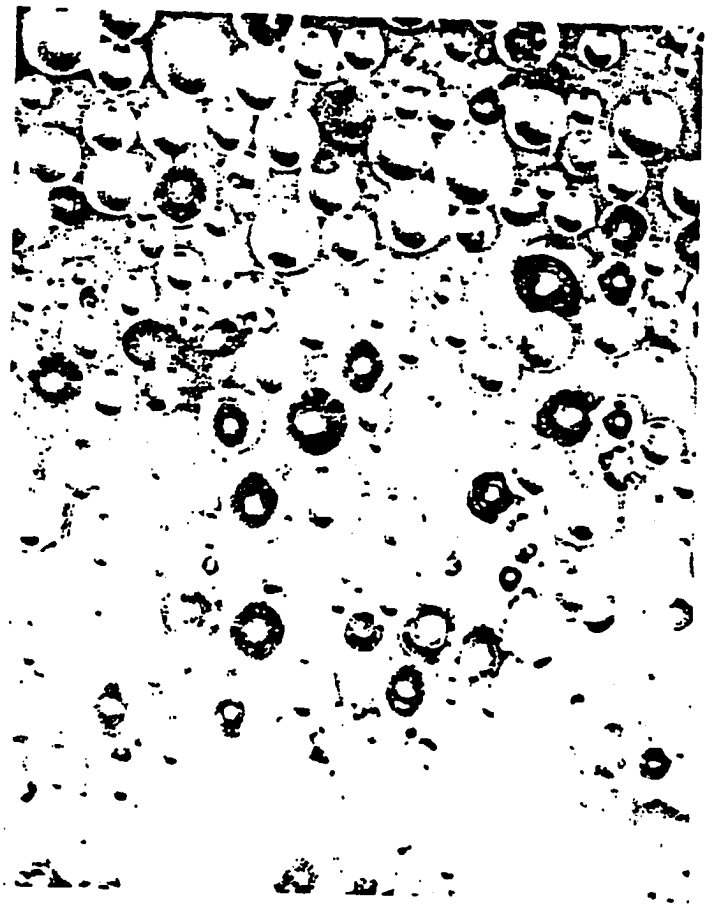

Figure 2.6: Photograph of 5-44 μm glass particles, magnification factor=320

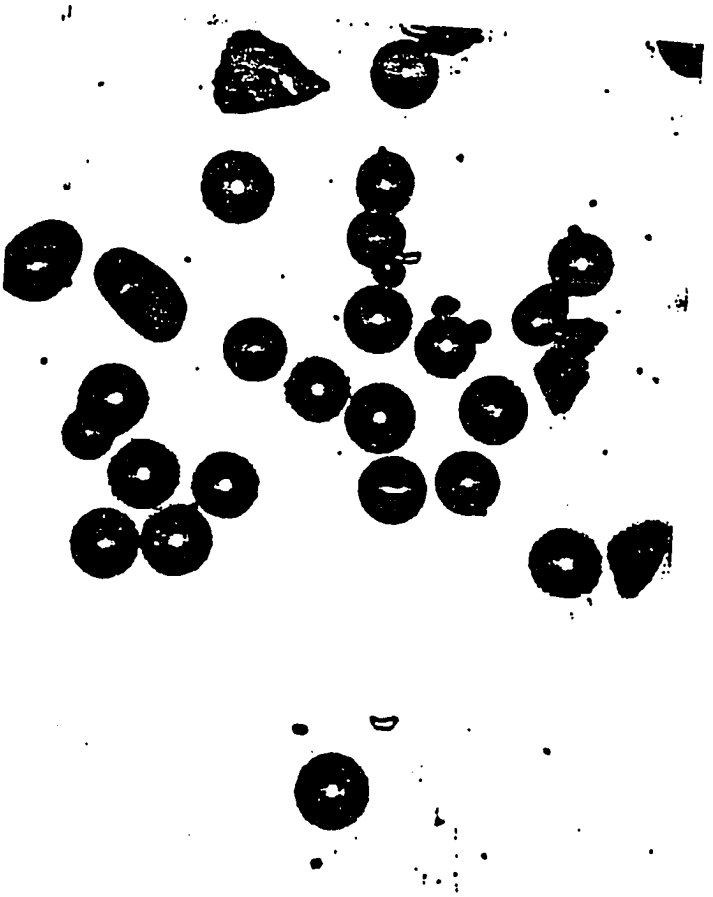

Figure 2.7: Photograph of 126-147 μm glass particles, magnification factor=64

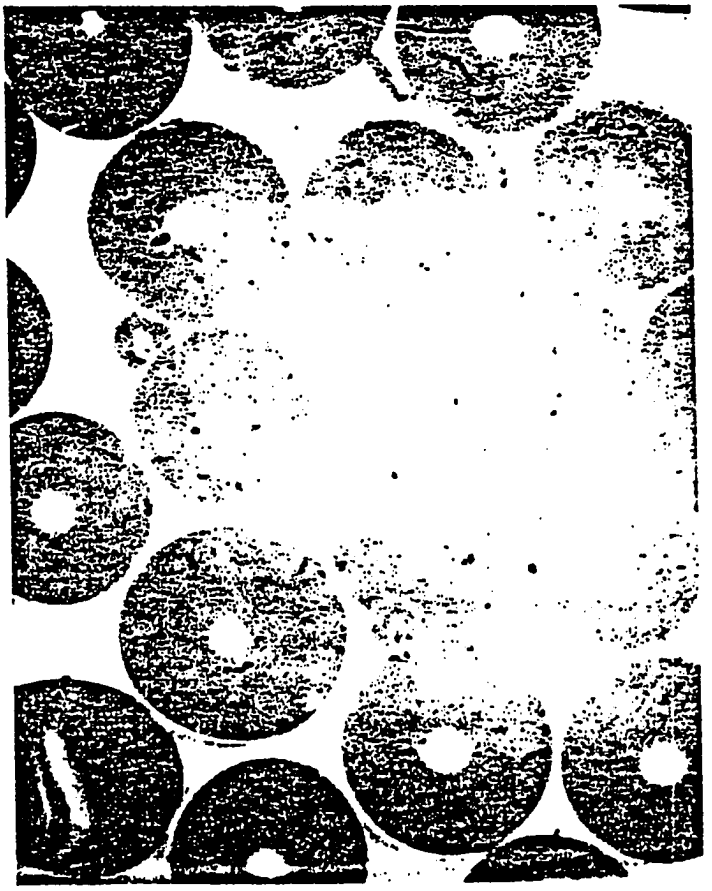

Figure 2.8: Photograph of 355-420 μm glass particles, magnification factor=64

data module (IADM) program written in FORTRAN 77. This setup allowed high rates of data acquisition (up to 500 readings/second). However, at this rate and without using any integrating circuit for filtering the signal, the main signal was affected by noise. Though this noise did not seem to affect the final result in terms of the heat transfer coefficient, a digital voltmeter was connected to the IEEE bus bar of the ADM unit and new software was developed to link the communication network between the PRO 380 computer and the HP digital voltmeter. The HP voltmeter was set up in such a way that it integrated the signal for about ten power cycles. In this way, the noise in the original signal was eliminated. However, the data recording rate was reduced to 3 to 4 temperature readings per second. This rate was deemed to be adequate for this study.

2.3 Experimental Procedure

In a typical experimental run, the height of the packed bed was kept at about 24 cm. The bed was fluidized by passing air at a specified superficial air velocity and the rotameter reading for the pressure of the air entering the rotameter, the pressure drop across the bed and the height of the fluidized bed were measured and were entered into the interactive computer program developed for data acquisition. Next the copper sphere was preheated to approximately 180-200 $^{\circ}C$ in the electrically heated heater cup filled with glass particles. The heating cup was manually removed and the D.C. motor driving the linear mechanism was started. For a stationary sphere experiment, the motor was shut down when the sphere reached a predetermined height of about 10 cm above the distributor plate. This height

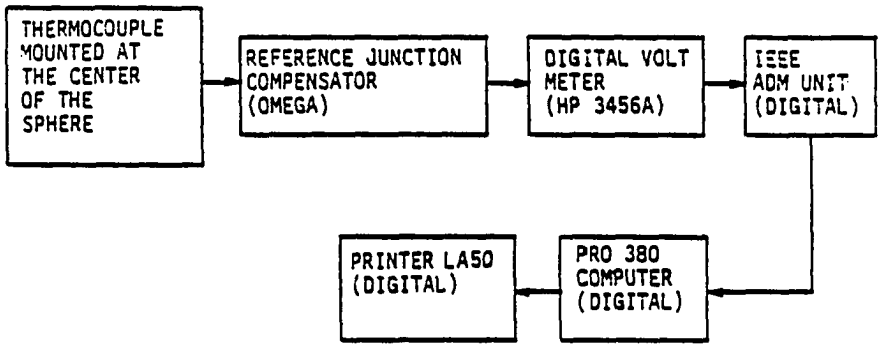

Figure 2.9: Computer controlled data acquisition system

corresponded to about half the bed depth of 24 cm. At this point, the data acquisition system was started quickly. The software program was set to stop the data acquisition as soon as the sphere temperature reaches to about 40 $^{\circ}$ C. The initial temperature of the sphere was always about 150 $^{\circ}C$. This was achieved in some cases by heating the sphere to a higher temperature. In the case of the initial temperature at the time of the start of a test the data acquisition system was higher than 150 $^{\circ}C$. The computer program was set to analyze data only at a temperature close to the specified value. All raw data in terms of thermocouple output voltage, including the rotameter reading, rotameter number, the pressure drop across the bed, the pressure at the outlet of the rotameter, the fluidized bed height, the packed bed height and the fluidized bed temperature were stored in a data file.

A computer program was written to reduce these data into an average heat transfer coefficient. The heat transfer experiment was repeated for various superficial velocities, three copper sphere diameters, and three glass particle sizes. Typically three to four runs were carried out for a constant superficial air velocity, to study the repeatability of the experiment. In some cases if the difference in average heat transfer coefficient was found to be greater than 15 to 20 % then five to six runs were made to improve the average value of the heat transfer coefficient obtained. In all of the heat transfer to a stationary sphere experiment about 600 runs were made. The average heat transfer coefficients for each set of runs were stored subsequently in the computer.

2.3.1 Linearly downward moving sphere

The mechanism shown in Figure 2.4 was used to move a sphere in a linearly downward direction. The data acquisition program was started and all required information such as: the sphere size, linear velocity, superficial air velocity, pressure drop across the bed, pressure at the rotameter outlet, bed temperature, and glass particle size were entered in to the computer. As in the case of the stationary sphere experiments, the copper sphere was preheated. The supporting steel rod was adjusted in such a way that the copper sphere was placed just above the fluidized bed surface. At this point the electric motor was turned on and as soon as the sphere was immersed fully into the fluidized bed the data acquisition system was turned on by simply pressing the return key on the key pad of PRO 380 computer. The temperature at the center of the copper sphere was recorded at the rate of three to four readings per second automatically over a preset time fed into the computer depending upon the linear velocity of the moving copper sphere. This time was predetermined in such a way that the sphere could traverse a constant distance of about 22 cm inside the fluidized bed. The time over which the sphere was in motion (similar to the data acquisition time) varied from about 3 seconds for the sphere moving at 7.5 cm/s to about 35 seconds for the sphere moving at 0.4 cm/s. Table 2.1 lists all the variables used in heat transfer experiments for the linearly downward moving sphere. For each linear velocity and superficial air velocity, typically three to four runs were made for a particular sphere and glass particle size. In all about 3000 runs for the linearly downward moving sphere case were made. The average heat transfer coefficients for each set of runs was recorded.

Table 2.1: List of variables used in the study of heat transfer from a linearly downward moving sphere

sphere diameter cm	1.0	1.4	2.0			
Glass particle size μm	5-44	126-147	355-420			
Range of superficial air velocity for 5-44 μm glass particles, cm/s	0.04	to	2.2			
Range of superficial air velocity for 126-147 μm glass particles, cm/s	1.58	to	18.5			
Range of superficial air velocity for 355-420 μm glass particles, cm/s	11.5	to	35.8			
Linearly downward velocity of sphere cm/s	0.4	1.1	1.9	3.0	4.6	7.5

2.3.2 Oscillating sphere

A mechanism shown in Figure 2.6 was used to oscillate the copper sphere inside the fluidized bed of glass particles. The preheated sphere was dropped quickly into the fluidized bed and adjusted (by tightening a set screw on the steel tube) to oscillate at about 10 cm above the distributor plate. This corresponded to about half the bed height. At this time the electric motor and the data acquisition system was started simultaneously. The sphere was adjusted to oscillate at a particular frequency and amplitude. The temperature history of the copper sphere was recorded until the temperature dropped to about 40 $^{\circ}C$ from its initial temperature of about 150 $^{\circ}C$. As explained previously the initial temperature of the copper sphere was adjusted to this value by trial and error. The frequency of the oscillation was varied from 1.1 to 2.85 Hz by varying the speed of the D.C motor. The amplitudes of the oscillation were varied from 6.9 cm to 1.8 cm by adjusting the position of the connecting rod inside a radial slot in the aluminum wheel. As in all the previous cases, about three to four runs were taken for the same conditions in order to study the repeatability of the experiment. Table 2.2 lists all of the variables used. About 3200 runs of heat transfer from an oscillating sphere were made. The average heat transfer coefficient for each set of runs was recorded.

2.4 Method of Evaluation of Average Heat Transfer Coefficient

In all the experiments, the Biot number of the heated spheres were kept sufficiently small so that the lumped heat capacity method was valid [Incropera and DeWitt, 1981]. Biot number can be defined as,

Table 2.2: List of variables used in the study of heat transfer from an oscillating sphere

Sphere diameter cm	1.0	1.4	2.0
Glass particle size μm	5-44	126-147	355-420
Range of superficial air velocity for 5-44 μm glass particles, cm/s	0.08	to	2.2
Range of superficial air velocity for 126-147 μm glass particles, cm/s	1.58	to	14.8
Range of superficial air velocity for 355-420 μm glass particles, cm/s	11.5	to	35.8
Peak-to-peak amplitude, cm	1.8	4.0	6.9
Frequency Hz	1.1	2.0	2.85

Table 2.3: Maximum Biot number and response time for immersed copper sphere-fluidized bed system

	Diameter, cm	h_{max}, w/m^2 K	Biot no.	τ_c
Copper sphere	1.0	~ 900	0.0039	6.4
Copper sphere	1.4	~ 800	0.0048	10.0
Copper sphere	2.0	~ 800	0.0069	14.3

$$Bi = \frac{hL_{ch}}{K_{cu}} \tag{2.1}$$

where for spheres,

$$L_{ch} = \frac{D_{sph}}{6} \tag{2.2}$$

As summarized in Table 2.3 the worst case Biot number corresponded to the maximum heat transfer coefficient and the largest size copper sphere tested was found to be less than 0.007. Table 2.3 also shows the calculated values of characteristic response time of the sphere-bed system.

$$\tau_c = \frac{\rho_{sph} C_{sph} V}{A_{sph} h} \tag{2.3}$$

This time constant is an indicator of the time of cooling required in a given run. For example, during the time corresponding to one time constant the copper sphere cools down to about 63.2 %. Since the Biot number is much less the 0.1, the internal resistance within the copper sphere can be safely neglected. An energy balance on the hot copper sphere immersed into the fluidized bed can be given as:

$$\rho_{sph} C_{sph} V \frac{dT}{dt} = h_t A_{sph} (T_b - T) \tag{2.4}$$

where, for the sphere,

$$\frac{V}{A_{sph}} = \frac{D_{sph}}{6} \tag{2.5}$$

A linear relationship was used for the heat capacity of the copper sphere.

$$C_{sph} = a + bT \tag{2.6}$$

where, for copper,

$$a = 351.2 J/KgK$$

$$b = 0.1085 J/KgK^2 (Valid\ for\ 27 - 327^{\circ}C)$$

Solution of equation 2.4 with the linear relationship for the heat capacity of the copper (equation 2.6) may be written as,

$$(a + bT_b)\left(ln\{\frac{(T_b - T)}{(T_b - T_0)}\}\right) + b(T - T_0) = -\left(\frac{h_t A_{sph}}{\rho_{sph} V}\right) t \qquad (2.7)$$

Equation 2.7 enables the determination of the total heat transfer coefficient h_t, averaged over time and sphere surface area from the slope of a plot of the left hand side of the above equation versus time. A regression fit was used in the computer program for the best slope. Correlation coefficients for the regression analysis were found typically to be 0.99 or greater.

The total heat transfer coefficient h_t was interpreted here to be that due to fluidized bed convection heat transfer coefficient h (particle convection and gas convection) and radiation heat transfer coefficient, h_r.

$$h = h_t - h_r \qquad (2.8)$$

where,

$$h_r = \sigma \epsilon_{sph} (T_0^2 - T_b^2)(T_0 + T_b) \qquad (2.9)$$

Example values for total heat transfer coefficient h_t and radiation heat transfer coefficient h_r are 245 W/m^2 K and 0.869 W/m^2 K, respectively. Here T_0 is the initial temperature of the sphere. It is assumed that the sphere is radiating to a

large black cavity. Thus the radiation heat transfer coefficient h_r considers the maximum possible radiation. In all experimental conditions the initial temperature range was low enough (about 160 to 140 $^{\circ}C$) so that radiation was negligible.

A typical thermocouple output voltage versus time is shown in Figure 2.10 for a stationary 2.0 cm diameter sphere during cooling in a bed of 355-420 μm glass particles at a superficial velocity of 15 cm/s. The superficial air velocity is just above the incipient fluidization. Figure 2.11 shows the cooling trace for the same sphere at the same conditions moving linearly downward through the bed at a speed of 3.0 cm/s.

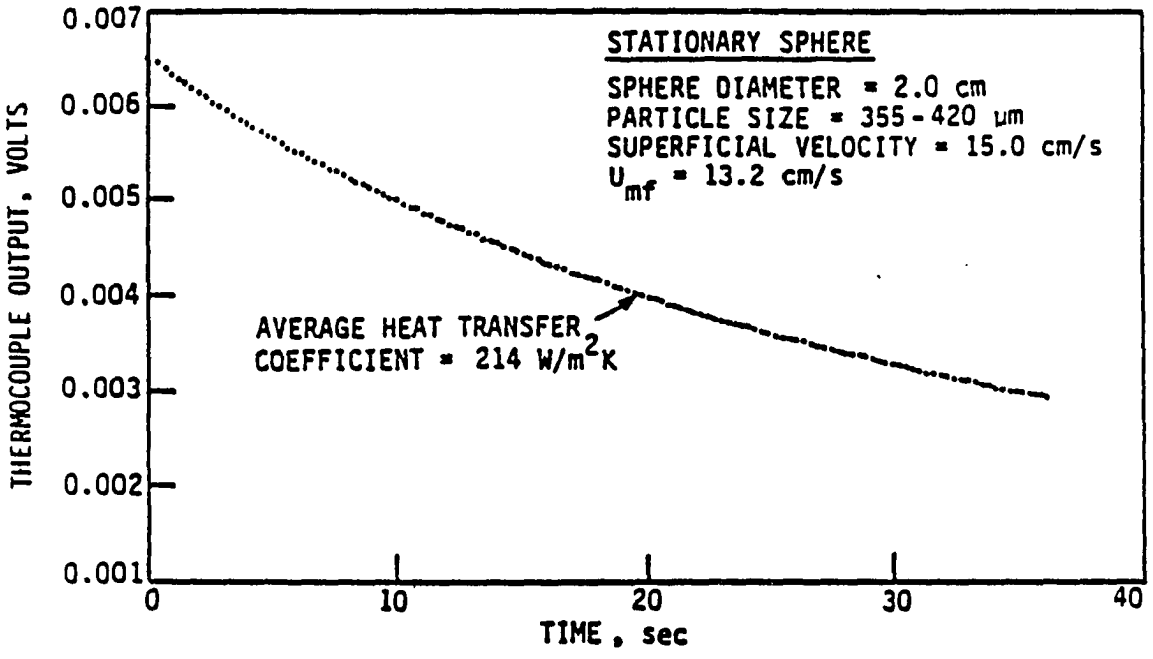

Figure 2.10: Typical thermocouple output versus time for 2 cm diameter stationary sphere

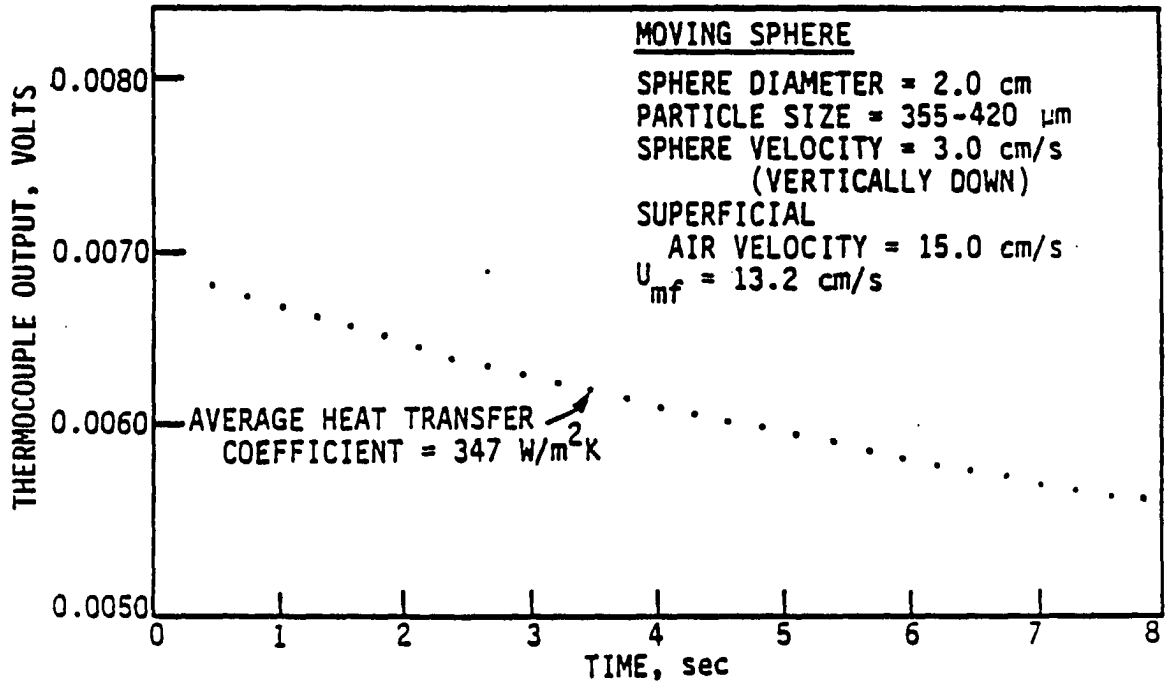

Figure 2.11: Typical thermocouple output versus time for 2 cm diameter linearly downward moving sphere at 3.0 cm/s

3 RESULTS AND DISCUSSION

The experimental results for heat transfer from stationary, linearly downward moving and oscillating spheres are presented in this Chapter. The pressure drop across the bed was used to calculate the minimum fluidization velocity for each glass particle size. A detailed tabulation of these experimental data is presented in the Appendix.

3.1 Minimum Fluidization Velocity and Classification of Glass Powder

The pressure drop across the fluidized bed was measured as a function of the superficial air velocity for each glass particle size. The minimum fluidization velocity was determined experimentally using the pressure drop data as shown in Figures 3.1, 3.2 and 3.3. At the minimum fluidization condition, as stated in Chapter 1, the force balance on the bed is;

$$(Drag\ force\ by\ upward\ moving\ gas) = (Weight\ of\ particles\ ) \qquad (3.1)$$

The pressure drop across the bed at minimum fluidization condition can be given as:

$$\frac{\Delta p}{L_{mf}} = (1 - \epsilon_{mf})(\rho_p - \rho_g)g \qquad (3.2)$$

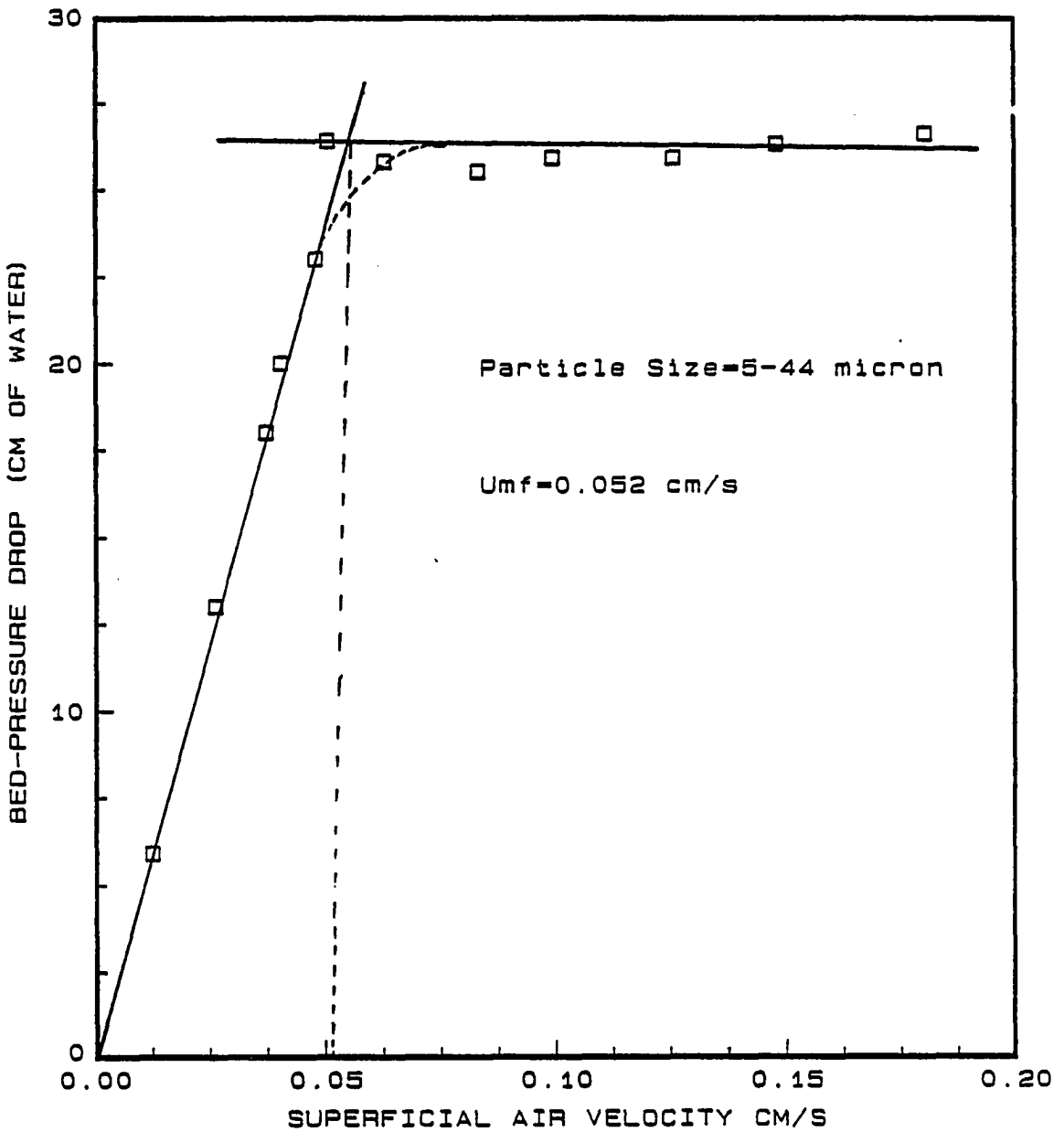

Figure 3.1: Bed-pressure drop vs. superficial air velocity for 5-44 μm glass particles

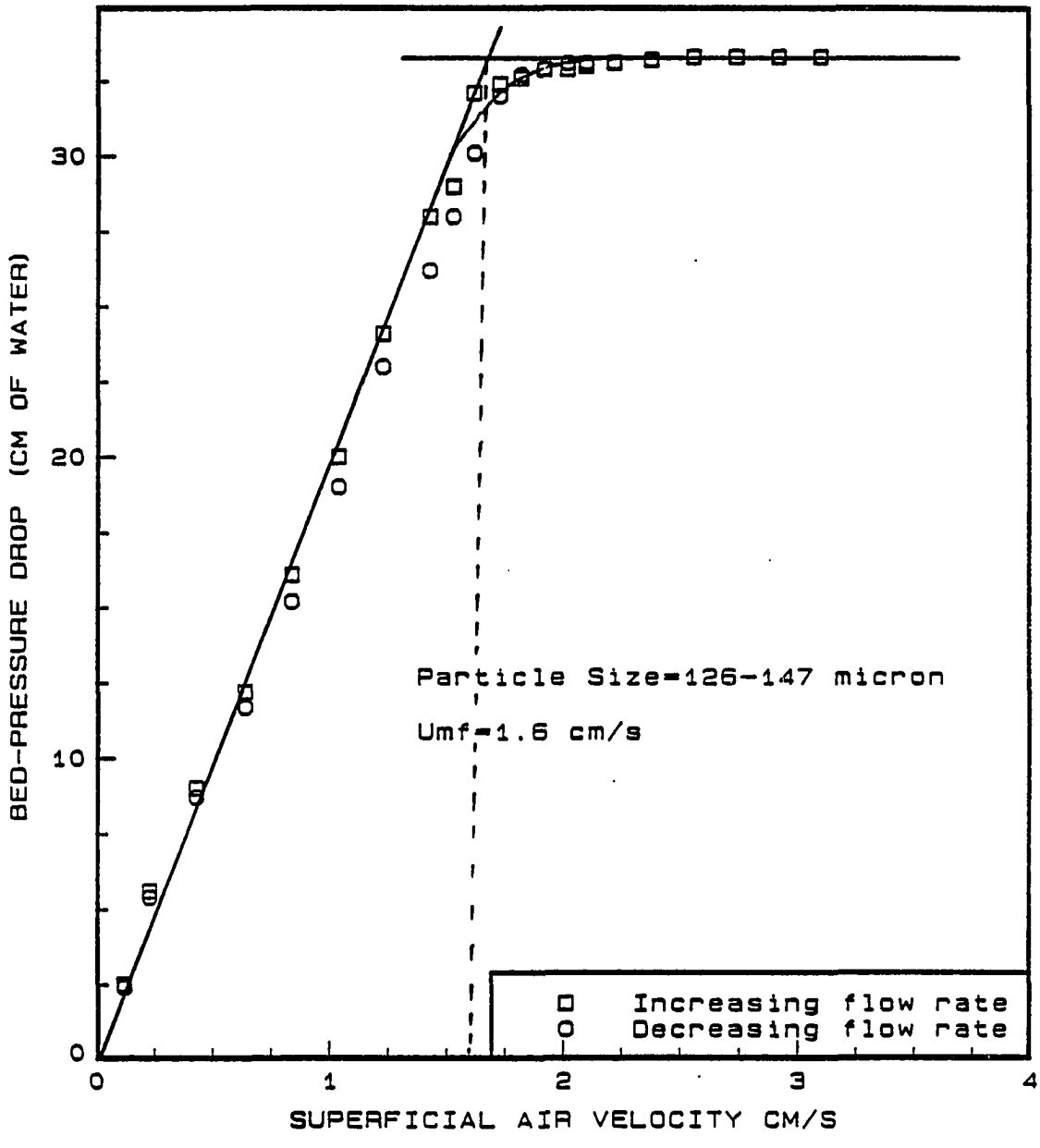

Figure 3.2: Bed-pressure drop vs. superficial air velocity for 126-147 μm glass particles

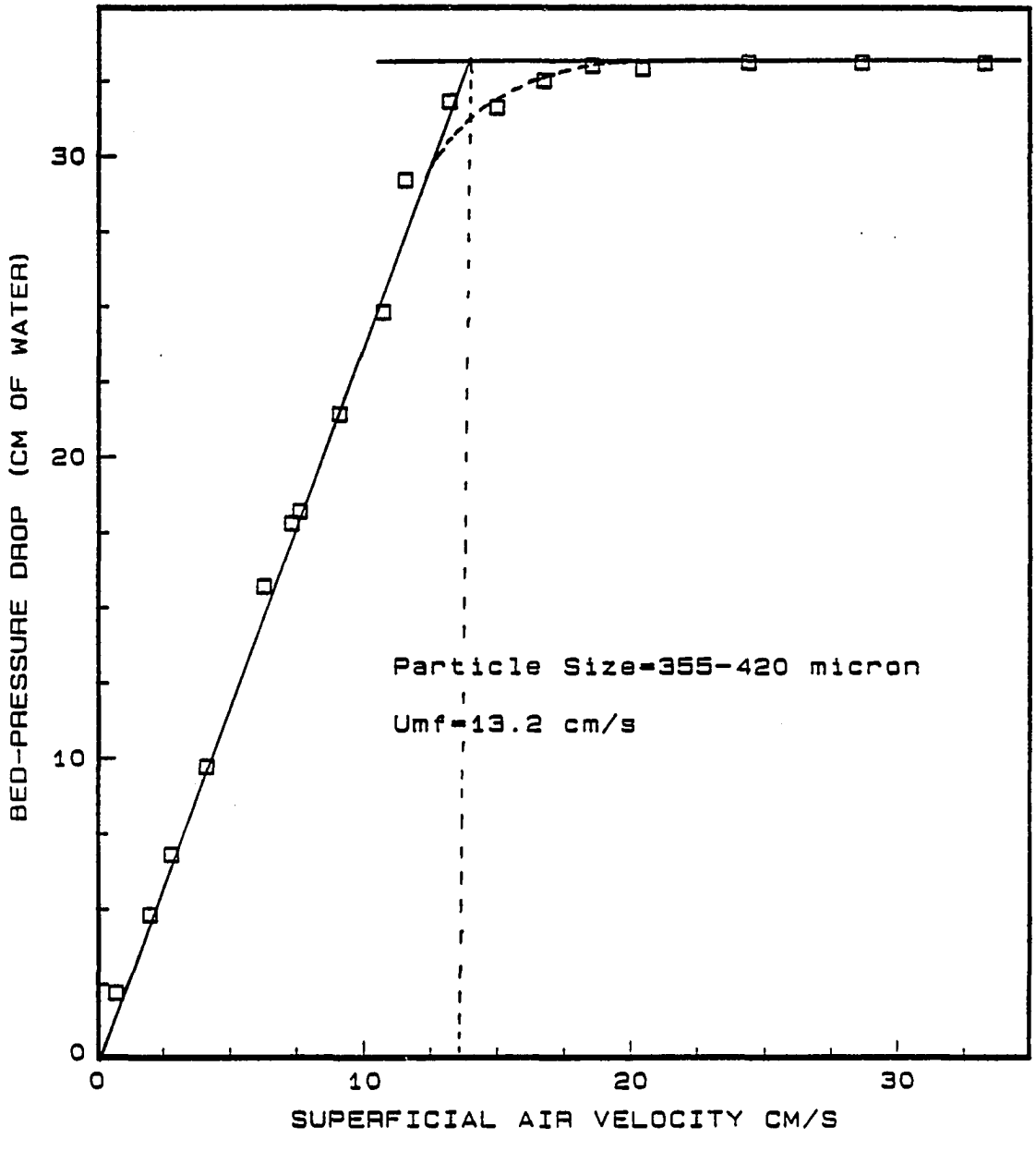

Figure 3.3: Bed-pressure drop vs. superficial air velocity for 355-420 μm glass particles

The experimental correlation for the pressure drop through packed beds of uniformly sized solids was obtained by Ergun [1952] as,

$$\frac{\Delta p}{L} = 150\frac{(1-\epsilon)^2}{\epsilon^3}\frac{\mu_g U}{(\phi_s d_p)^2} + 1.75\frac{1-\epsilon}{\epsilon^3}\rho_g U^2 \phi_s d_p \tag{3.3}$$

The first term in the above equation represents the pressure drop due to viscous energy loss while the second term is the loss from kinetic energy. The expression for the minimum fluidization velocity can be obtained by combining equations 3.2 and 3.3. Furthermore, it was found experimentally [Kunii and Levenspiel, 1969] that for a wide variety of systems $1/\phi_s \epsilon_{mf}^3 \approx 14$ and $(1-\epsilon_{mf})/\phi_s^2 \epsilon_{mf}^3 \approx 11$. Using this result, the expression for minimum fluidization velocity reduces to,

$$U_{mf} = \frac{d_p^2(\rho_p - \rho_g)g}{1650\mu_g} \quad for \quad Re_p < 20 \tag{3.4}$$

and

$$U_{mf}^2 = \frac{d_p(\rho_p - \rho_g)g}{24.5\rho_g} \quad for \quad Re_p > 1000 \tag{3.5}$$

The Reynolds number based on the particle diameter was found to be much less than 20 for all three glass particle sizes used in the present study. Hence equation 3.5 was used to calculate the minimum fluidization velocities. The terminal velocity of the glass particles can be estimated by force balance on a single particle under steady state condition,

$$U_t = \left(\frac{4d_p(\rho_p - \rho_g)g}{3C_D\rho_g}\right)^{\frac{1}{2}} \tag{3.6}$$

Using the values of the drag coefficients according to the Reynolds number range, the expression for the terminal velocity can be given as,

$$C_D = \frac{24}{Re_p} \quad Re_p < 0.4, \quad U_t = \frac{g(\rho_p - \rho_g)d_p^2}{18\mu_g} \tag{3.7}$$

$$C_D = \frac{10}{\sqrt{Re_p}} \quad 0.4 < Re_p < 500 \quad U_t = \left(\frac{4g^2(\rho_p - \rho_g)^2}{225\rho_g\mu_g} \right)^{\frac{1}{2}} d_p \qquad (3.8)$$

Table 3.1 lists the maximum particle Reynolds number, the minimum fluidization velocity as obtained from equation 3.5 and from the experiment, and the terminal velocity for each glass particle size.

As shown in Table 3.1, the difference between the minimum fluidization velocity as obtained from the equation 3.5 and by experiment is about 20 %. Considering the fact that equation 3.5 utilizes two empirical correlations namely, from Ergun [1952] and Wen and Yu [1966], this discrepancy in the results is acceptable.

The hydrodynamic behavior of a fluidized bed depends on the properties of the powder used. The powders have been classified in four groups: C , A, B and D in the order of increasing particle size [Geldart, 1986]. Group C powders are very cohesive and normal fluidization is very difficult. Channeling occurs because the inter-particle forces are greater than the drag force of the fluid exerted on the particles. Generally particles less than 20 μm exhibits such behavior. The pressure drop across the bed is lower than the theoretical value (bed-weight per unit cross-sectional area). The heat transfer between a surface to fluidized bed is much poorer than with group A and group B powders because of poor particle mixing. Group A powders are characterized by considerable expansion of the bed between minimum fluidizing velocity U_{mf}, and minimum bubbling velocity U_{mb}. These powders are slightly cohesive. A further increase in the superficial velocity beyond U_{mb}, increases the size and the number of bubbles. Small number of bubbles produce rapid particle mixing and the surface of the bed resembles a boiling liquid. In

Table 3.1: Maximum particle Reynolds number, minimum fluidization and terminal velocity for each glass particle-air system

Glass Particle size, μm	Maximum Reynolds number based on maximum U	Terminal Velocity cm/s	Reynolds number based on terminal velocity cm/s	Minimum Fluidization Velocity from experiment cm/s	Minimum Fluidization Velocity from equation 3.5 cm/s
5-44	0.029	3.96	0.061	0.052	0.043
126-147	1.103	105.2	9.02	1.6	1.34
355-420	7.52	300.0	7.30	13.2	10.85

contrast to group A powders, group B powders have negligible inter-particle forces and formation of bubbles starts at or slightly above minimum fluidization velocity. Bed expansion is small and the bed collapses very rapidly when the gas supply is cut off. There is little powder circulation in the absence of bubbles and bubbles burst at the surface of the bed as discrete entities. Also most bubbles rise more quickly than the interstitial gas velocity and bubble size increases with both bed height and excess gas velocity $U - U_{mf}$. Group D powders are coarse and/or dense. All but the largest bubbles rise more slowly than the interstitial fluidizing gas so that the gas flows into the base of the bubble and out of the top, providing the mode of gas-exchange and by-passing which is different from the group A or group B powders. A quantitative description of these properties of the powders belonging to these groups is given in Table 3.2 [Geldart,'1986]. Recently A new class of powder belonging to group named AC has been characterized [Geldart, 1986] by the absence of a meaningful incipient fluidization point and the absence of a contraction of the bed when bubbles first appear.

The three glass powders used in this experiment have been classified in these four groups. Using the Figure 3.4 [Geldart, 1986] for $\rho_p - \rho_g$=2500 kg/m^3, it is found that the glass particles in size range of 5-44 μm with a mean diameter of 24.5μm belongs to group of A powders. The glass particles ranging in size 126-147 μm and 355-420 μm with mean diameters of 136.5μm and 387.5μm respectively, belong to group B powders.

Although the 5-44 μm glass particles with a mean diameter of 24.5 μm falls in the range of group A powder. As shown in Figure 3.4, it is very close to the boundary

Table 3.2: Summary of group property [Geldart, 1986]

Increasing size and density →

Group		C	A	B	D
Most Obvious Characteristic		Cohesive, difficult to fluidize.	Bubble-free range of fludization	Starting bubbles at U mf	Coarse Solids
Property \ Typical solids		Flour Cement	Cracking catalyst	Building sand table salt	Crushed limestone coffee beans
1. Bed expansion		Low when bed channels, can be high when fluidized	High	Moderate	Low
2. Deaeration rate		Initially fast, exponential	Slow, linear	Fast	Fast
3. Bubble properties		No bubbles, channels, and cracks	Splitting, recoalescence predominate; maximum size exists; large wake	No limit on size	No known upper size; small wake
4. Solids mixing		Very low	High	Moderate	Low
5. Gas backmixing		Very low	High	Moderate	Low
6. Slug properties		Solid slugs	Axisymmetric	Axisymmetric asymmetric	Horizontal voids, solids slugs, wall slugs
7. Spouting		No	No except in very shallow beds	Shallow beds only	Yes, even in deep beds
Effect on properties 1 to 7 of:	Mean Particle size within group	Cohesiveness increases as dp decreases	Properties improve as size decreases.	Properties improve as size decreases	Not known
	Particle size distribution	Not known	Increasing less than 45 micron fraction improves properties	None	Increases segregation
	Increasing pressure, temperature, viscosity, density of gas	Probably Improves	Definitely improves	Uncertain, some possibly	Uncertain, some possibly

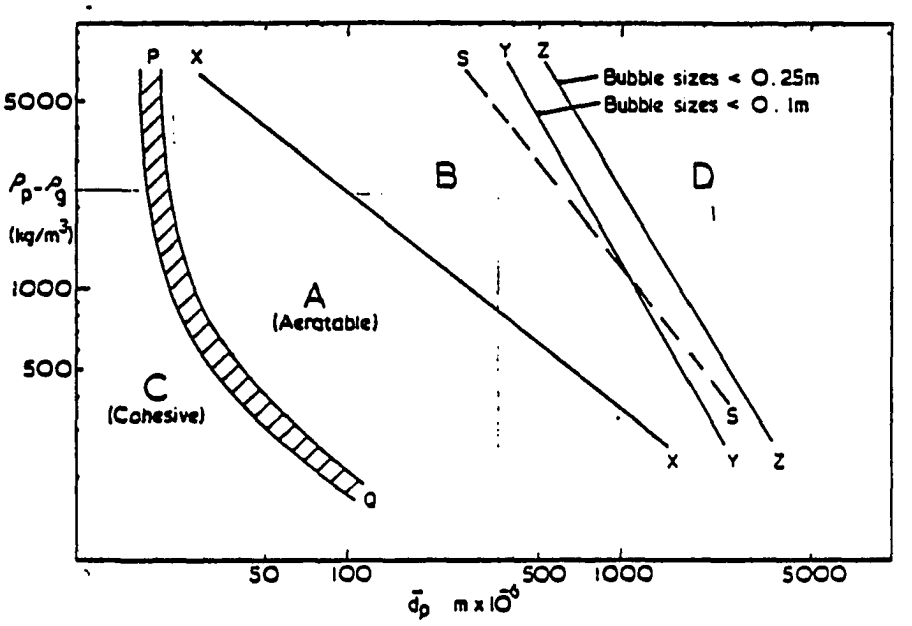

Figure 3.4: Diagram for powder classification into groups [Geldart, 1986]

of powder A and powder C. Moreover, a study of the fluidization characteristics of this powder revealed the presence of extensive channeling in the bed up to a superficial air velocity of 0.1 cm/s, then resembling more like C powder. At higher superficial velocities, this powder showed reasonably good fluidization behavior as a group A powder.

The remaining two powders sizes of 126-147 and 355-420 μm, clearly behaves as group B powders. As expected for this group, bubbling starts very close to the minimum fluidization condition.

3.2 Stationary Sphere

Experimental investigation was carried out to study the effect of sphere size, superficial air velocity and glass particle size on the average heat transfer coefficient for a stationary sphere immersed in an air fluidized bed. All experiments were carried out with the copper sphere positioned at about 10 cm from the bottom of the bed. The experimental values of time averaged heat transfer coefficient h are plotted (Figures 3.5, 3.6 and 3.7) against the superficial air velocity for each sphere size and glass particle size. Most of the systems showed similar trends and their behavior could be characterized by the three zones, referring to Figures 3.6 and 3.7 for the fluidized bed of 126-147 μm and 355-420 μm glass particles.

1. In the first region where the superficial air velocity is less than that of minimum fluidization velocity, the bed behaves almost like a packed bed. The glass particles are not in motion with respect to the other particles or the immersed sphere. In this region, the heat transfer coefficient was found to

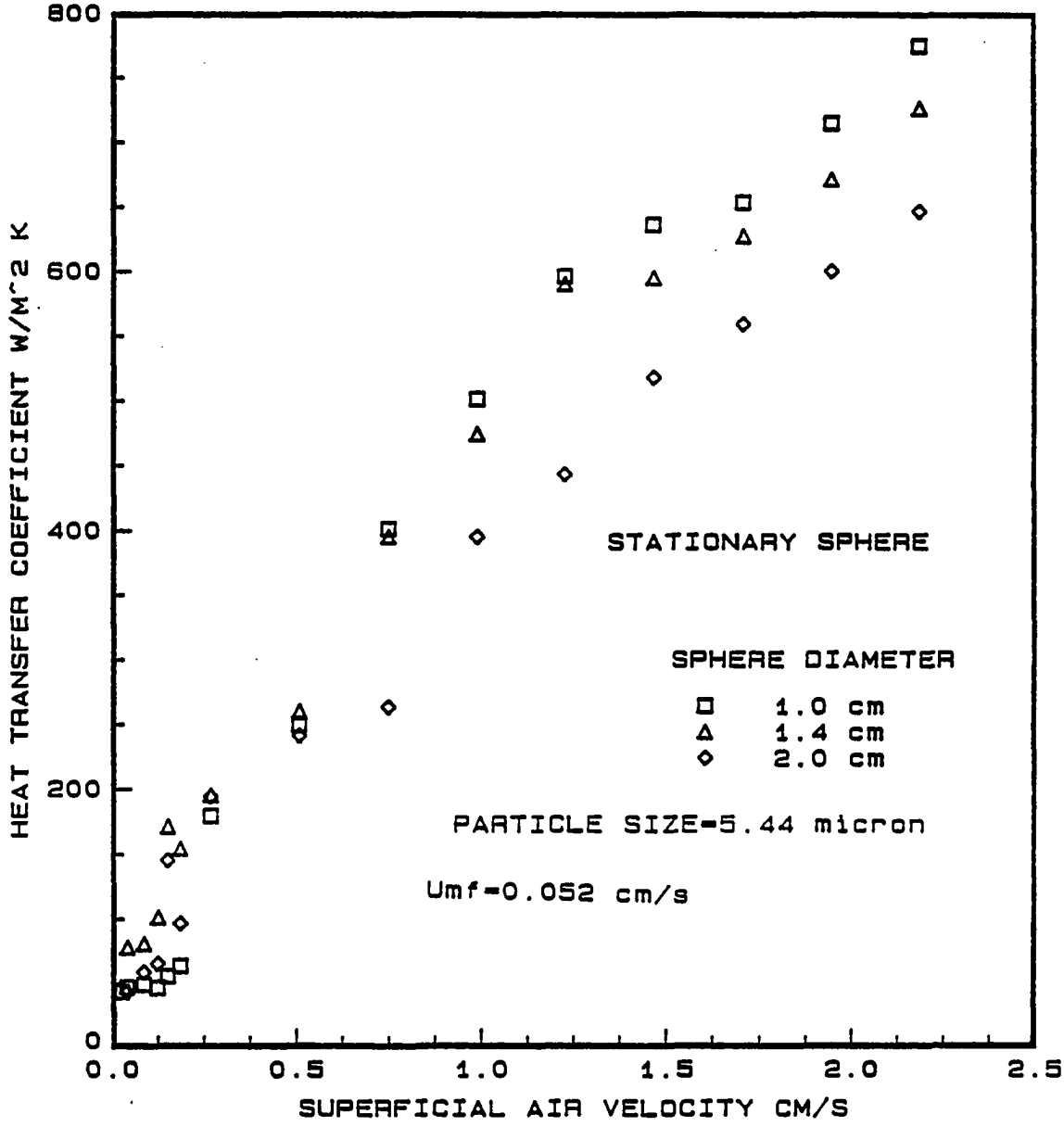

Figure 3.5: Heat transfer coefficient vs. superficial air velocity for 5-44 μm glass particles and various size copper spheres

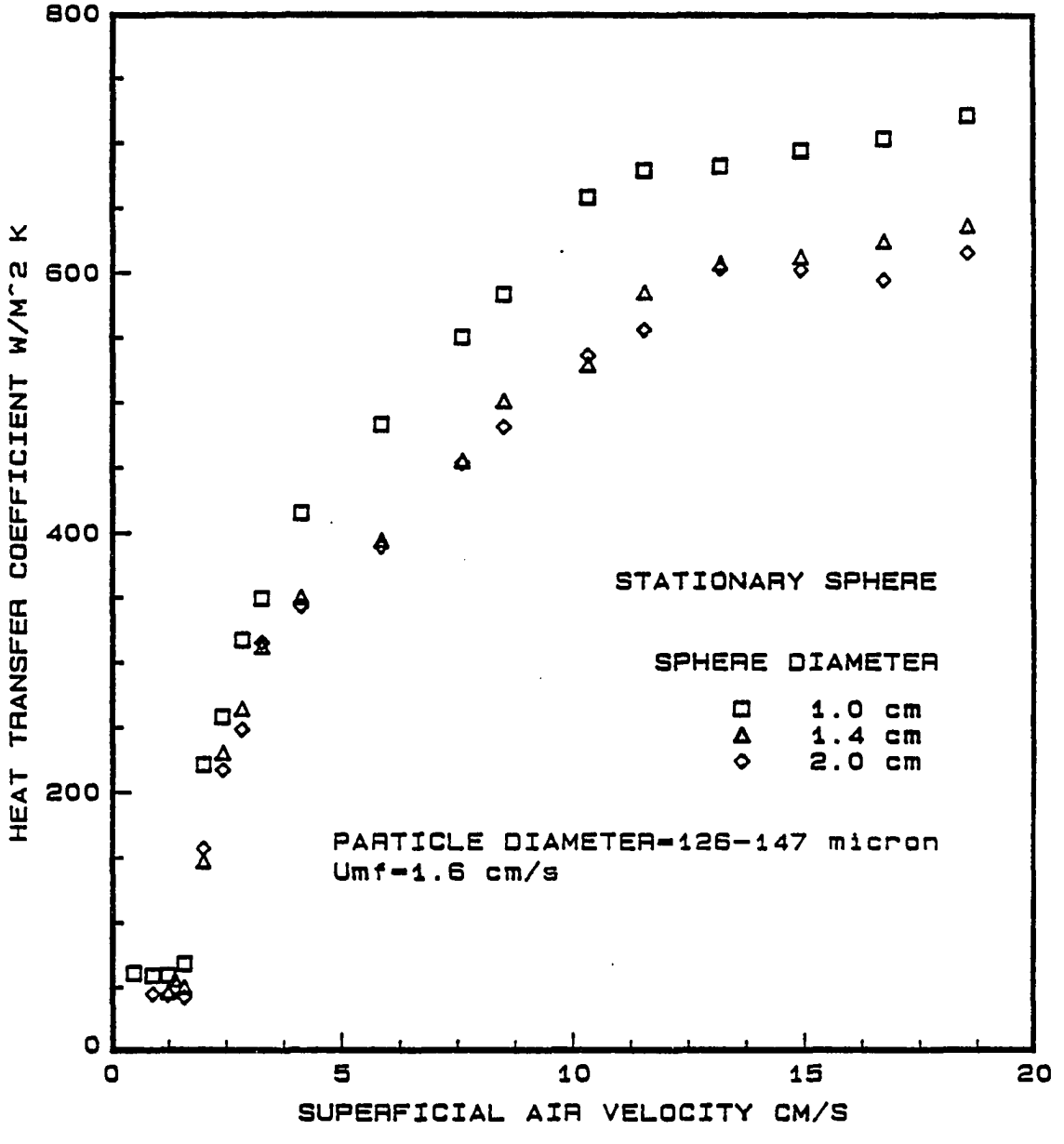

Figure 3.6: Heat transfer coefficient vs. superficial air velocity for 126-147 μm size glass particles and various size copper spheres

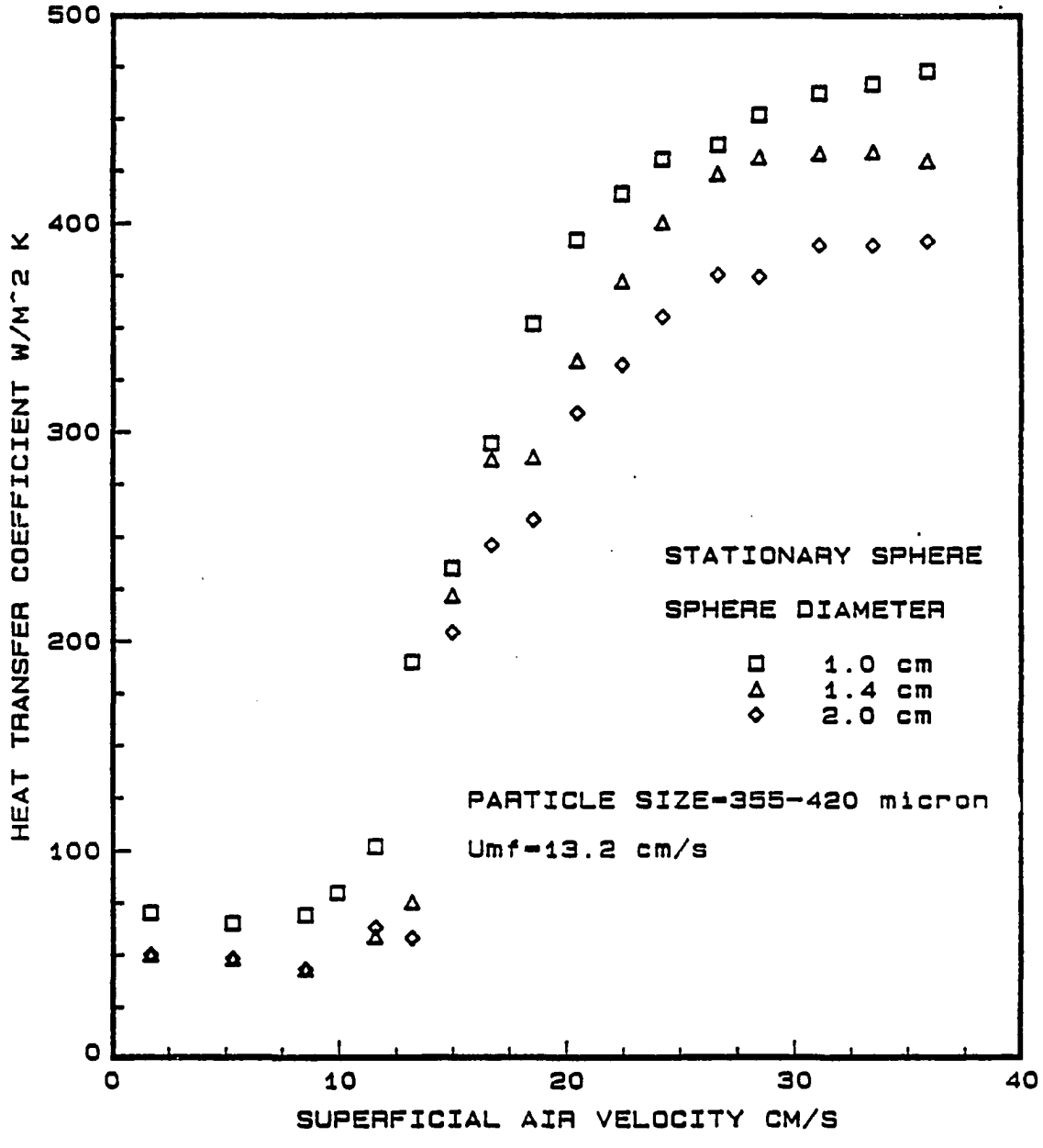

Figure 3.7: Heat transfer coefficient vs. superficial air velocity for 355-420 μm size glass particles and various size copper spheres

be very low as there is no circulation of the particulate phase. Although it seems that the heat transfer coefficient is almost constant, close examination of the numerical values revealed that the heat transfer coefficient decreased slightly as the superficial velocity increased until it reached the minimum fluidization velocity. This slight decrease in the heat transfer coefficient might be explained as follows: the expansion of the bed caused by the upward flowing air increases the void fraction and, thus, decreases the effective thermal conductivity of the bed in the region close to the heated copper sphere.

2. In the second region, where the ratio of superficial air velocity to the minimum fluidization velocity varies from 1 to 6 as in the case of 126-147 μm glass particles and from 1 to 2 for the case of 355-420 μm particles, the heat transfer coefficient rises very rapidly. The particle movement increases as small bubbles form within the bed. These small bubbles increase the circulation of the particulate phase near the sphere, decreasing the residence time of the emulsion packet.

3. At a higher superficial velocity, the heat transfer coefficient begins to level off. In this region, large bubbles appear in the bed and the bed behaves very close to a slugging bed as the bubble diameter grows to the same size as the column diameter of the fluidized bed. As the size of the bubble increases, the copper sphere is engulfed by more and more bubbles. During the time when the sphere is surrounded by a bubble, only gas phase heat transfer takes place. The resulting low thermal conductivity and heat capacity of the air phase, compared to the glass particles, reduces the overall heat transfer coefficient

even though the increased frequency of bubbles decreases the residence time of the emulsion packet.

The above trends explained in terms of three regions applies, more or less to all three sizes of the copper spheres and the glass particle sizes of 126-147 μm and 355-420 μm. For the smallest size glass particles tested (5-44 μm) the observed behavior is slightly different. For the ratio of U/U_{mf} up to about 2, the heat transfer coefficient is very low and remains almost constant as the inter-particle forces produce severe channeling while prevents smooth fluidization. This is followed by a gradual increase in the heat transfer coefficient up to the point when the superficial air velocity reaches about 0.7 cm/s. In this region small bubbles start to form in the bed giving rise to a local particulate circulation. As the superficial air velocity increases, the frequency and the size of the bubbles increases and the surface movement of the bed starts. At this point the heat transfer coefficient rises rapidly without a maximum or minimum. At about a superficial air velocity of 1.5 to 2.0 cm/s, attrition of small size glass particle starts and bursting of large bubbles near the upper surface causes vigorous bed movement. This increases the heat transfer coefficient continuously with superficial velocity as circulation of the particulate phase becomes very effective for this size of glass particles. At a superficial velocity close to or greater than that of the terminal velocity of the particles, leveling off or even a decrease in the heat transfer coefficient could be expected as the particulate phase becomes leaner.

Kharchenko and Makhorin [1964] reported maxima in the heat transfer coefficients when plotted versus superficial velocity, an effect that was more pronounced

with an increase in the bed temperature for a spherical alpha-calorimeter of 6 cm in diameter. The existence of a maximum heat transfer coefficient is well established trend particularly for internal objects such as plates, cylinders and heat transfer probes [Davidson and Harrison, 1971]. However, Yamazaki and Jimbo [1970] showed only a leveling off of the heat transfer curve with an increase in the superficial velocity for a 1.2 cm steel sphere immersed in a fluidized bed of limestone or molding sand tested over a variety of particle sizes and values of U/U_{mf} up to 45. Ziegler and Brazelton [1964] obtained almost constant heat transfer coefficients for the range of U/U_{mf} of 3 to 7 for a half inch clay-like sphere immersed in a fluidized bed of glass particles. Shirai et al.[1966] also showed that the heat transfer coefficient leveled off above the value of U/U_{mf}=10, for a 3 cm diameter sphere immersed in a fluidized bed of active carbon, alumina, silica gel and sand particles, having minimum fluidization velocities from 1.6 cm/s to 10.5 cm/s. More recently, similar trend was obtained by Pillai [1976] for spheres ranging in size from 5 to 15 mm in diameter and a fluidized bed of silica sand, zircon sand and silicon carbide at 550 $^{\circ}C$. The heat transfer coefficients were found to be almost constant above U/U_{mf}=3. This absence of a maximum heat transfer coefficient and subsequent decrease in heat transfer coefficient seems to be yet another trend as can be inferred from the four previous research works cited and the present study, particularly for the case of a spherical object immersed in an air fluidized bed.

The effect of diameter of the copper sphere on the average heat transfer coefficient is shown in Figures 3.5, 3.6 and 3.7 for various glass particle sizes. Figures 3.6 and 3.7 show clearly a decrease in the average heat transfer coefficient with increase

in the sphere diameter. This increase in heat transfer coefficient with decrease in sphere diameter is more predominant at superficial air velocities higher than that of minimum fluidization velocity. This decrease in heat transfer coefficient will be explained qualitatively. The residence time of an emulsion packet on any surface immersed in a fluidized bed can be defined as;

$$\tau = \frac{L_h}{u_p} \tag{3.9}$$

where l_h is the projected or equivalent length of heat transfer surface and u_{ep} is the relative velocity of the emulsion packet with respect to the heat transfer surface. For a smaller copper sphere, the emulsion packet has to travel less distance to cover the projected length of the sphere and hence the residence time of the packet is less. This increases the heat transfer coefficient for a small sphere as compared to a larger sphere. Shirai et al. [1966] showed that heat transfer coefficient decreases with an increase in sphere diameter varying from 0.45 to 5.0 cm in an air fluidized bed. Moreover, Prins et al. [1985] found that the mass transfer coefficient decreased with increasing test sample diameter up to a certain limit which was roughly characterized by a gas contact time of 25 microseconds. This gas contact time was defined as;

$$t_{cg} = \frac{\epsilon_{mf} D_{sph}}{U_{mf}} \tag{3.10}$$

At superficial velocities below that of minimum fluidization, the particulate phase circulation within the bed is almost absent, making the residence time of the emulsion packet very large. Hence, in this region the effect of sphere diameter is not prominent as can be seen from the Figures 3.5, 3.6 and 3.7. Furthermore, from Figure 3.5, it is evident that this normal trend of decreasing the heat transfer co-

efficient with increasing sphere diameter is not observed in the lower superficial air velocity region.

The effect of the mean powder size of the bed particles can be seen in Figures 3.8, 3.9 and 3.10 for various sizes of the copper spheres. In general the average heat transfer coefficient is higher for smaller size particles. The increase is a result of the higher mobility of the smaller size particles which in turn reduces the residence time of the emulsion packet. Furthermore, decreasing the particle diameter causes an increase in the heat transfer coefficient due to the reduction in the gas film between the body and the aggregates of particles. In a fluidized bed the heat transfer is viewed in terms of two resistances in series, a) a contact resistance R_c due to an increase in voidage near the heat transfer surface and b) the resistance inside the emulsion packet itself. For large particles the contact resistance becomes the controlling factor and heat transfer mainly occurs through a gas film. Hence, the heat transfer coefficient decreases with an increase in the glass particle diameter. This effect has also been observed by Kharchenko and Makhorin [1964], Richardson and Shakiri [1979], Yamazaki and Jimbo [1970] and Kunii and Levenspiel [1969].

The scatter in the heat transfer coefficients are shown in Figure 3.11. The spread is comparatively larger near the minimum fluidization condition. This plot clearly emphasizes the difficulties in obtaining reproducible heat transfer data in fluidized bed studies. This scatter in the heat transfer coefficients which is rarely reported in the literature is mainly due to dynamic conditions of the fluidized bed.

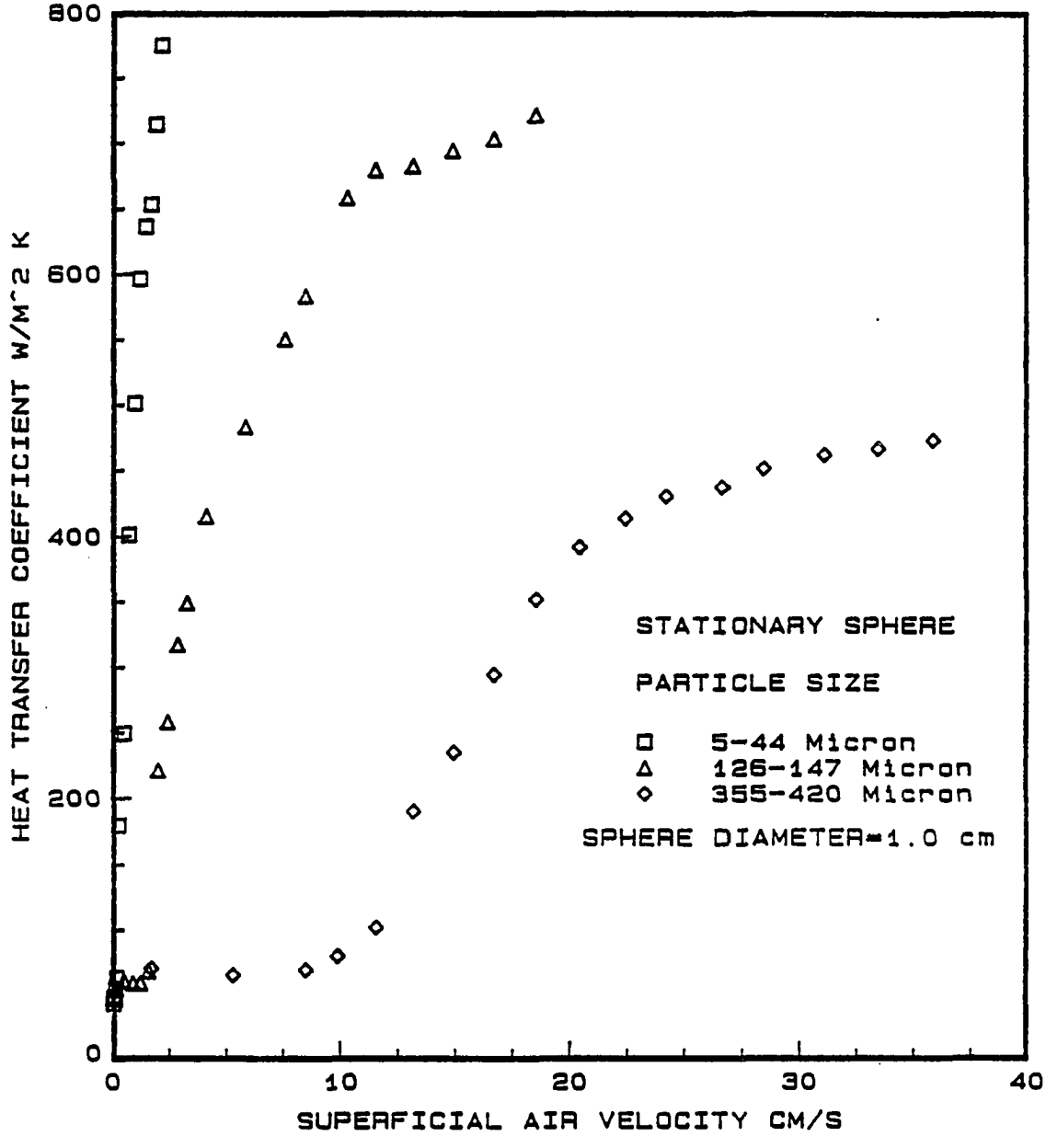

Figure 3.8: Heat transfer coefficient vs. superficial air velocity for a copper sphere diameter of 1.0 cm and various size glass particles

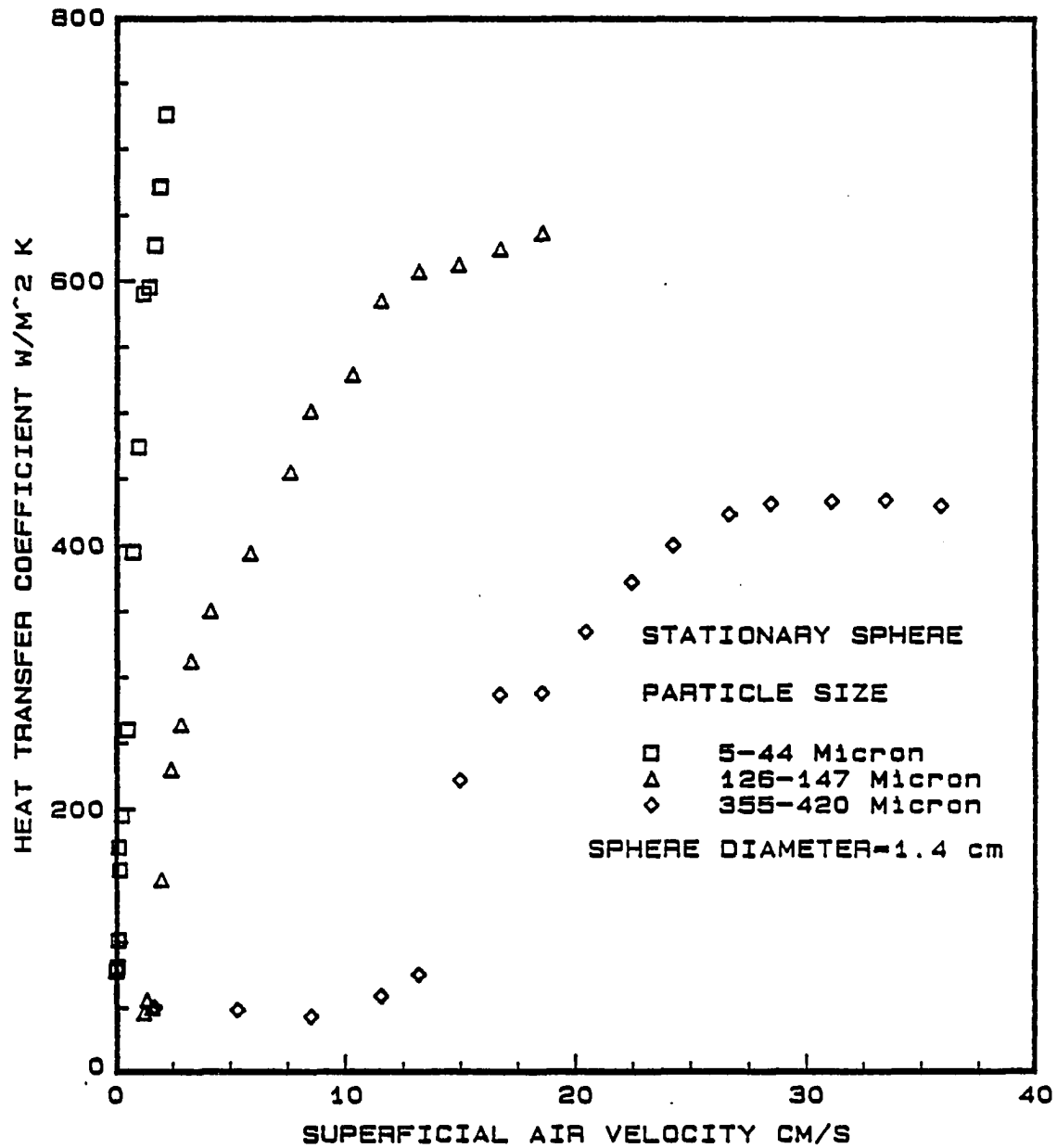

Figure 3.9: Heat transfer coefficient vs. superficial air velocity for a copper sphere diameter of 1.4 cm and various size glass particles

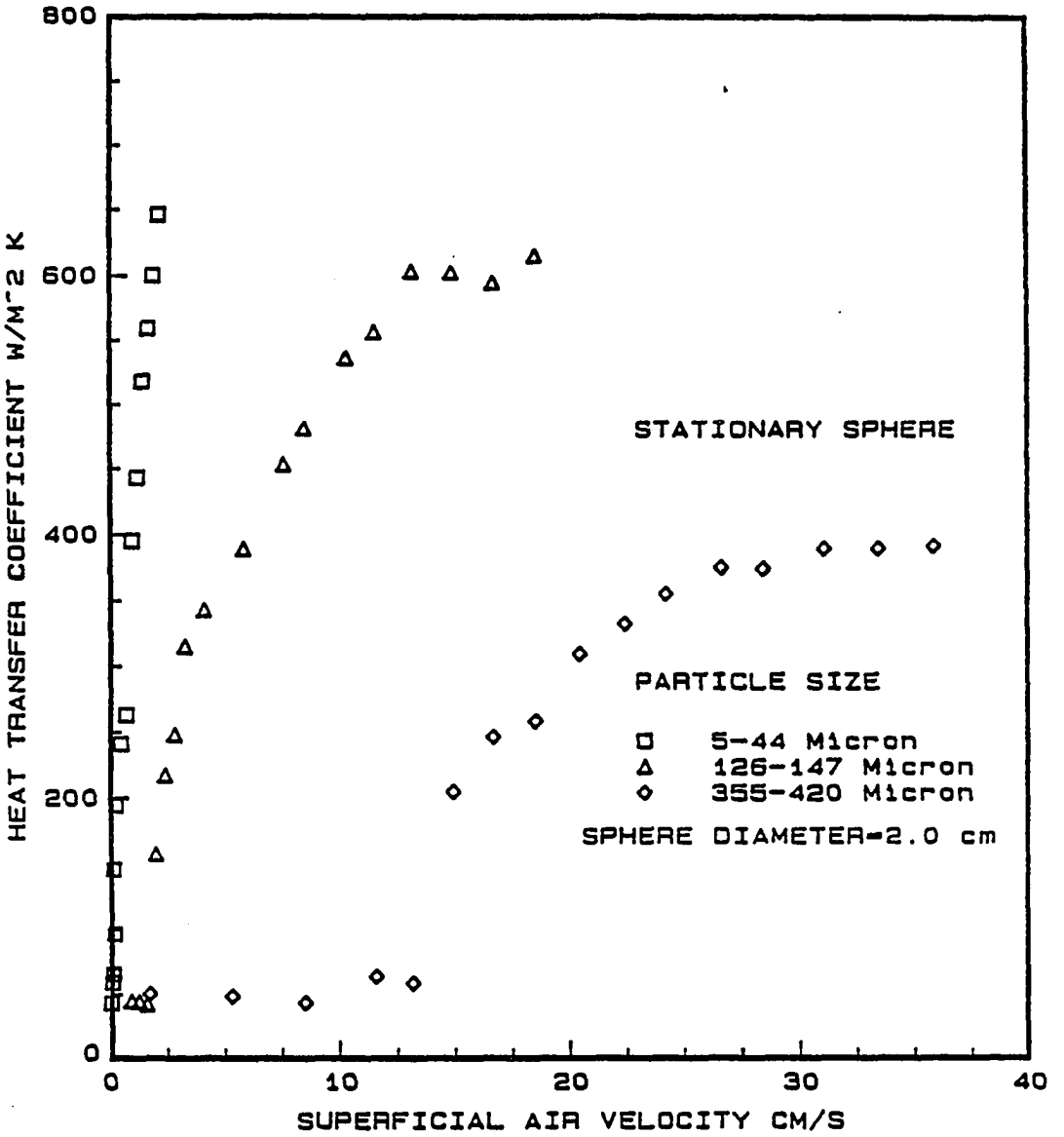

Figure 3.10: Heat transfer coefficient vs. superficial air velocity for a copper sphere of 2.0 cm diameter and various size glass particles

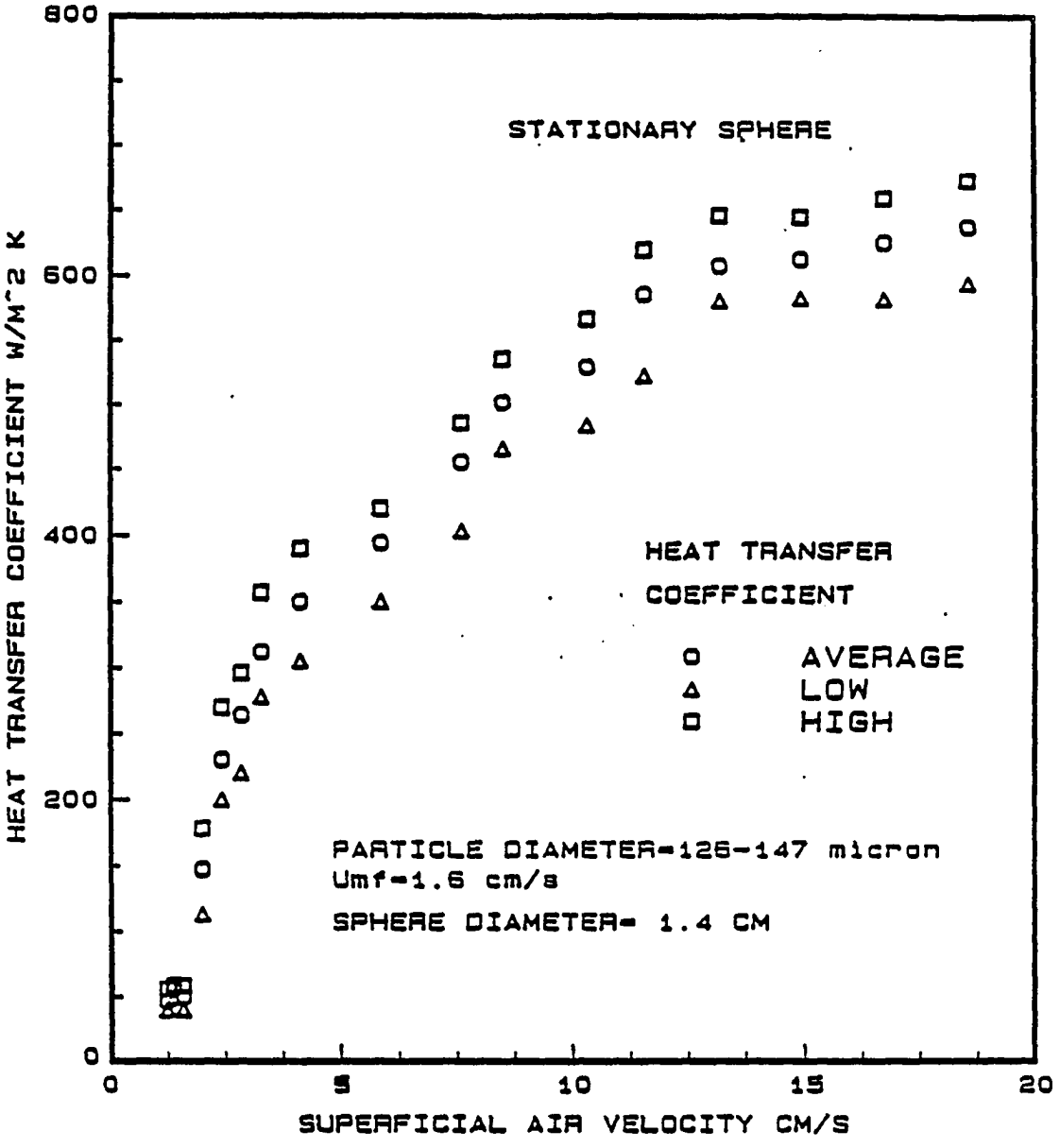

Figure 3.11: Scatter in heat transfer coefficient as a function of the superficial air velocity for a copper sphere of 1.4 cm diameter and 126-147 μm glass particles

3.2.1 Role of Particle and Gas Convective Heat Transfer

The average heat transfer coefficient h, may be considered as the sum of two terms; namely, particle convective transport h_{pc}, and gas convective transport h_{gc} in the absence of the radiation heat transfer.

$$h = h_{gc} + h_{pc} \tag{3.11}$$

The gas convective heat transfer coefficient can be estimated from the Ranz and Marshal [1952] correlation for an isolated sphere.

$$NU = 2 + 0.6Re^{1/2}Pr^{1/3} \tag{3.12}$$

The ratio of the fraction of the total average heat transfer coefficient for the sphere due to gas convective transport, h_{gc}/h is shown in Figures 3.12, 3.13 and 3.14 for 1.4 cm copper sphere immersed in the fluidized bed of various sizes of glass particles. A comparison of these three powder sizes shows that the percentage heat transfer carried by the particle convection is larger for the smaller glass particles. The particle heat transport observed to be about 98 % for the 5-44 μm glass particles, about 94 % for the 126-147 μm glass particles and about 92 % for the 355-420 μm glass particles. At lower superficial air velocities, the gas convection heat transport is as high as 37 % for the 355-420 μm glass particles. In all the cases the particle convective component is higher for the small particle sizes as compare to the large particle system.

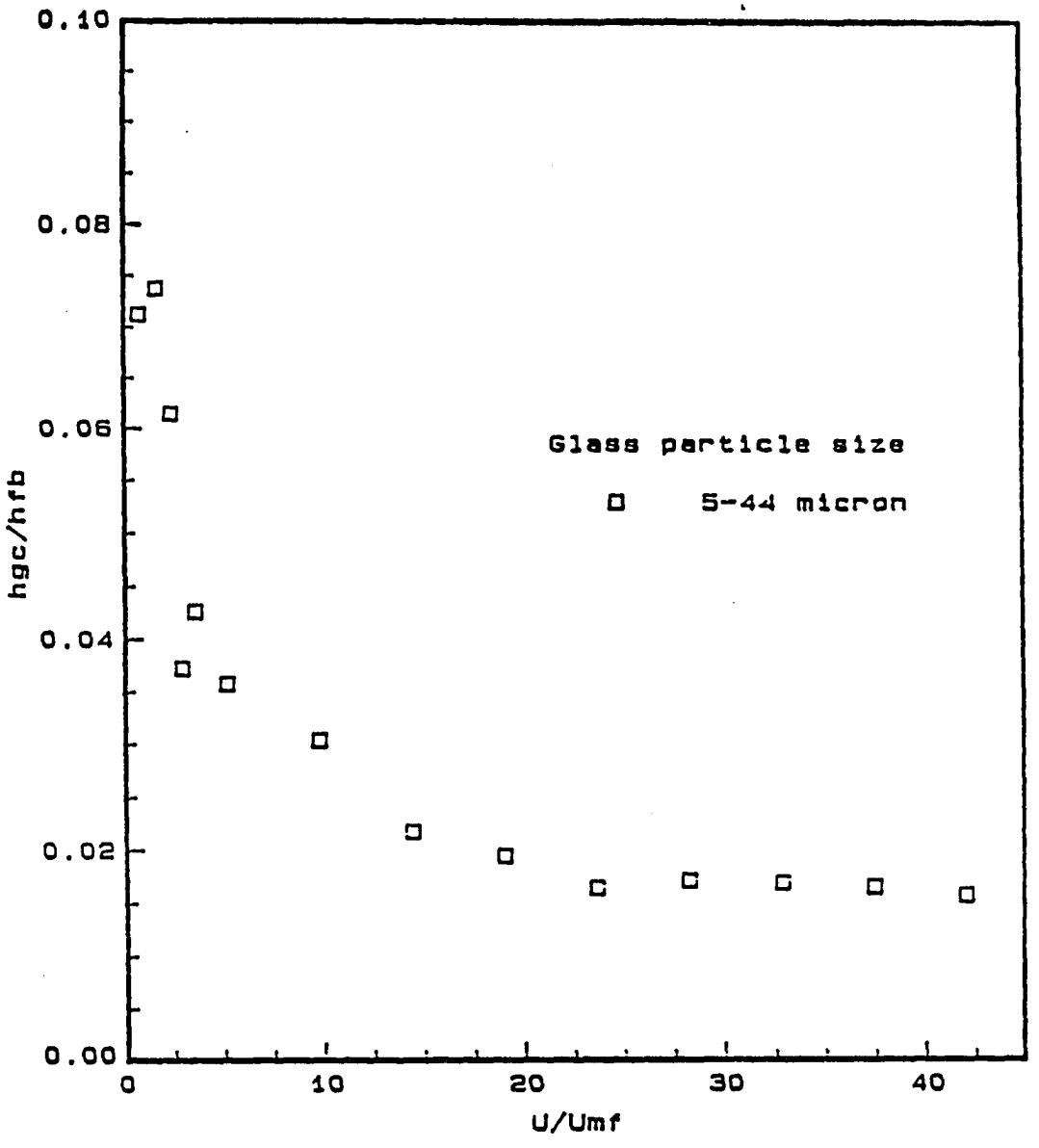

Figure 3.12: Contribution of gas convection heat transfer to particle convection heat transfer for a 1.0 cm copper sphere immersed in a fluidized bed of 5-44 μm glass partic.

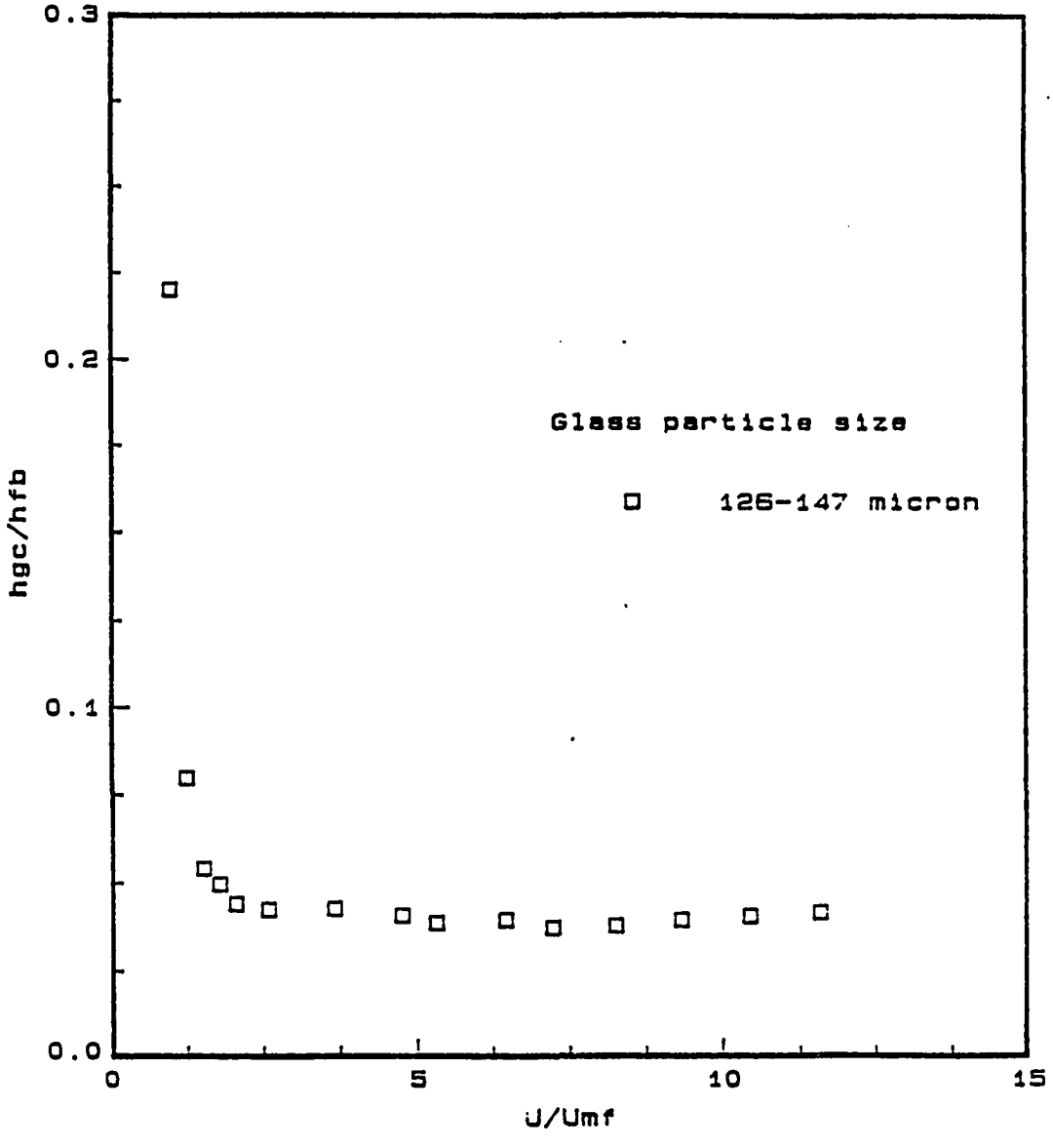

Figure 3.13: Contribution of gas convection heat transfer to particle convection heat transfer for a 1.0 cm copper sphere immersed in a fluidized bed of 126-147 μm glass particles

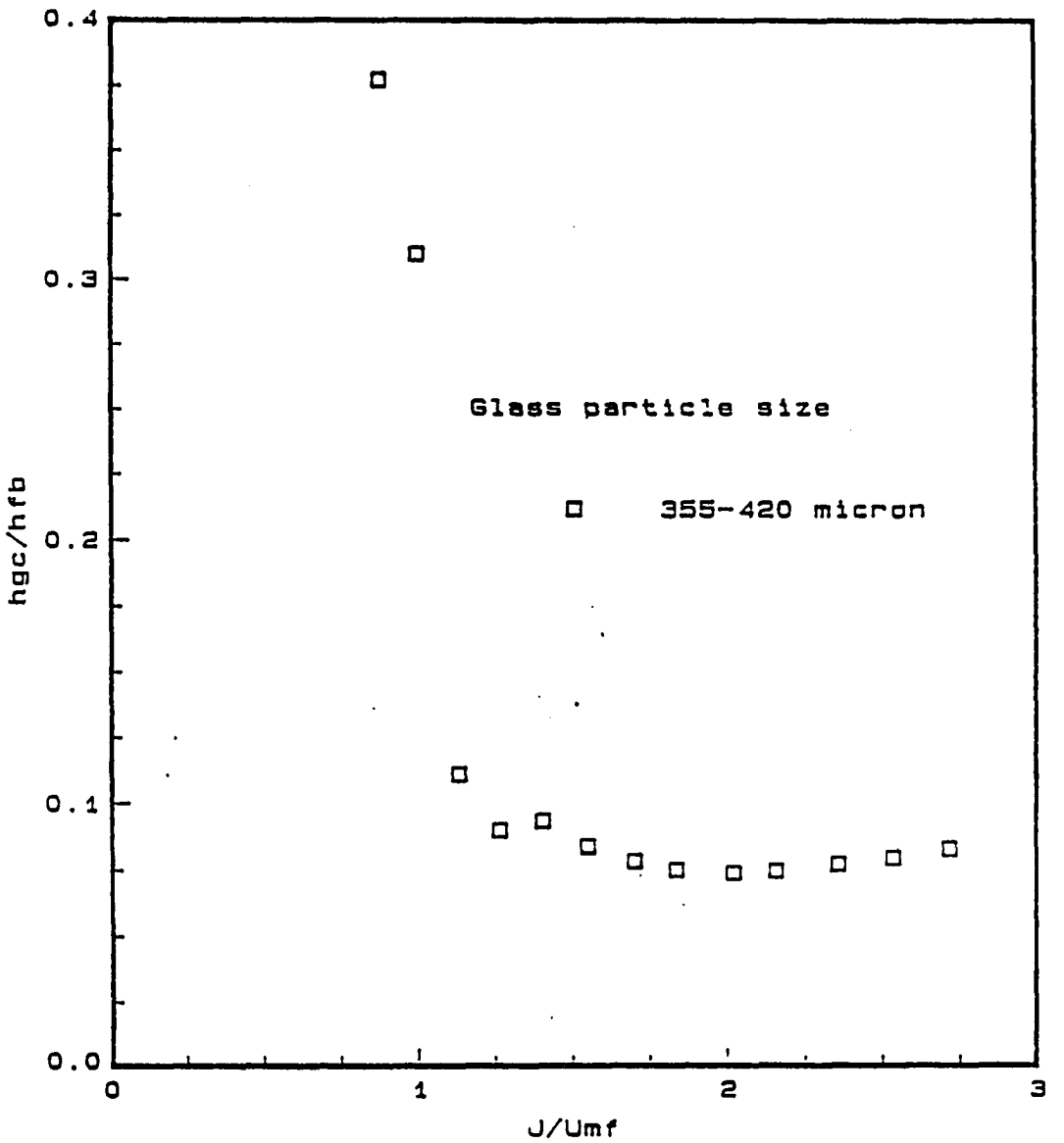

Figure 3.14: Contribution of gas convection heat transfer to particle convection heat transfer for a 1.0 cm copper sphere immersed in a fluidized bed of 355-420 μm glass particles

3.2.2 Heat transfer coefficient as a function of average sphere temperature

As indicated in Chapter 2, the average heat transfer coefficient is calculated from a cooling curve obtained for a copper sphere-air fluidized bed system. A typical cooling curve is shown in Figure 2.12. The average heat transfer coefficient is evaluated for the whole curve where the initial sphere temperature is about 420 to 400 K and the final sphere temperature is about 300 K. Dividing one cooling curve into a number of smaller curves, each representing a sphere temperature drop of 5 K, the heat transfer coefficient for each individual temperature step was calculated. As for example one complete cooling curve from 400 K to 300 can be divided into 20 temperature steps such that during the first step the sphere temperature would drop from 400 K to 395 K etc. For each 5 K temperature drop, the heat transfer coefficient was evaluated and plotted against the average sphere temperature as shown in Figure 3.15 for 1.0 cm copper sphere immersed in a fluidized bed of 126-147 μm glass particles. For this study, a high speed data acquisition system (ADM module) was used with the frequency range of 10 to 50 readings per second. The average sphere temperature is the arithmetic mean between the initial and the final sphere temperatures during each temperature step. The time required for a temperature step of 5 K varies from 0.6 second for the higher average sphere temperatures to 0.9 second for the lower average sphere temperatures. Considering this, the heat transfer coefficient obtained for this temperature step can be considered as almost an instantaneous heat transfer coefficient. High values of the instantaneous heat transfer coefficient suggests that during that period a fresh (cold) packet of

emulsion might have come in the contact with the copper sphere. While the low values of the instantaneous heat transfer coefficient implies that the copper sphere might have been engulfed by a large bubble during that period. Although the heat transfer coefficients are very much scattered, the general trend as shown in Figure 3.15 is that of a decreasing heat transfer coefficient with a decreasing average sphere temperature. The same cooling curve was also divided into the various other temperature steps such as; 10 K, 15 K, 20 K, and 30 K. The heat transfer coefficients for each of the temperature steps are plotted against the average sphere temperature as shown in Figures 3.15 to 3.19.

The spread in the heat transfer coefficient is almost negligible for larger temperature steps as shown in Figures 3.15 to 3.19. However as noted earlier, the heat transfer coefficient decreases with the average sphere temperature for all temperature steps. This decrease is probably a result of the changing thermophysical properties of the packet of emulsion with the average film temperature. However the heat transfer coefficient decreases by 12 to 20 % as the average sphere temperature varies from 400 K to 310 K. Considering the range of the average sphere temperatures, it is not likely that the change in the thermophysical properties of the emulsion packet will contribute to this considerable reduction in the heat transfer coefficient. Hence this reduction in the heat transfer coefficient could be attributed partly to change in the thermophysical properties of the emulsion packet and partly to the dynamic conditions of the fluidized bed during the respective temperature steps. Furthermore it can be inferred from the scatter in the heat transfer coefficients that in order to obtain the average value of heat transfer coefficient, the

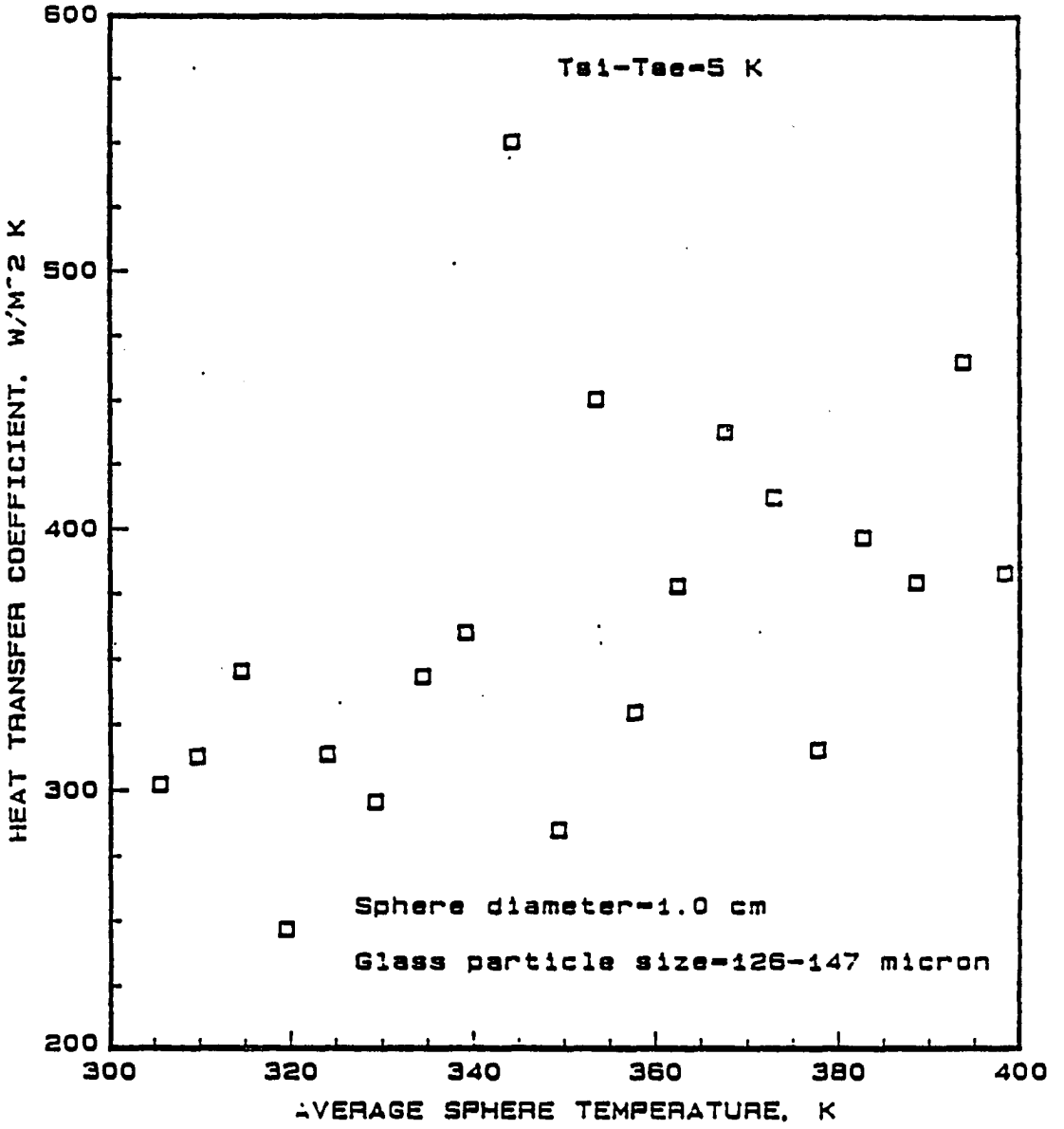

Figure 3.15: Heat transfer coefficient vs. average sphere temperature for a temperature step of 5 K and for a 1.0 cm copper sphere immersed in a fluidized bed of 126-147 μm glass particles

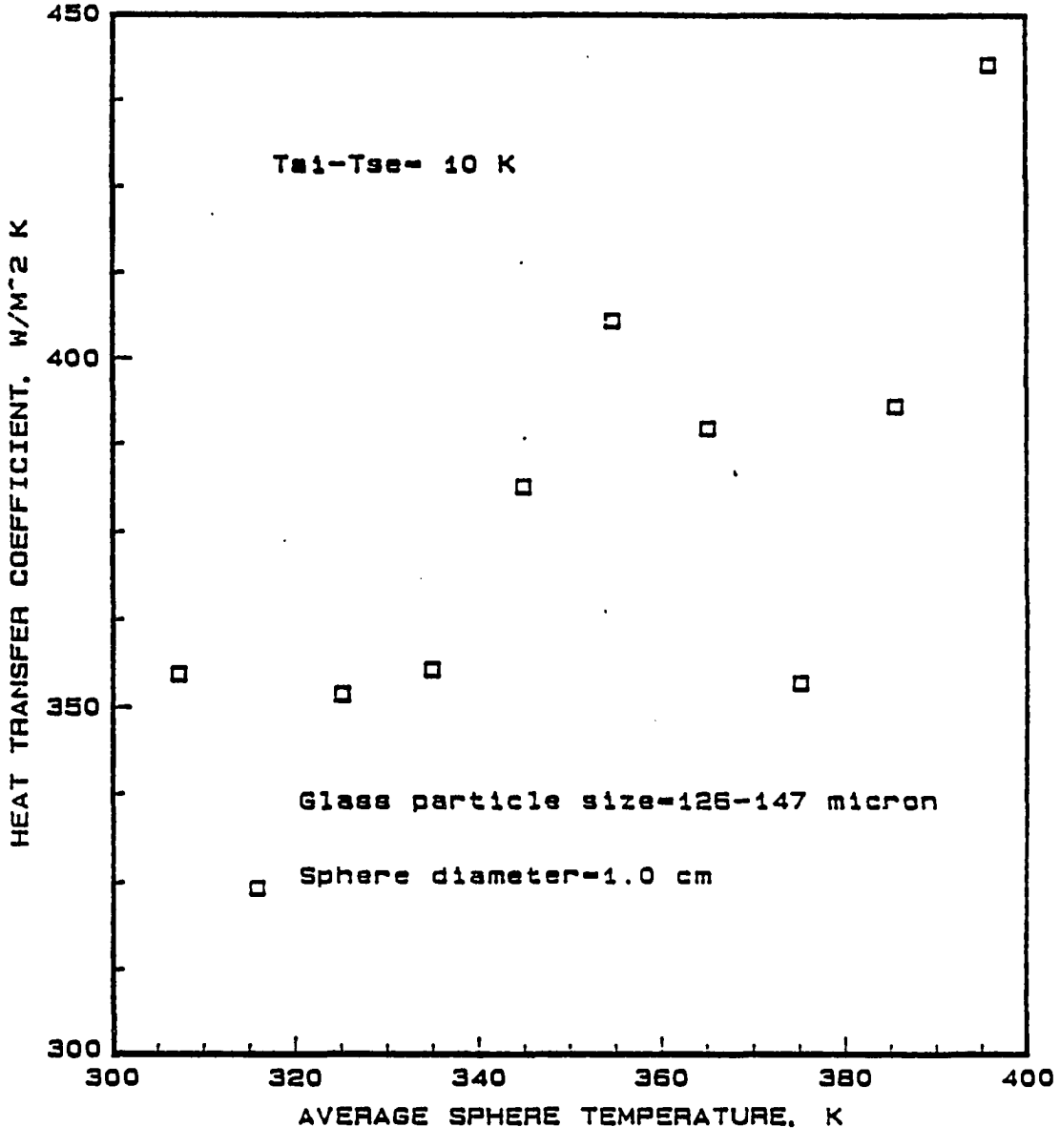

Figure 3.16: Heat transfer coefficient vs. average sphere temperature for a temperature step of 10 K and for a 1.0 cm copper sphere immersed in a fluidized bed of 126-147 μm glass particles

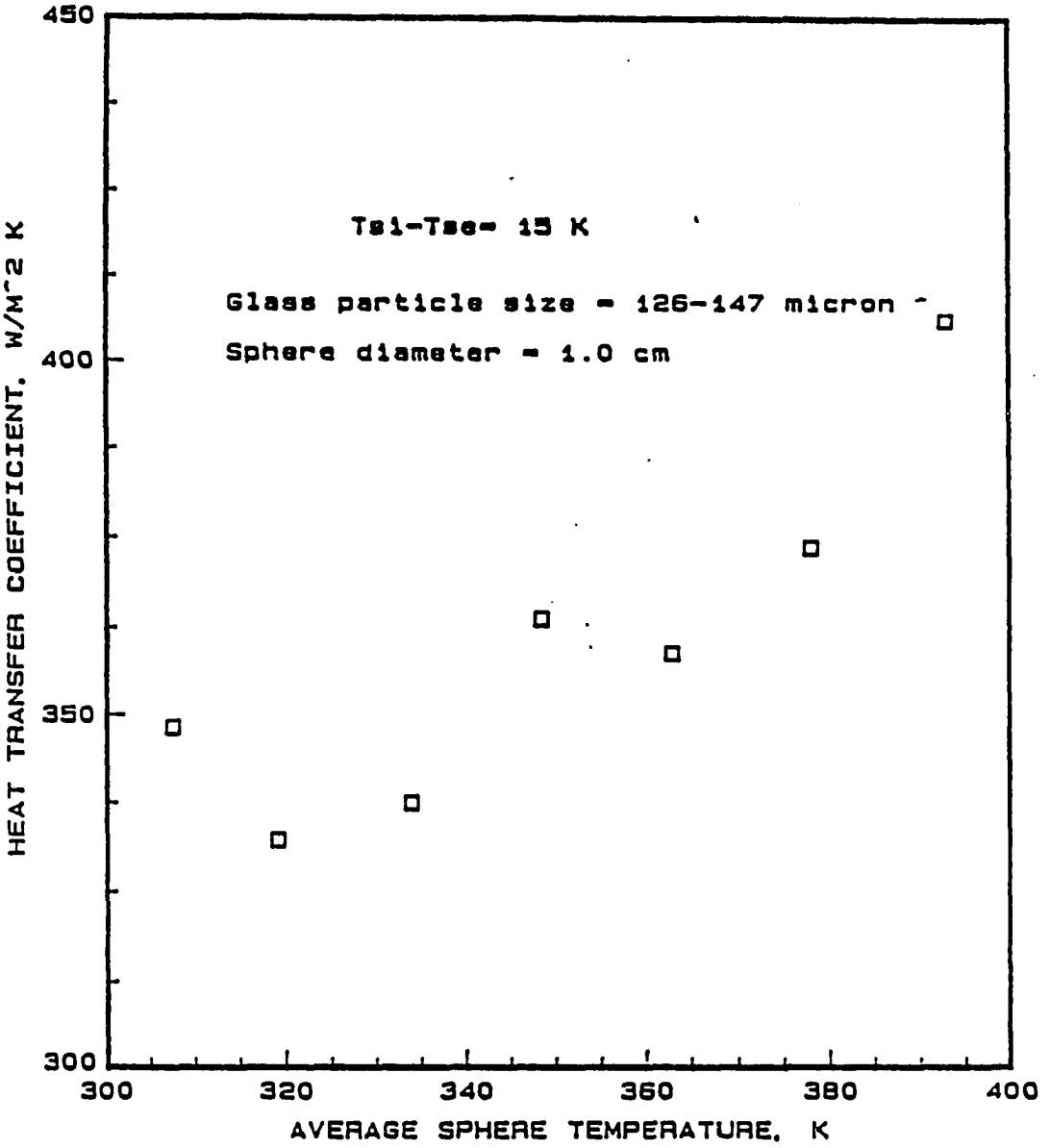

Figure 3.17: Heat transfer coefficient vs. average sphere temperature for a temperature step of 15 K and for a 1.0 cm copper sphere immersed in a fluidized bed of 126-147 μm glass particles

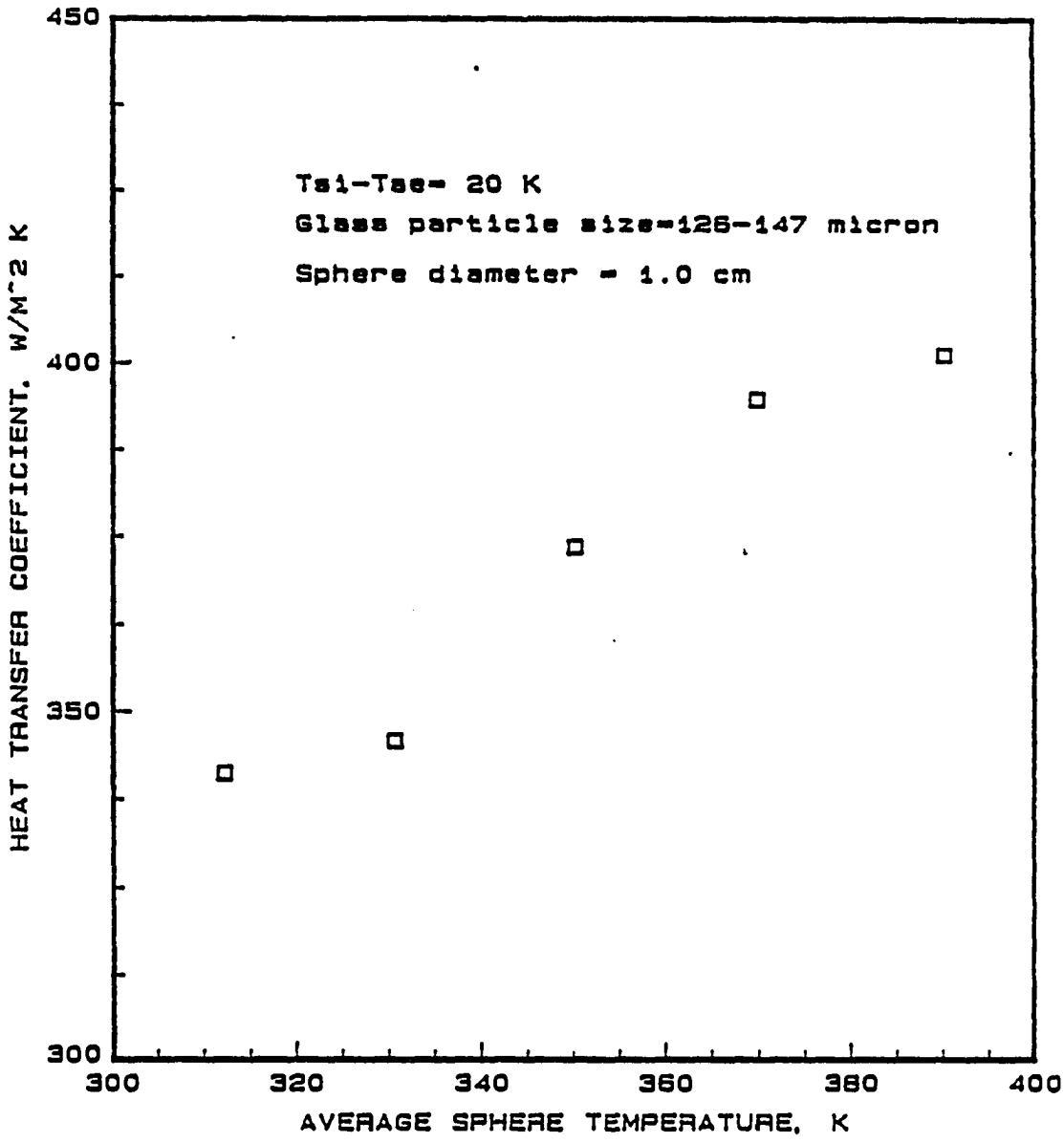

Figure 3.18: Heat transfer coefficient vs. average sphere temperature for a temperature step of 20 K and for a 1.0 cm copper sphere immersed in a fluidized bed of 126-147 μm glass particles

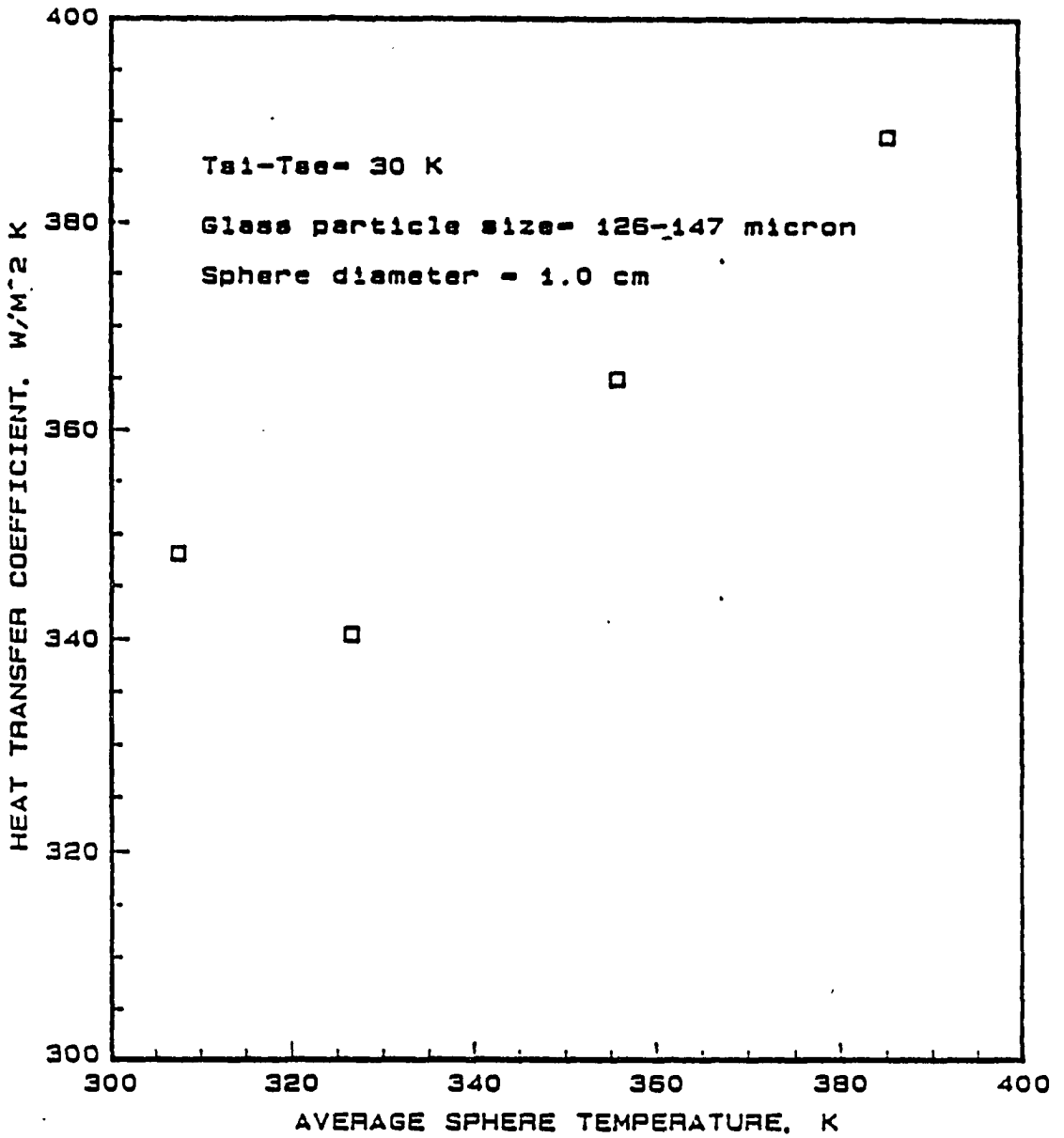

Figure 3.19: Heat transfer coefficient vs. average sphere temperature for a temperature step of 30 K and for a 1.0 cm copper sphere immersed in a fluidized bed of 126-147 μm glass particles

temperature step should be more than 20 K.

The study of the temperature dependence characteristics of the heat transfer coefficient was also extended to the packed beds. Figure 3.20 shows the heat transfer coefficient as a function of the average sphere temperature obtained from a single cooling curve for a system of hot copper sphere immersed in a packed bed of 126-147 μm glass particles. In a packed bed due to the absence of the particulate phase circulation, the residence time of the emulsion packet surrounding the sphere is essentially infinite. The heat transfer coefficient is very high for the initial time as the emulsion packet is cold, but slowly the temperature of the emulsion packet rises, decreasing the temperature potential and also the heat transfer coefficient. This temperature dependence property of the heat transfer coefficient can be verified by a better suited experimental method of steady state heat transfer from an immersed surface to the bed. This can be achieved by inserting a heater in side the object or by electrically heating the object and monitoring the power required to maintain the constant temperature of the immersed object.

3.3 Heat Transfer from Linearly Downward Moving Sphere

Heat transfer coefficients were evaluated for spheres moving linearly downward at various velocities in an air fluidized bed of various size glass particles. Figures 3.21 to 3.29 shows such plots. The copper sphere was moved in a downwardly direction by the gear train mechanism as shown in Figure 2.4. The time required for a sphere to traverse the fluidized bed from the top to the bottom of the fluidized bed varied from 60 second for a sphere moving at 0.4 cm/s velocity to 3.2 second

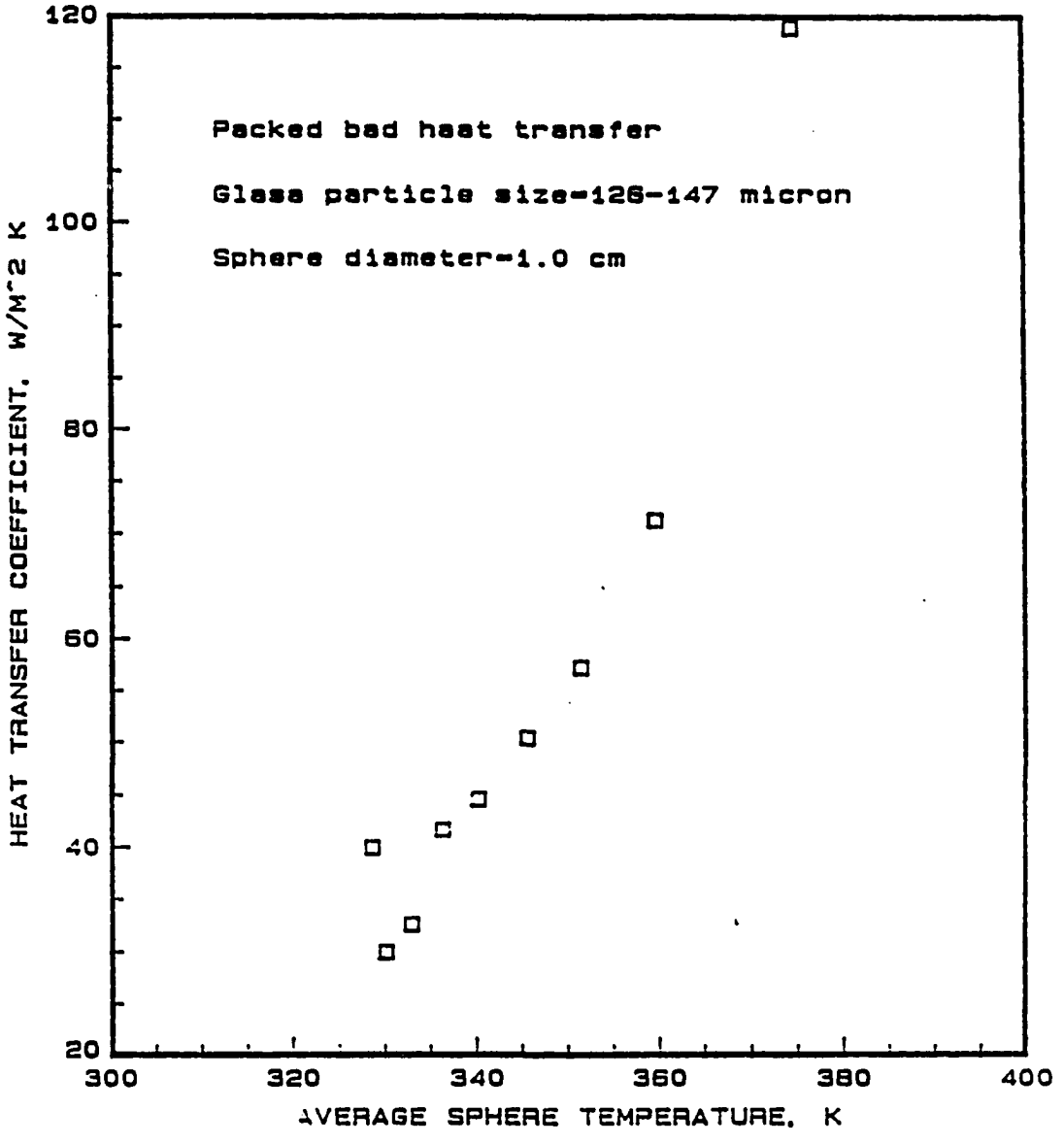

Figure 3.20: Heat transfer coefficient vs. average sphere temperature for a 1.0 cm copper sphere immersed in a packed bed of 126-147 μm glass particles

for a sphere moving at 7.5 cm/s. Even though it takes only 3.2 second for a fast moving sphere to traverse the fluidized bed from the top to the bottom, the high heat transfer coefficient associated with the motion of the sphere ensured that the sphere temperature dropped at least by 30° to 40 ° C during this time. As established earlier, this much temperature drop is necessary to get the average heat transfer coefficient.

It is reasonable to expect that the heat transfer between an immersed object and a fluidized bed to closely depend on the flow configuration around the object. Figures 3.21, 3.22 and 3.23 shows plots of the heat transfer coefficient versus superficial air velocity at various average sphere velocity in downward direction for a fluidized bed of 5-44 μm glass particles and various size copper spheres. Near minimum fluidization the heat transfer coefficient for the case of the sphere moving at 7.5 cm/s is observed to increase about 10 to 13 times as compared to that of a stationary sphere. Even at a sphere velocity of 0.4 cm/s, the increase in the heat transfer coefficient is about 25 % for the 1.4 cm sphere and about 280% for the 1.0 cm sphere. As seen in Figures 3.21, 3.22 and 3.23, each plot can be divided in to two regions. In region one where the superficial air velocity is less than 0.5 cm/s the heat transfer coefficient increases continuously with the linear velocity of the sphere. Moreover, the heat transfer coefficient decreases with an increase in the superficial air velocity at higher sphere velocities while it increases with superficial air velocity at lower sphere velocities. Even though there is a considerable amount of scatter in the data, this general trend is fairly well established. It is interesting to note that the heat transfer coefficient remains almost constant with the superficial

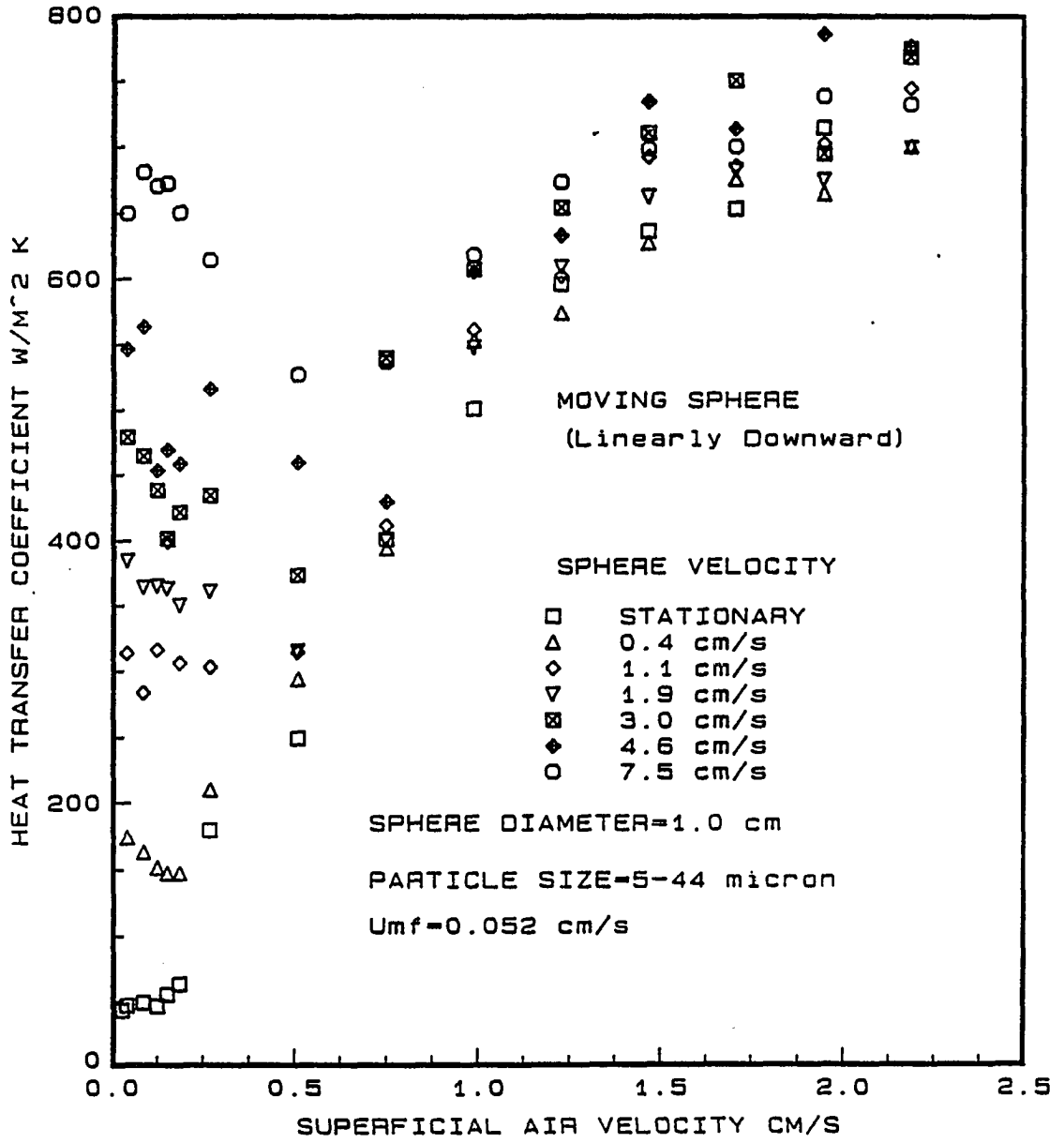

Figure 3.21: Heat transfer coefficient for a 1.0 cm copper sphere in linearly downward motion (various speeds) versus superficial air velocity for a fluidized bed of 5-44 μm glass particles

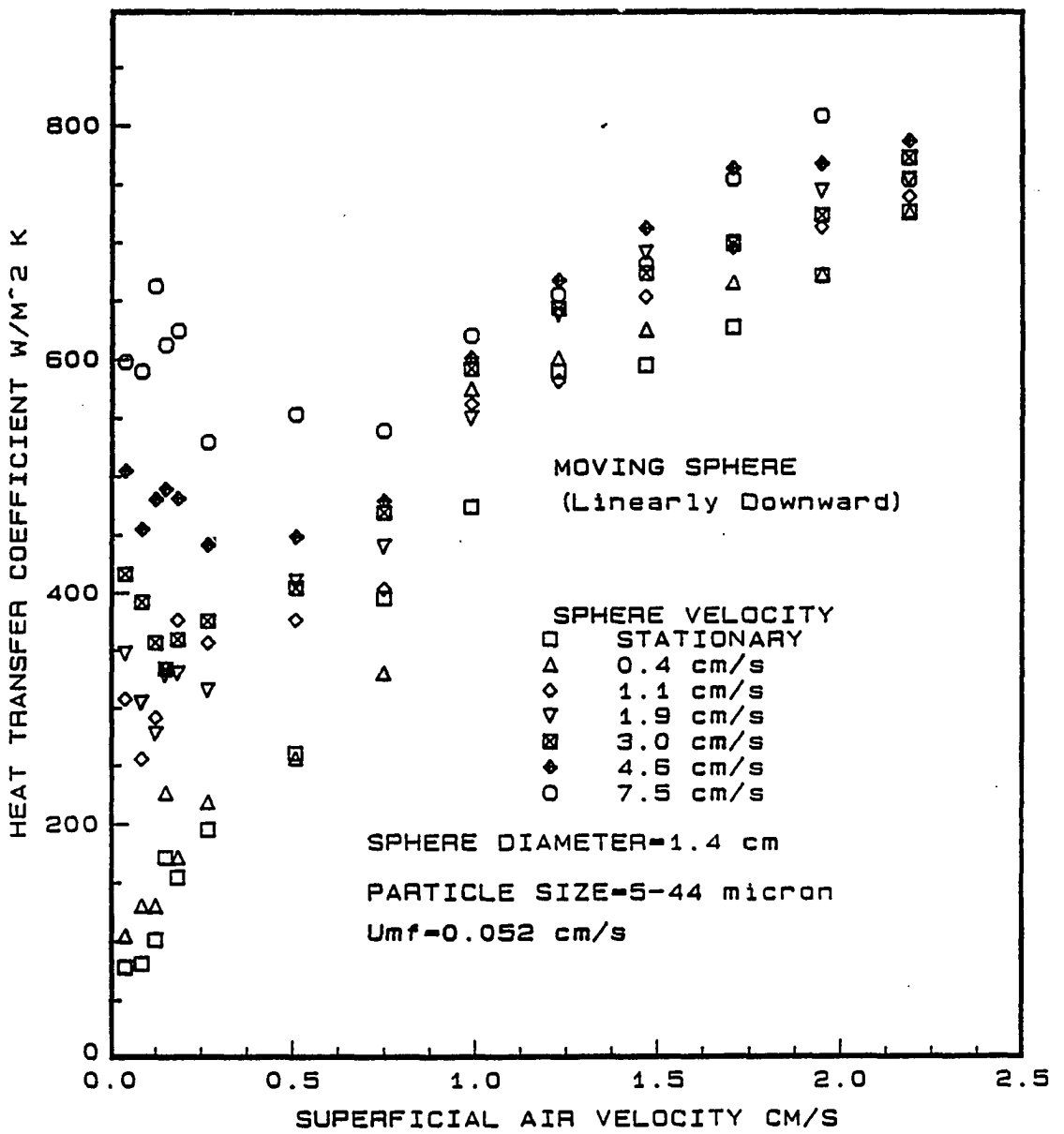

Figure 3.22: Heat transfer coefficient of a 1.4 cm copper sphere in linearly downward motion (various speeds) versus superficial air velocity for a fluidized bed of 5-44 μm glass particles

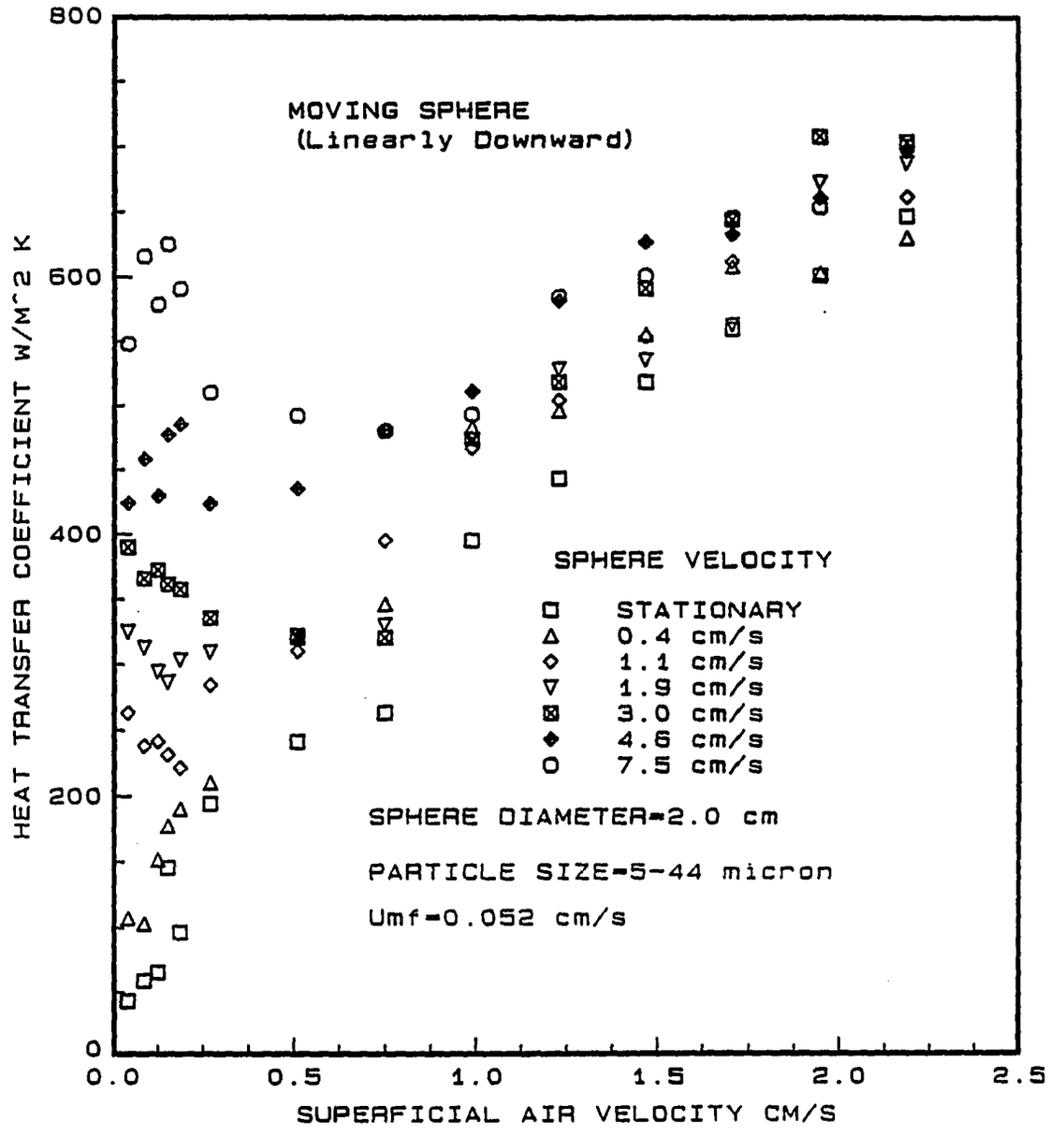

Figure 3.23: Heat transfer coefficient of a 2.0 cm copper sphere in linearly downward motion (various speeds) versus superficial air velocity for a fluidized bed of 5-44 μm glass particles

air velocity for 1.0 cm diameter sphere moving at 1.1 and 1.9 cm/s. In the region two, where the superficial velocity is greater than 0.5 cm/s, the increase in the heat transfer coefficient with the sphere velocity is very small and scatter in the data is larger compared to the region one.

In Figures 3.24 to 3.26 and 3.27 to 3.29, the average heat transfer coefficients are plotted against the superficial air velocity for various sphere velocities and fluidized beds of 126-147 and 355-420 μm glass particles respectively. The general trend of increasing heat transfer coefficient with sphere velocity in region one where the superficial air velocity is lower than 5 cm/s for the 126-147 μm glass particles and 20 cm/s for the 355-420 μm glass particles, remains the same as mentioned previously. As shown in Figures 3.24 to 3.26, in region two, where the superficial air velocity is greater than 5 cm/s, the increase in the heat transfer coefficient with sphere velocity is much lower than that for the fluidized bed of 5-44 μm glass particles. Moreover for 355-420 μm glass particles, the heat transfer coefficient remains almost constant for all sphere velocities in region two where the superficial air velocity is greater than 22 cm/s. The increase in the heat transfer coefficient for the 1.0 cm sphere at 7.5 cm/s in the fluidized bed of 126-147μm is about 10 to 12 times as compared to the stationary sphere near minimum fluidization condition.

As shown in the Figure 3.29, the heat transfer coefficient remains almost constant for 2.0 cm diameter sphere moving at 3 cm/s in the fluidized bed of 355-420 μm glass particles. Furthermore, the scatter in the data is less compare to that of the 5-44 μm glass particles. In this case the heat transfer coefficient increases by 4 to 5 times near the minimum fluidization condition for the sphere moving at 7.5

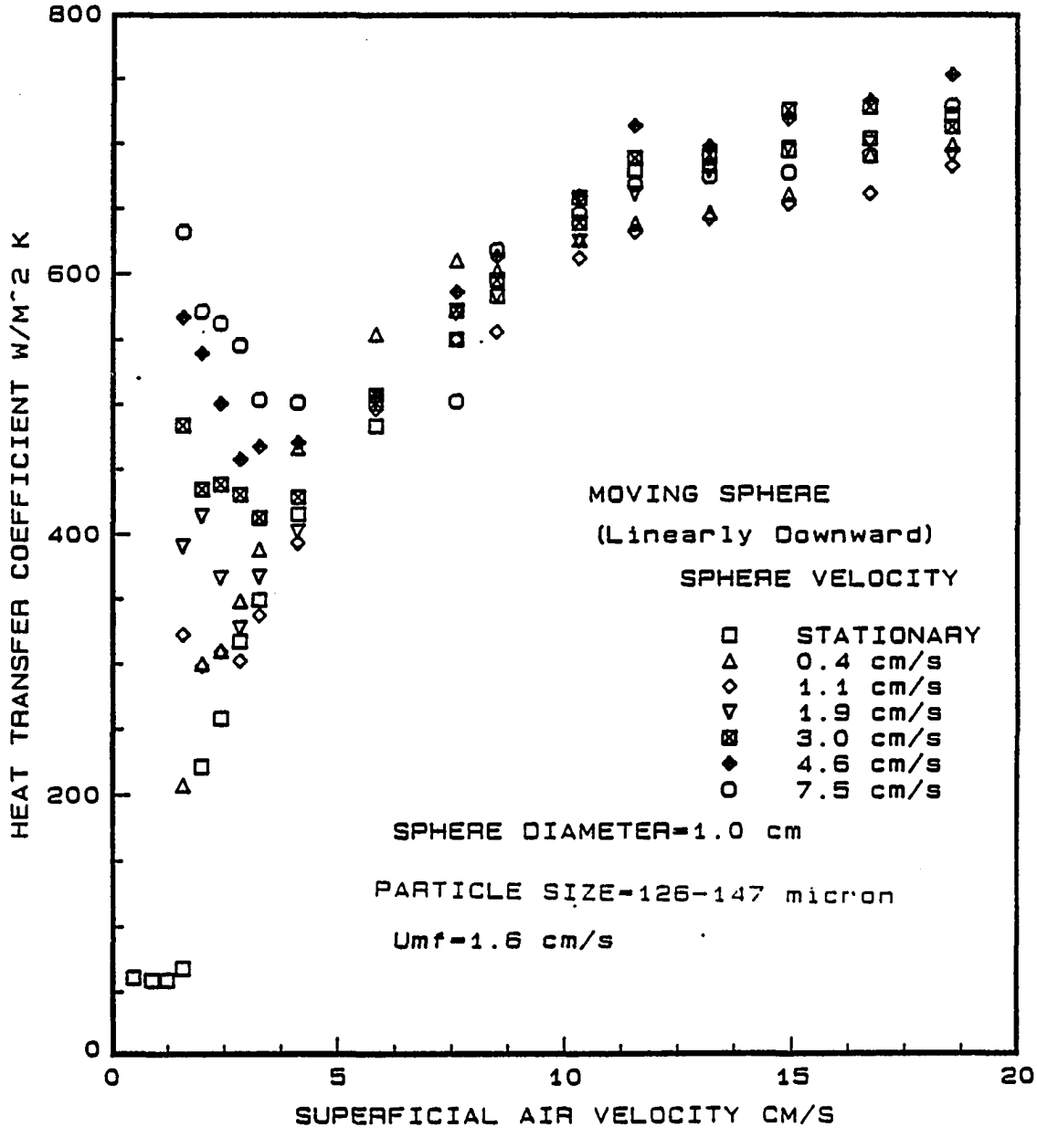

Figure 3.24: Heat transfer coefficient of a 1.0 cm copper sphere in linearly downward motion (various speeds) versus superficial air velocity for a fluidized bed of 126-147 μm glass particles

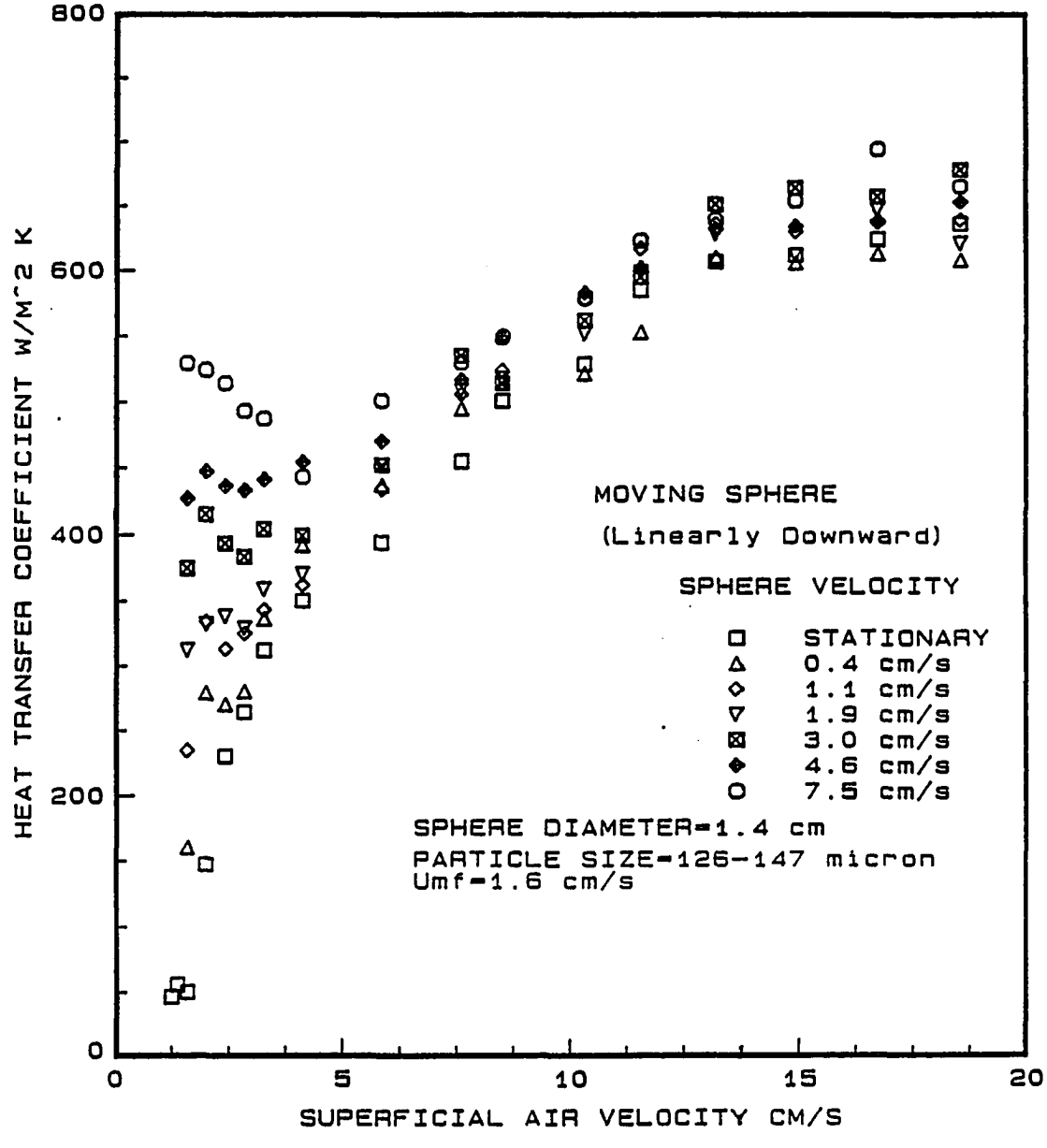

Figure 3.25: Heat transfer coefficient of a 1.4 cm copper sphere in linearly downward motion (various speeds) versus superficial air velocity for a fluidized bed of 126-147 μm glass particles

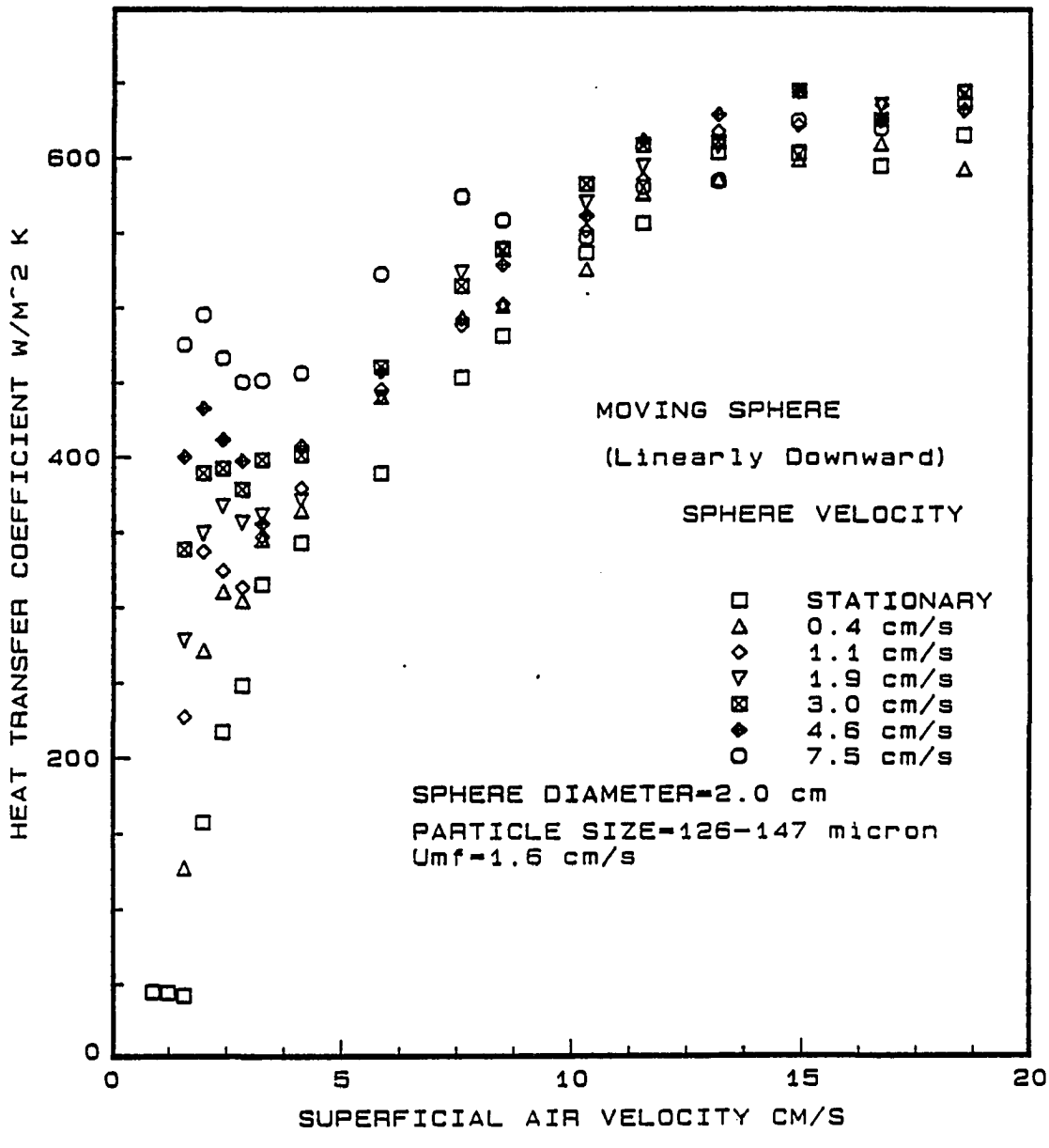

Figure 3.26: Heat transfer coefficient of a 2.0 cm copper sphere in linearly downward motion (various speeds) versus superficial air velocity for a fluidized bed of 126-147 μm glass particles

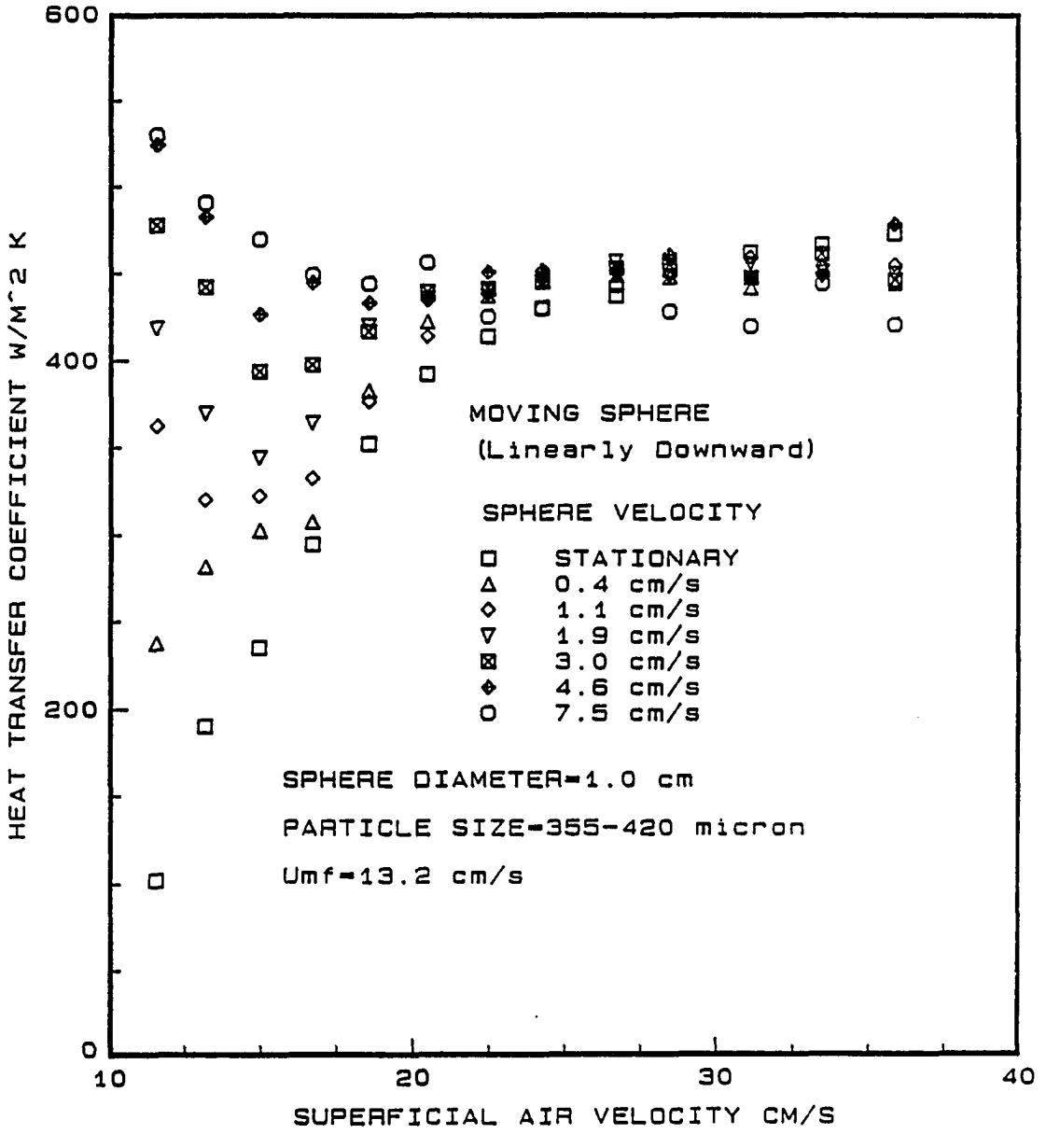

Figure 3.27: Heat transfer coefficient of a 1.0 cm copper sphere in linearly downward motion (various speeds) versus superficial air velocity for a fluidized bed of 355-420 μm glass particles

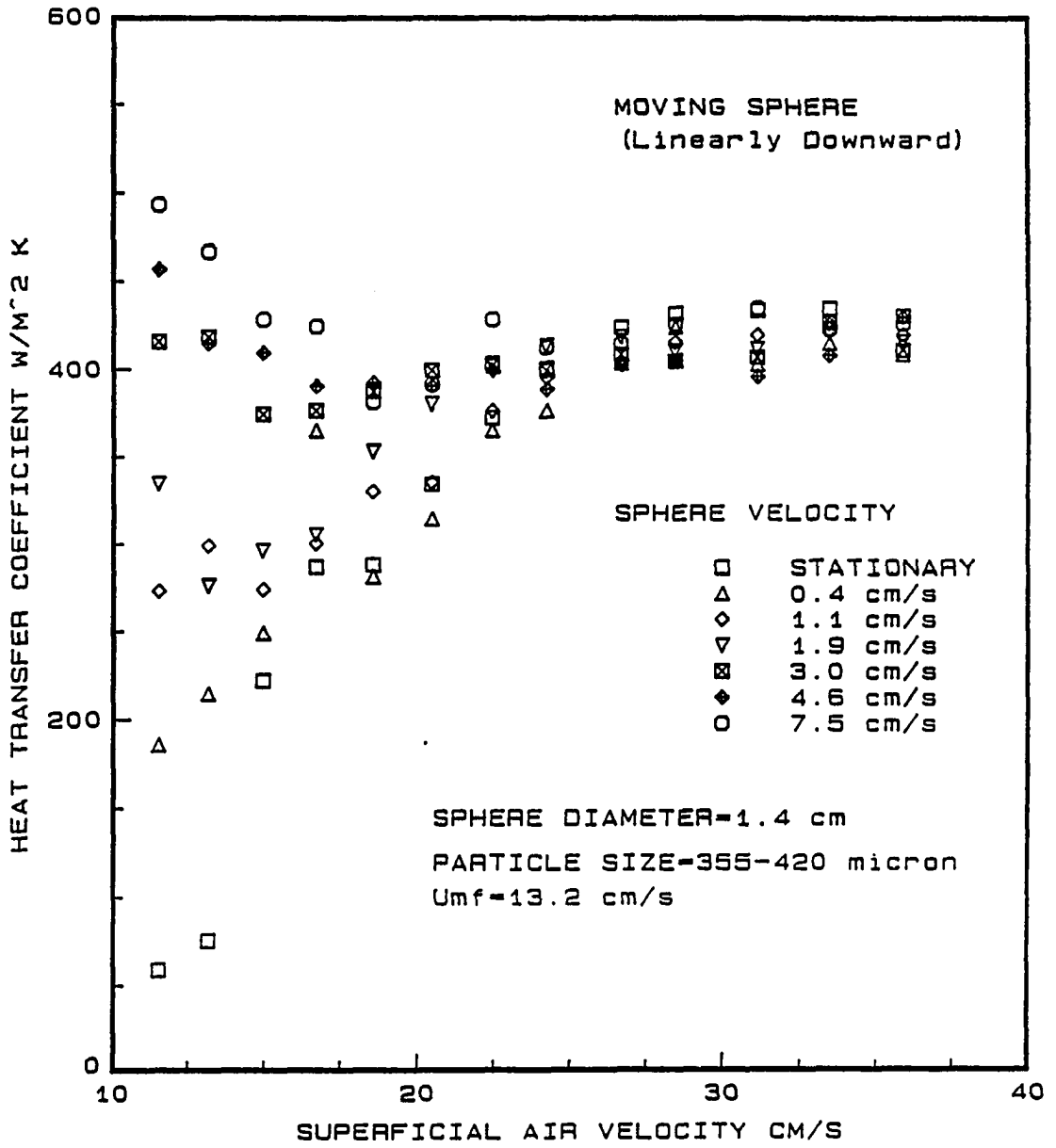

Figure 3.28: Heat transfer coefficient of a 1.4 cm copper sphere in linearly downward motion (various speeds) versus superficial air velocity for a fluidized bed of 355-420 μm glass particles

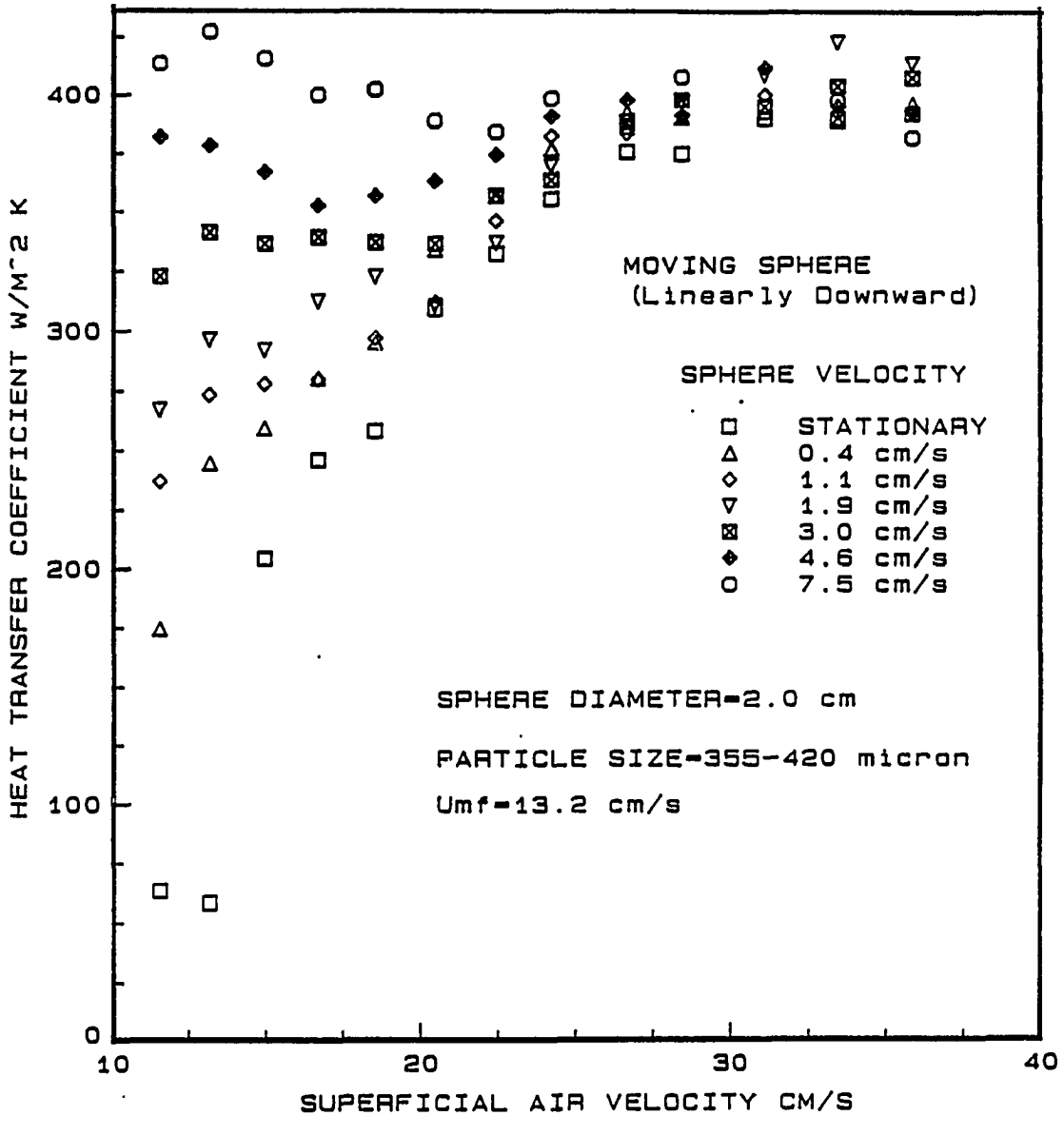

Figure 3.29: Heat transfer coefficient of a 2.0 cm copper sphere in linearly downward motion (various speeds) versus superficial air velocity for a fluidized bed of 355-420 μm glass particles

cm/s.

As mentioned above in all the cases the heat transfer coefficient for a sphere moving at 7.5 cm/s is observed to increase by about 4 to 13 times with respect to the stationary sphere. However at higher superficial air velocities, the difference between the heat transfer coefficient for a moving and a stationary sphere is diminished. This might be explained as follows: at lower superficial air velocities, the absence of appreciable circulation of the particulate phase makes the residence time of the emulsion packet very large for a stationary sphere. Thus, the motion of the sphere at the low superficial air velocities decreases the residence time considerably and improving the heat transfer coefficient. At higher superficial air velocities, the circulation of the particles around the sphere is already high and the motion of the sphere does not significantly change the residence time of the emulsion packet, thus, the influence of the forced motion of the sphere on the heat transfer coefficient is reduced.

The effect of the glass particle size on the heat transfer coefficient for a moving sphere is the same as that of the stationary sphere: the heat transfer coefficient increases with a decrease in the glass particle size. However the well established trend of increasing heat transfer coefficient for a stationary sphere with a decrease in the sphere diameter is not very clearly established for a moving sphere.

The effect of the forced linear motion of the heat transfer surface on heat transfer coefficient is not recorded in the literature. However, a limited amount of work has been done on the heat transfer between a moving bed of solid particles and an immersed surface. Heat transfer between a surface and a fluidized or moving

packed bed is determined by the time of contact of the solid particles with the surface and the porosity of the bed. At the same contact time a dense moving bed may be considered as a hypothetical fluidized bed whose porosity is equal to that of a dense bed. Colakyan and Levenspiel [1984] observed that the heat transfer coefficient increases with linear solid velocity up to 10.0 cm/s and after that it levels off for a packed bed of 0.27 and 0.8 mm silica sand moving over a heated cylinder. At the minimum fluidization condition, the sphere moving within a fluidized bed is analogous to a moving bed of particles passing through a heat transfer surface. The existence of the maximum heat transfer coefficient with the solid velocity suggests that the continuous increase in the heat transfer coefficient at minimum fluidization condition observed in the present work may levelled off at higher sphere velocities.

Botterill and Denloye [1978a] used a flowing packed bed to model the heat transfer behavior of a freely fluidized bed of solid particles. The residence time of the bed material adjacent to the transfer surface was regulated by controlling the downward rate of the flow of the bed past a small exposed heat transfer surface. They found that the flowing packed bed to surface heat transfer coefficient increases with increase in solid velocity. Dunsky et al. [1966] carried out an experiment in which the residence time of the solids on a heat transfer surface was controlled by the spining action of an annular packed bed column. They showed that the heat transfer coefficient increases with an increase in the speed of the moving bed and gradually reached the maximum value which was different for each size of particles. In recent studies, the sphere was allowed to move freely which tends to follow the natural motion of the bulk circulation. Prins et al. [1986] measured the heat

transfer coefficient from a gas fluidized bed to a fixed and nearly freely moving single sphere over a wide range of bed particles and heat transfer sphere diameters. The heat transfer coefficient for a fixed sphere was found to be higher; however, the difference was relatively small and decreased for larger bed particles. Rios and Gibert [1984] showed that the heat transfer coefficient increases by 170% for a freely moving sphere when compared to a stationary sphere at $U = 2.3U_{mf}$. This increase follows the same trend as established in the present research.

3.3.1 Industrial figure of merit

The cost of nitrogen fluidizing gas is a significant operational cost in industrial heat treatment processes. A trade-off now seems possible between nitrogen gas throughput and object motion such that the same or improved heat transfer rate is maintained. To demonstrate this Figure 3.30 plots an industrial figure of merit. This is defined here as the ratio of the heat transfer coefficient to the superficial gas velocity plotted versus superficial air velocity based on the data of Figure 3.26 and normalized to the maximum value of figure of merit for the stationary sphere [i.e $(h_m/U)/(h_s/U)_{max}$. A high figure of merit (i.e., greater than 1) compared to the stationary sphere indicates overall improvement in heat transfer at reduced operating cost of the bed. In fact, not only is the figure of merit improved at reduced superficial air velocity of the bed (reduced cost of inert gas), but the absolute value of the heat transfer coefficient is also increases above the maximum value attained for the stationary sphere when the sphere is moved linearly downward at 7.5 cm/s.

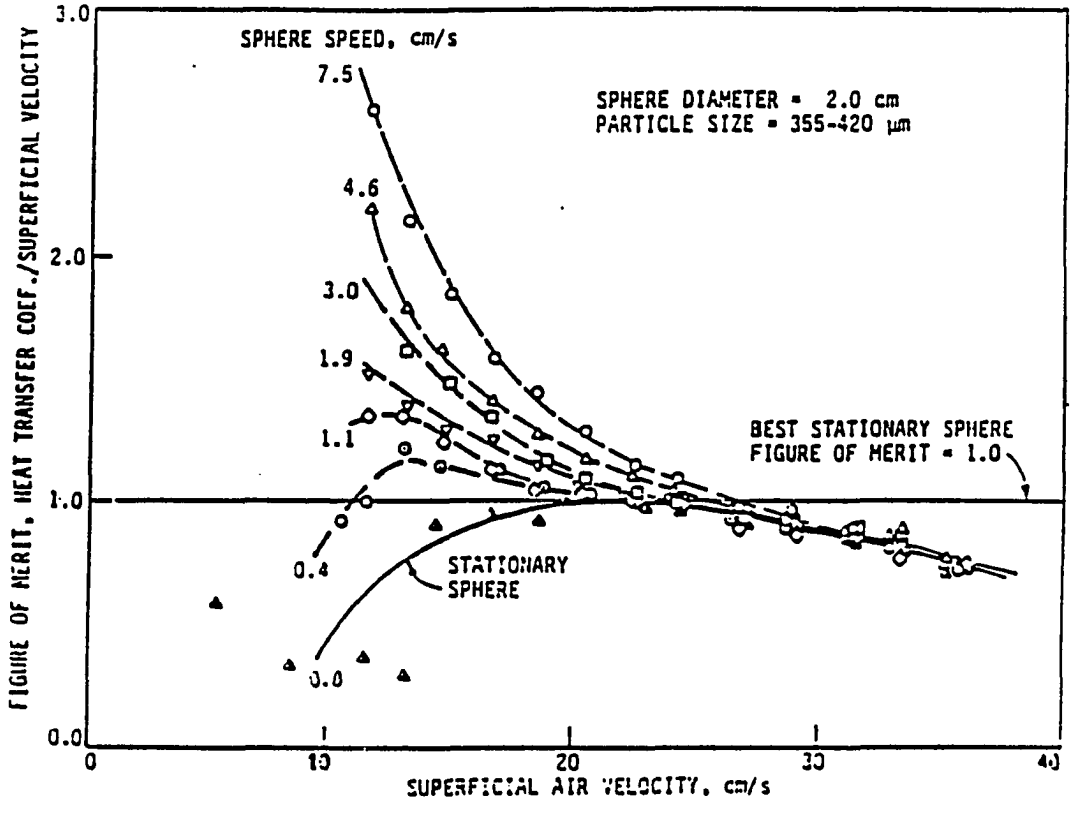

Figure 3.30: Industrial figure of merit, heat transfer to operating cost ratio, normalized to the best stationary sphere operation of the bed

3.4 Heat Transfer from Oscillating Spheres

The fluidizing action of the mechanical stirrer has been utilized to aid in handling particulate solids in various processes. Oscillating, rotating and impeller type agitators have been used to blend various solid components in cement manufacturing. Rotating stirrers have been used in laboratory cracking catalyst activity evaluation. Vibrating objects immersed in beds of solids have been used as an aid in fluidization at low superficial gas velocities. Relative motion between the immersed object and solid particle is the major factor contributing to the enhanced heat transfer coefficient in the fluidized beds. In this study, hot spheres of various diameters were allowed to oscillate at various frequencies and amplitudes in order to study the effect of oscillating motion on the heat transfer coefficient.

Figures 3.31, 3.32 and 3.33 shows the heat transfer coefficient as a function of superficial air velocity for various frequencies of a 1.0 cm oscillating sphere and peak-to-peak amplitudes of 1.8 cm, 4.0 cm and 6.9 cm respectively. The heat transfer coefficient increases by 7.5 to 14 times for a sphere oscillating when compared to the stationary sphere at 2.85 hz as the peak-to-peak amplitude increases from 1.8 to 6.9 cm. As shown in Figure 3.31, the heat transfer coefficient increases continuously with the superficial air velocity at lower peak-to-peak amplitude of 1.8 cm. Whereas at higher peak-to-peak amplitudes, the heat transfer coefficient increases rapidly at the lower superficial air velocities followed by a gradual increase or leveling off at the higher superficial air velocities. At the peak-to-peak amplitude of 4.0 cm and 6.9 cm and the oscillating frequency of 2.85 hz, the heat transfer coefficient remains almost constant for a superficial air velocity greater than 0.2 cm/s.

Figures 3.34-3.36 and Figures 3.37-3.39 show the plots of heat transfer coefficient versus the superficial air velocity for 1.4 and 2.0 cm sphere oscillating at various frequencies and peak-to-peak amplitudes within a fluidized bed of 5-44 μm glass particles. The general trend remains the same as in the previous case; for the lower peak-to-peak amplitude, the heat transfer coefficient increased continuously with the superficial air velocity, while for higher amplitudes the heat transfer coefficient increases rapidly at lower superficial air velocities and remains almost constant at higher superficial air velocities.

Figures 3.40 to 3.48 shows plots of the heat transfer coefficient for various peak-to-peak amplitudes and sphere diameters versus the superficial air velocity for the fluidized bed of 126-147 μm glass particles. Figures 3.49 to 3.57 shows plots of the heat transfer coefficient for various peak-to-peak amplitudes and sphere diameters versus the superficial air velocity for the fluidized bed of 355-420 μm glass particles.

As shown in these figures, the general trend remains the same as the heat transfer coefficient increases with increasing frequency and peak-to-peak amplitude.

The oscillating motion of the sphere can be converted into an average velocity assuming a sinusoidal motion of the sphere.

$$V_{avg} = 2A_s F_s \tag{3.13}$$

Table 3.2 shows the equivalent average velocity of the sphere oscillating at a particular frequency and peak-to-peak amplitude.

The heat transfer coefficients are plotted as a function of superficial air velocities for different equivalent average sphere velocities in Figure 3.58. The heat transfer coefficient increases gradually as the average sphere velocity increases. However,

Table 3.3: Average velocity of the sphere oscillating at various frequencies and amplitudes

Peak-to-peak amplitude, cm	Frequency Hz	Average Velocity cm/s
1.8	1.1	3.96
4.0	2.0	7.20
4.0	1.1	8.80
1.8	2.85	10.26
6.9	1.1	15.18
4.0	2.00	16.00
4.0	2.85	22.8
6.9	2.00	27.6
6.9	2.85	39.33

at the average sphere velocities of 8.8 cm/s and 16.0 cm/s the heat transfer coefficient decreased unexpectedly. The increase in heat transfer coefficient was found to be more at the lower superficial air velocities as compared to the higher superficial air velocities. The variation in the heat transfer coefficient with the average velocity for four different superficial air velocities is shown in Figure 3.59. The heat transfer coefficient increases rapidly with increasing average sphere velocity at lower superficial velocity, e.g., at superficial velocity of 0.087 cm/s, the heat transfer coefficient increases by more than three times as the average sphere velocity increases from 3.96 cm/s to 39.33 cm/s. Whereas, at superficial air velocity of 1.95 cm/s, the heat transfer coefficient increases only by 20 % in the same range of the average sphere velocity. Figure 3.60 shows the heat transfer coefficient versus the superficial air velocity for various average velocity for a 1.0 cm sphere oscillating in a fluidized bed of 126-147 μm glass particles. The heat transfer coefficient increases rapidly with the average sphere velocity at lower superficial air velocity and increases gradually at higher superficial air velocity. At superficial air velocities of 7.6 cm/s and 14.9 cm/s the heat transfer coefficient remains almost constant as shown in Figure 3.61.

The heat transfer coefficient does not increase rapidly with the average sphere velocity at lower superficial air velocities in case of the 355-420 μm glass particles. As shown in Figure 3.63 an increase in the heat transfer coefficient with the average sphere velocity is very gradual and the scatter in data is much greater as compared to the other two powders. It is interesting to note that the heat transfer coefficient decreases with an increasing average sphere velocity for the fluidized bed of 355-420 μm glass particles. As shown in Figure 3.63, the heat transfer coefficient is about

7 % lower for the average sphere velocity of 27.6 cm/s as compare to the average sphere velocity of 3.96 cm/s at the superficial air velocity of 13.2 cm/s. At higher superficial velocities, the heat transfer coefficient decreases with increasing average sphere velocity. In fact for the superficial air velocities of 16.7, 18.5, 24.4 and 33.2 cm/s the heat transfer coefficient is lowest for the highest average sphere velocity of 39.33 cm/s. This decrease in the heat transfer coefficient with increase in the average sphere velocity is very peculiar and it is found only for the 355-420 μm glass particles.

3.4.1 Comparison with linearly downward moving sphere

The oscillating motion of the sphere can be converted in to an equivalent average linear velocity. The average velocities obtained by the equation 3.13 is listed in Table 3.3. Using this average sphere velocity for an oscillating sphere, the heat transfer results obtained for an oscillating sphere can be compared with that of the linearly downward moving sphere. In case of the linearly downward moving sphere, the sphere was allowed to travel in six different velocities; 0.4, 1.1, 1.9, 3.0, 4.6, 7.5 cm/s. Whereas, the average sphere velocity varies from 3.96 to 39.33 cm/s in case of the oscillating sphere. In Figures 3.64, 3.65 and 3.66, the heat transfer coefficient for 1.0 cm sphere moving in a linearly downward motion at 4.6 cm/s and 7.5 cm/s in a fluidized beds of various size glass particles is compared to the heat transfer coefficient for a sphere oscillating at an average velocity of 3.96 cm/s and 7.20 cm/s respectively under the same conditions. At the minimum fluidization condition, the heat transfer coefficient for an oscillating sphere with an average sphere velocity

of 7.2 cm/s is 250 W/M^2 K and for a sphere moving in linearly downward direction at 7.5 cm/s is 650 W/M^2 K. The heat transfer coefficient was observed to be about 260 % higher for the linearly moving sphere when compared to the oscillating sphere with almost the same average velocity at lower superficial air velocity. At higher superficial air velocities, the difference in the heat transfer coefficients for the oscillating and linearly moving spheres is negligible.

Figure 3.65 shows the heat transfer coefficient as a function of the superficial air velocity and for various average sphere velocities for an oscillating and linearly moving sphere in side the fluidized bed of 126-147 μm glass particles. The heat transfer coefficient at minimum fluidization condition for the case of an oscillating sphere is about 1.5 times lower than that of a linearly downward moving sphere which is lower than that of 5-44 μm glass particle system. However the general trend is the same as that of the 5-44 μm glass particle system. At higher superficial air velocities, the heat transfer coefficient remains almost constant for the range of the average sphere velocities shown in the Figure 3.65.

For 355-420 μm glass particles, the heat transfer coefficient is only about 40 % higher for a linearly downward moving sphere at 7.5 cm/s as compared to an oscillating sphere with an average sphere velocity of 7.2 cm/s near minimum fluidization condition. The two curves, for the oscillating sphere and the linearly downward moving sphere crosse at a superficial air velocity of 17 cm/s as shown in Figure 3.66. For superficial air velocities, greater than 17 cm/s, the heat transfer coefficient is consistently higher for the case of an oscillating sphere than a linearly downward moving sphere. Thus, the oscillating sphere is the more efficient for 355-

420 μm glass particles system as it gives a higher heat transfer coefficients at higher superficial air velocities. The high heat transfer coefficient obtained for the case of a linearly downward moving sphere as compare to the oscillating sphere at lower superficial air velocities can be physically explained as follow: at low superficial air velocity, the particulate phase circulation is absent, and hence, the oscillating sphere, comes in contact with the same emulsion packet again and again increasing the temperature of the emulsion packet and reducing the overall heat transfer coefficient. However, in case of a linearly downward moving sphere, although there is no particulate circulation at low superficial air velocities, the sphere moving through the bed comes in contact with a fresh (cold) emulsion packet as it moves down the fluidized bed and hence the heat transfer coefficient is very high.

As can be seen from the table 3.3, for certain combinations of peak-to-peak amplitudes and frequencies, the average sphere velocity remains the same, e.g., at peak-to-peak amplitude of 6.9 cm and frequency of 1.0 Hz, the average sphere velocity is 15.18 cm/s while, for a peak-to-peak amplitude of 4.0 cm and frequency of 2.0 Hz, the average sphere velocity is 16.0 cm/s. Hence it is reasonable to expect that the heat transfer coefficients obtained for these two combination should be close. Figures 3.67, 3.68 and 3.68 compares two such cases for each glass powder and each sphere. The heat transfer coefficients remains the same for the two combinations of the amplitudes and frequencies for which the average sphere velocities are almost the same for each sphere size. Furthermore, as in case of a stationary sphere, the heat transfer coefficient increases with decreasing sphere diameter for an oscillating sphere.

It follows in general from the aforementioned results that the heat transfer coefficient increases with increasing frequency and amplitude. The only exception found in this study was for the 355-420 μm glass particle system, in which the heat transfer coefficient at the higher frequency was observed to decrease. The motion of the heat transfer surface relative to the particulate phase and to the gas phase generates a greater disturbance, enhancing the heat transfer. Reed and Fenske [1955] conducted an experiment to study the effect vibration of an hollow element with extended surface on heat transfer coefficient in a fluidized beds of nickel powder, lead powder, steel shot and carbon granules. They showed that at low superficial air velocity of 6.1 cm/s, the heat transfer coefficient increased by 66 % for a plate vibrating at 2000 cycles/min and 0.795 cm stroke when compared to a stationary plate. For a superficial air velocity at and below 30.5 cm/s the vibrating motion of the plate was effective in enhancing the heat transfer coefficient. At higher superficial air velocities of 115 cm/s and 228.6 cm/s used to fluidized steel shot, the vibrating motion of the plate had essentially no effect on the heat transfer coefficient. Moreover they showed that the heat transfer coefficient increased with the vibration frequency up to 1000 cycles/min and a stroke of 0.795 cm for nickel powder fluidized by air at 6.1 cm/s superficial velocity. Beyond this vibration frequency, the heat transfer coefficient was observed to decrease with increasing frequency.

Recently, some experiments have been carried out in which instead of vibrating the heat transfer surface, the fluidized bed itself is mounted on a vibrating table, in order to study its effect on heat transfer coefficient. Lu Wei-Ming et al. [1976] and Malhotra and Majumdar [1987] studied such effect. They found that

the heat transfer coefficient to a stationary sphere increases as the amplitude and frequency of the fluidized bed vibration increased in lower superficial gas velocity region. Wei-Ming Lu et al. found that for values of Reynold number based on the sphere diameter and gas properties greater than 1000, the effect of the fluidized bed vibration on the heat transfer was negligible. Their results also showed that the higher gas flow rate did not increase the heat transfer coefficient of the system if the vibration intensity, $a\omega^2/g$ is greater than 3. These findings are similar in nature with the present investigation.

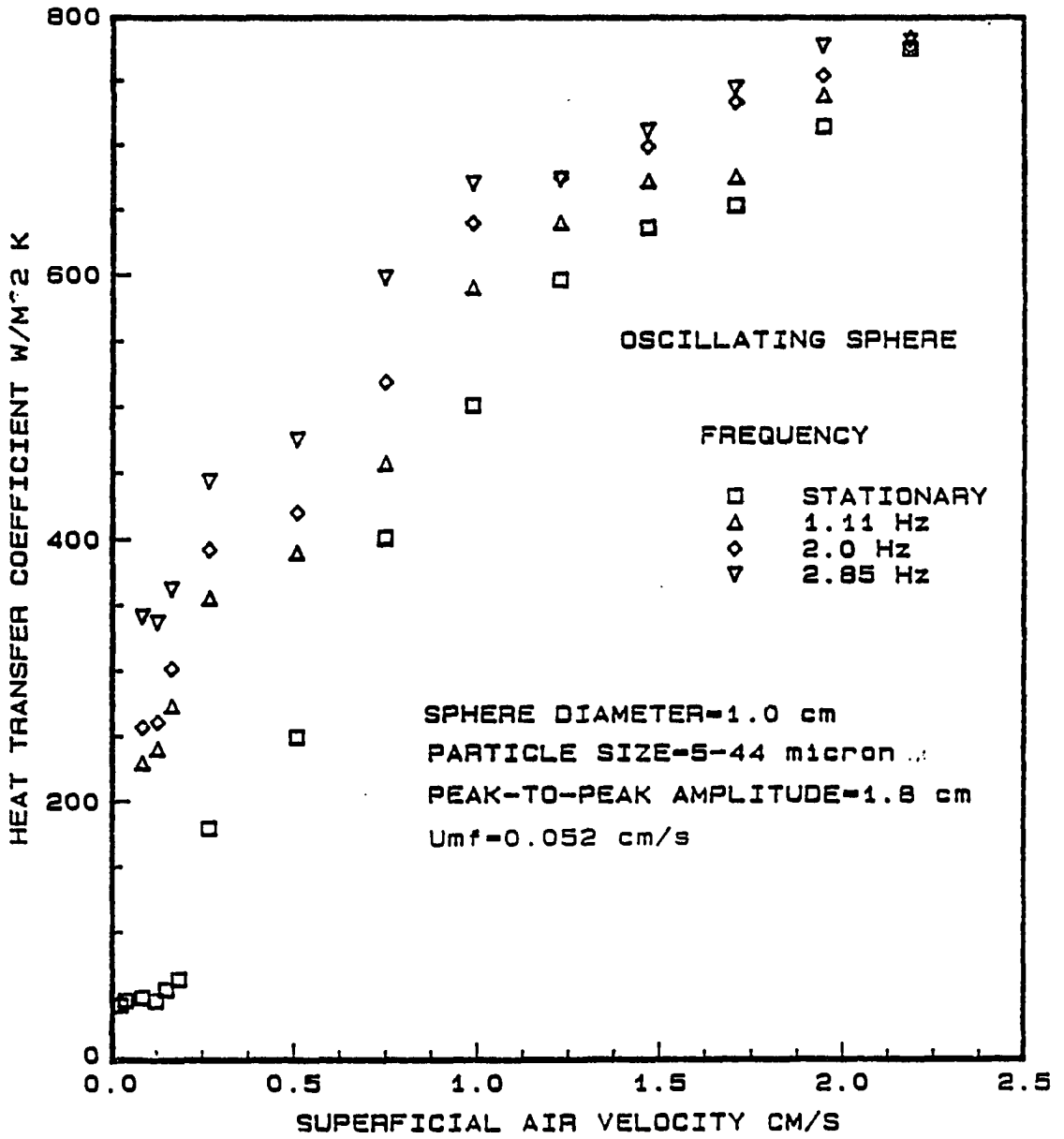

Figure 3.31: Heat transfer coefficient of a 1.0 cm copper sphere in oscillating motion (various frequencies) with the peak-to-peak amplitude of 1.8 cm versus superficial air velocity for a fluidized bed of 5-44 μm glass particles

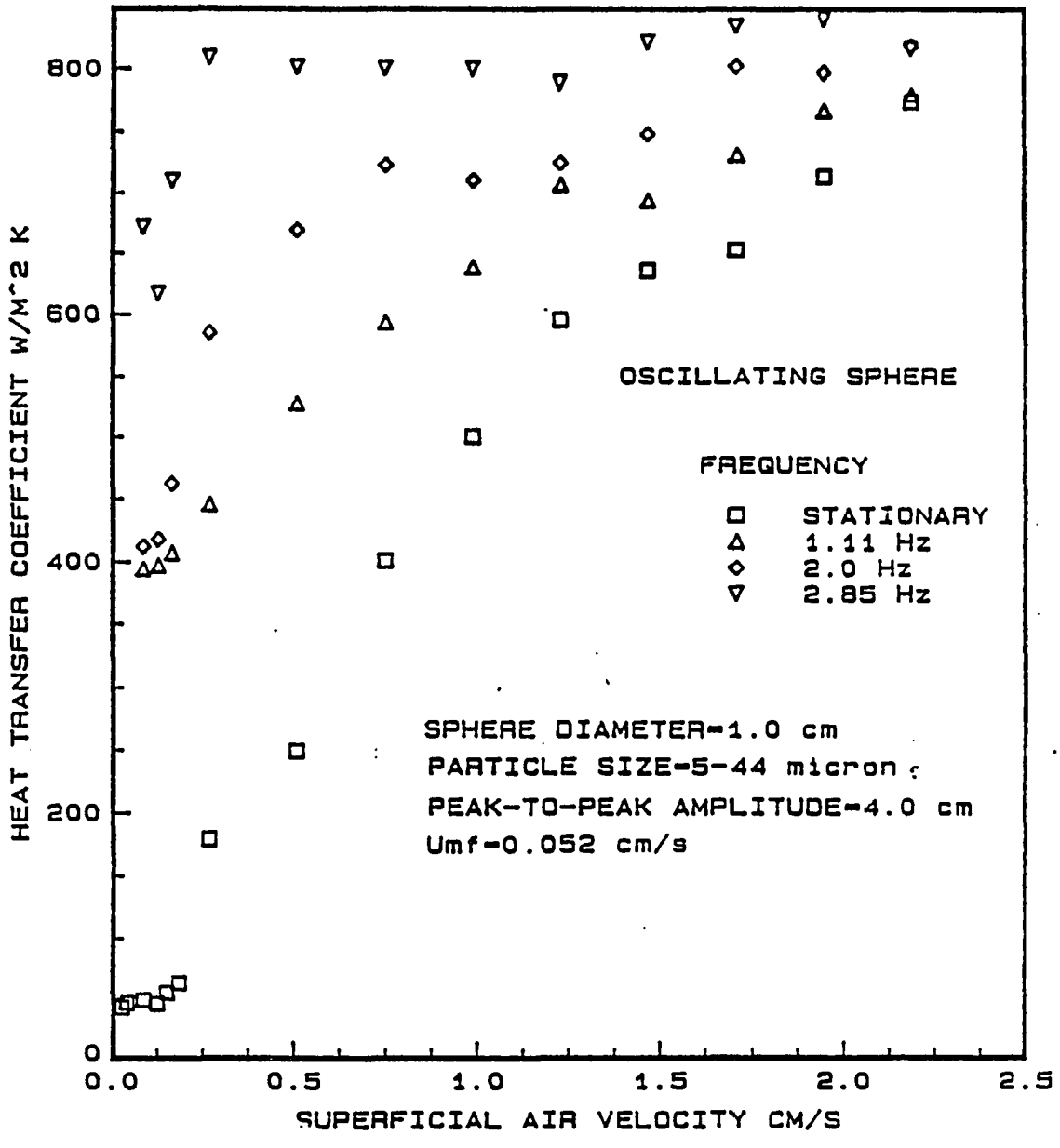

Figure 3.32: Heat transfer coefficient of a 1.0 cm copper sphere in oscillating motion (various frequencies) with the peak-to-peak amplitude of 4.0 cm versus superficial air velocity for a fluidized bed of 5-44 μm glass particles

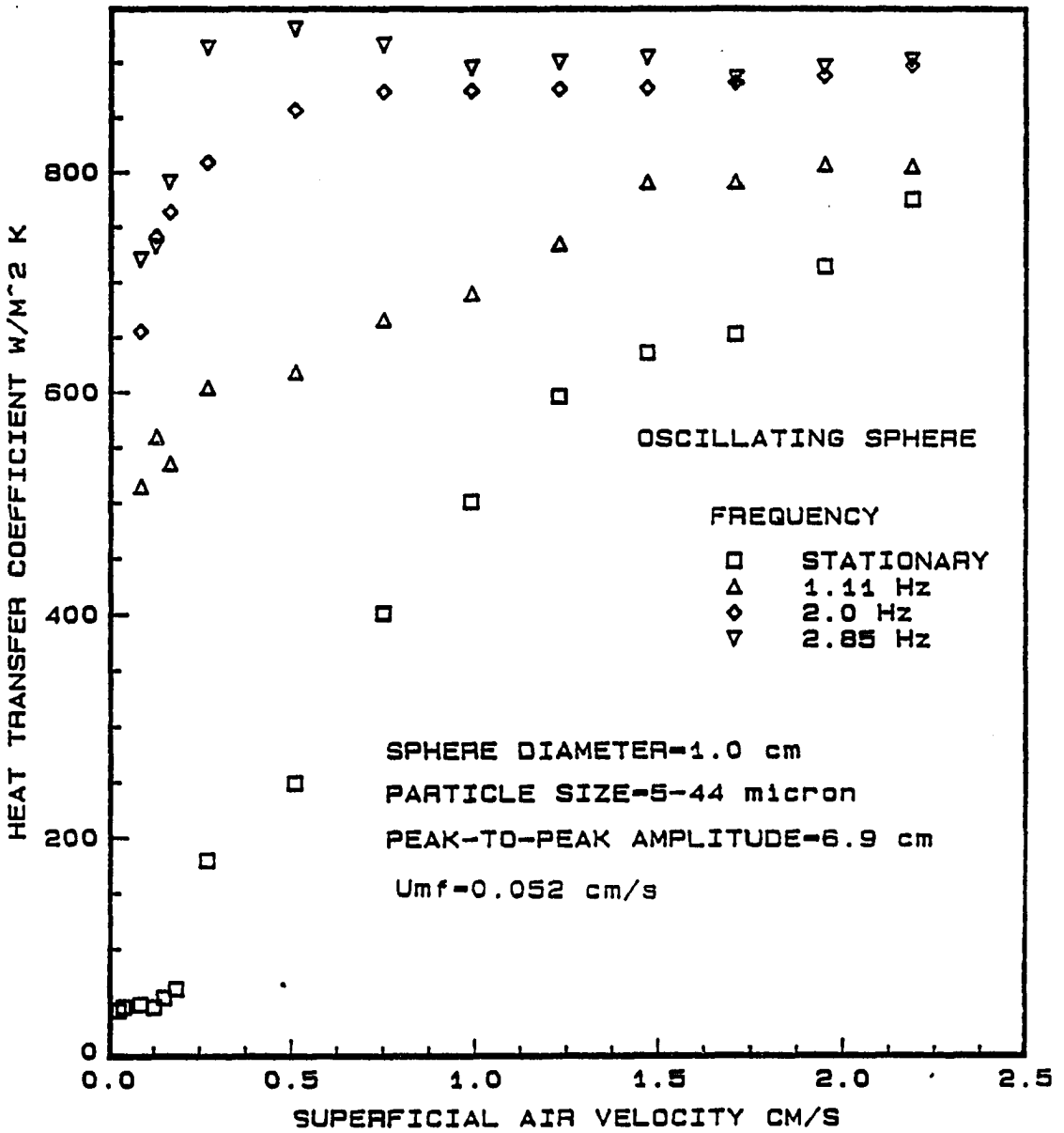

Figure 3.33: Heat transfer coefficient of a 1.0 cm copper sphere in oscillating motion (various frequencies) with the peak-to-peak amplitude of 6.9 cm versus superficial air velocity for a fluidized bed of 5-44 μm glass particles

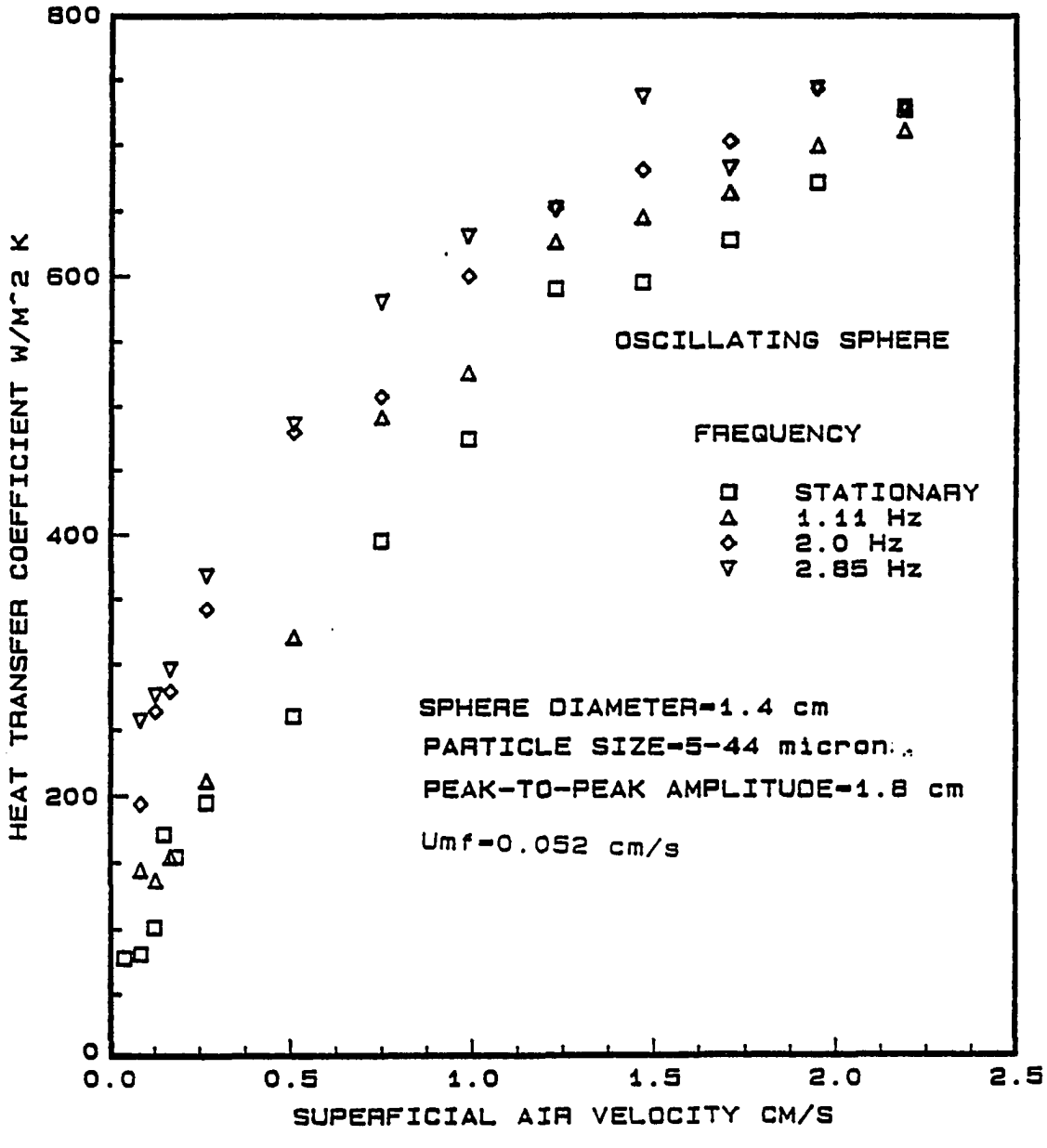

Figure 3.34: Heat transfer coefficient of a 1.4 cm copper sphere in oscillating motion (various frequencies) with the peak-to-peak amplitude of 1.8 cm versus superficial air velocity for a fluidized bed of 5-44 μm glass particles

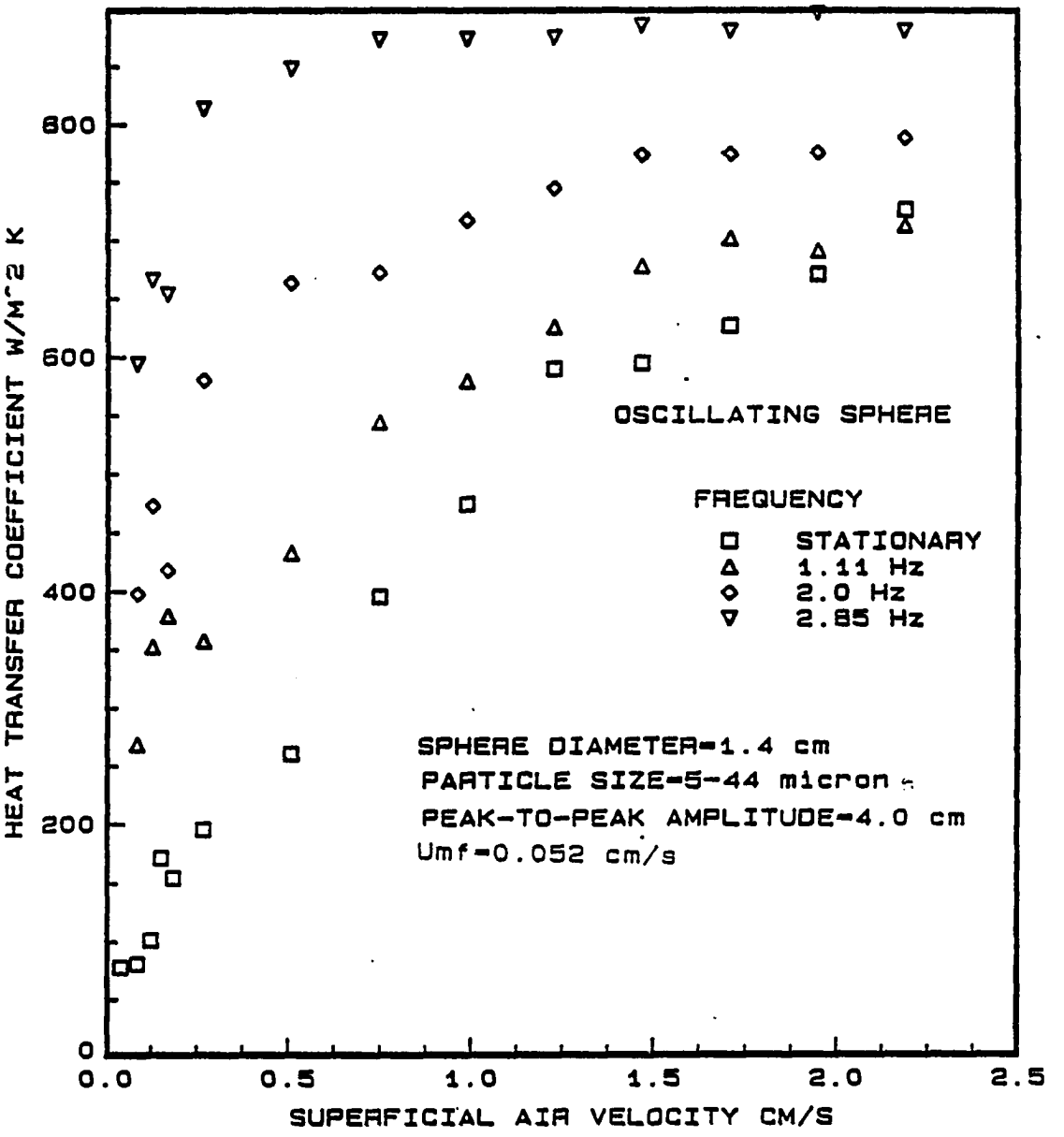

Figure 3.35: Heat transfer coefficient of a 1.4 cm copper sphere in oscillating motion (various frequencies) with the peak-to-peak amplitude of 4.0 cm versus superficial air velocity for a fluidized bed of 5-44 μm glass particles

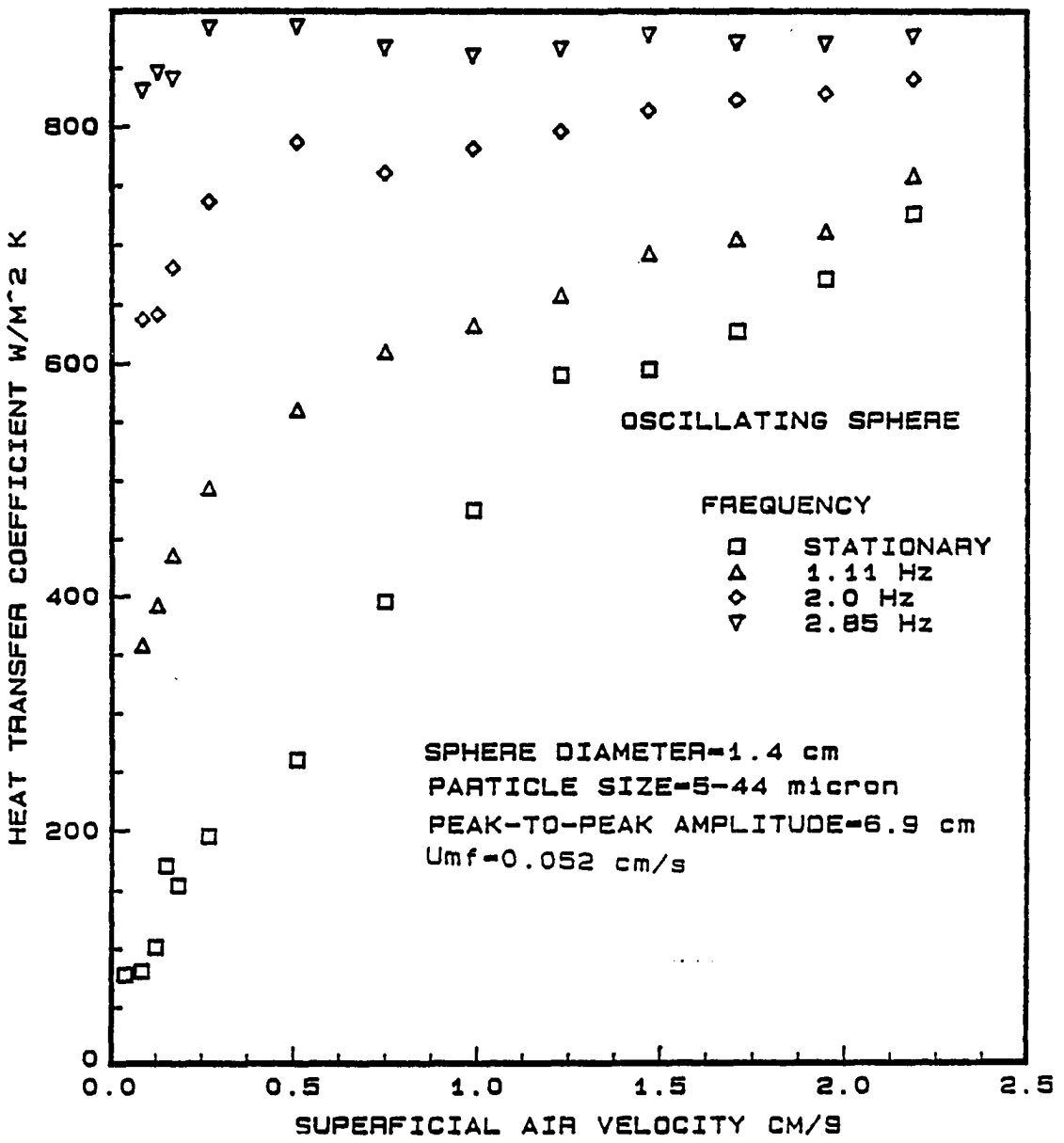

Figure 3.36: Heat transfer coefficient of a 1.4 cm copper sphere in oscillating motion (various frequencies) with the peak-to-peak amplitude of 6.9 cm versus superficial air velocity for a fluidized bed of 5-44 μm glass particles

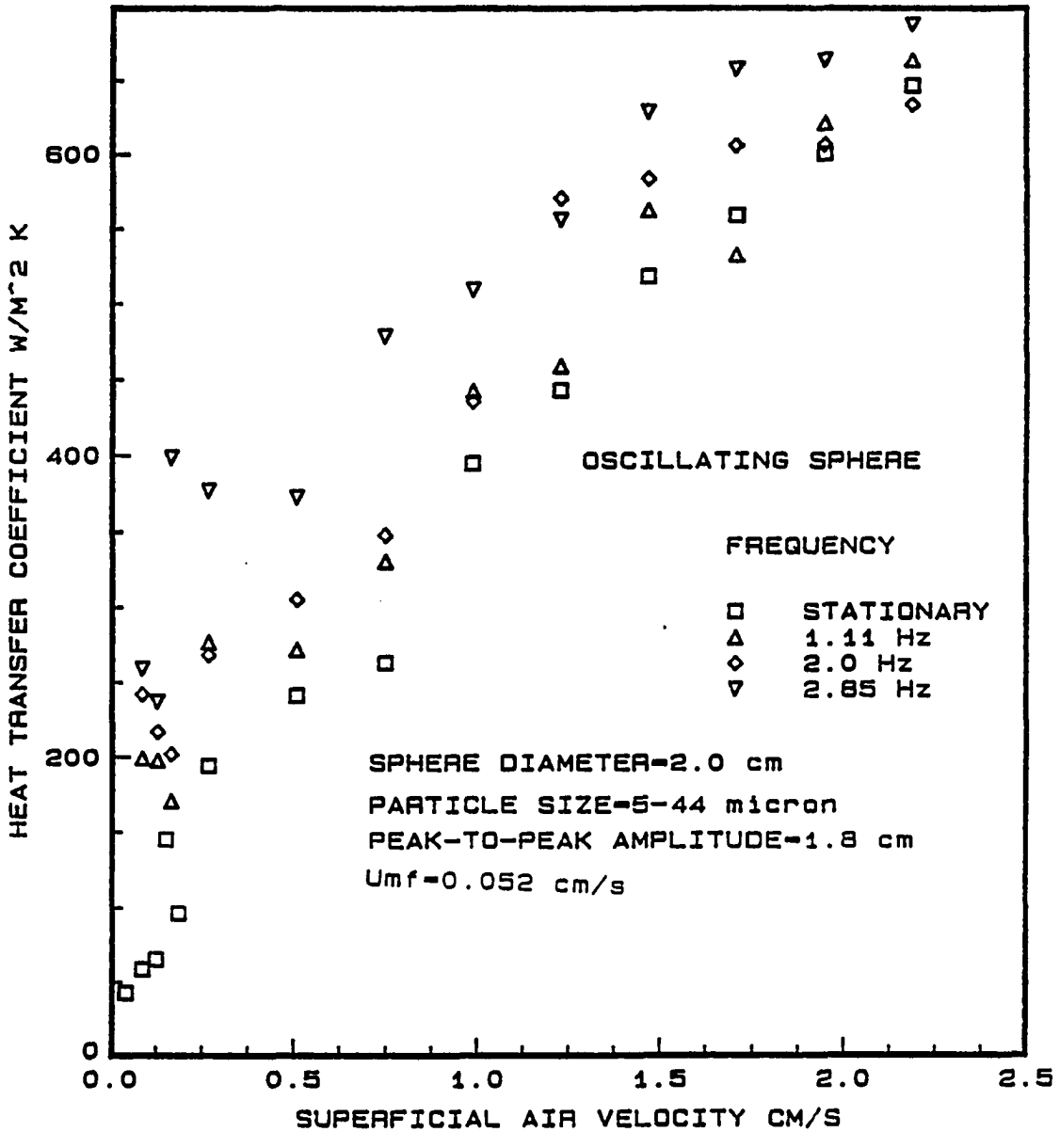

Figure 3.37: Heat transfer coefficient of a 2.0 cm copper sphere in oscillating motion (various frequencies) with the peak-to-peak amplitude of 1.8 cm versus superficial air velocity for a fluidized bed of 5-44 μm glass particles

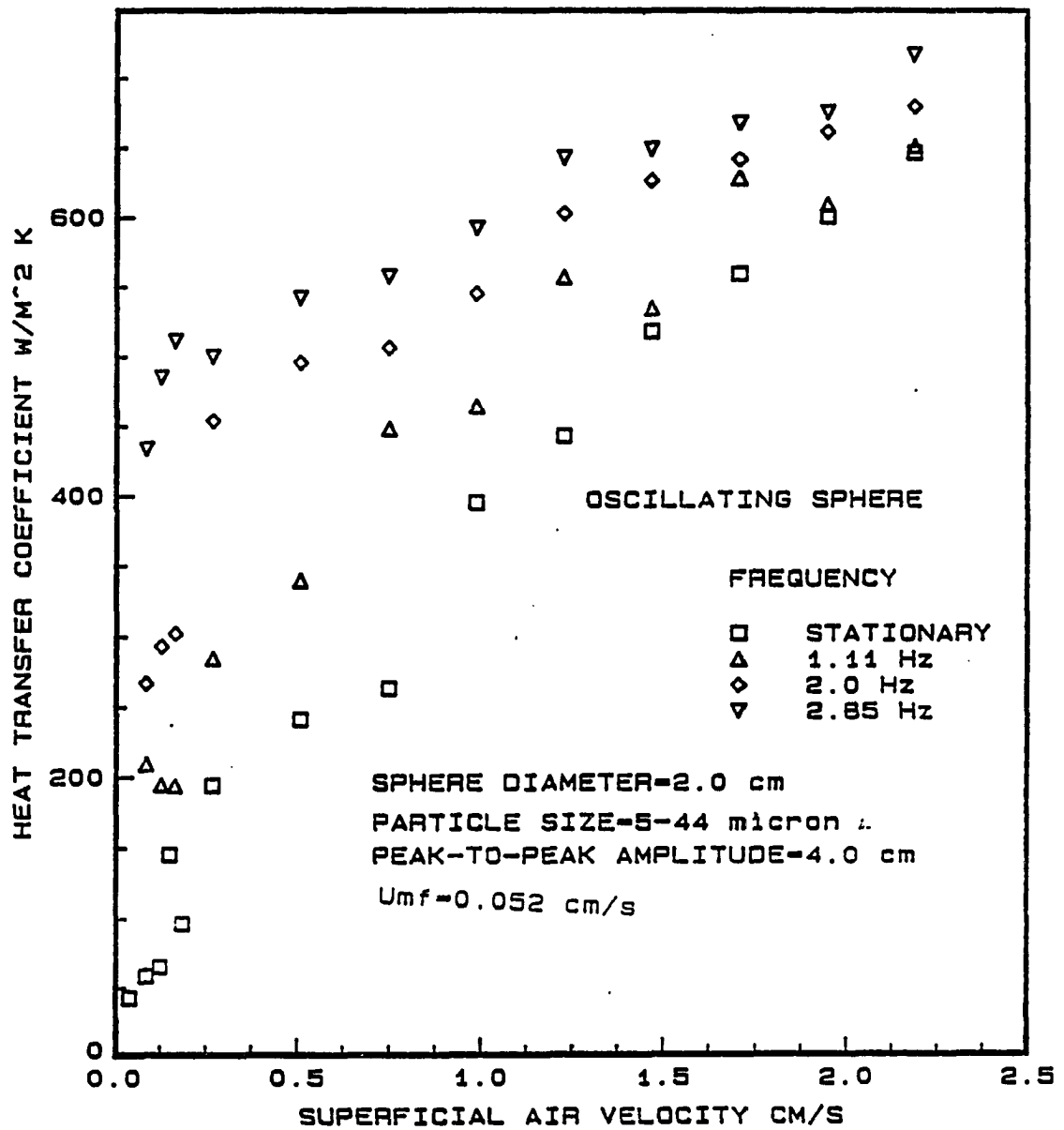

Figure 3.38: Heat transfer coefficient of a 2.0 cm copper sphere in oscillating motion (various frequencies) with the peak-to-peak amplitude of 4.0 cm versus superficial air velocity for a fluidized bed of 5-44 μm glass particles

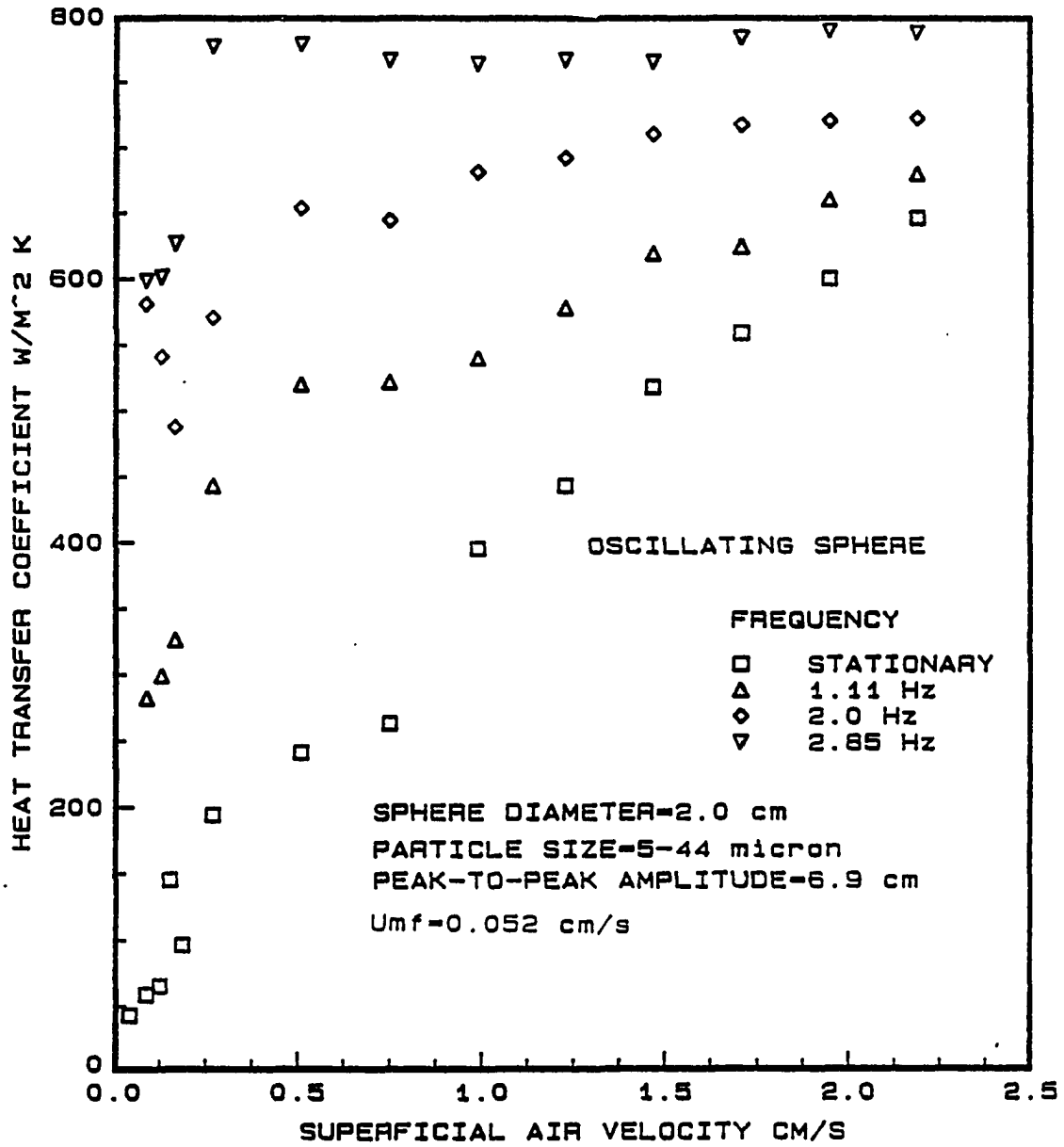

Figure 3.39: Heat transfer coefficient of a 2.0 cm copper sphere in oscillating motion (various frequencies) with the peak-to-peak amplitude of 6.9 cm versus superficial air velocity for a fluidized bed of 5-44 μm glass particles

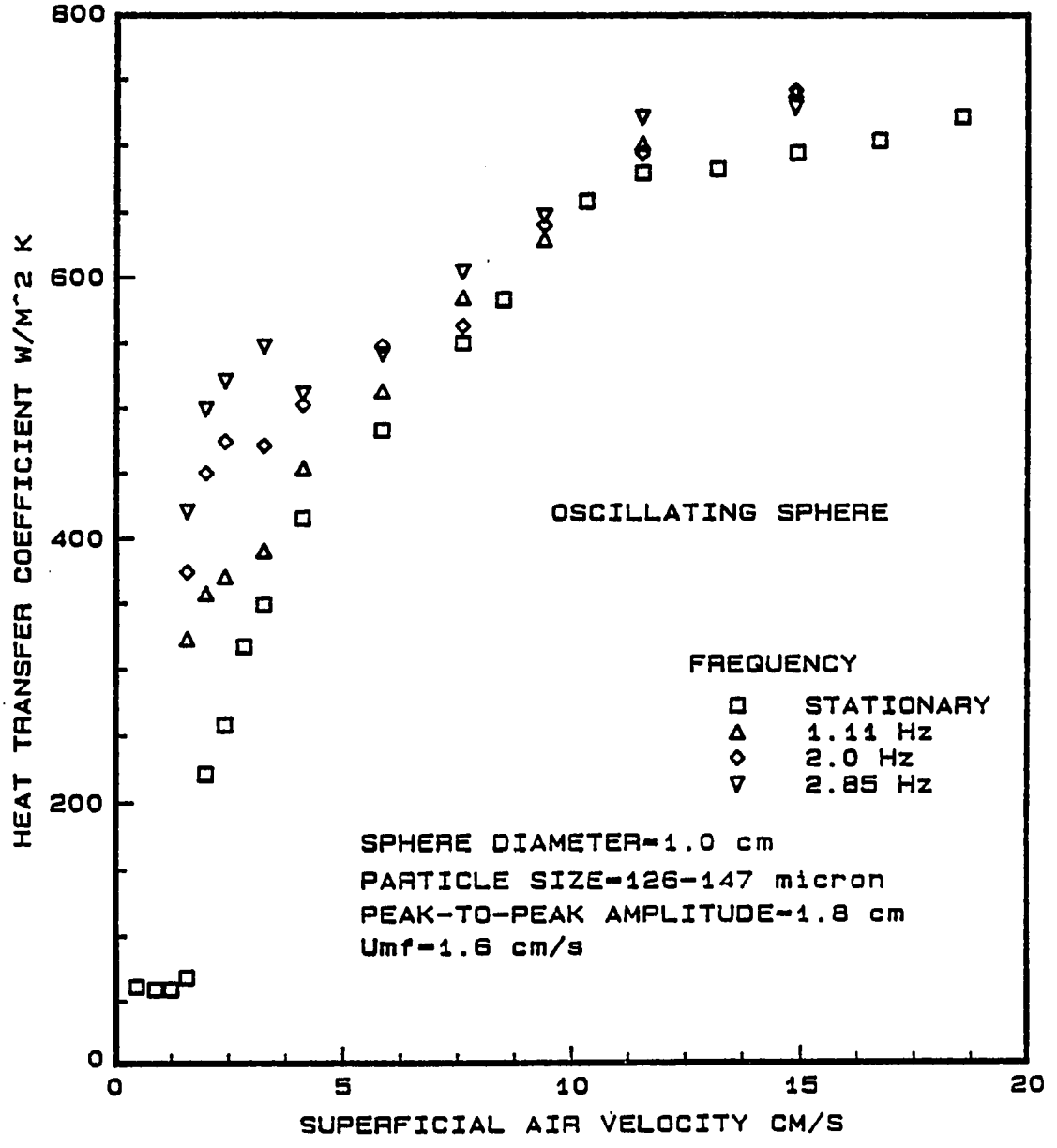

Figure 3.40: Heat transfer coefficient of a 1.0 cm copper sphere in oscillating motion (various frequencies) with the peak-to-peak amplitude of 1.8 cm versus superficial air velocity for a fluidized bed of 126-147 μm glass particles

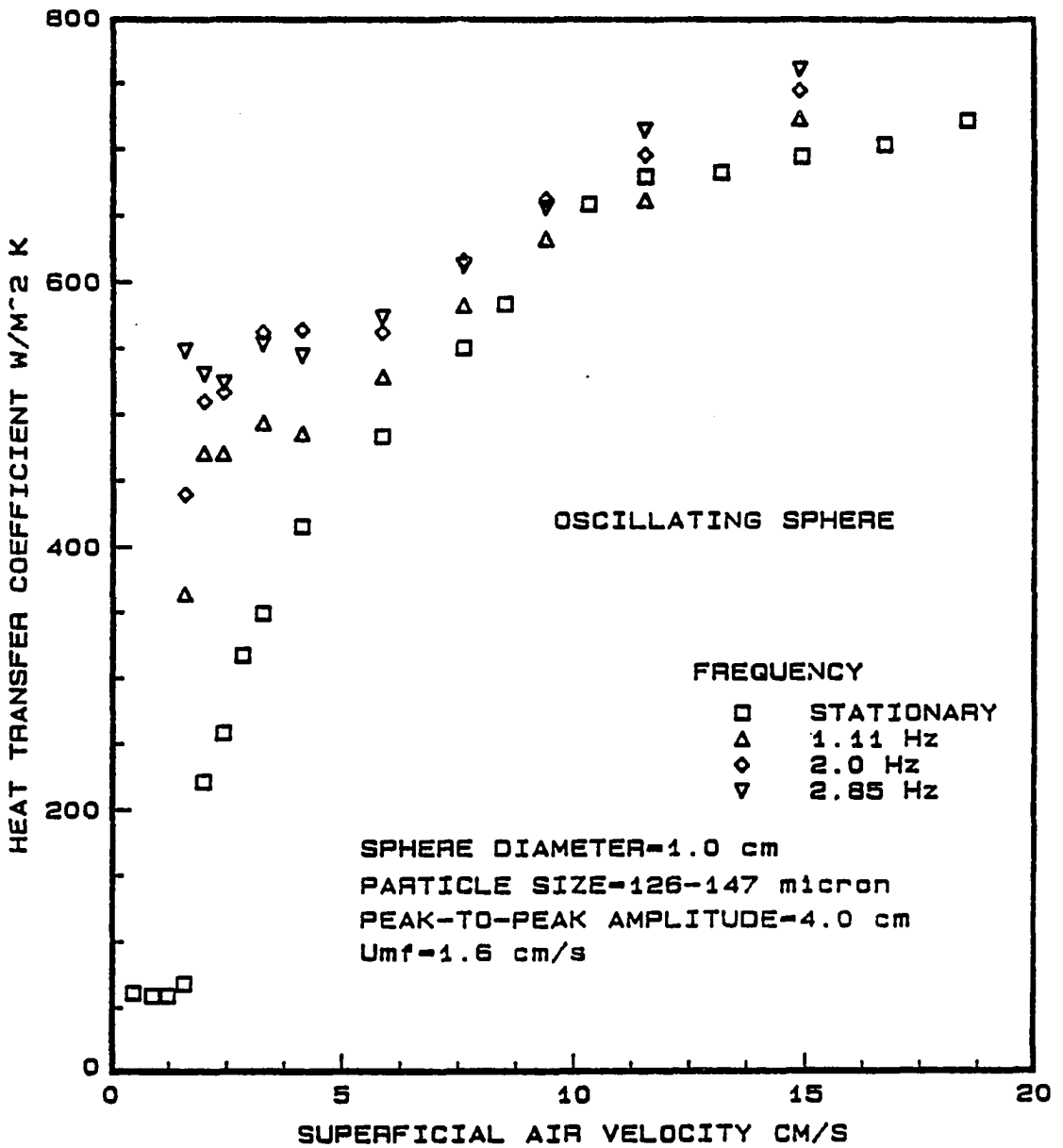

Figure 3.41: Heat transfer coefficient of a 1.0 cm copper sphere in oscillating motion (various frequencies) with the peak-to-peak amplitude of 4.0 cm versus superficial air velocity for a fluidized bed of 126-147 μm glass particles

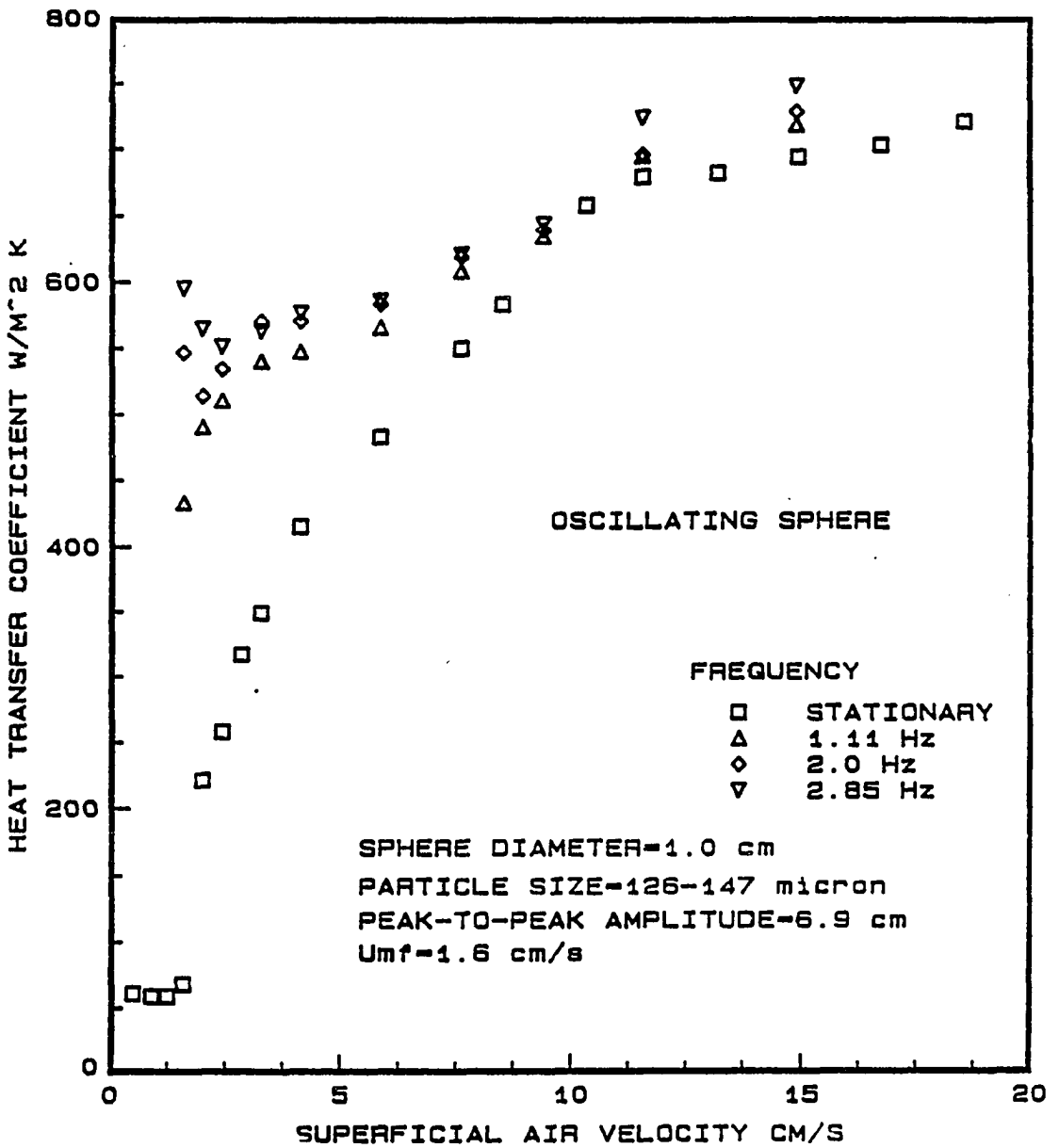

Figure 3.42: Heat transfer coefficient of a 1.0 cm copper sphere in oscillating motion (various frequencies) with the peak-to-peak amplitude of 6.9 cm versus superficial air velocity for a fluidized bed of 126-147 μm glass particles

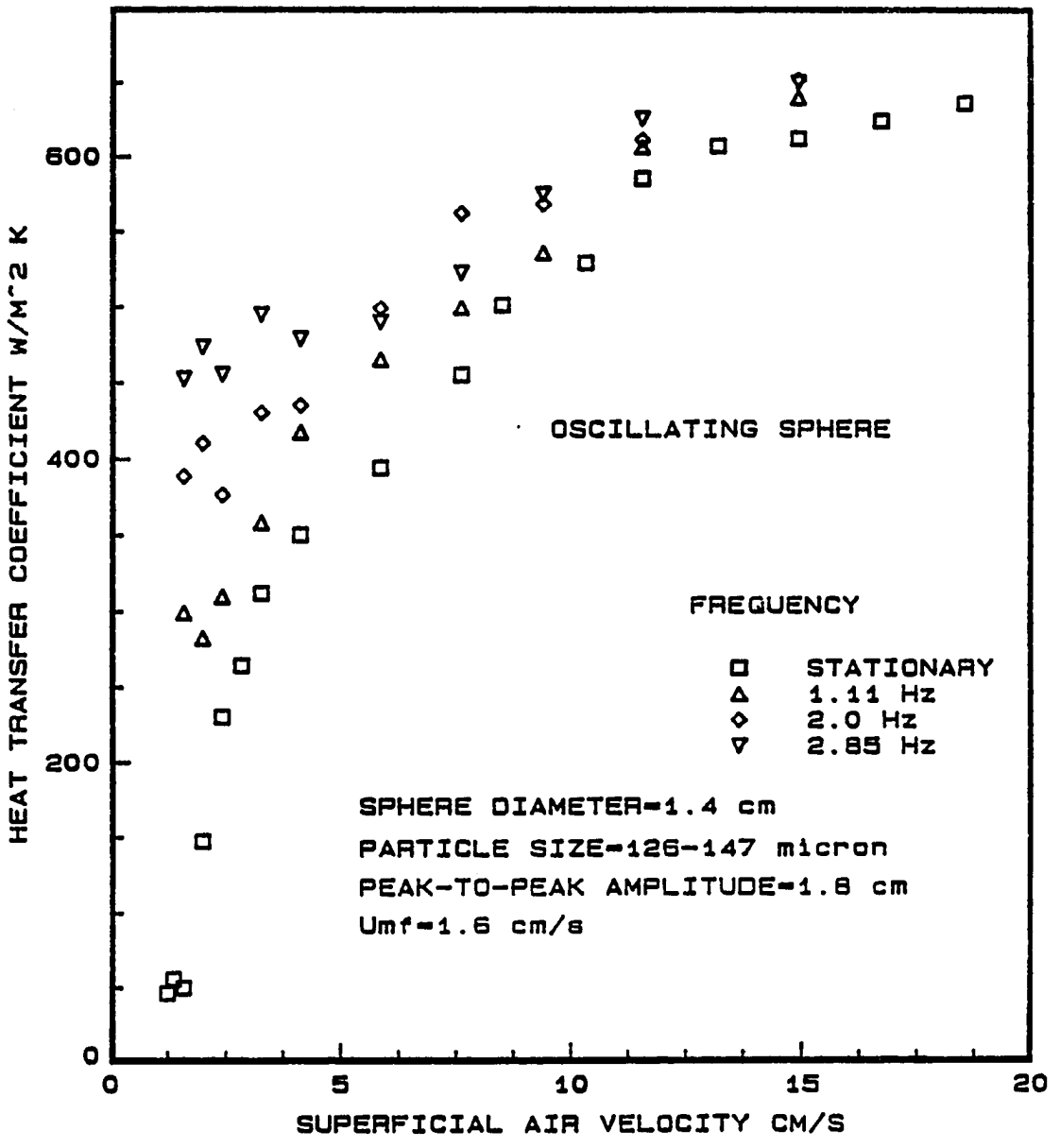

Figure 3.43: Heat transfer coefficient of a 1.4 cm copper sphere in oscillating motion (various frequencies) with the peak-to-peak amplitude of 1.8 cm versus superficial air velocity for a fluidized bed of 126-147 μm glass particles

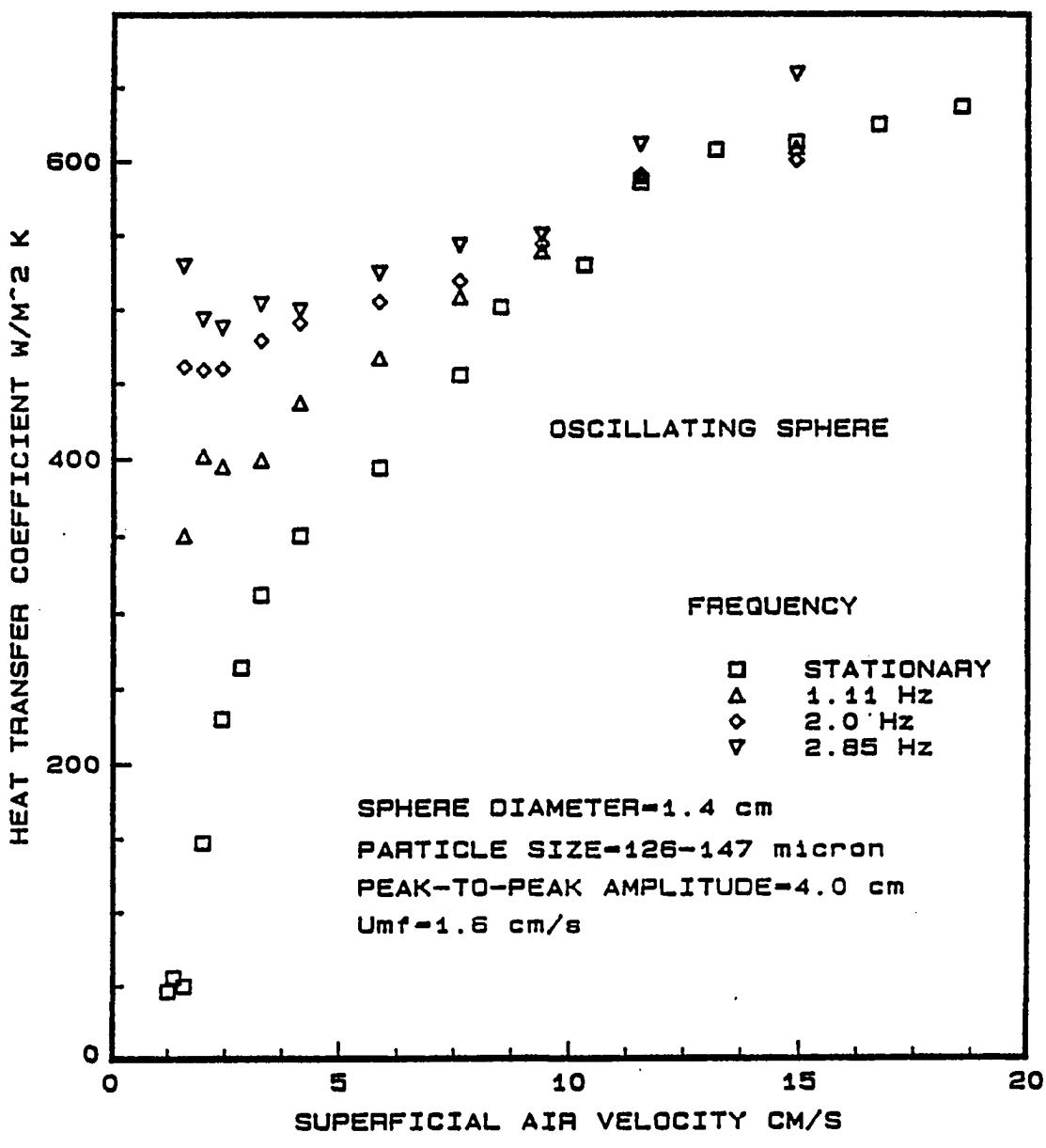

Figure 3.44: Heat transfer coefficient of a 1.4 cm copper sphere in oscillating motion (various frequencies) with the peak-to-peak amplitude of 4.0 cm versus superficial air velocity for a fluidized bed of 126-147 μm glass particles

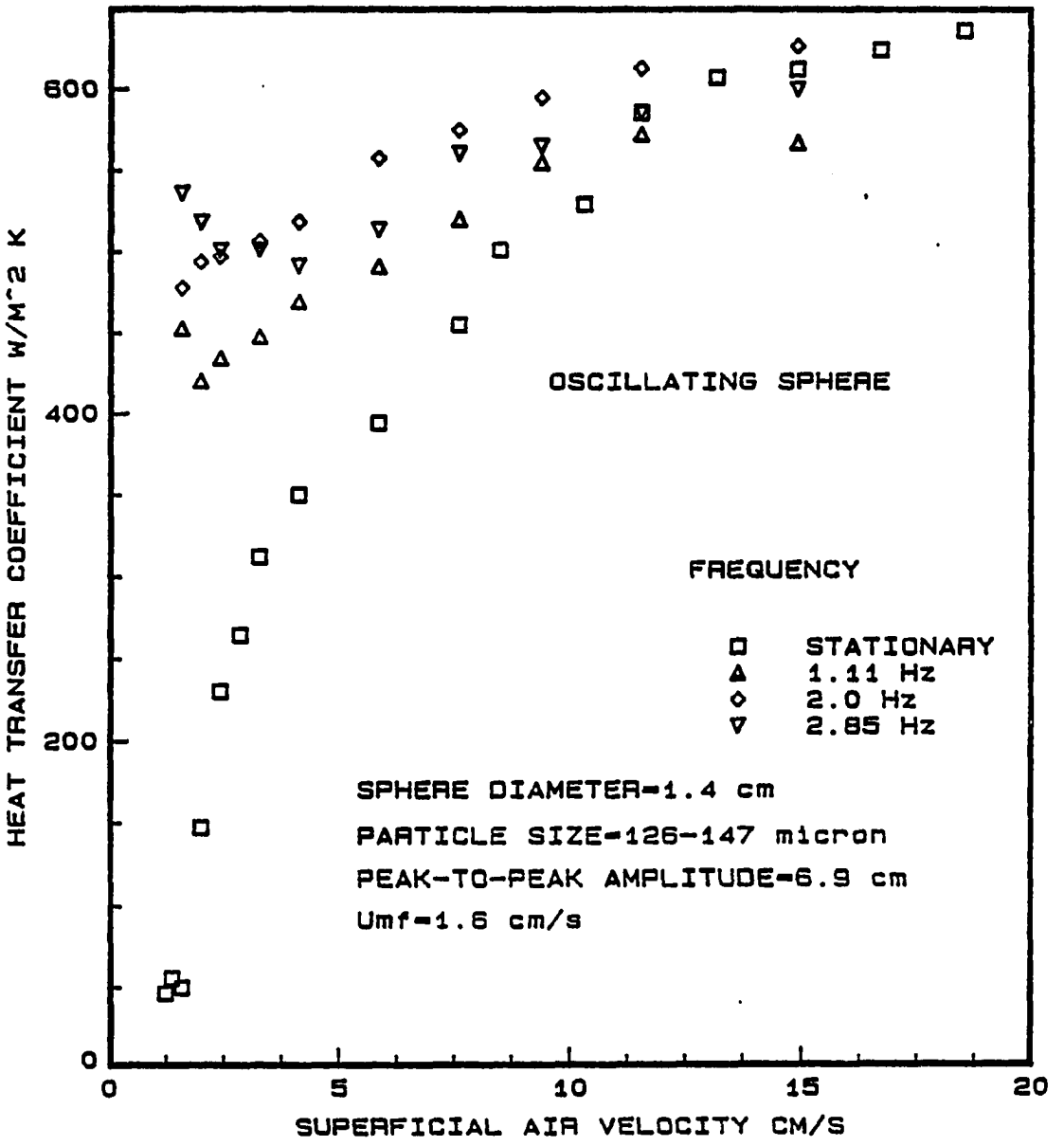

Figure 3.45: Heat transfer coefficient of a 1.4 cm copper sphere in oscillating motion (various frequencies) with the peak-to-peak amplitude of 6.9 cm versus superficial air velocity for a fluidized bed of 126-147 μm glass particles

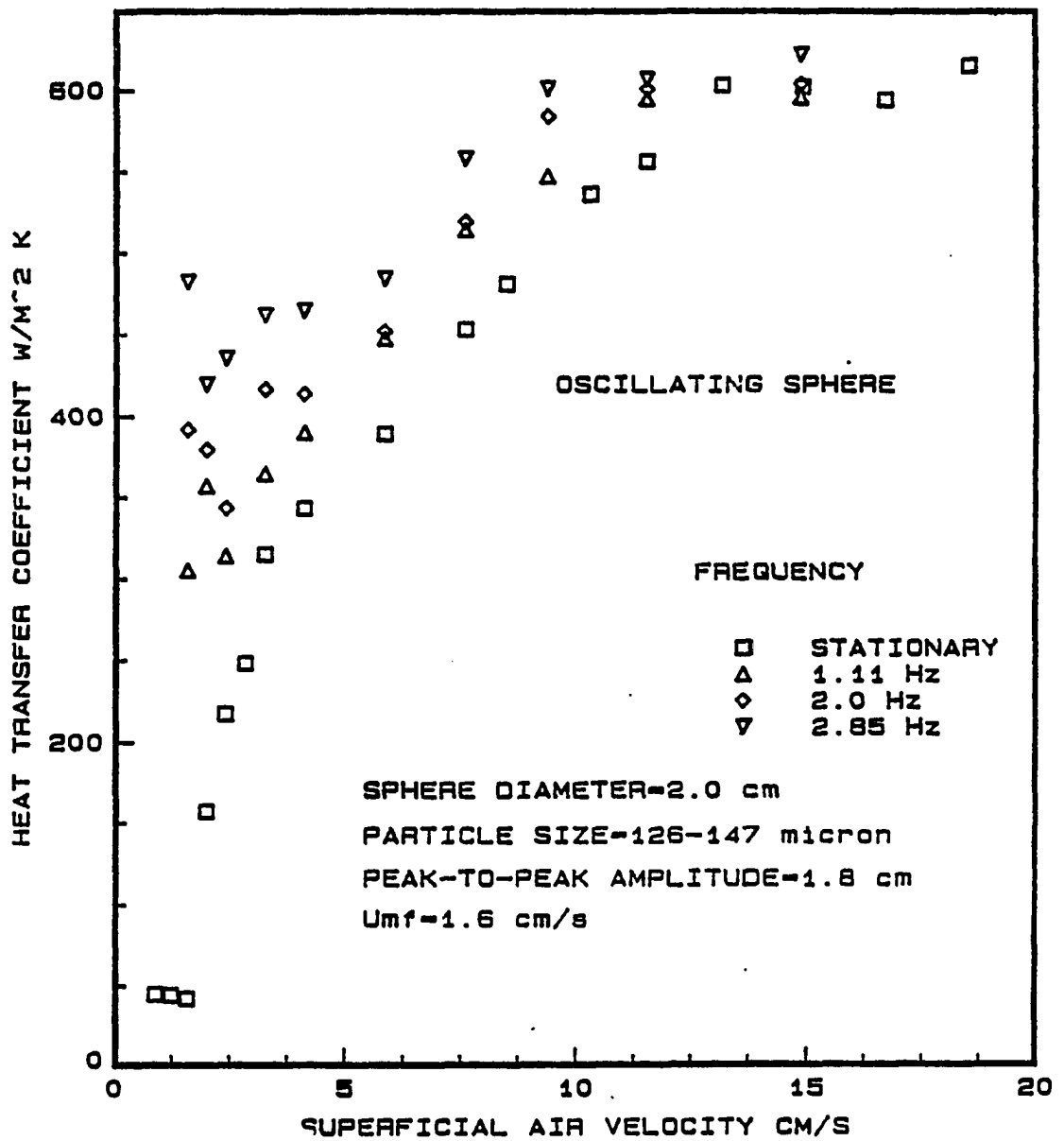

Figure 3.46: Heat transfer coefficient of a 2.0 cm copper sphere in oscillating motion (various frequencies) with the peak-to-peak amplitude of 1.8 cm versus superficial air velocity for a fluidized bed of 126-147 μm glass particles

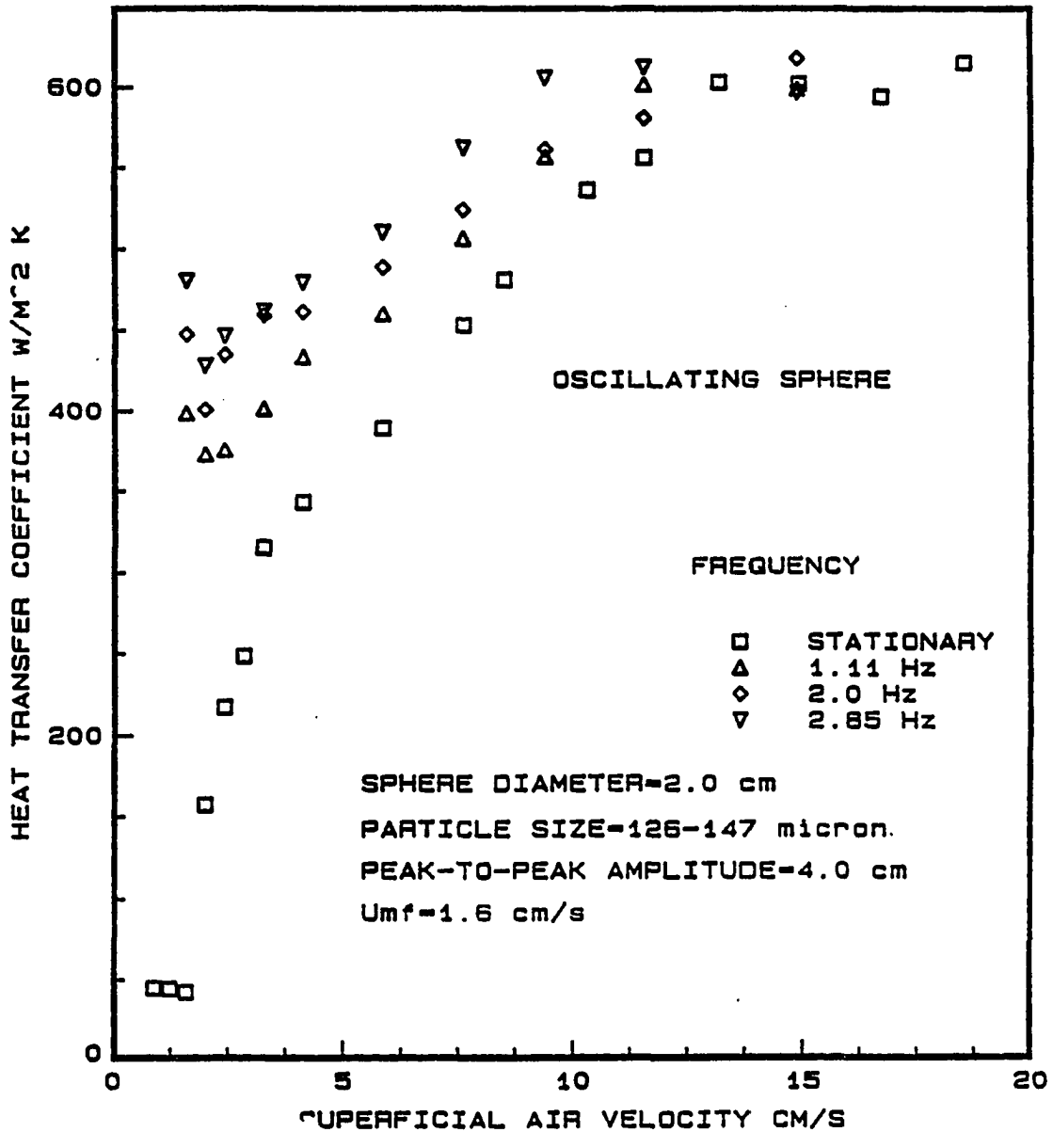

Figure 3.47: Heat transfer coefficient of a 2.0 cm copper sphere in oscillating motion (various frequencies) with the peak-to-peak amplitude of 4.0 cm versus superficial air velocity for a fluidized bed of 126-147 μm glass particles

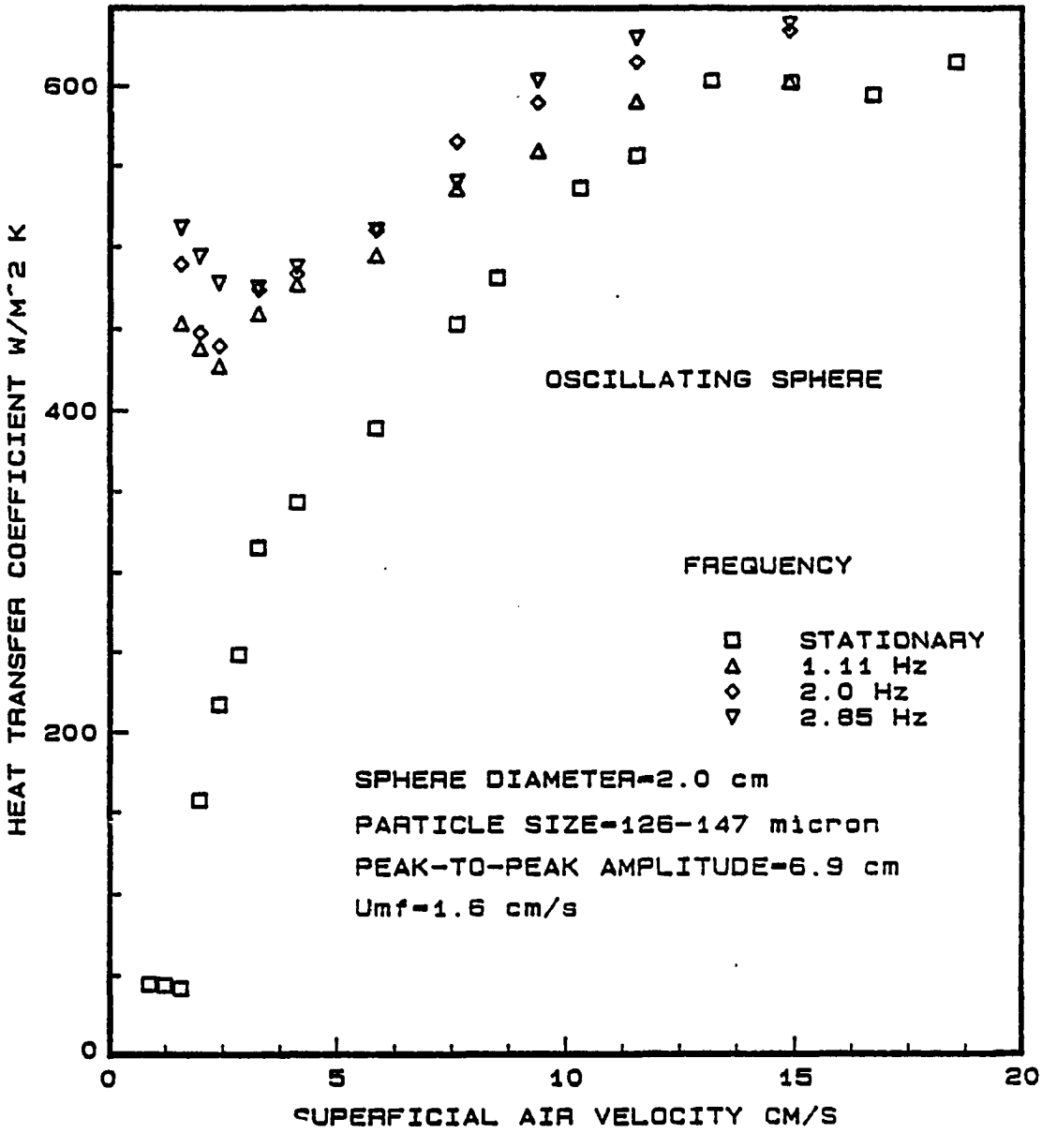

Figure 3.48: Heat transfer coefficient of a 2.0 cm copper sphere in oscillating motion (various frequencies) with the peak-to-peak amplitude of 6.9 cm versus superficial air velocity for a fluidized bed of 126-147 μm glass particles

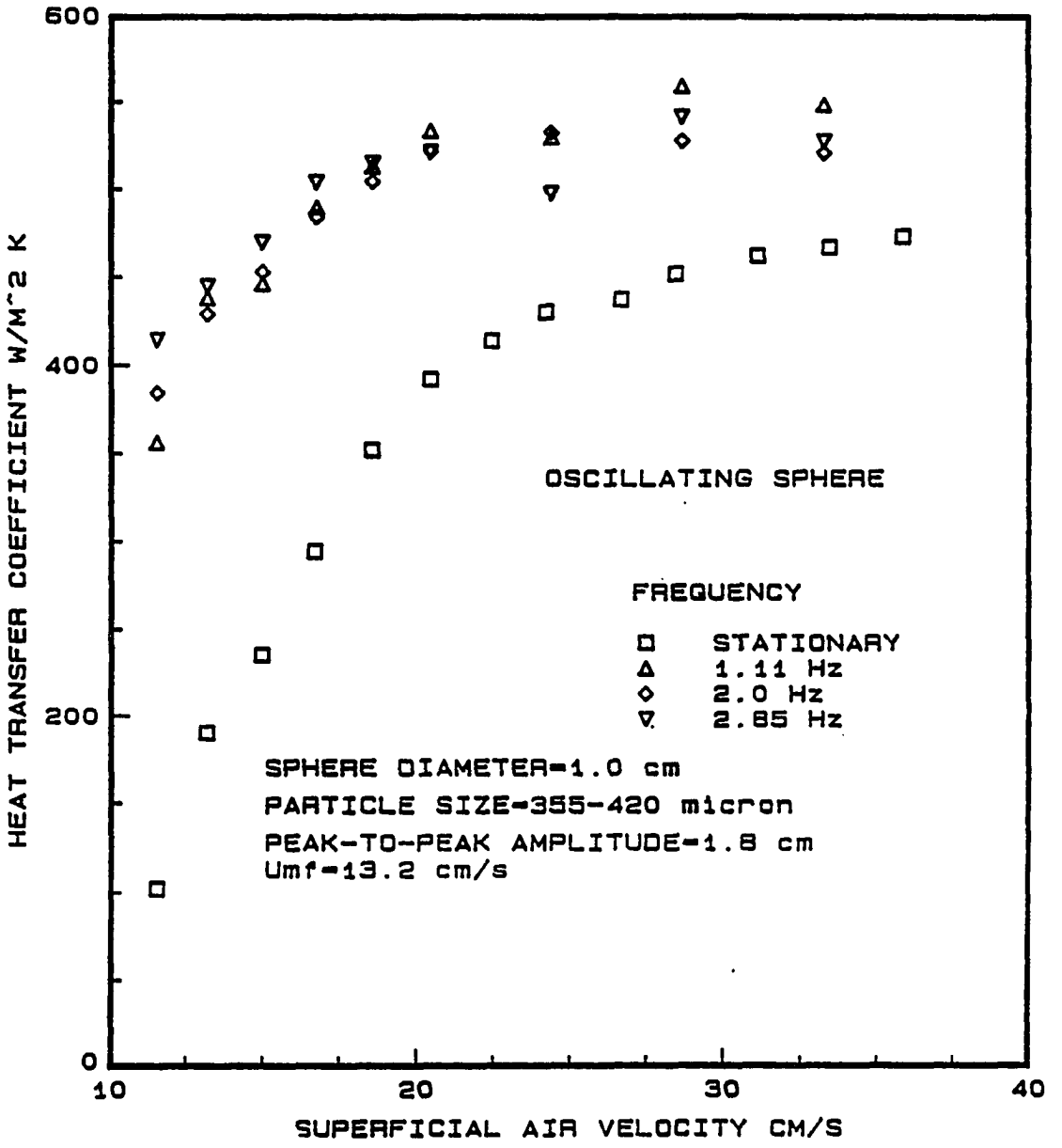

Figure 3.49: Heat transfer coefficient of a 1.0 cm copper sphere in oscillating motion (various frequencies) with the peak-to-peak amplitude of 1.8 cm versus superficial air velocity for a fluidized bed of 355-420 μm glass particles

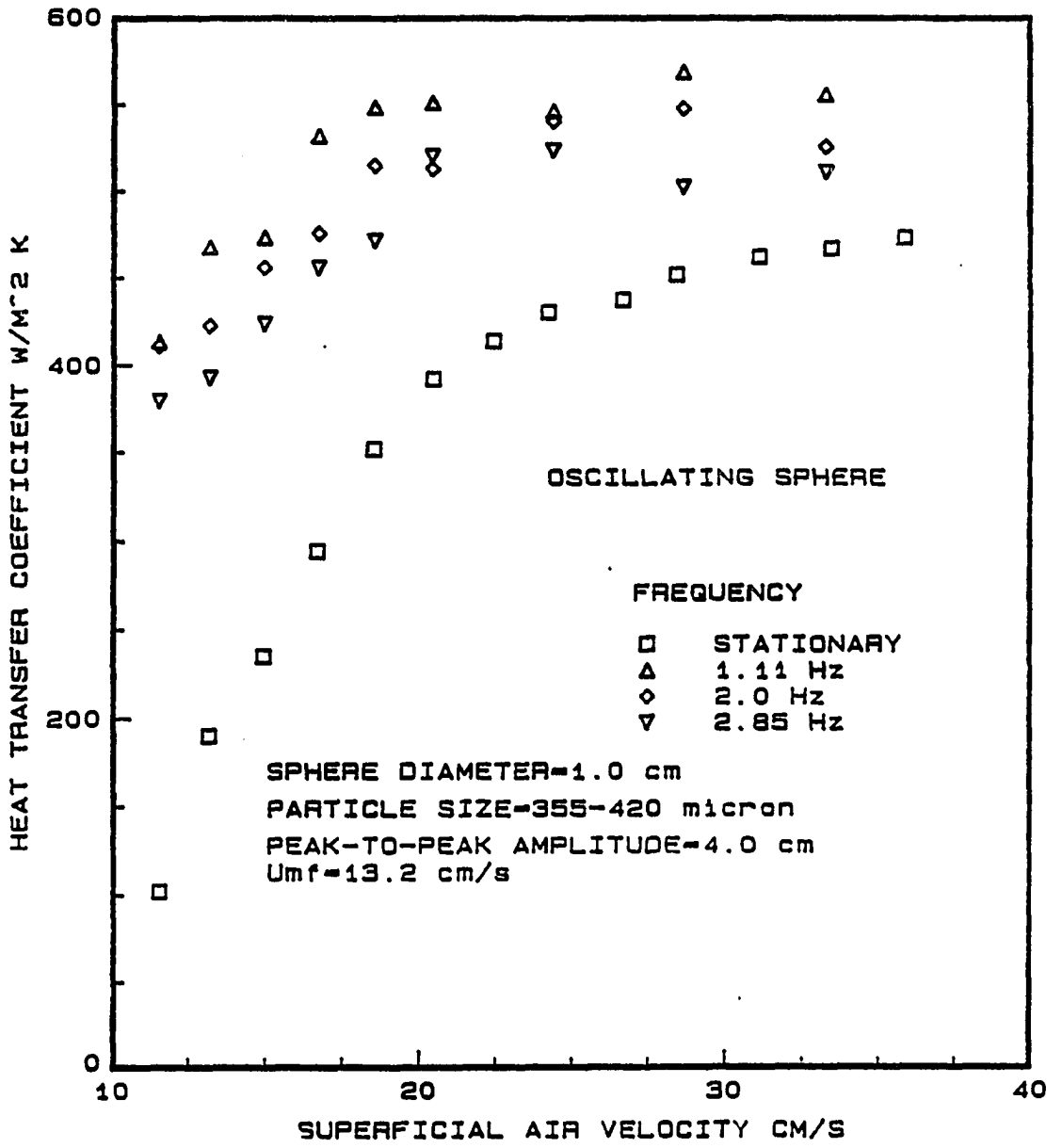

Figure 3.50: Heat transfer coefficient of a 1.0 cm copper sphere in oscillating motion (various frequencies) with the peak-to-peak amplitude of 4.0 cm versus superficial air velocity for a fluidized bed of 355-420 μm glass particles

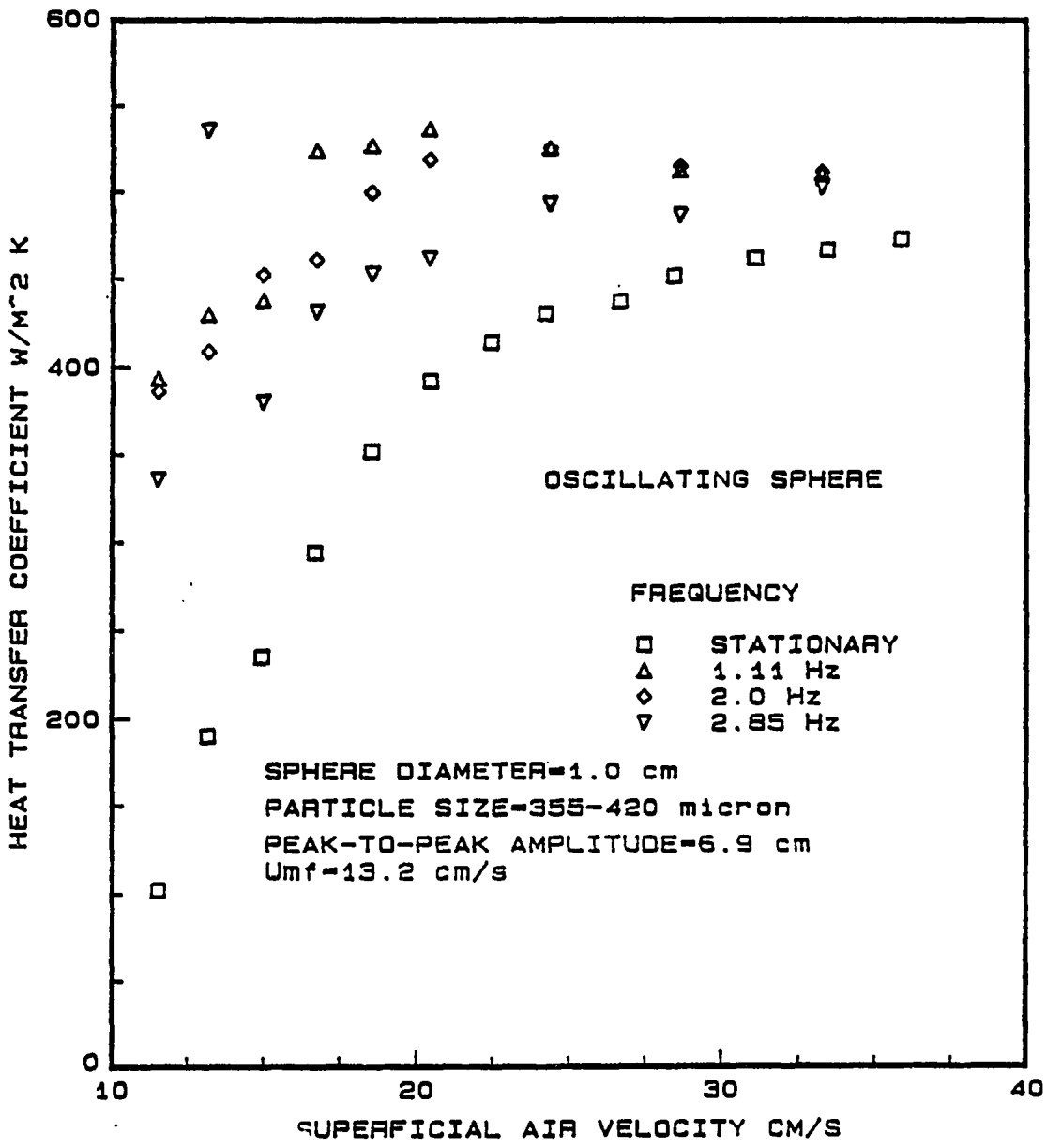

Figure 3.51: Heat transfer coefficient of a 1.0 cm copper sphere in oscillating motion (various frequencies) with the peak-to-peak amplitude of 6.9 cm versus superficial air velocity for a fluidized bed of 355-420 μm glass particles

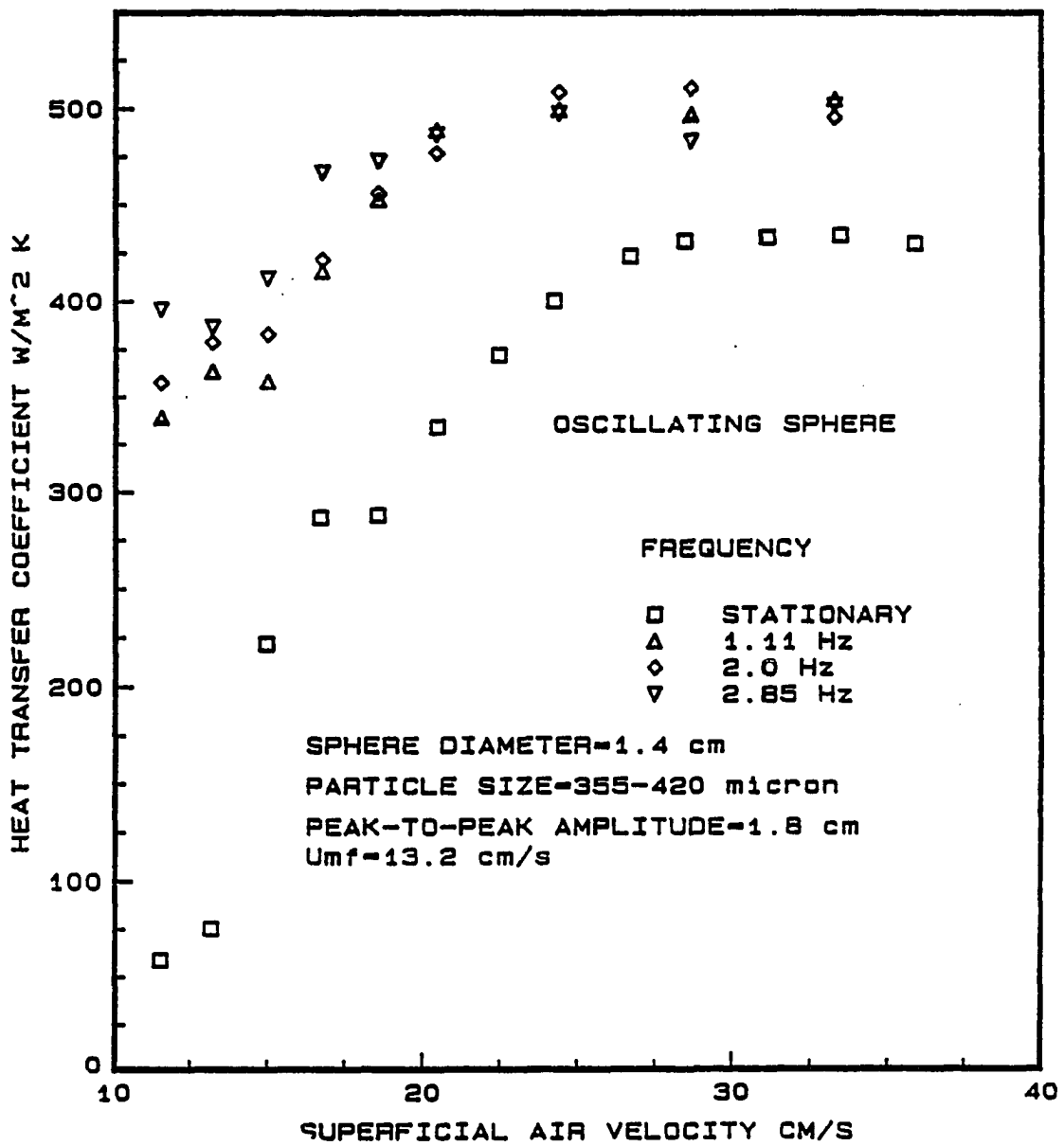

Figure 3.52: Heat transfer coefficient of a 1.4 cm copper sphere in oscillating motion (various frequencies) with the peak-to-peak amplitude of 1.8 cm versus superficial air velocity for a fluidized bed of 355-420 μm glass particles

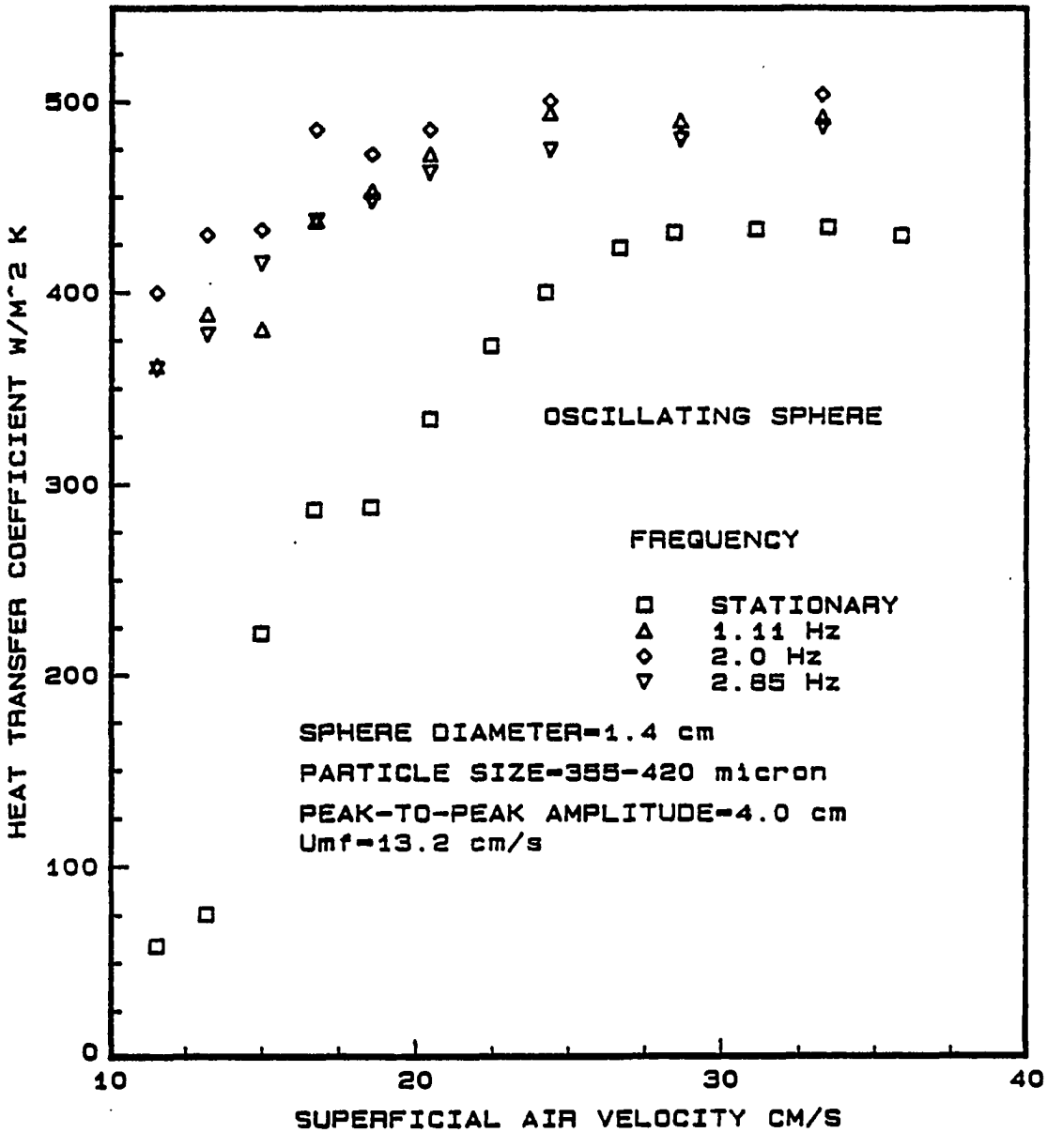

Figure 3.53: Heat transfer coefficient of a 1.4 cm copper sphere in oscillating motion (various frequencies) with the peak-to-peak amplitude of 4.0 cm versus superficial air velocity for a fluidized bed of 355-420 μm glass particles

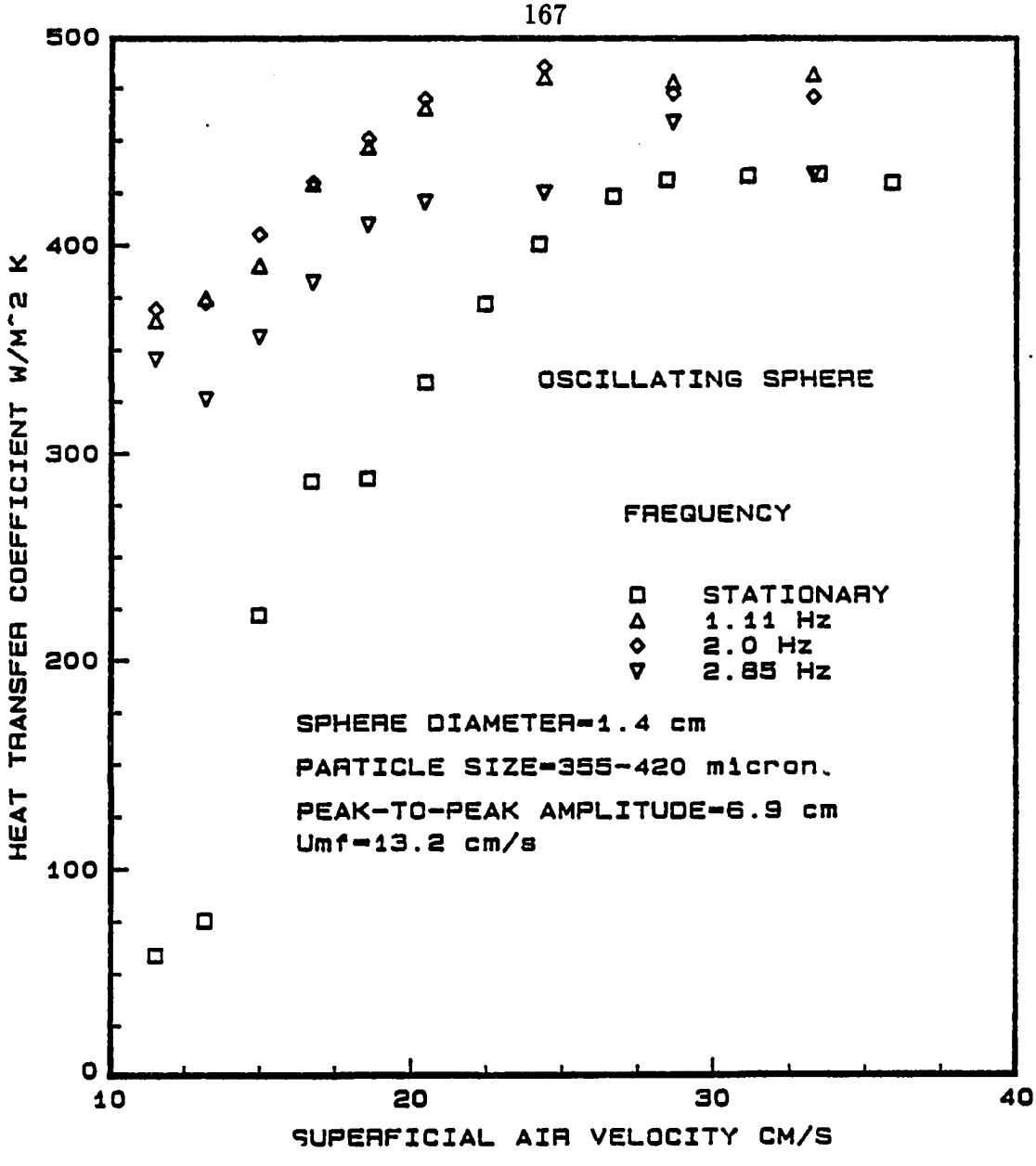

Figure 3.54: Heat transfer coefficient of a 1.4 cm copper sphere in oscillating motion (various frequencies) with the peak-to-peak amplitude of 6.9 cm versus superficial air velocity for a fluidized bed of 355-420 μm glass particles

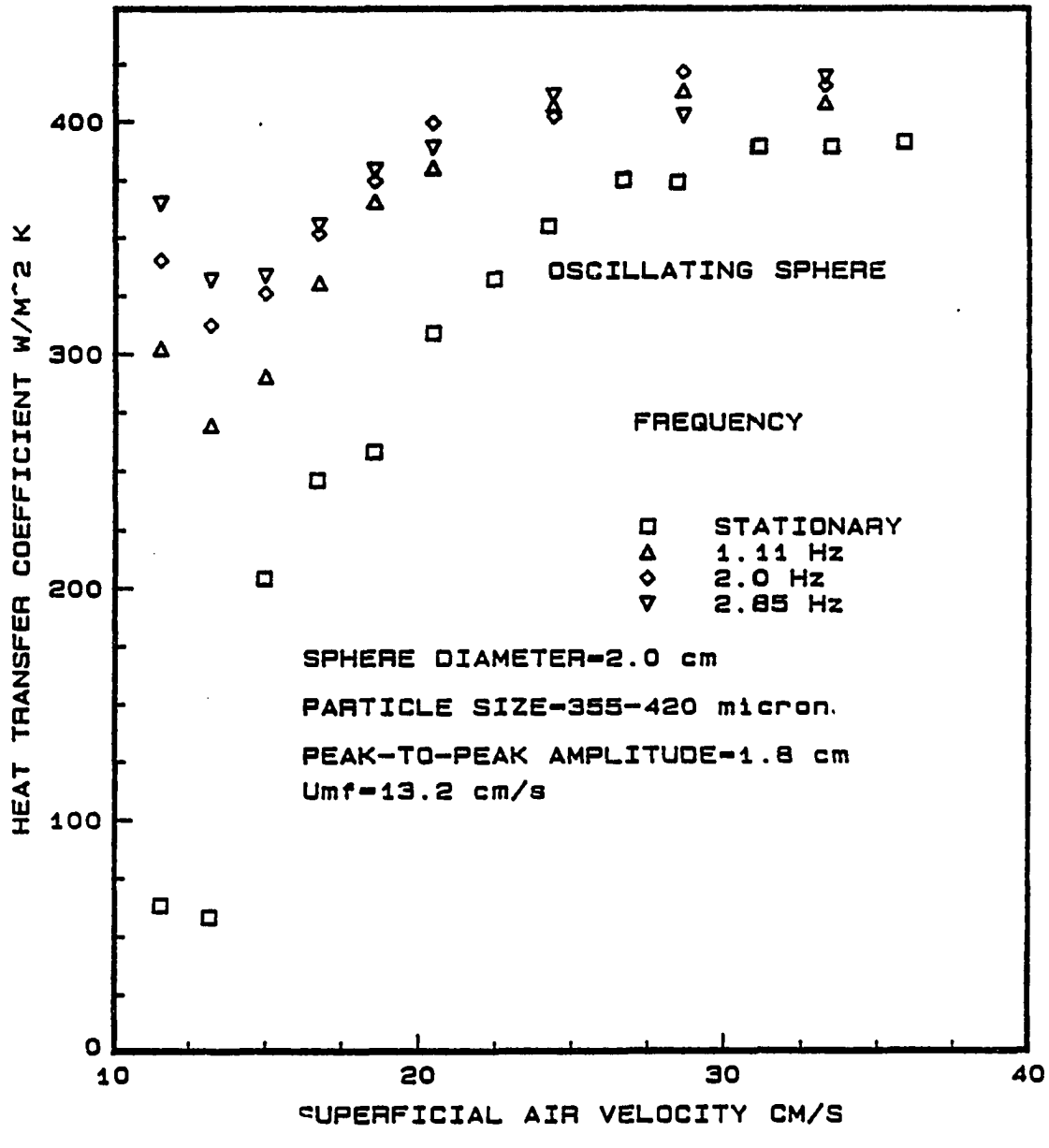

Figure 3.55: Heat transfer coefficient of a 2.0 cm copper sphere in oscillating motion (various frequencies) with the peak-to-peak amplitude of 1.8 cm versus superficial air velocity for a fluidized bed of 355-420 μm glass particles

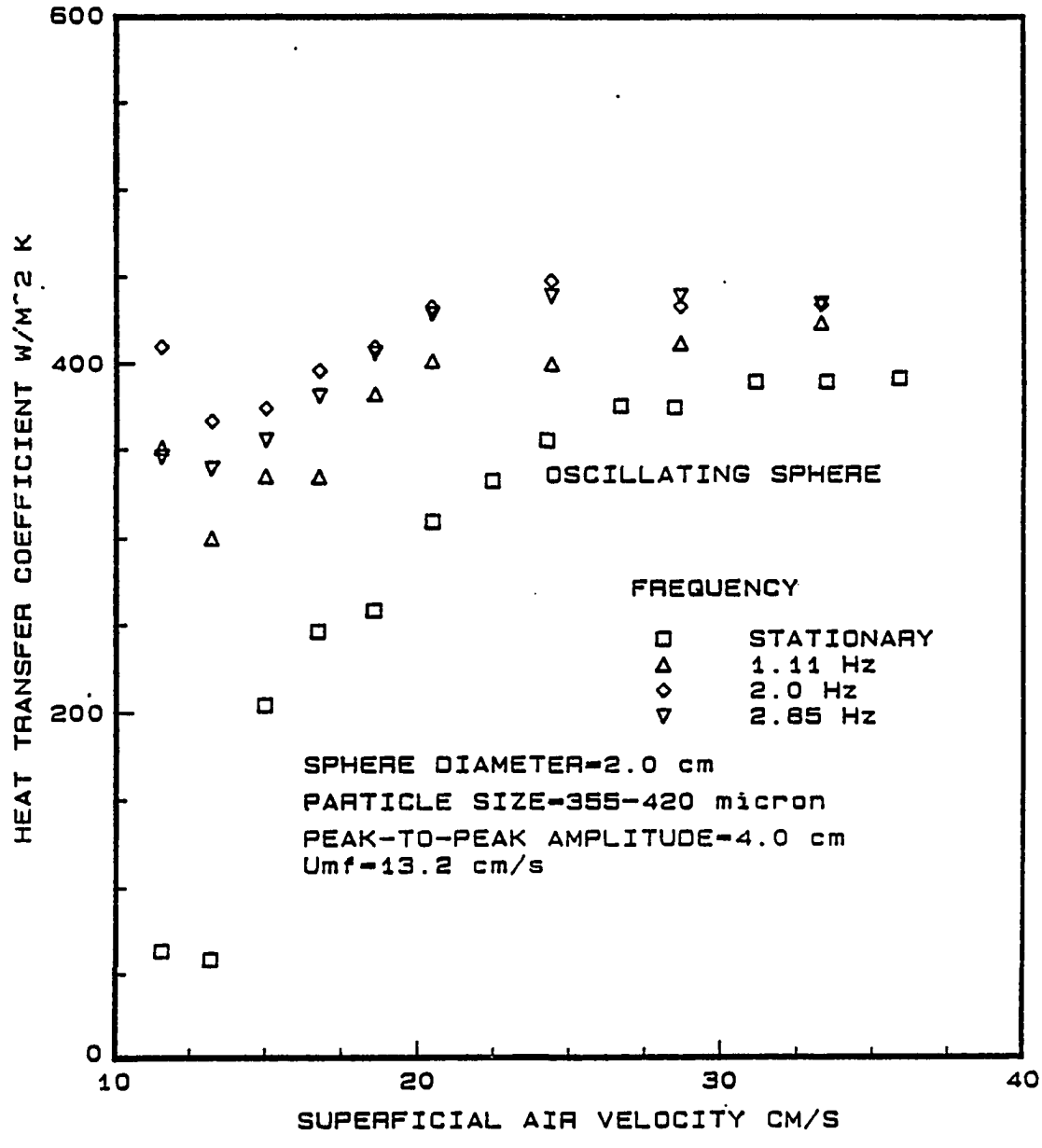

Figure 3.56: Heat transfer coefficient of a 2.0 cm copper sphere in oscillating motion (various frequencies) with the peak-to-peak amplitude of 4.0 cm versus superficial air velocity for a fluidized bed of 355-420 μm glass particles

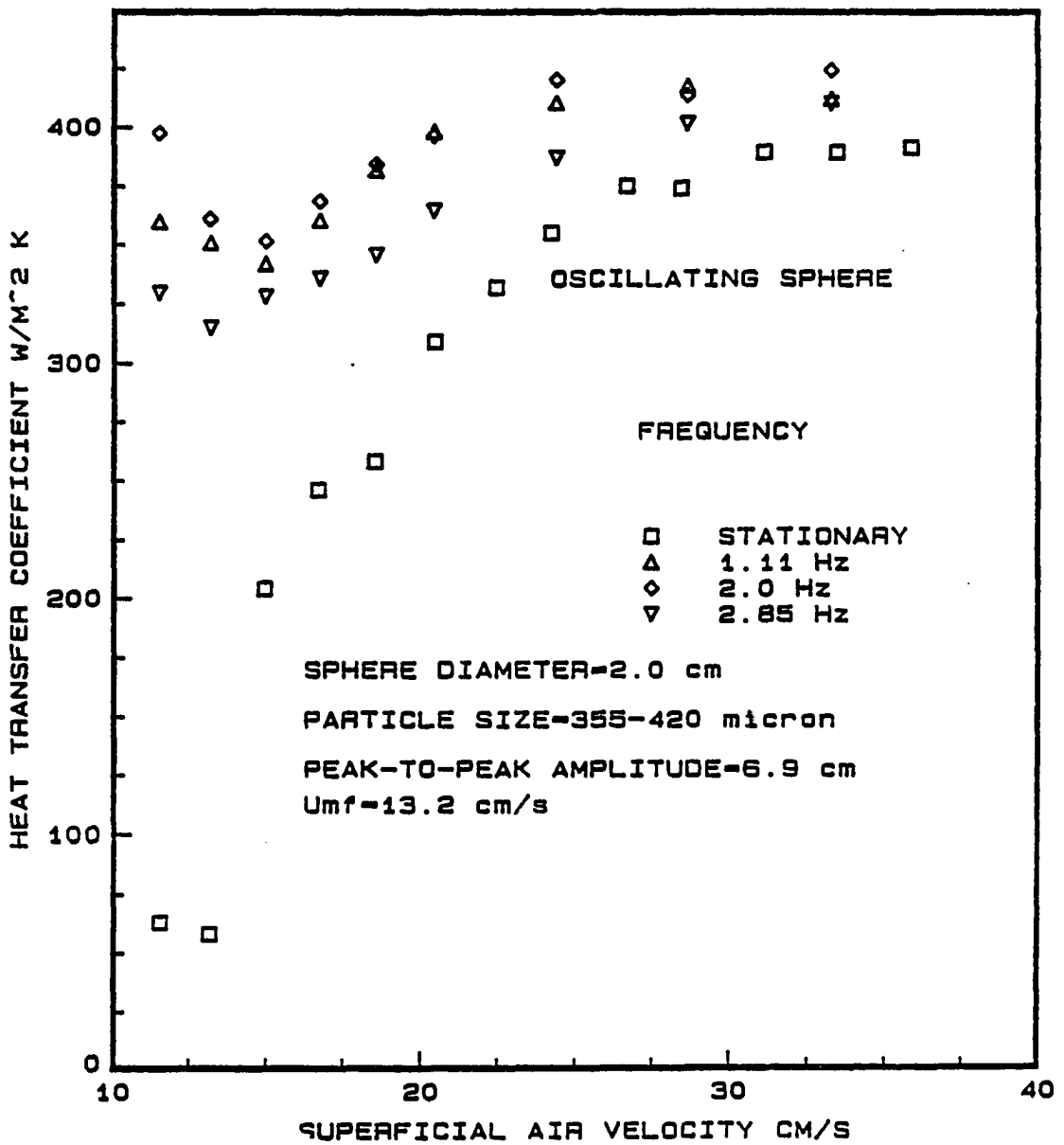

Figure 3.57: Heat transfer coefficient of a 2.0 cm copper sphere in oscillating motion (various frequencies) with the peak-to-peak amplitude of 6.9 cm versus superficial air velocity for a fluidized bed of 355-420 μm glass particles

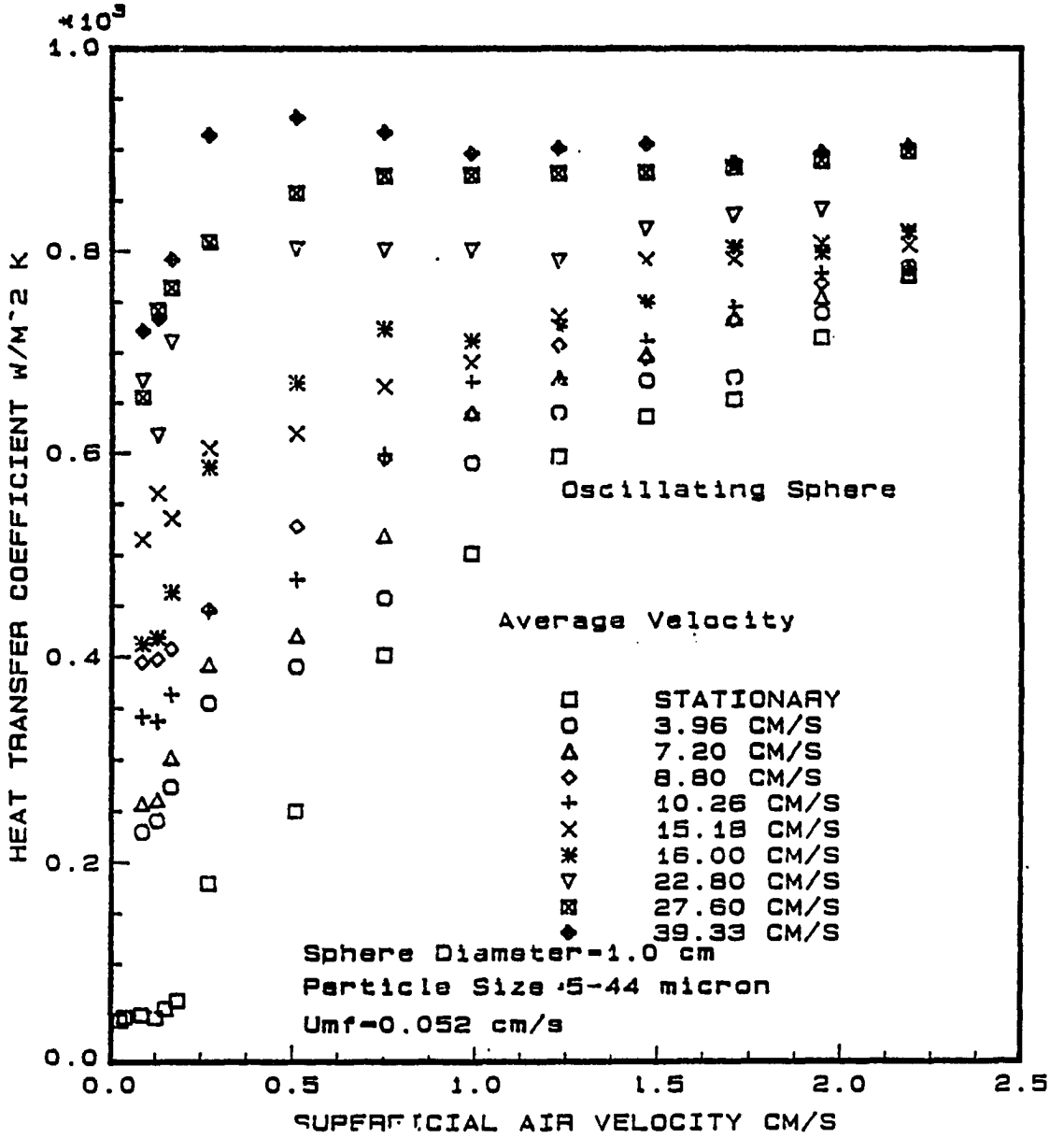

Figure 3.58: Heat transfer coefficient of a 1.0 cm oscillating copper sphere moving at various equivalent average sphere velocities versus superficial air velocity for a fluidized bed of 5-44 μm glass particles

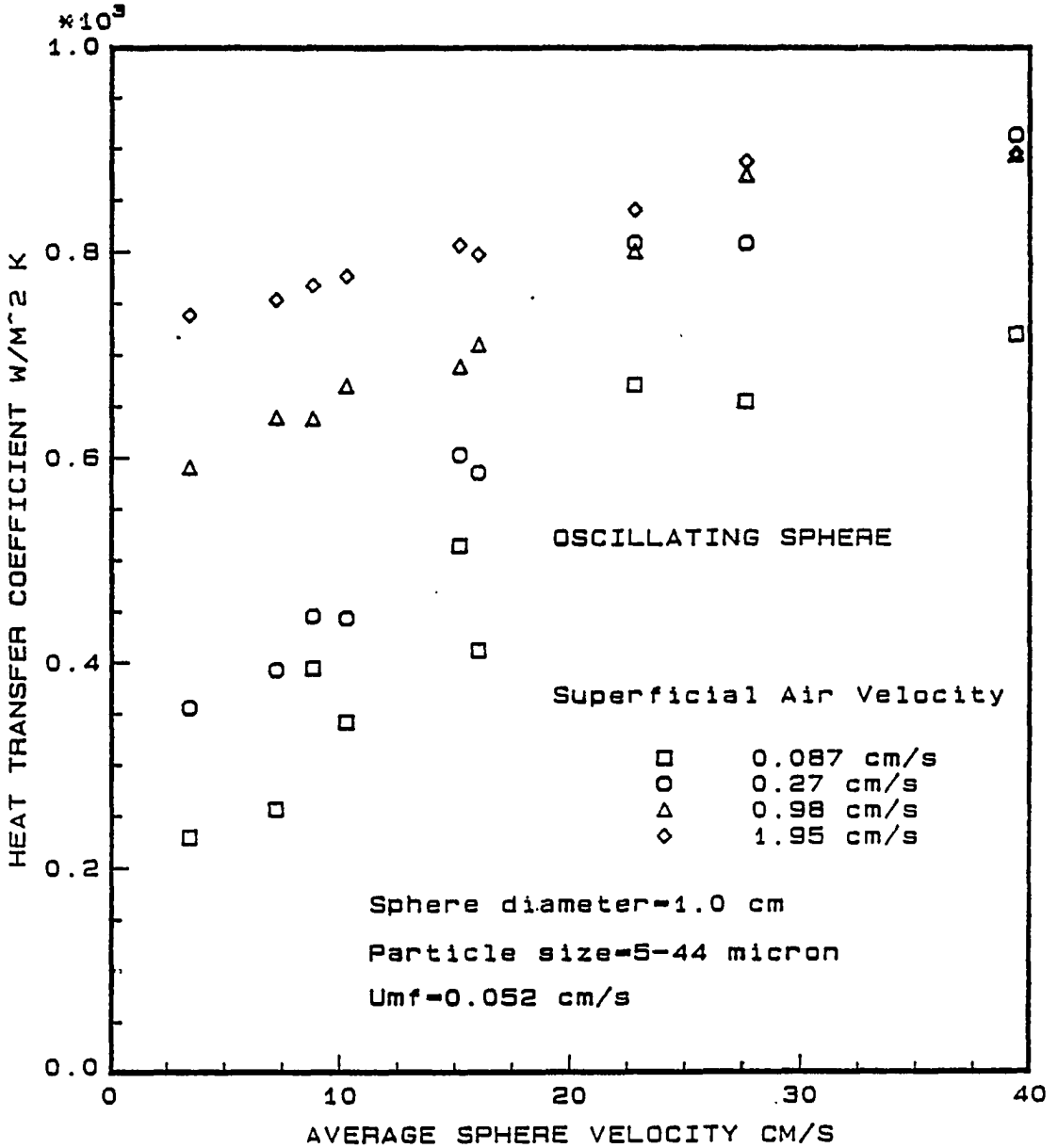

Figure 3.59: Heat transfer coefficient of a 1.0 cm oscillating copper sphere versus average sphere velocity for various superficial air velocities.

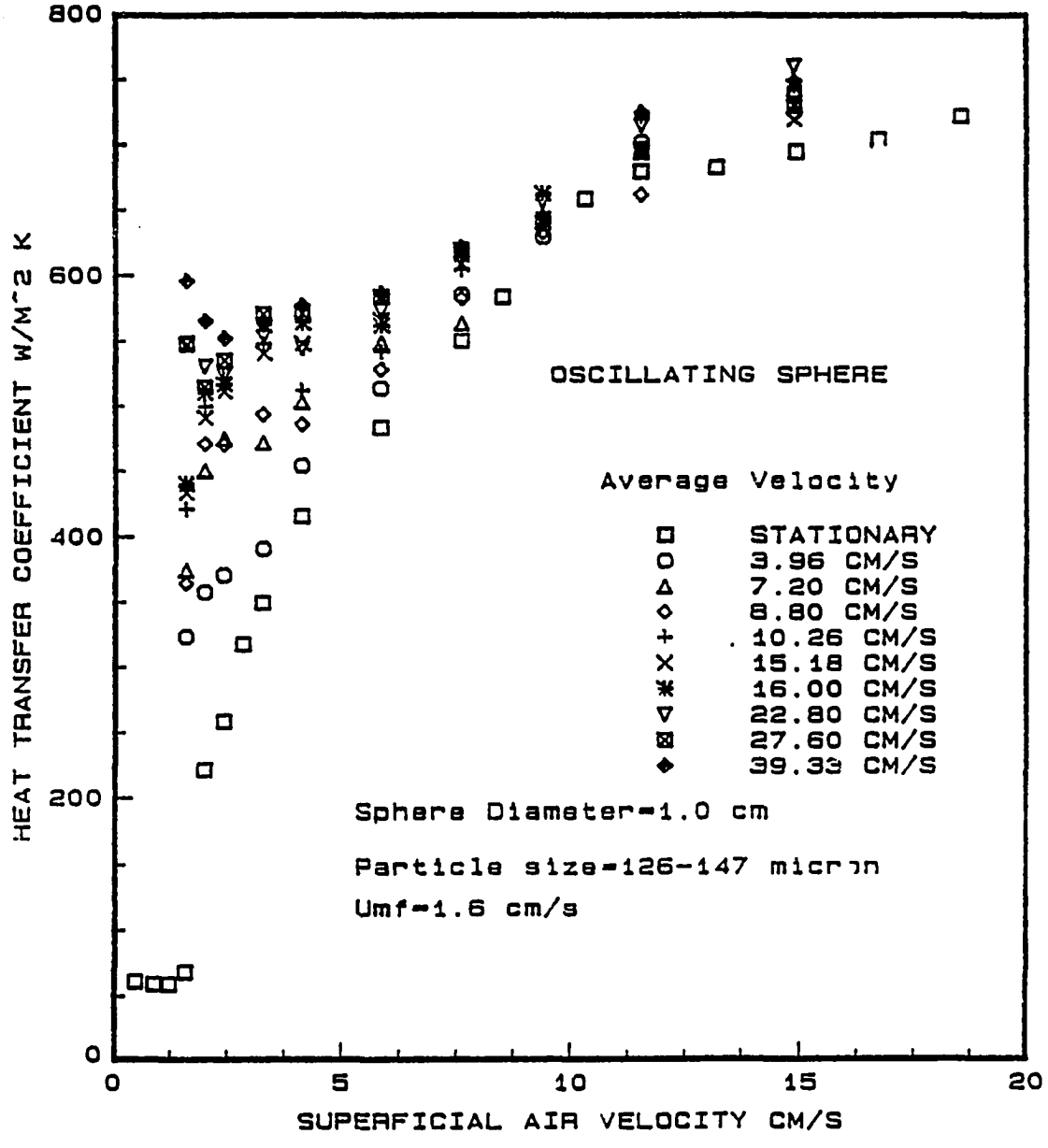

Figure 3.60: Heat transfer coefficient of a 1.0 cm oscillating copper sphere moving at various equivalent average sphere velocities versus superficial air velocity for a fluidized bed of 126-147 μm glass particles

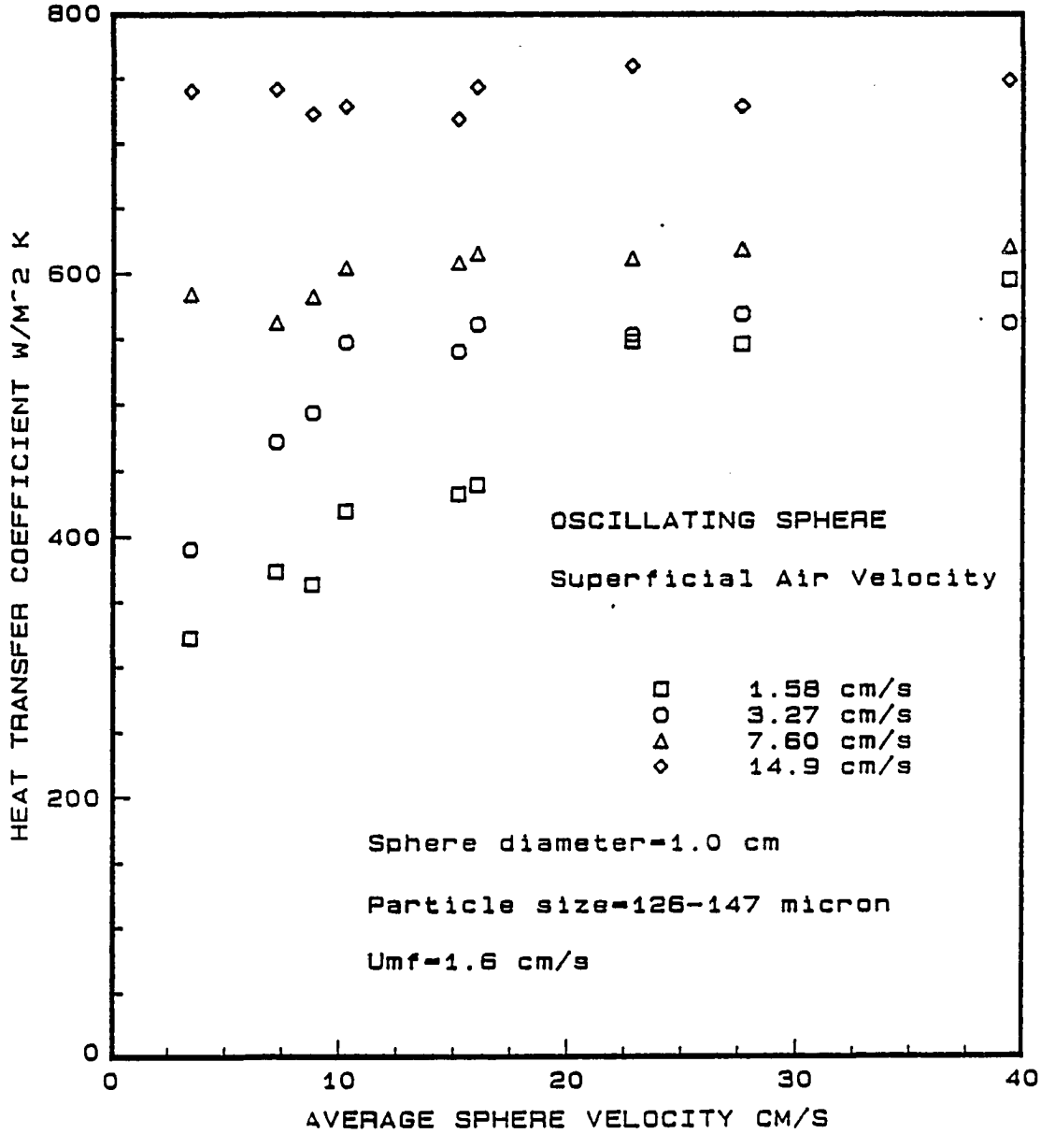

Figure 3.61: Heat transfer coefficient of a 1.0 cm oscillating copper sphere versus average sphere velocity for various superficial air velocities

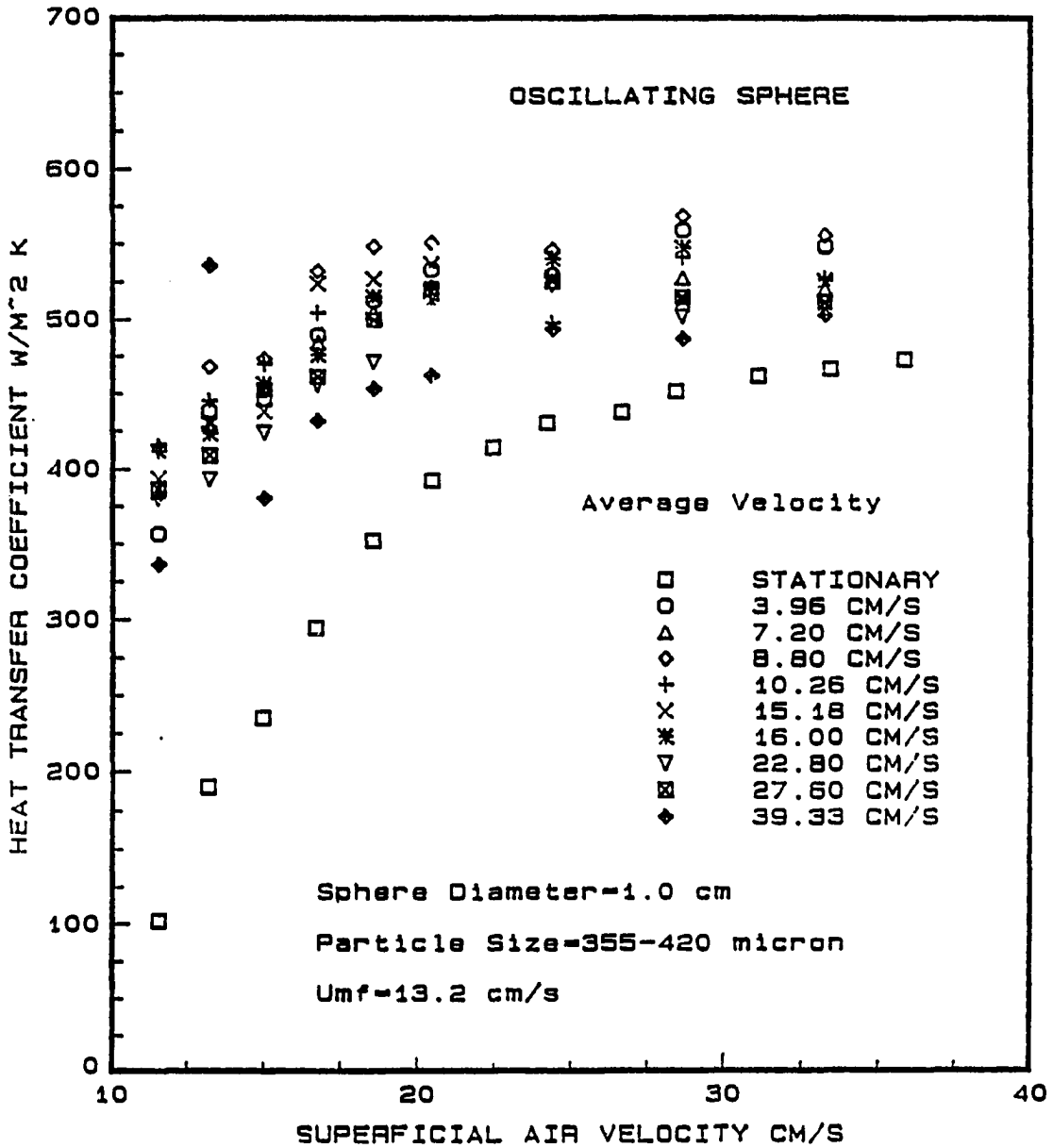

Figure 3.62: Heat transfer coefficient of a 1.0 cm oscillating copper sphere moving at various equivalent average sphere velocities versus superficial air velocity for a fluidized bed of 355-420 μm glass particles

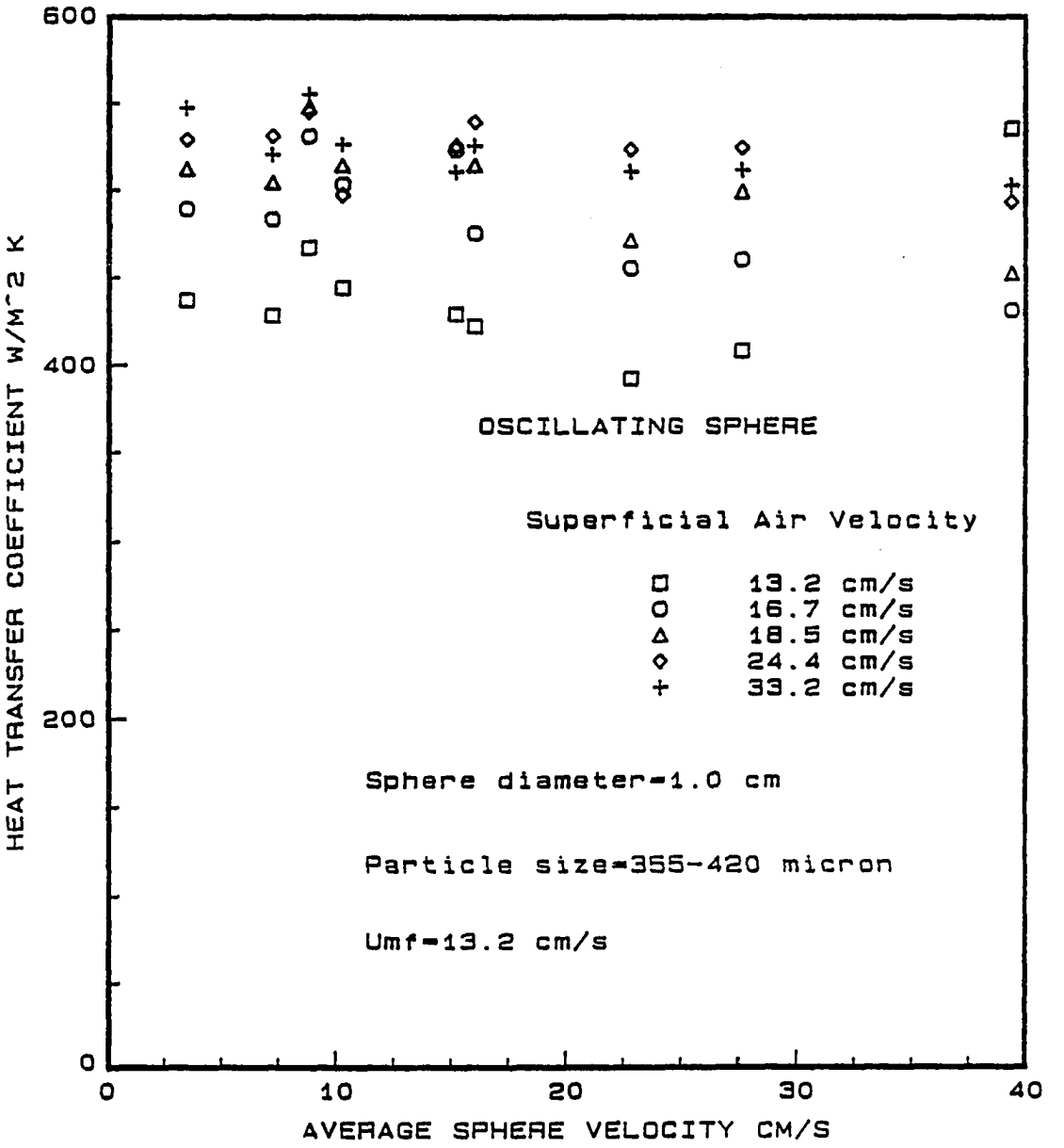

Figure 3.63: Heat transfer coefficient of a 1.0 cm oscillating copper sphere versus average sphere velocity for various superficial air velocities

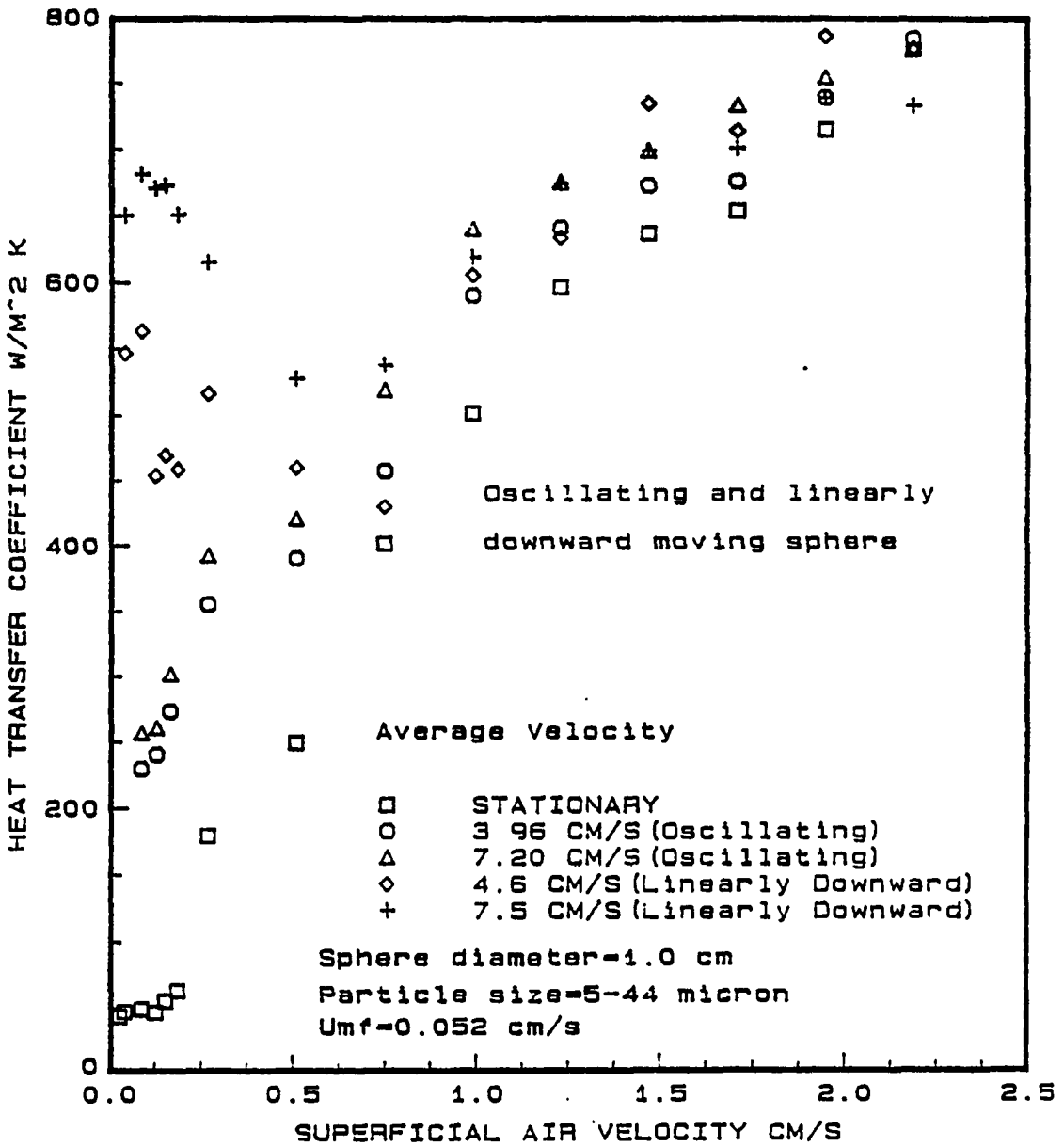

Figure 3.64: Heat transfer coefficient of a 1.0 cm oscillating and linearly downward moving copper sphere versus superficial air velocities for various average velocities and 5-44 μm glass particles

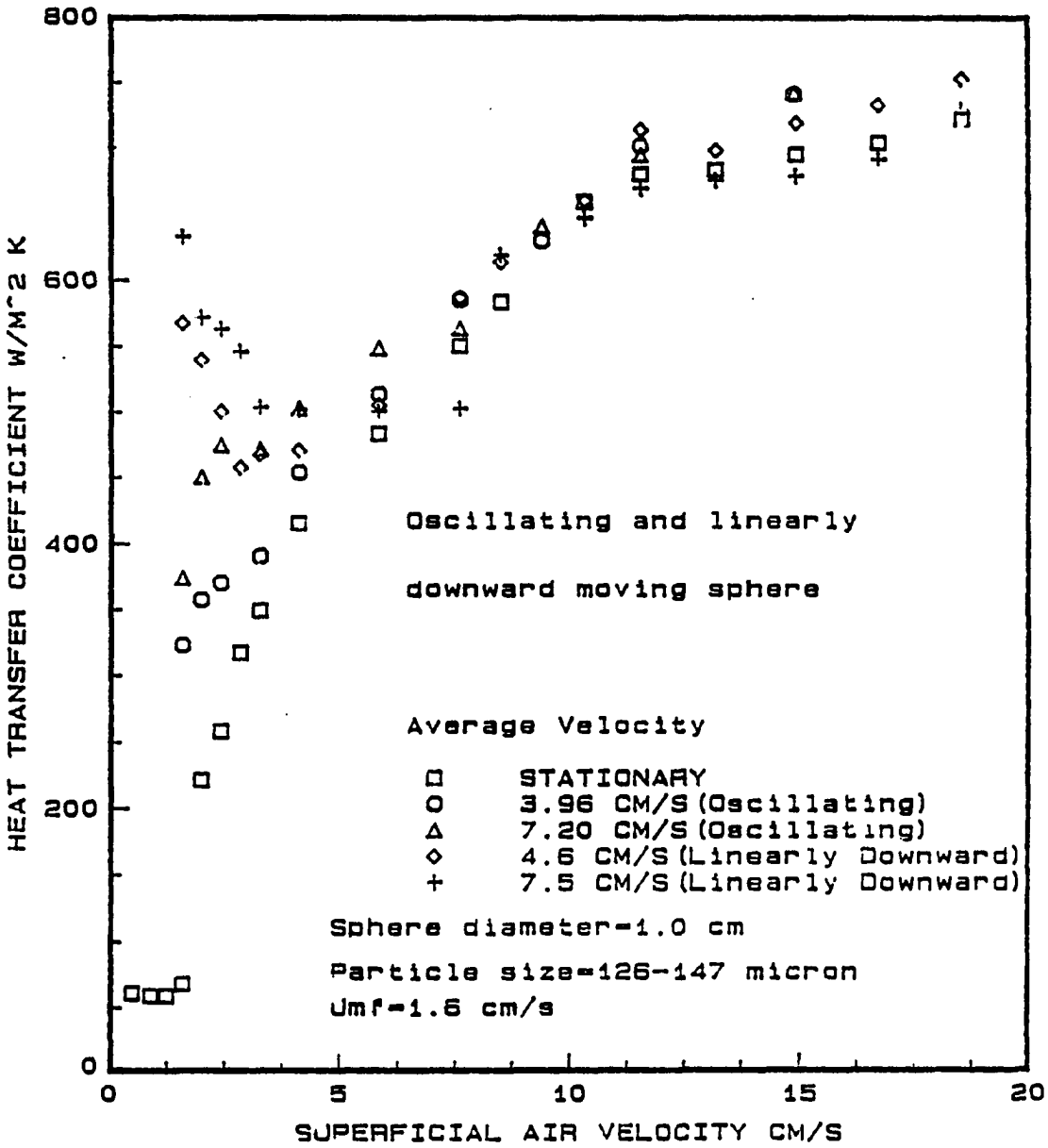

Figure 3.65: Heat transfer coefficient of a 1.0 cm oscillating and linearly downward moving copper sphere versus superficial air velocities for various average velocities and 126-147 μm glass particles

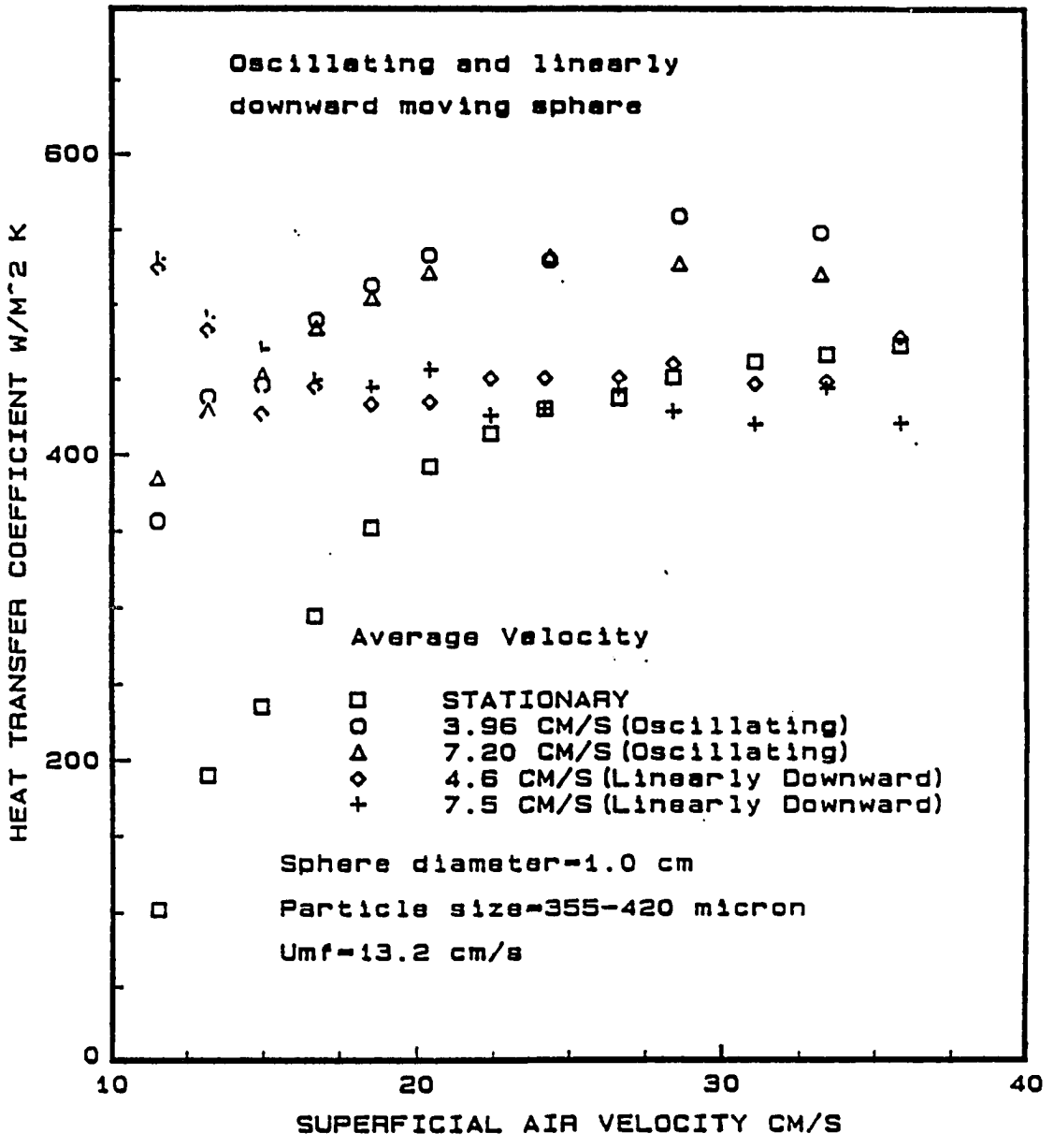

Figure 3.66: Heat transfer coefficient of a 1.0 cm oscillating and linearly downward moving copper sphere versus superficial air velocities for various average velocities and 355-420 μm glass particles

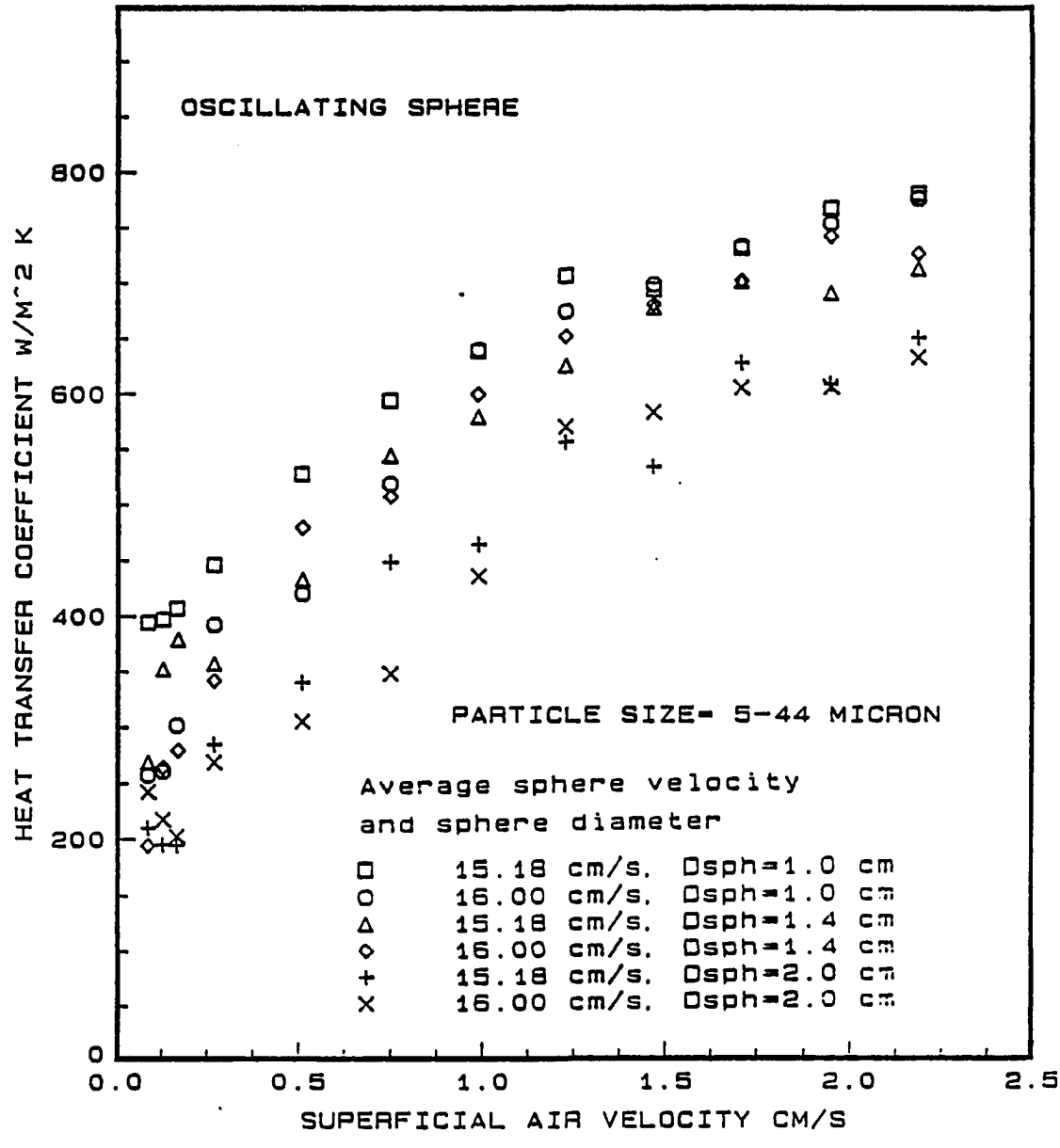

Figure 3.67: Heat transfer coefficient for various sphere diameters versus superficial air velocity for the same linear average velocity and 5-44 μm glass particles

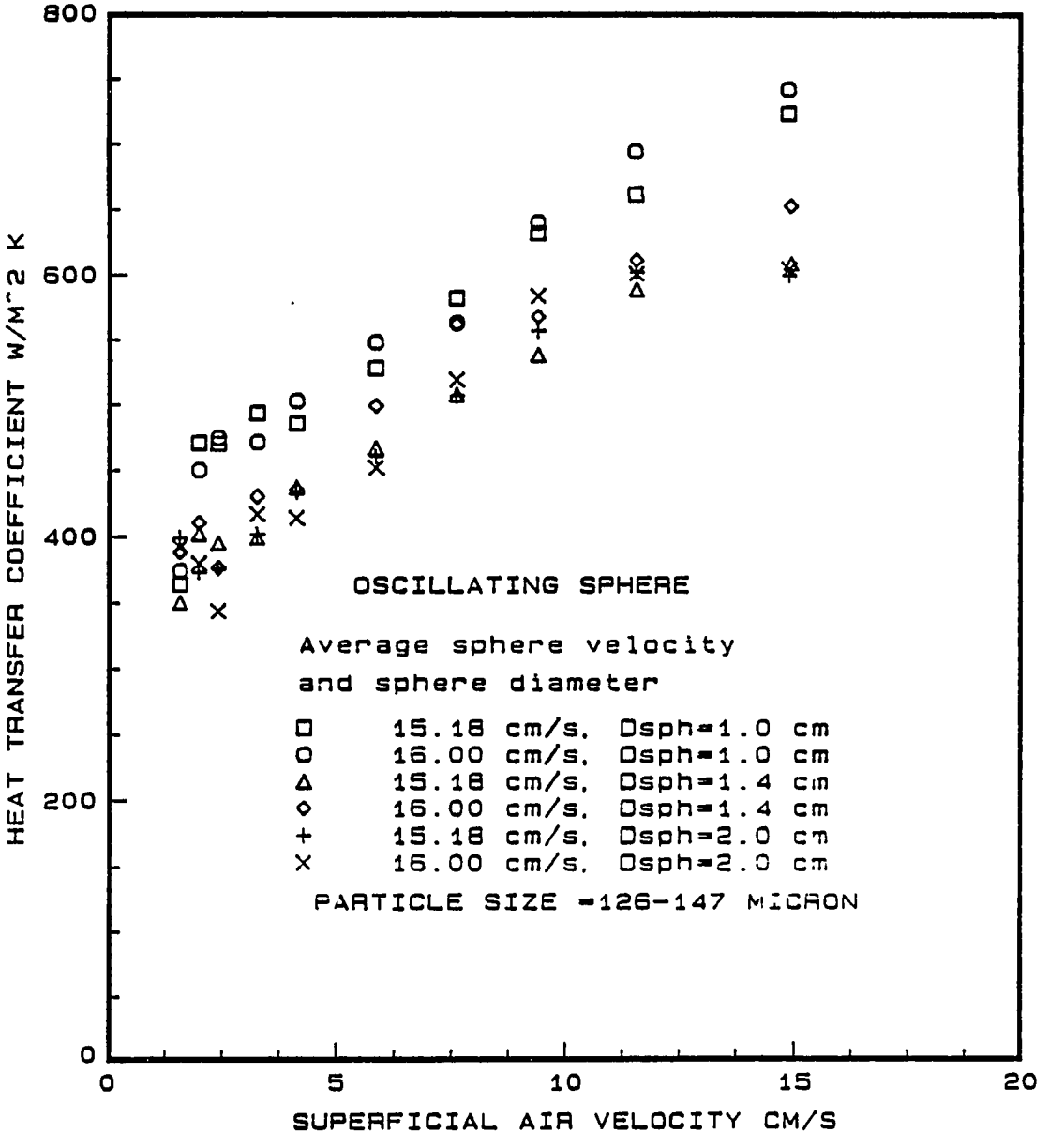

Figure 3.68: Heat transfer coefficient for various sphere diameters versus superficial air velocity for the same linear average velocity and 126-147 μm glass particles

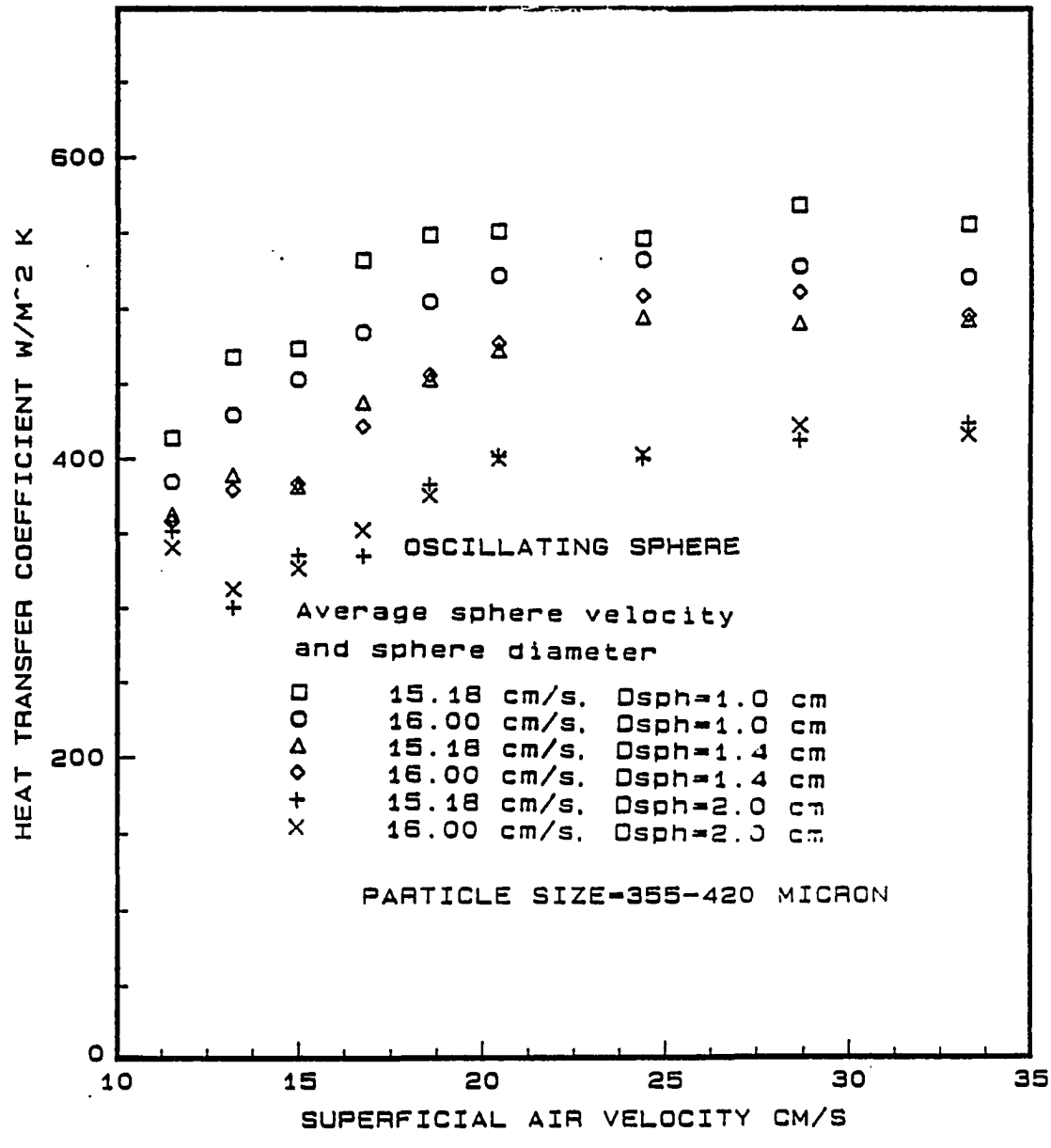

Figure 3.69: Heat transfer coefficient for various sphere diameters versus superficial air velocity for the same linear average velocity and 355-420 μm glass particles

4 HEAT TRANSFER CORRELATION

Heat transfer correlations were obtained for each of three cases, namely, for the stationary sphere, the linearly downward moving sphere, and the oscillating sphere. SAS and RS/1 statistical packages were used to correlate the experimental data. Instead of relying on the statistical parameters such as, correlation coefficient, residuals, etc., the correlations were directly compared with the experimental data in its original form for each case.

4.1 Heat Transfer Correlation for a Stationary Sphere

The heat transfer coefficient for a stationary sphere system incorporated the following independent variables: glass particle diameter, sphere diameter and superficial air velocity. The empirical correlation was proposed in the following form,

$$Nu_s = C_{s1}\left(\frac{U}{U_{mf}}\right)^{C_{s2}}\left(\frac{g d_p^3 \rho_g(\rho_p - \rho_g)}{\mu_g^2}\right)^{C_{s3}}\left(\frac{D_{sph}}{d_p}\right)^{C_{s4}} \qquad (4.1)$$

In the above formulation Nusselt number is based on the sphere diameter and the properties of air. The constants, C_{s1}, C_{s2}, C_{s3} and C_{s4} were evaluated from a multiple log-linear regression analysis. The range of this equation was confined to the fluidized region only (i.e., not including packed bed) as shown in Figure 4.1. Most practical application apply to the fluidized bed region and, moreover, because

of the shape of the plot of the heat transfer coefficient versus the superficial air velocity, it is not possible to correlate all the data with the log-linear correlation model assumed for this case. The result of the log-linear multi-variable regression obtained using SAS program for a stationary sphere with ±25 % is given as follow;

$$Nu_s = 0.176 \left(\frac{U}{U_{mf}}\right)^{0.664} \left(\frac{g d_p^3 \rho_g (\rho_p - \rho_g)}{\mu_g^2}\right)^{0.44} \left(\frac{D_{sph}}{d_p}\right)^{0.798} \qquad (4.2)$$

The range of the application of this correlation and the agreement between the predicted and the experimental heat transfer coefficients are shown in Figures 4.1, 4.2 and 4.3. For the glass particle size of 5-44 μm, the correlated values of the heat transfer coefficient agrees within ±25 % in the fluidized bed region as shown in Figure 4.1. However for the glass particle size of 126-147 μm (Figure 4.2), where the heat transfer coefficients are underpredicted by as much as 20 %. The heat transfer coefficient levels off above the superficial velocity of 25 cm/s for the glass particle system of 355-420 μm where the change in the slope of the curve in which the proposed correlation is not adequately flexible to adopt. The empirical correlation (equation 4.2) obtained implies that, the heat transfer coefficient h is proportional to $D_{sph}^{-0.2}$. Shirai et al. [1966] found that $h \propto D_{sph}^{-0.06}$. The direct relation of the heat transfer coefficient to the glass particle diameter is $d_p^{0.52}$. This result is contradictory to the experimental findings of an increasing heat transfer coefficient with a decrease in the glass particle diameter (Figures 3.5, 3.6 and, 3.7). However, considering the dependence of the minimum fluidizing velocity U_{mf} on the glass particle diameter, expressed in the equation 3.4, the heat transfer coefficient

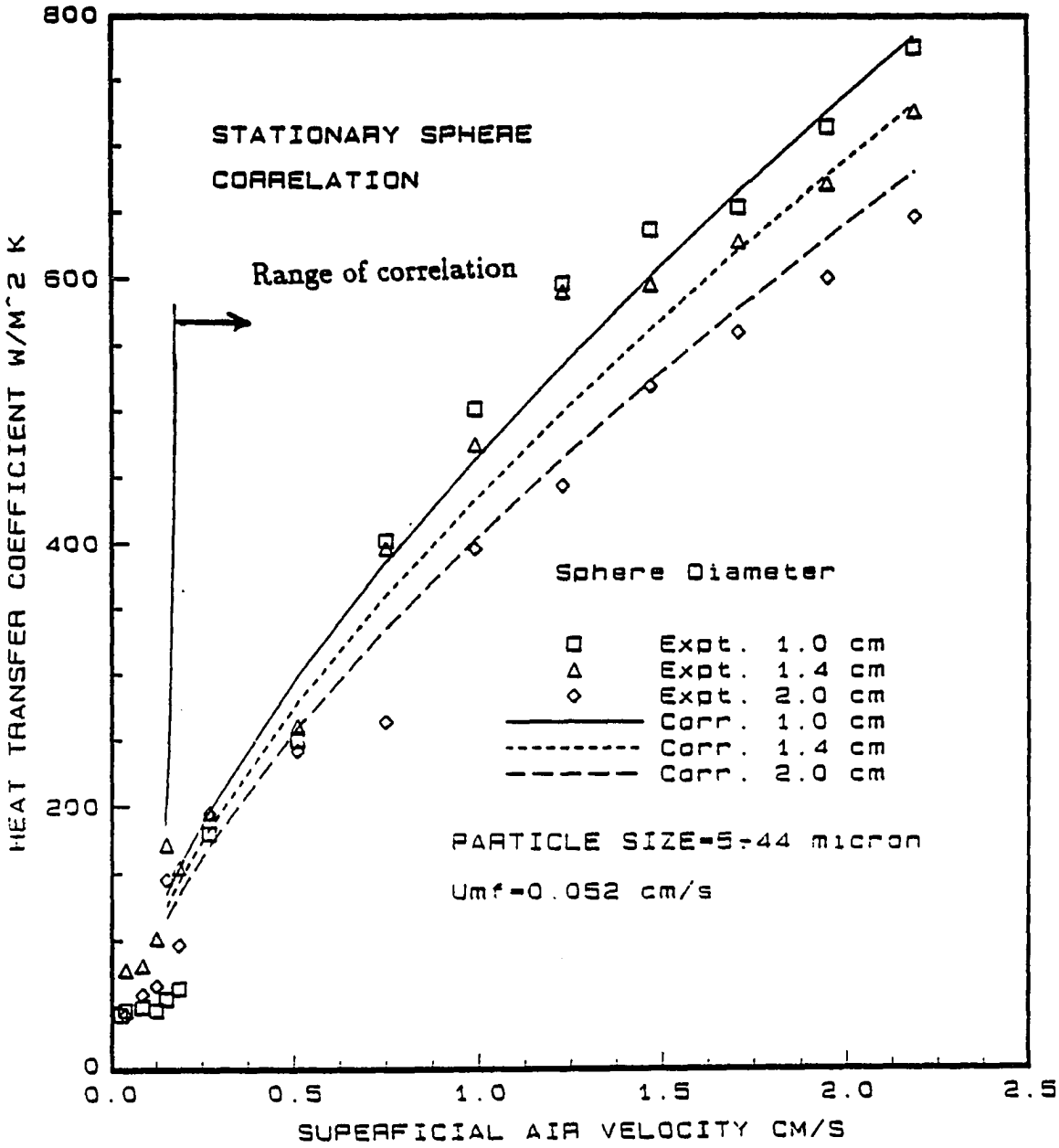

Figure 4.1: Experimental and predicted heat transfer coefficients as a function of superficial air velocity for the fluidized bed of 5-44 μm glass particles and stationary sphere

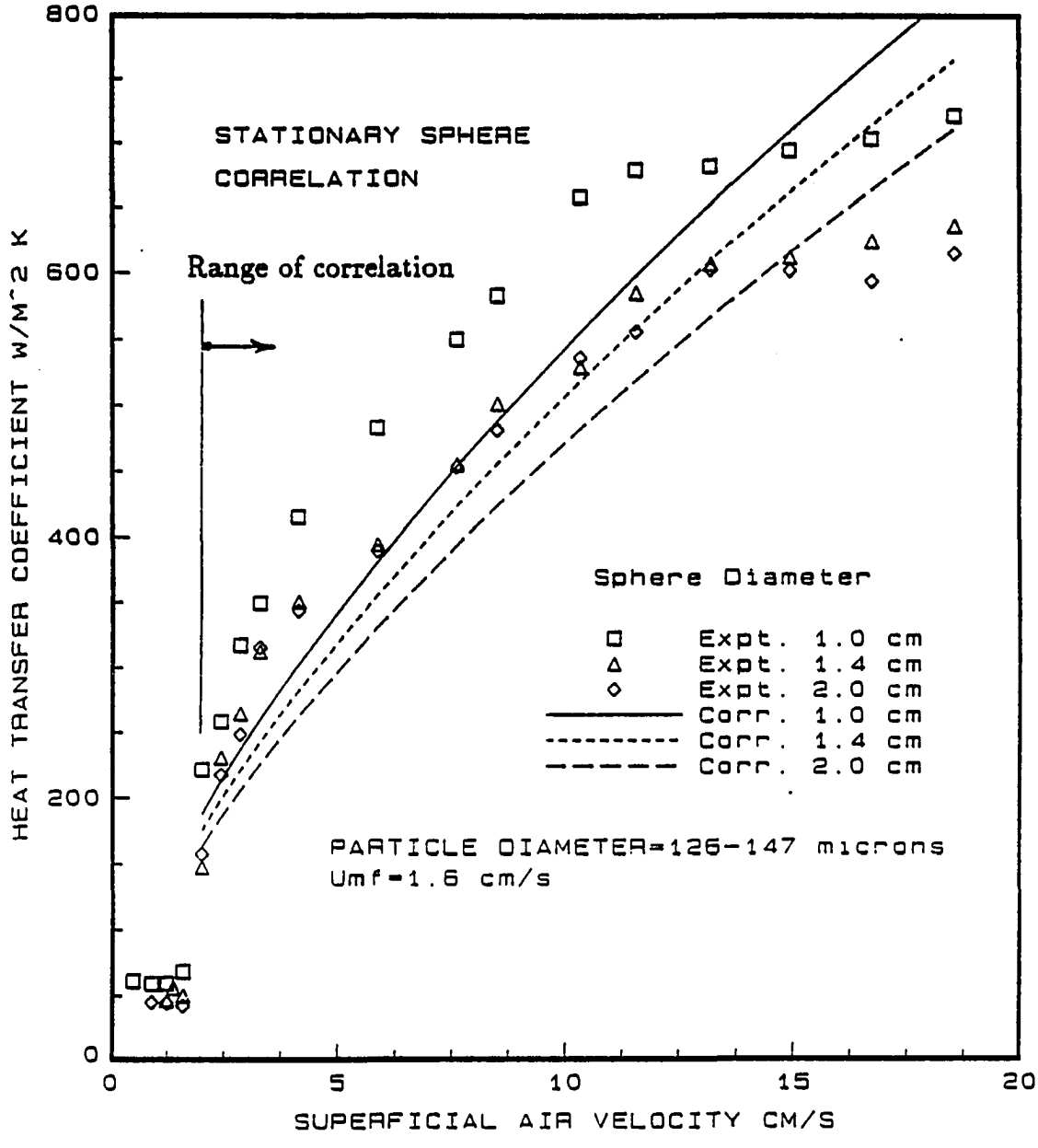

Figure 4.2: Experimental and predicted heat transfer coefficients as a function of superficial air velocity for the fluidized bed of 126-147 μm glass particles and stationary sphere

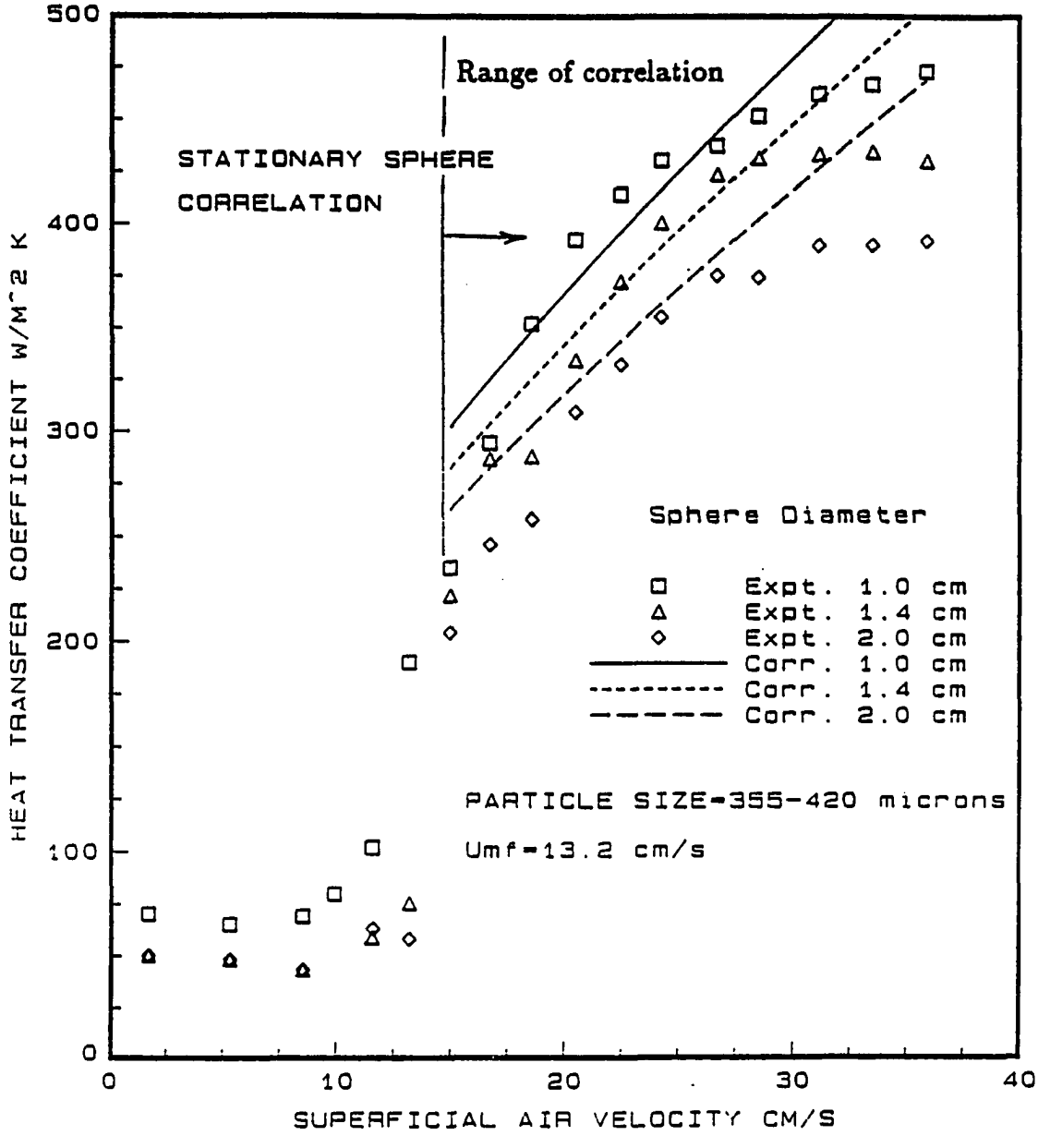

Figure 4.3: Experimental and predicted heat transfer coefficients as a function of superficial air velocity for the fluidized bed of 355-420 μm glass particles and stationary sphere

h is proportional to $d_p^{-0.79}$. This result can be compared to the following results documented by various researchers.

$$h \propto d_p^{-0.23} \quad (Dow\ and\ Jacob[1951])$$

$$h \propto d_p^{-0.50} \quad (Yamazaki\ and\ Jimbo[1970])$$

Figure 4.4 shows the plot of the heat transfer coefficient versus the left hand side of the equation 4.2 without the coefficient 0.176 (XSCORR) and the experimental values of the heat transfer coefficient. The correlation obtained agrees reasonably well with the experimental data.

4.2 Heat Transfer Correlation for Linearly Downward Moving Sphere

The heat transfer results for the linearly downward moving sphere were correlated in the form suggested by the equation 4.1 with an added term to include the linear velocity of the sphere V_{sph}. The first attempt for a moving sphere was to correlate all the experimental data in one single correlation as given bellow (within about ±30 %):

Correlation I

$$Nu_m = 0.498 \left(\frac{U}{U_{mf}}\right)^{0.251} \left(\frac{g d_p^3 \rho_g (\rho_p - \rho_g)}{\mu_g^2}\right)^{0.385} \left(\frac{D_{sph}}{d_p}\right)^{0.793} \times \left(\frac{V_{sph}}{U_{mf}}\right)^{0.132} \tag{4.3}$$

The above correlation is compared with the experimental values of the heat transfer coefficient given in Figures 4.5, 4.6 and 4.7. As seen from these Figures,

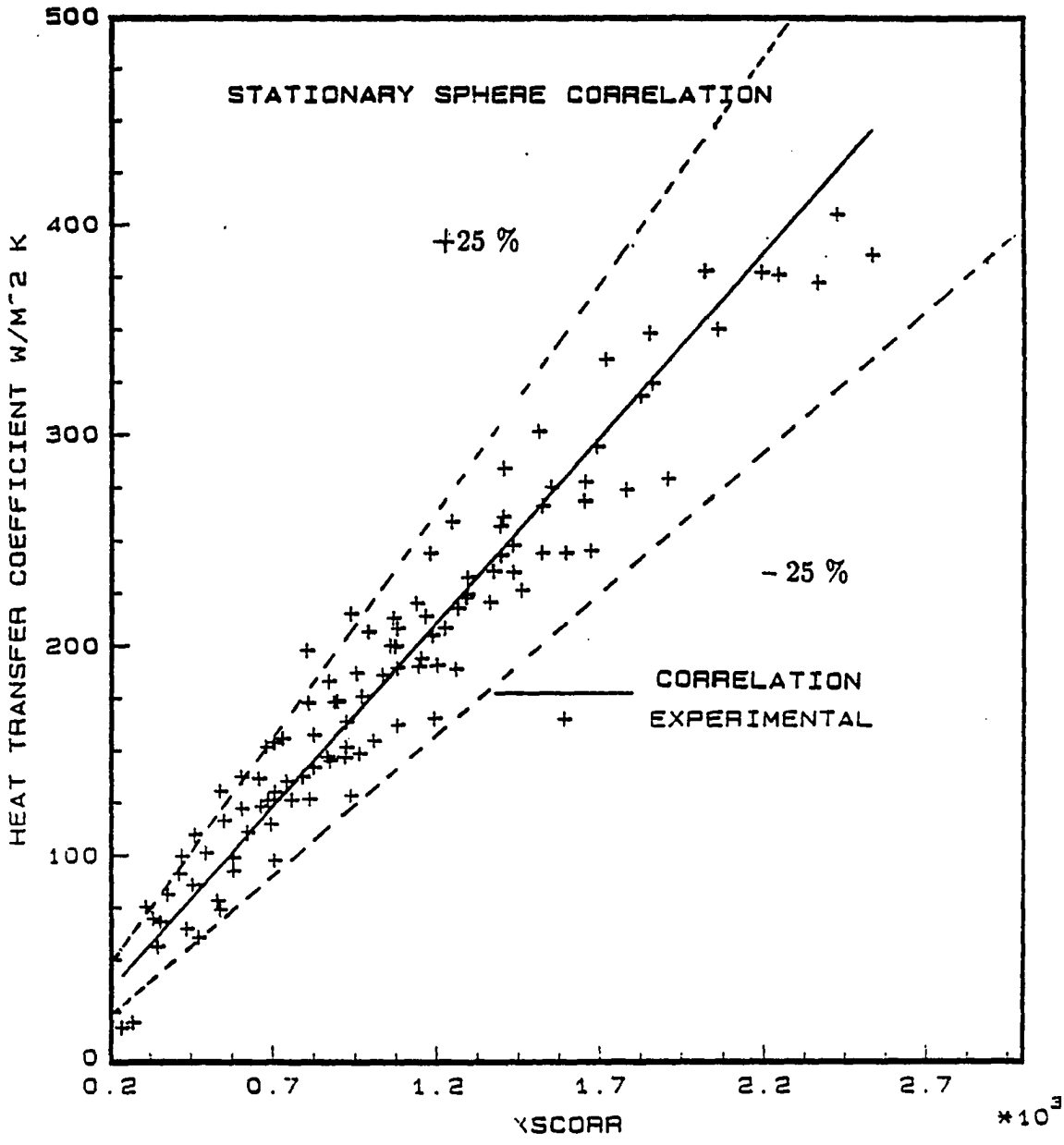

Figure 4.4: Experimental and predicted heat transfer coefficients as a function of XSCORR

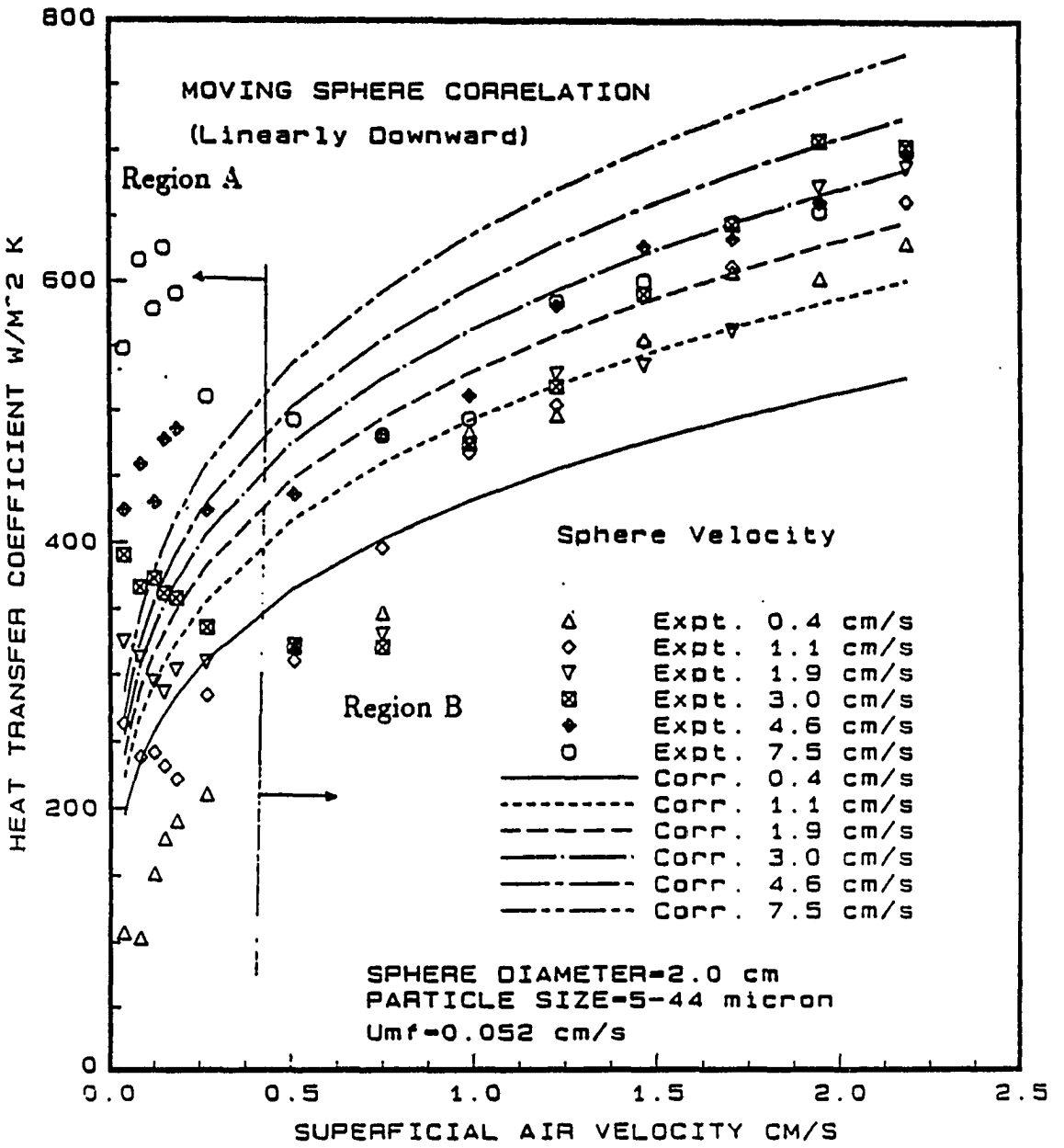

Figure 4.5: Experimental and predicted heat transfer coefficients (correlation I. equation 4.3) as a function of superficial air velocity for the linearly downward moving sphere in a fluidized bed of 5-44 μm glass particles

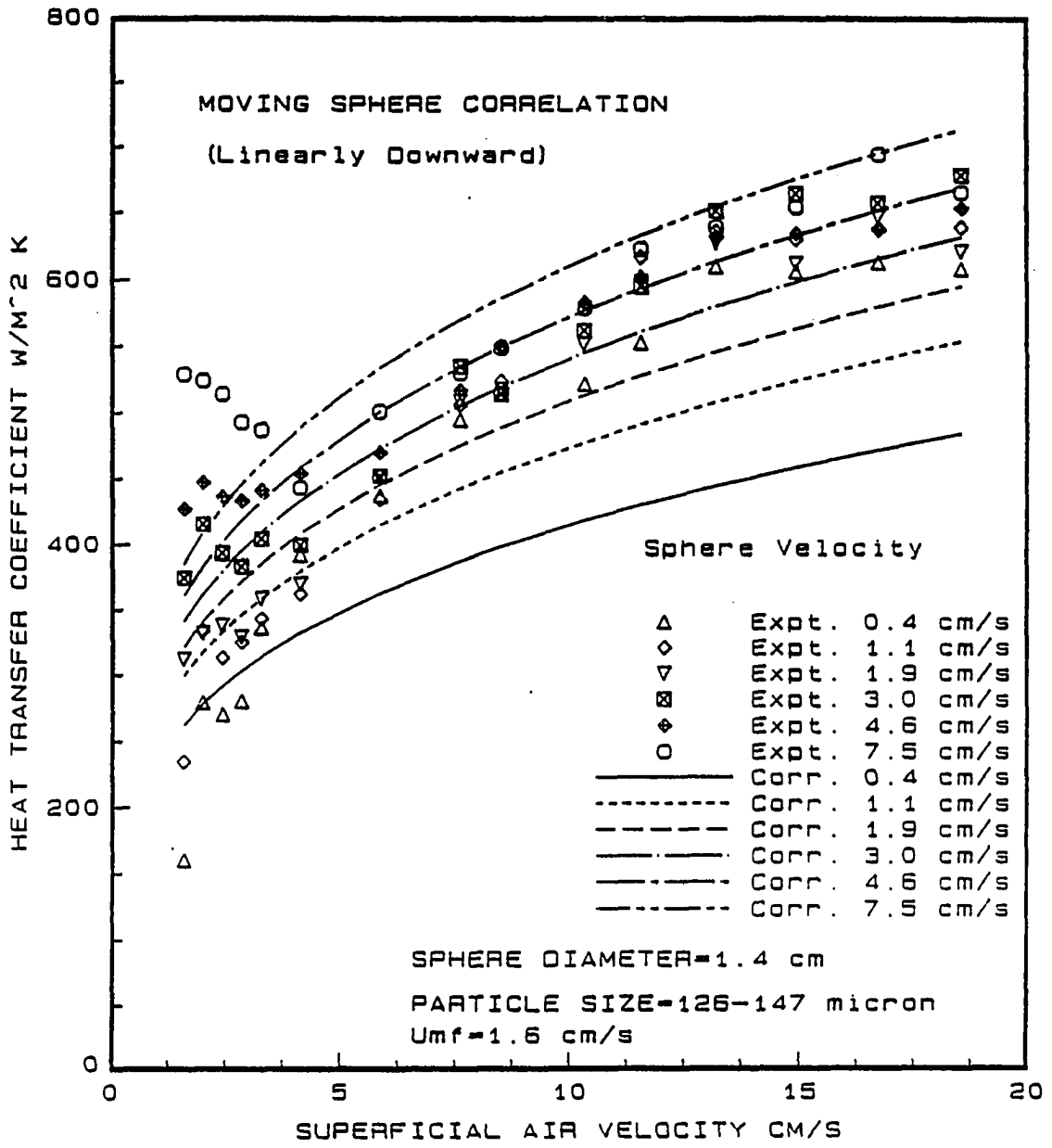

Figure 4.6: Experimental and predicted heat transfer coefficients (correlation I, equation 4.3) as a function of superficial air velocity for the linearly downward moving sphere in a fluidized bed of 126-147 μm glass particles

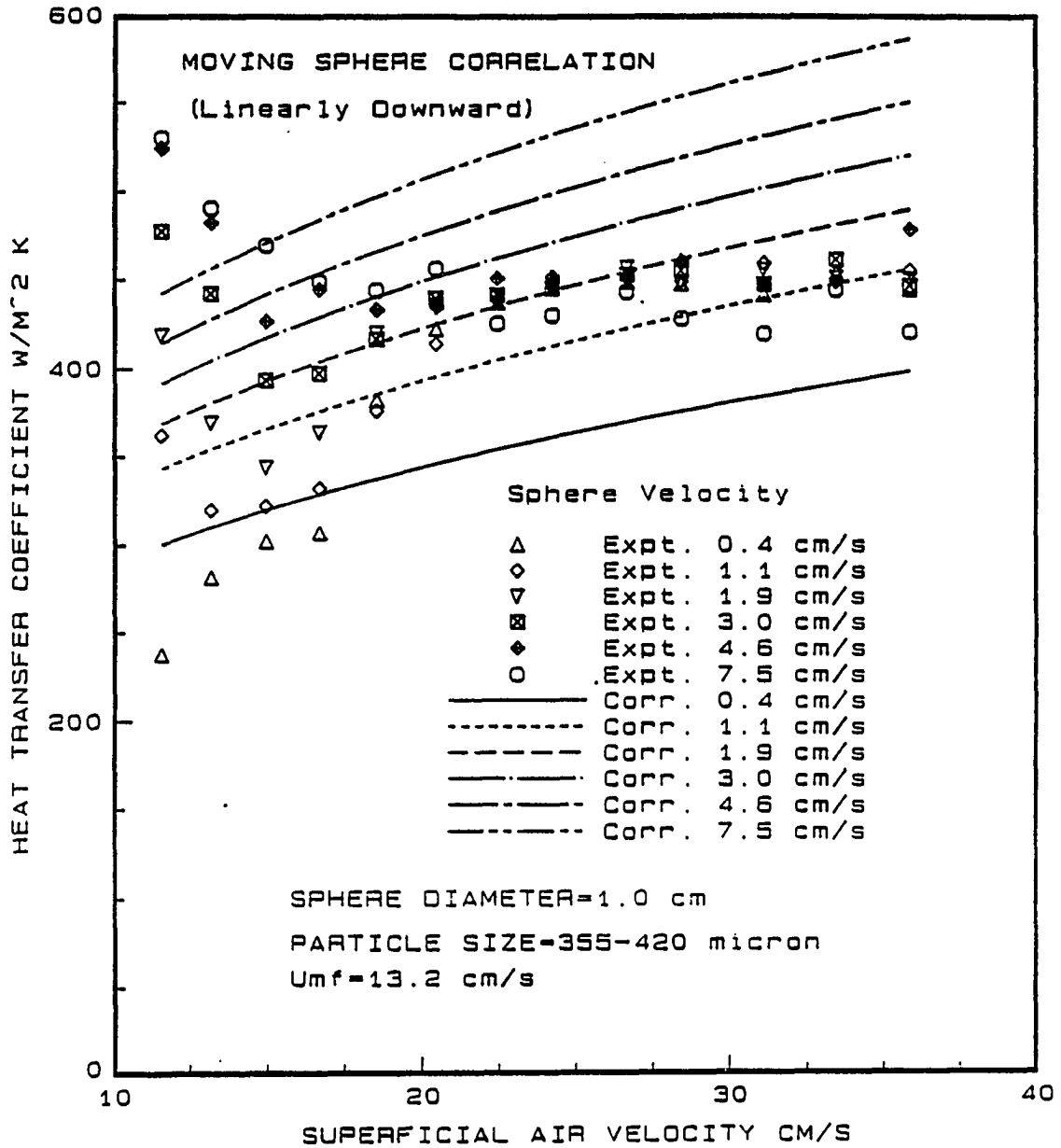

Figure 4.7: Experimental and predicted heat transfer coefficients (correlation I. equation 4.3) as a function of superficial air velocity for the linearly downward moving sphere in a fluidized bed of 355-420 μm glass particles

the correlation does not represent the experimental results entirely correctly. One obvious problem occurs in the region of lower superficial air velocities and higher sphere velocities, where the heat transfer coefficient decreases with increase in the superficial air velocity up to certain value of the superficial air velocity, as in Figure 4.5 above V_{sph} = 0.4 cm/s and than either increases or remains nearly constant, changing the slope of the curve from negative to positive. However, the proposed form of the correlation does not permit such a change of the slope.

In order to obtain a better correlation, the heat transfer results were divided into two regions according to the observed trend of the plot of the heat transfer coefficient versus the superficial air velocity as shown in Figure 4.5. In the region A, the heat transfer coefficient is either decreasing or increasing with increase in the superficial air velocity. In the region B, the heat transfer coefficient remains nearly constant or increases with increase in the superficial air velocity. The transition from the region A to the region B occurs at different superficial air velocity for each glass particle size such as; 0.325 cm/s, 3.744 cm/s and 20.0 cm/s for 24.5, 136.5 and 387.5 μm mean diameter glass particles respectively. This transition point can be defined by one single parameter for all the glass particle sizes and sphere diameters as;

$$Parameter1 = \left(\frac{\frac{U}{U_{mf}} d_p}{\left(\frac{(1-\epsilon_{mf})}{\epsilon_{mf}} \right)^3} \right) = 191 \mu m \tag{4.4}$$

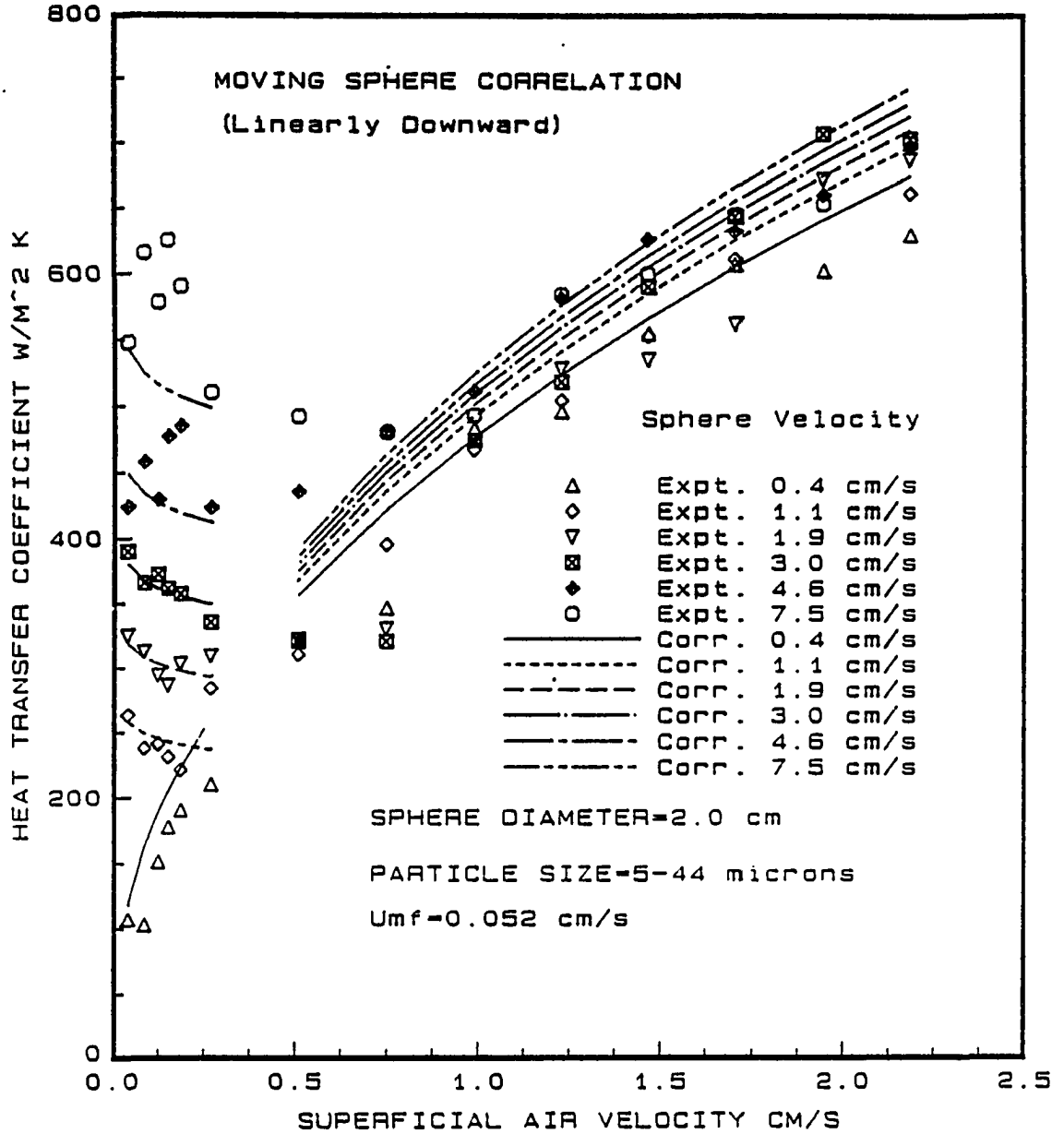

Figure 4.8: Experimental and predicted heat transfer coefficients (correlation II, equation 4.5) as a function of superficial air velocity for the linearly downward moving sphere in a fluidized bed of 5-44 μm glass particles

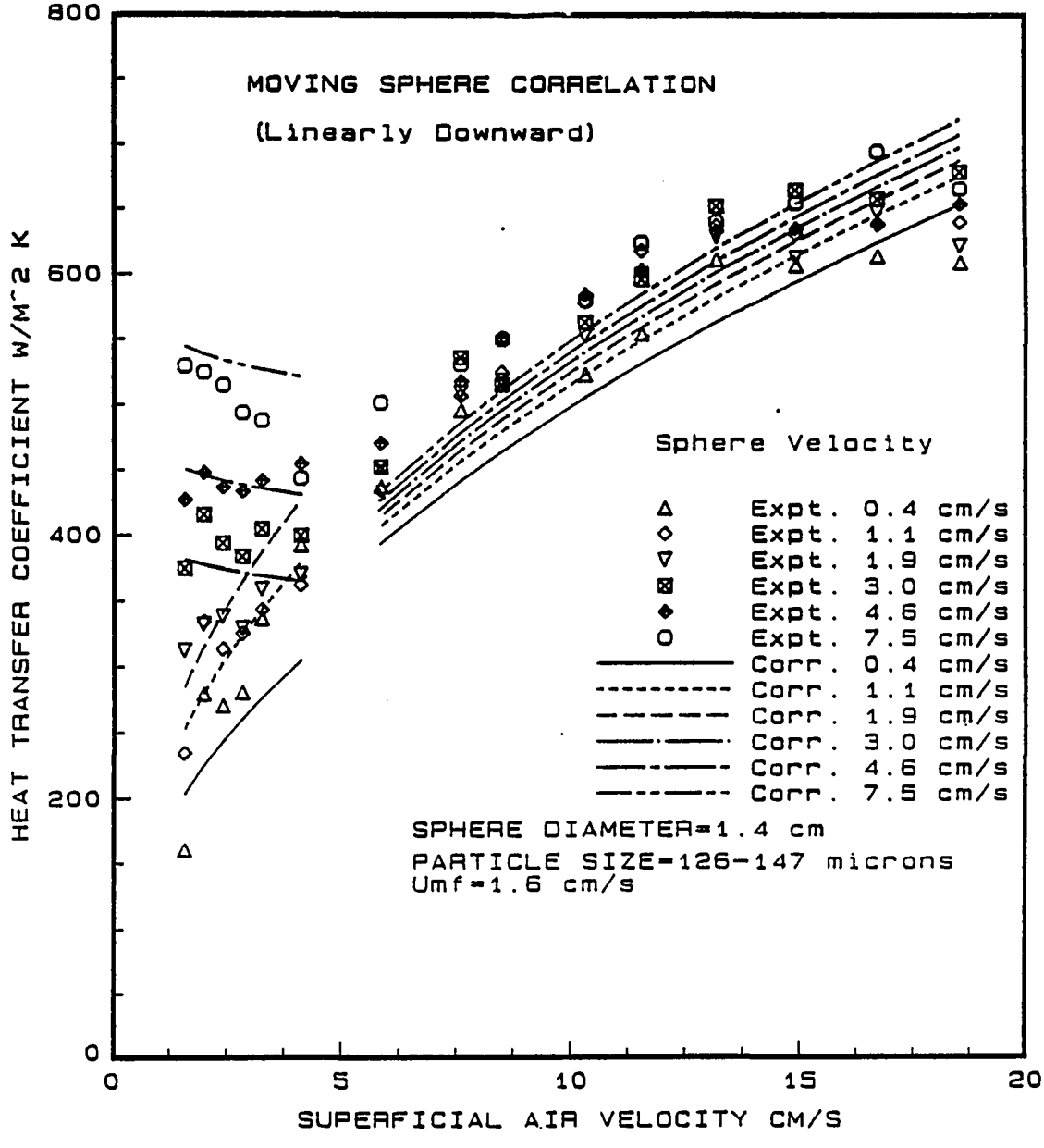

Figure 4.9: Experimental and predicted heat transfer coefficients (correlation II, equation 4.5) as a function of superficial air velocity for the linearly downward moving sphere in a fluidized bed of 126-147 μm glass particles

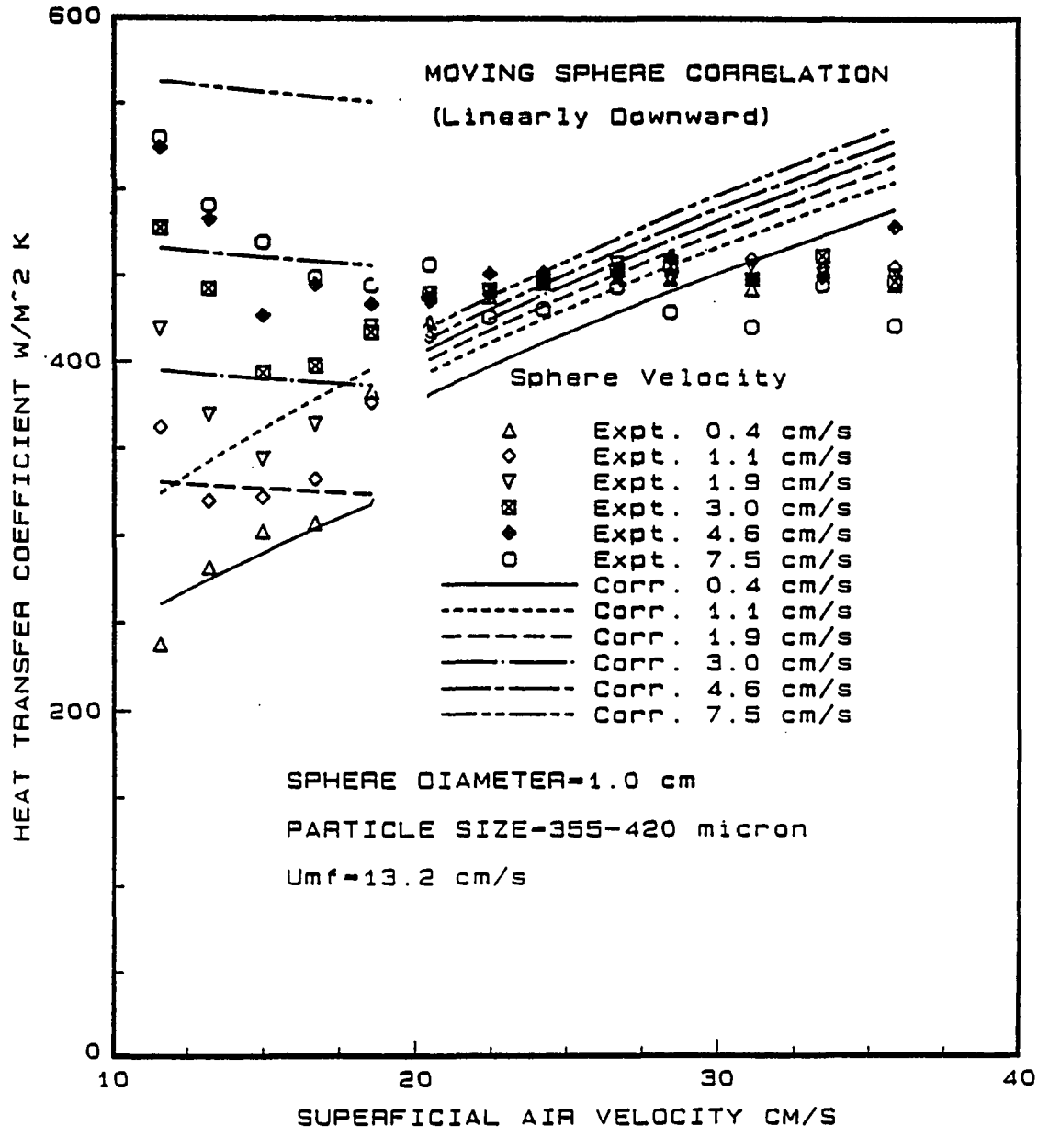

Figure 4.10: Experimental and predicted heat transfer coefficients (correlation II. equation 4.5) as a function of superficial air velocity for the linearly downward moving sphere in a fluidized bed of 355-420 μm glass particles

When the value of this parameter1 is less than 191 μm, the observed trend in the heat transfer coefficient is that of the region A, i.e., either increasing or decreasing with an increase in the superficial air velocity. Whereas, if the value of the parameter1 is greater than 191 μm, the trend of the region B is observed. Furthermore, the region A can also be divided in to two subdivisions namely A1 and A2, representing the decreasing and increasing trend of the heat transfer coefficient with increasing superficial air velocity respectively. The general form of the correlation is given by(within $\pm$ 25 %);

Correlation II

$$Nu_m = C_{m1}\left(\frac{U}{U_{mf}}\right)^{C_{m2}}\left(\frac{gd_p^3\rho_g(\rho_p-\rho_g)}{\mu_g^2}\right)^{C_{m3}}\left(\frac{D_{sph}}{d_p}\right)^{C_{m4}} \times\left(\frac{V_{sph}}{U_{mf}}\right)^{C_{m5}} \tag{4.5}$$

The coefficients C_{m1} to C_{m4} for each region and the corresponding condition for the application of the correlation is listed in Table 4.1. The sphere velocities are defined as,

$$V_1 = 0.4cm/s \quad V_2 = 1.1cm/s \quad V_3 = 1.9cm/s \quad V_4 = 3.0cm/s$$
$$V_5 = 4.6cm/s \text{ and } V_6 = 7.5cm/s$$

As shown in Figures 4.8 to 4.10, the agreement between the predicted and the observed values of the heat transfer coefficient is better than the previous correlation. However for the case of the 355-420 μm glass particles, the correlation does

Table 4.1: Coefficients for the equation 4.5 and corresponding range of application for all glass particle size

Region	C_{m1}	C_{m2}	C_{m3}	C_{m4}	C_{m5}	Range of Application
A1	0.404	-0.0406	0.481	0.719	0.389	Parameter1 $\leq$ 191 μm For 5-44 μm D_{sph}=1.0 cm, V_1 to V_6 D_{sph} = 1.4cm V_3 *to* V_6 D_{sph} = 2.0cm V_2 *to* V_6 For 126-147 μm D_{sph}=1.0 cm, V_3 to V_6 D_{sph} = 1.4cm V_4 *to* V_6 D_{sph} = 2.0cm V_5 *to* V_6 For 355-420 μm D_{sph}=1.0 cm, V_3 to V_6 D_{sph} = 1.4cm V_4 *to* V_6 D_{sph} = 2.0cm V_4 *to* V_6
A2	0.406	0.424	0.456	0.729	0.216	Parameter1 $\leq$ 191 μm For 5-44 μm D_{sph} = 1.4cm V_1 *to* V_2 D_{sph} = 2.0cm V_1 For 126-147 μm D_{sph}=1.0 cm, V_1 to V_2 D_{sph} = 1.4cm V_1 *to* V_3 D_{sph} = 2.0cm V_1 *to* V_4 For 355-420 μm D_{sph}=1.0 cm, V_1 to V_2 D_{sph} = 1.4cm V_1 *to* V_3 D_{sph} = 2.0cm V_4 *to* V_6
B	0.334	0.439	0.384	0.814	0.033	Parameter1 $\geq$ 191 μm for all range of glass particles and copper spheres used

not follow the experimental trend in the heat transfer coefficient at low superficial air velocity and high sphere velocity.

In order to improve the correlation further, each powder size was correlated separately in the following form;

$$Nu_m = C_{mm1} \left(\frac{U}{U_{mf}}\right)^{C_{mm2}} \left(\frac{D_{sph}}{d_p}\right)^{C_{mm3}} \left(\frac{V_{sph}}{U_{mf}}\right)^{C_{mm4}} \tag{4.6}$$

In this proposed correlation the Archimedes' number is not included as an independent variable as the correlation is sought for each particle size range. Tables 4.2, 4.3 and 4.4 lists the coefficients for each glass particle size and the range of application of the correlation.

Figures 4.11 to 4.19 shows the experimental and the predicted heat transfer coefficients as a function of superficial air velocity for each glass particle size and copper sphere diameter. Furthermore, Figures 4.20, 4.21 and 4.22 show the overall goodness of fit of the correlation.

4.3 Heat Transfer Correlation For Oscillating Sphere

Heat transfer results for an oscillating sphere were correlated in the same general format as given by the equation 4.1. Instead of the linear velocity of the sphere, the average translational sphere velocity given by the product of the frequency and the peak-to-peak amplitude of the oscillation was used.

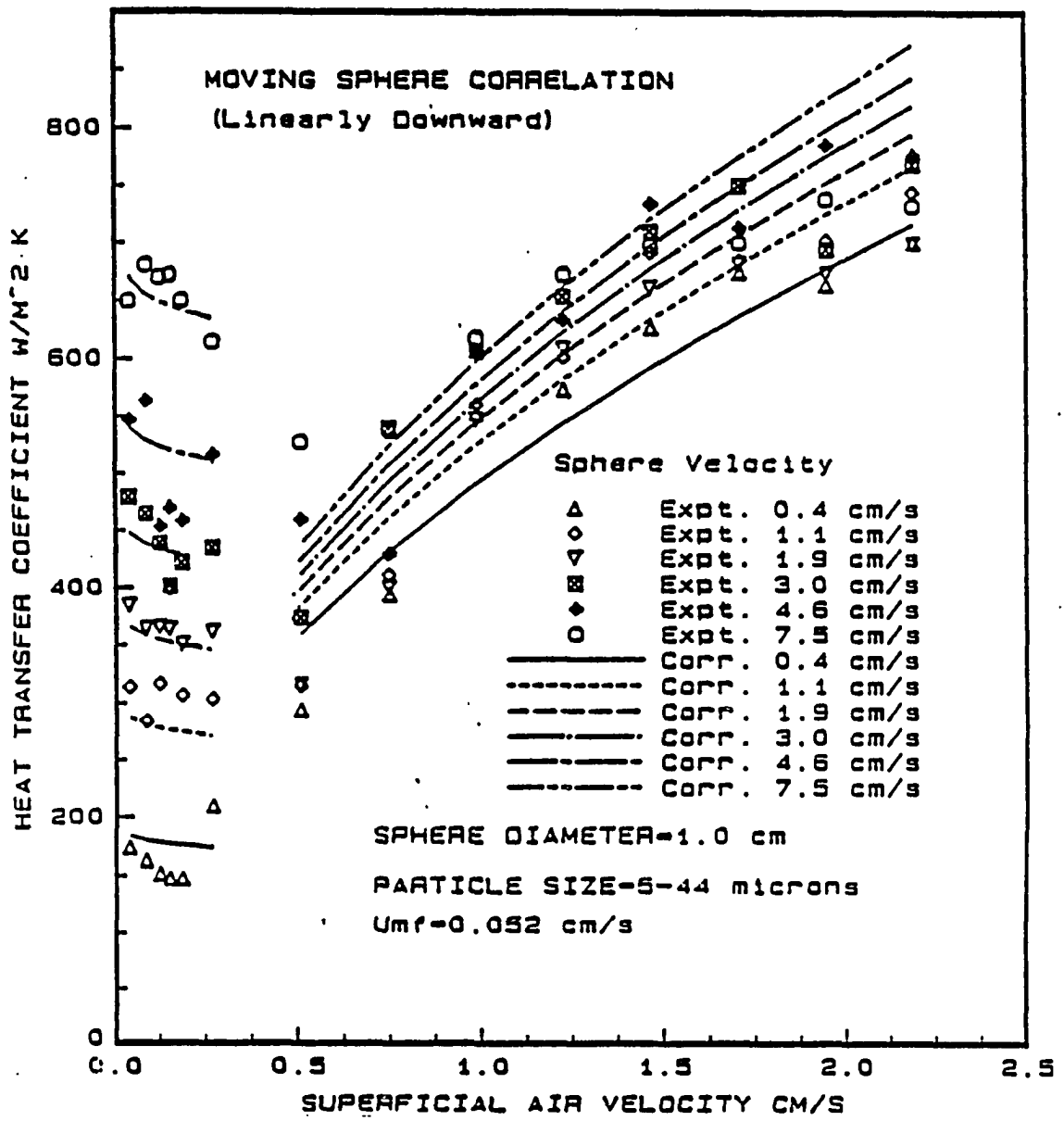

Figure 4.11: Experimental and predicted heat transfer coefficients (correlation III. equation 4.6) as a function of superficial air velocity for the linearly downward moving 1.0 cm diameter sphere in a fluidized bed of 5-44 μm glass particles

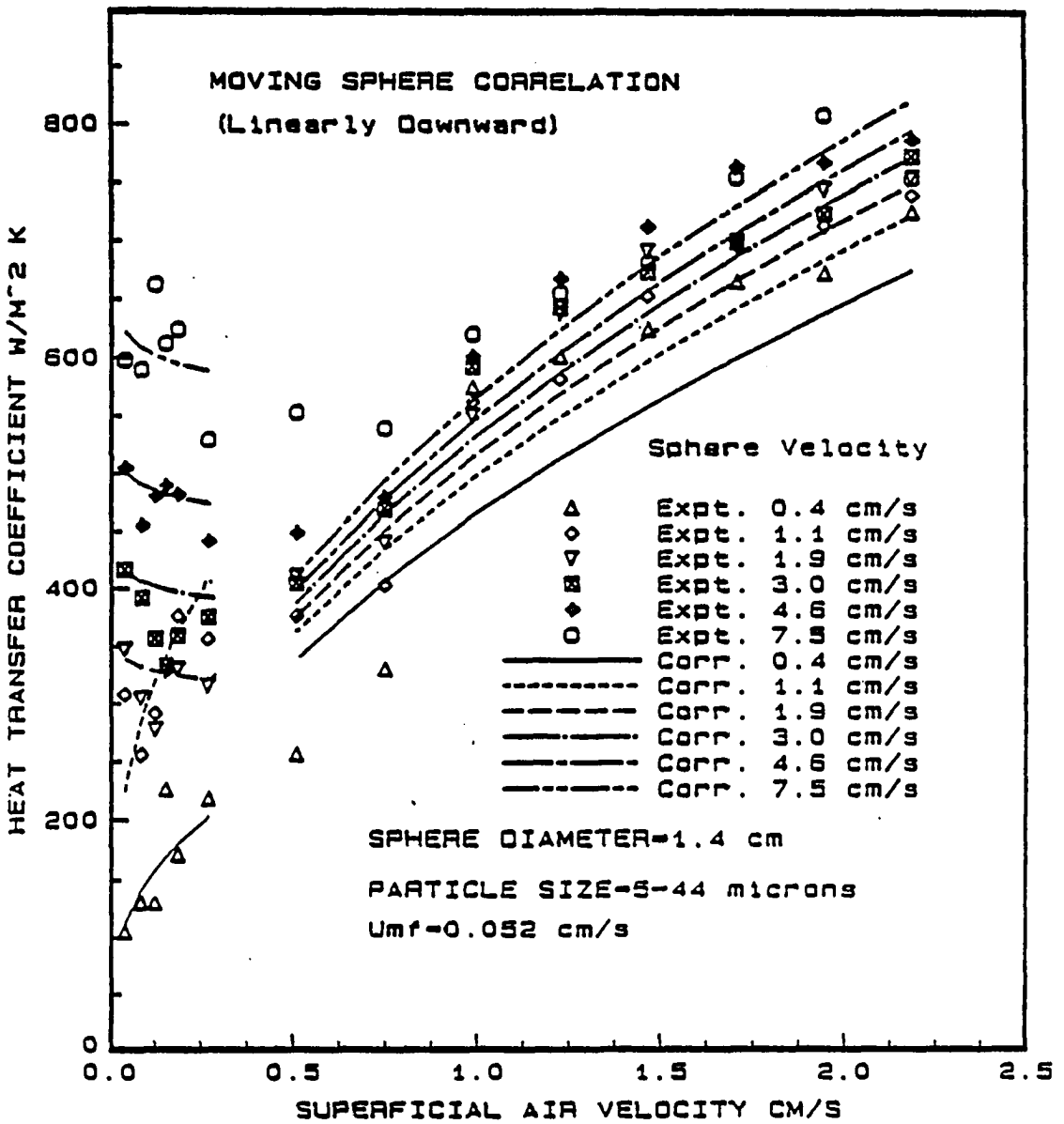

Figure 4.12: Experimental and predicted heat transfer coefficients (correlation III. equation 4.6) as a function of superficial air velocity for the linearly downward moving 1.4 cm diameter sphere in a fluidized bed of 5-44 μm glass particles

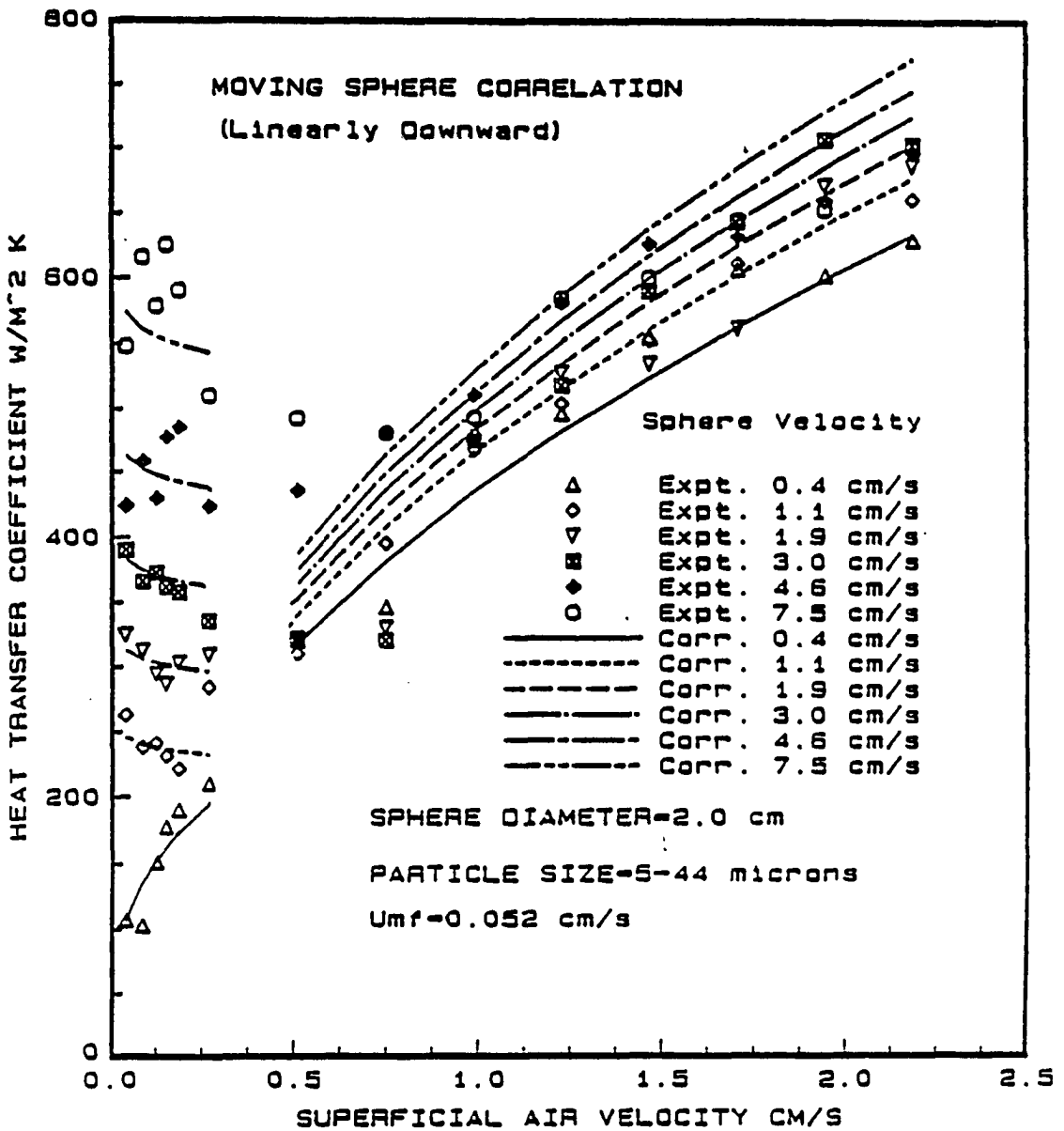

Figure 4.13: Experimental and predicted heat transfer coefficients (correlation III, equation 4.6) as a function of superficial air velocity for the linearly downward moving 2.0 cm diameter sphere in a fluidized bed of 5-44 μm glass particles

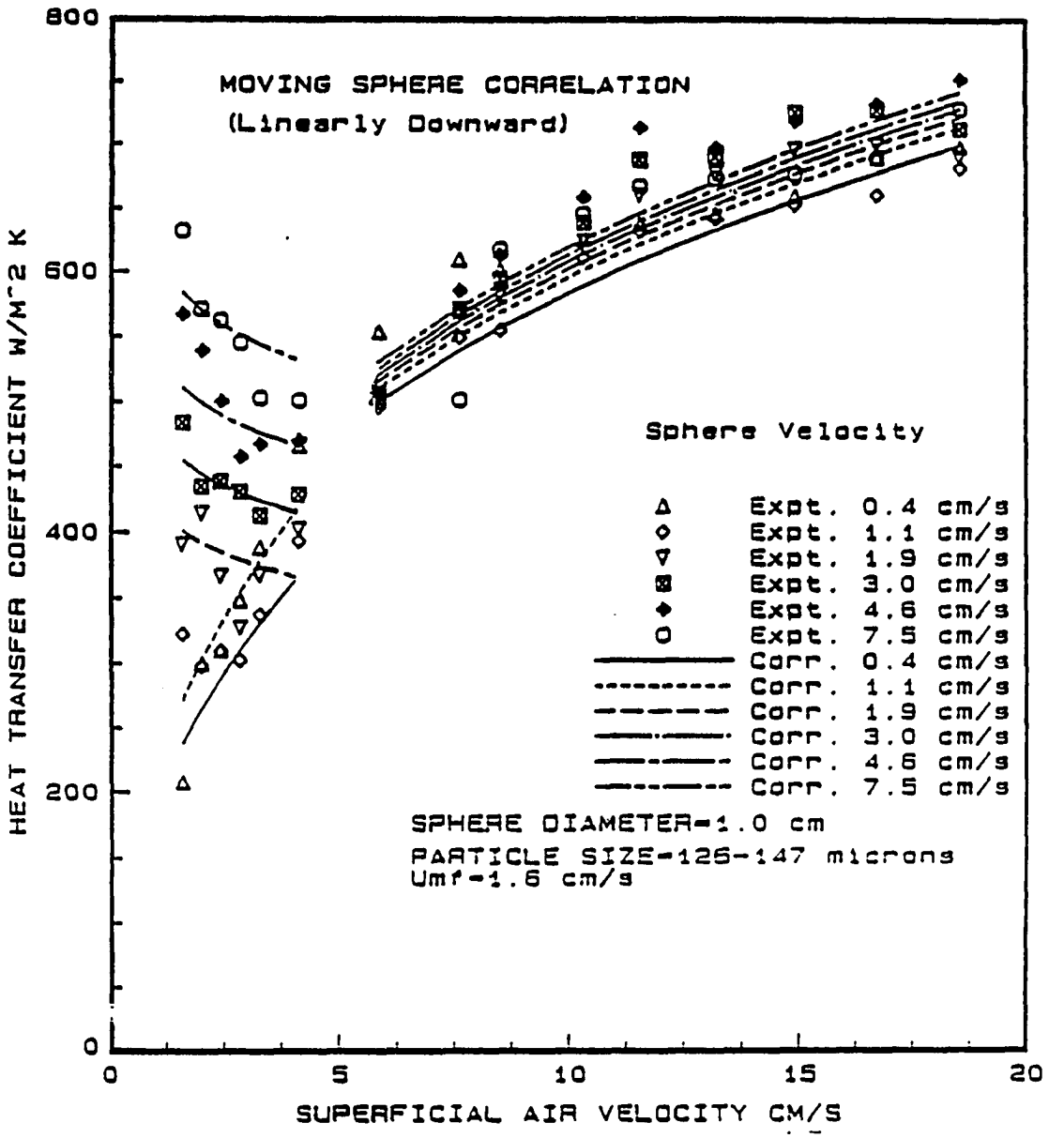

Figure 4.14: Experimental and predicted heat transfer coefficients (correlation III, equation 4.6) as a function of superficial air velocity for the linearly downward moving 1.0 cm diameter sphere in a fluidized bed of 126-147 μm glass particles

Table 4.2: Coefficients for equation 4.6 and the corresponding range of application for 5-44 μm glass particle system

Region	C_{mm1}	C_{mm2}	C_{mm3}	C_{mm4}	Range of Application
A1	0.219	-0.0301	0.774	0.443	Parameter1 $\leq$ 191 μm D_{sph}=1.0 cm, V_1 to V_6 $D_{sph} = 1.4cm$ V_3 *to* V_6 $D_{sph} = 2.0cm$ V_2 *to* V_6
A2	0.045	0.322	0.886	0.696	Parameter1 $\leq$191 μm $D_{sph} = 1.4cm$ V_1 *to* V_2 $D_{sph} = 2.0cm$ V_1
B	0.238	0.474	0.823	0.0667	Parameter1 $\geq$ 191 μm of glass particles and copper spheres used

Table 4.3: Coefficients for equation 4.6 and the corresponding range of application for 126-147 μm glass particle system

Region	C_{mm1}	C_{mm2}	C_{mm3}	C_{mm4}	Range of Application
A1	5.398	-0.099	0.721	0.274	Parameter1 $\leq$ 191 μm D_{sph}=1.0 cm, V_3 to V_6 $D_{sph} = 1.4cm$ V_4 *to* V_6 $D_{sph} = 2.0cm$ V_5 *to* V_6
A2	1.85	0.456	0.903	0.132	Parameter1 $\leq$191 μm $D_{sph} = 1.0cm$ V_1 *to* V_2 $D_{sph} = 1.4cm$ V_1 *to* V_3 $D_{sph} = 2.0cm$ V_1 *to* V_4
B	3.01	0.289	0.839	0.02	Parameter1 $\geq$ 191 μm of glass particles and copper spheres used

Table 4.4: Coefficients for equation 4.6 and the corresponding range of application for 355-420 μm glass particle system

Region	C_{mm1}	C_{mm2}	C_{mm3}	C_{mm4}	Range of Application
A1	16.88	-0.239	0.716	0.166	Parameter1 $\leq$ 191 μm D_{sph}=1.0 cm, V_3 to V_6 $D_{sph} = 1.4cm$ V_4 *to* V_6 $D_{sph} = 2.0cm$ V_4 *to* V_6
A2	12.83	0.549	0.717	0.778	Parameter1 $\leq$191 μm $D_{sph} = 1.0cm$ V_1 *to* V_2 $D_{sph} = 1.4cm$ V_1 *to* V_3 $D_{sph} = 2.0cm$ V_1 *to* V_3
B	9.91	0.175	0.778	0.011	Parameter1 $\geq$ 191 μm of glass particles and copper spheres used

$$Nu_o = 0.794\left(\frac{U}{U_{mf}}\right)^{0.228}\left(\frac{gd_p^3\rho g(\rho_p-\rho_g)}{\mu_g^2}\right)^{0.361}\left(\frac{D_{sph}}{d_p}\right)^{0.685} \times\left(\frac{2F_{sph}A_{sph}}{U_{mf}}\right)^{0.159} \quad (4.7)$$

Figures 4.23 to 4.25 shows the goodness of fit for the above correlation. The difference in the predicted and the experimental heat transfer coefficient is about $\pm$ 30 % for the case of the 5-44 μm glass particle at higher frequency and higher peak-to-peak amplitude as seen in Figure 4.23.

The correlations obtained given here can serve as guidelines for a reasonable prediction of the heat transfer coefficient under certain conditions. The validity of these correlations beyond the range of the present experiment is questionable. The heat transfer characteristics of a fluidized bed depends largely on the hydrodynamics of the bed. Many variables affect the hydrodynamic behavior of the bed such as the distributor plate design, the physical dimensions of the bed, the geometry of the immersed object, and the properties of the fluidized particles.

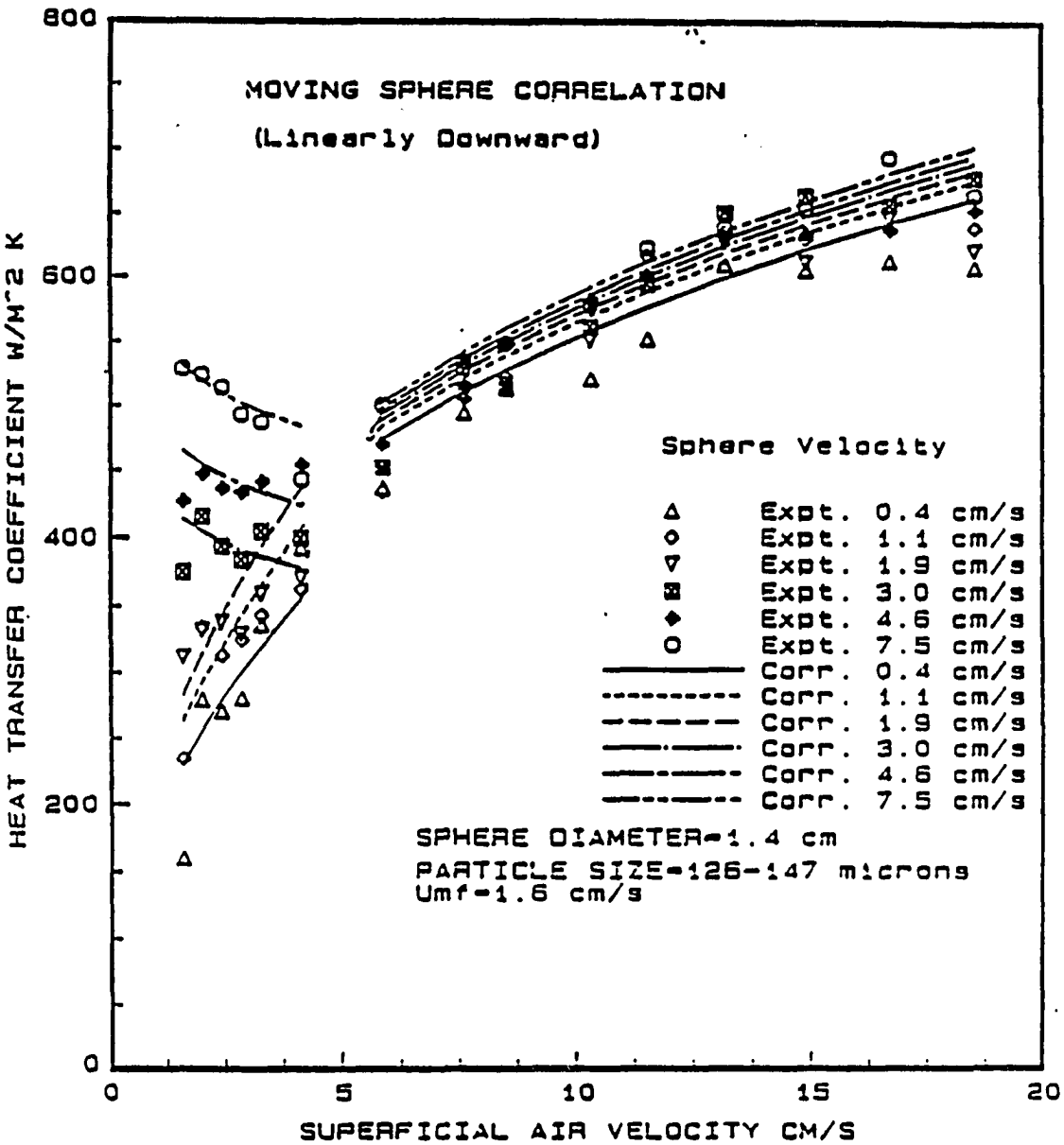

Figure 4.15: Experimental and predicted heat transfer coefficients (correlation III, equation) as a function of superficial air velocity for the linearly downward moving 1.4 cm diameter sphere in a fluidized bed of 126-147 μm glass particles

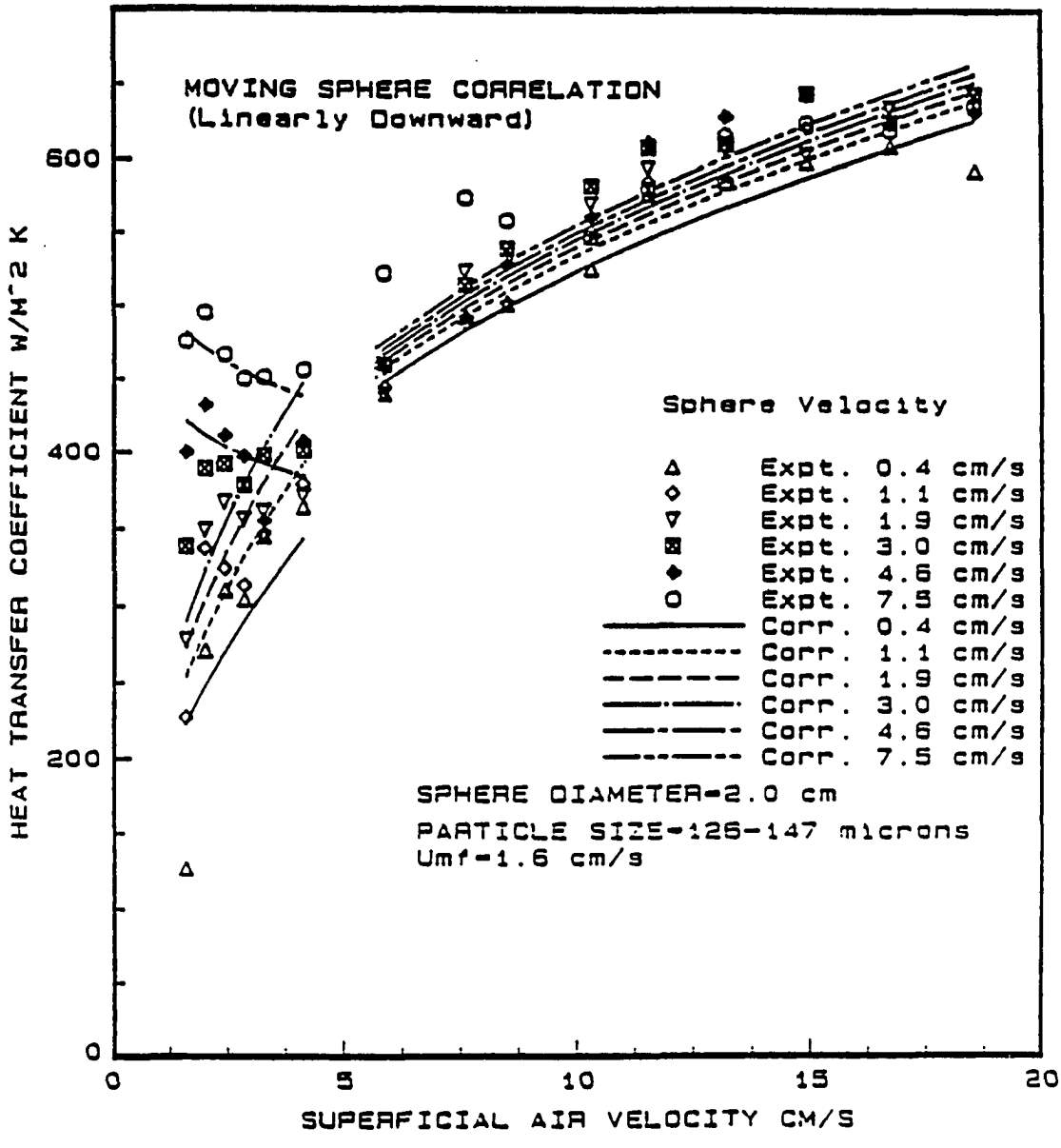

Figure 4.16: Experimental and predicted heat transfer coefficients (correlation III, equation 4.6) as a function of superficial air velocity for the linearly downward moving 2.0 cm diameter sphere in a fluidized bed of 126-147 μm glass particles

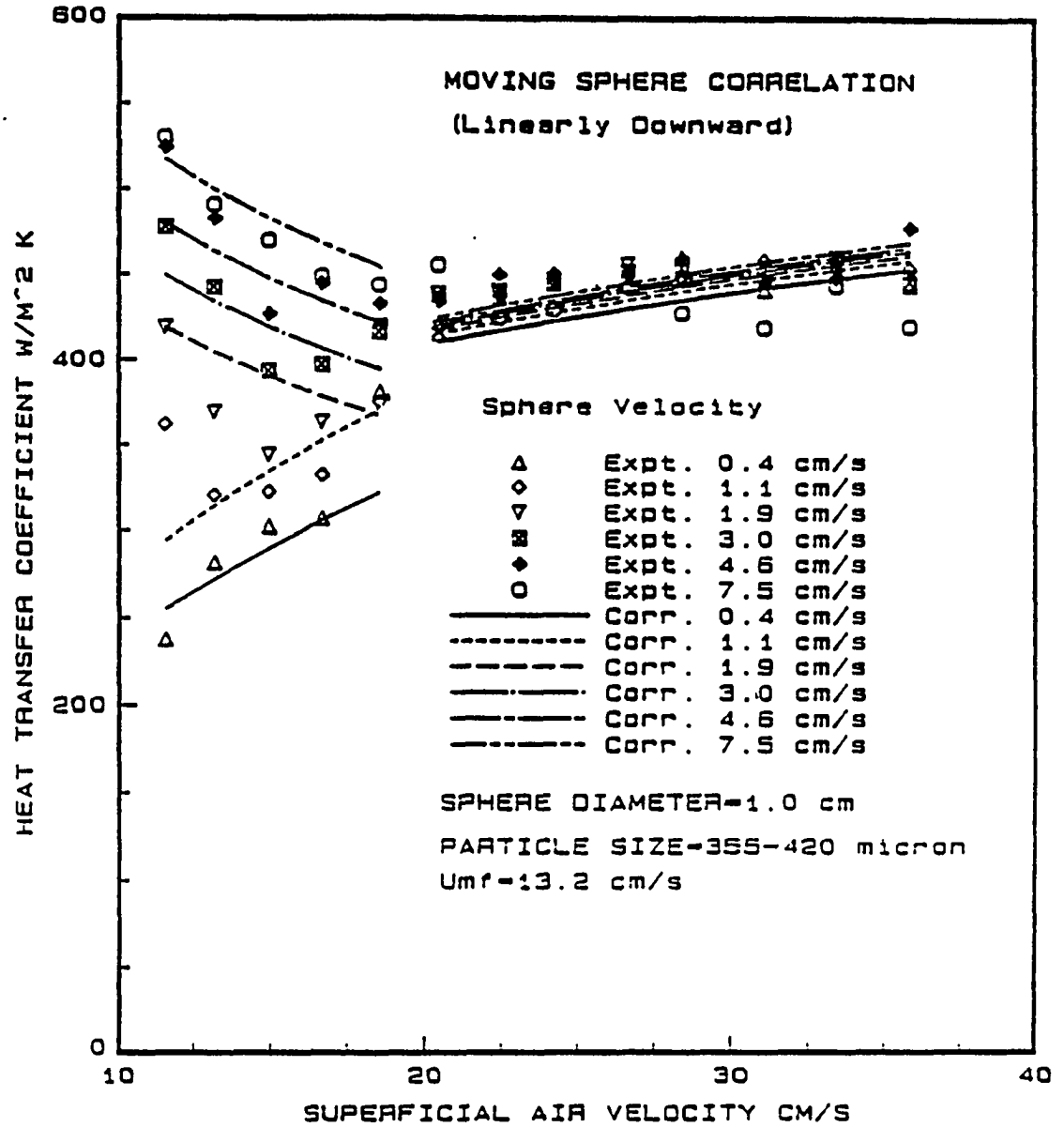

Figure 4.17: Experimental and predicted heat transfer coefficients (correlation III, equation 4.6) as a function of superficial air velocity for the linearly downward moving 1.0 cm diameter sphere in a fluidized bed of 355-420 μm glass particles

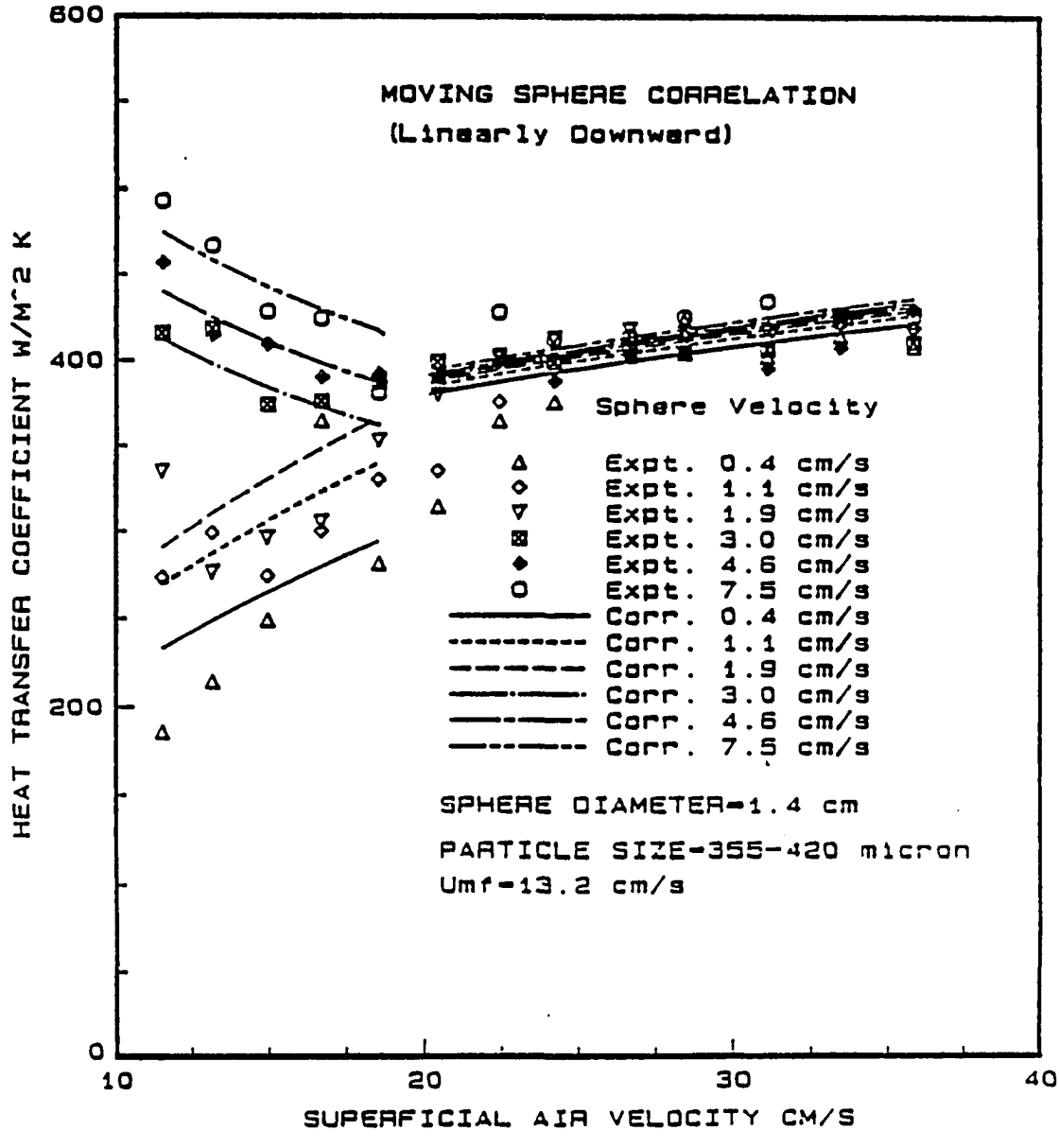

Figure 4.18: Experimental and predicted heat transfer coefficients (correlation III, equation 4.6) as a function of superficial air velocity for the linearly downward moving 1.4 cm diameter sphere in a fluidized bed of 355-420 μm glass particles

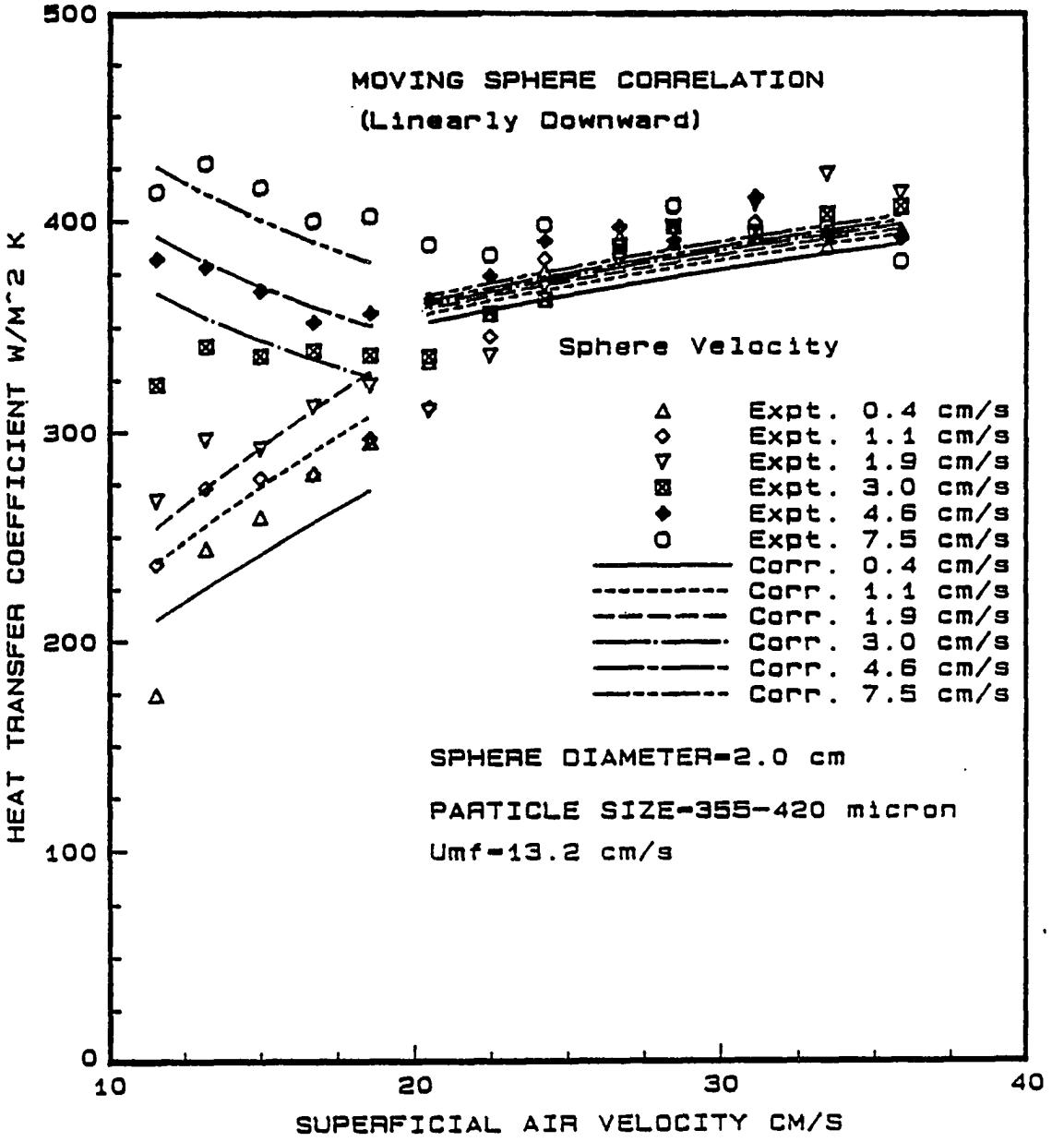

Figure 4.19: Experimental and predicted heat transfer coefficients (correlation III, equation 4.6) as a function of superficial air velocity for the linearly downward moving 2.0 cm diameter sphere in a fluidized bed of 355-420 μm glass particles

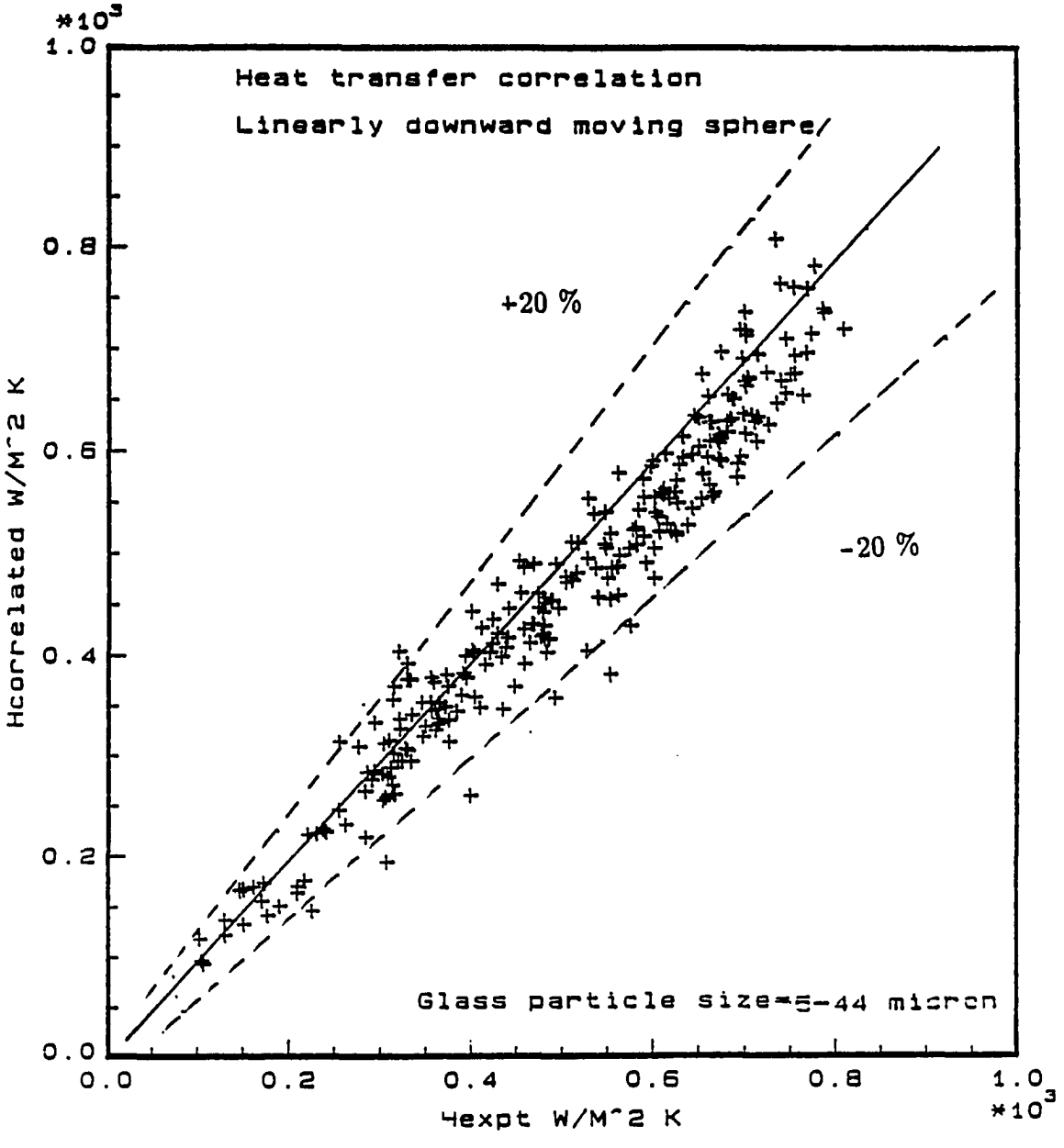

Figure 4.20: Predicted heat transfer coefficients (correlation III. equation 4.6) as a function of the experimental heat transfer coefficient for a fluidized bed of 5-44 μm glass particles

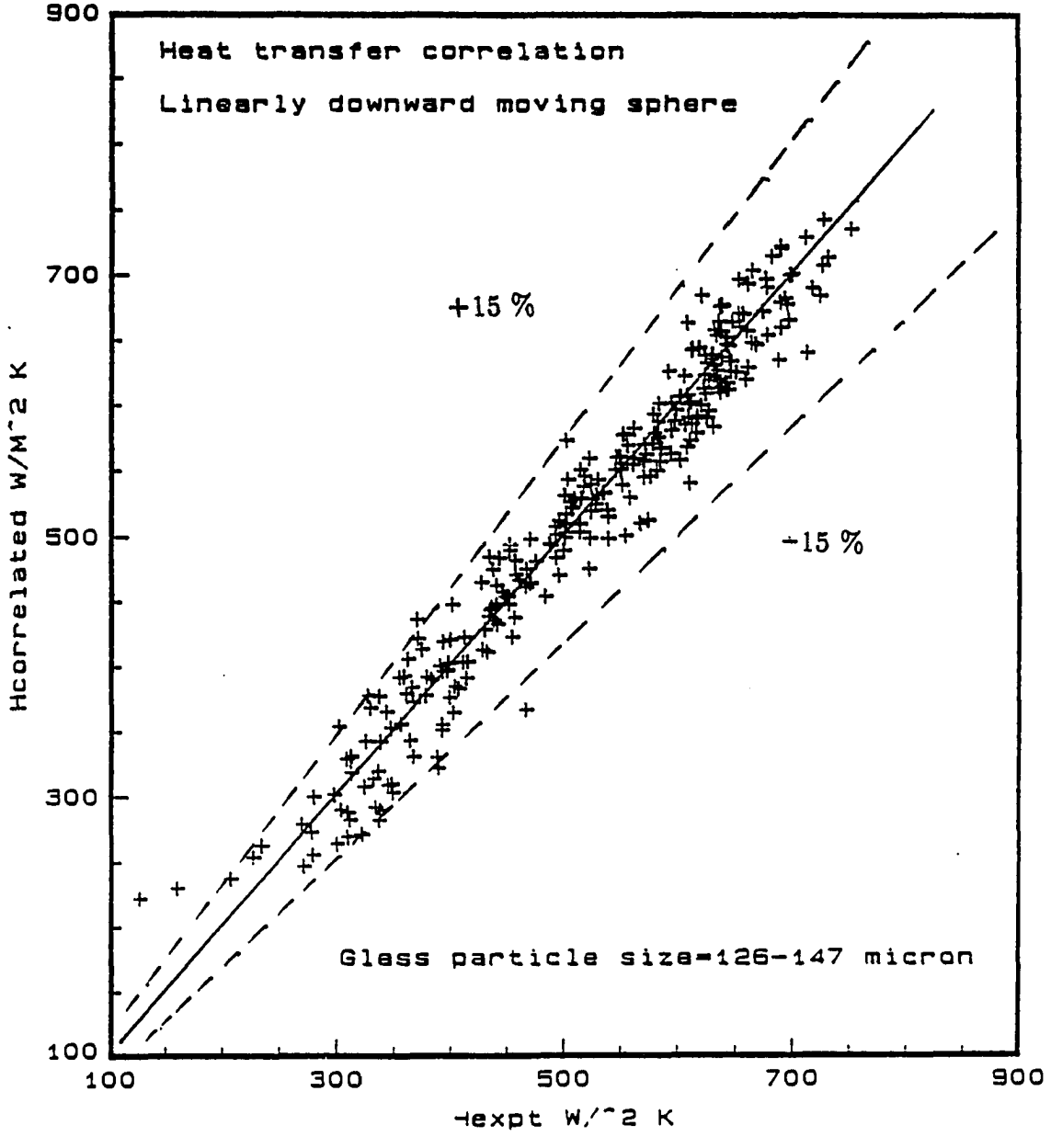

Figure 4.21: Predicted heat transfer coefficients (correlation III, equation 4.6) as a function of the experimental heat transfer coefficient for a fluidized bed of 126-147 μm glass particles

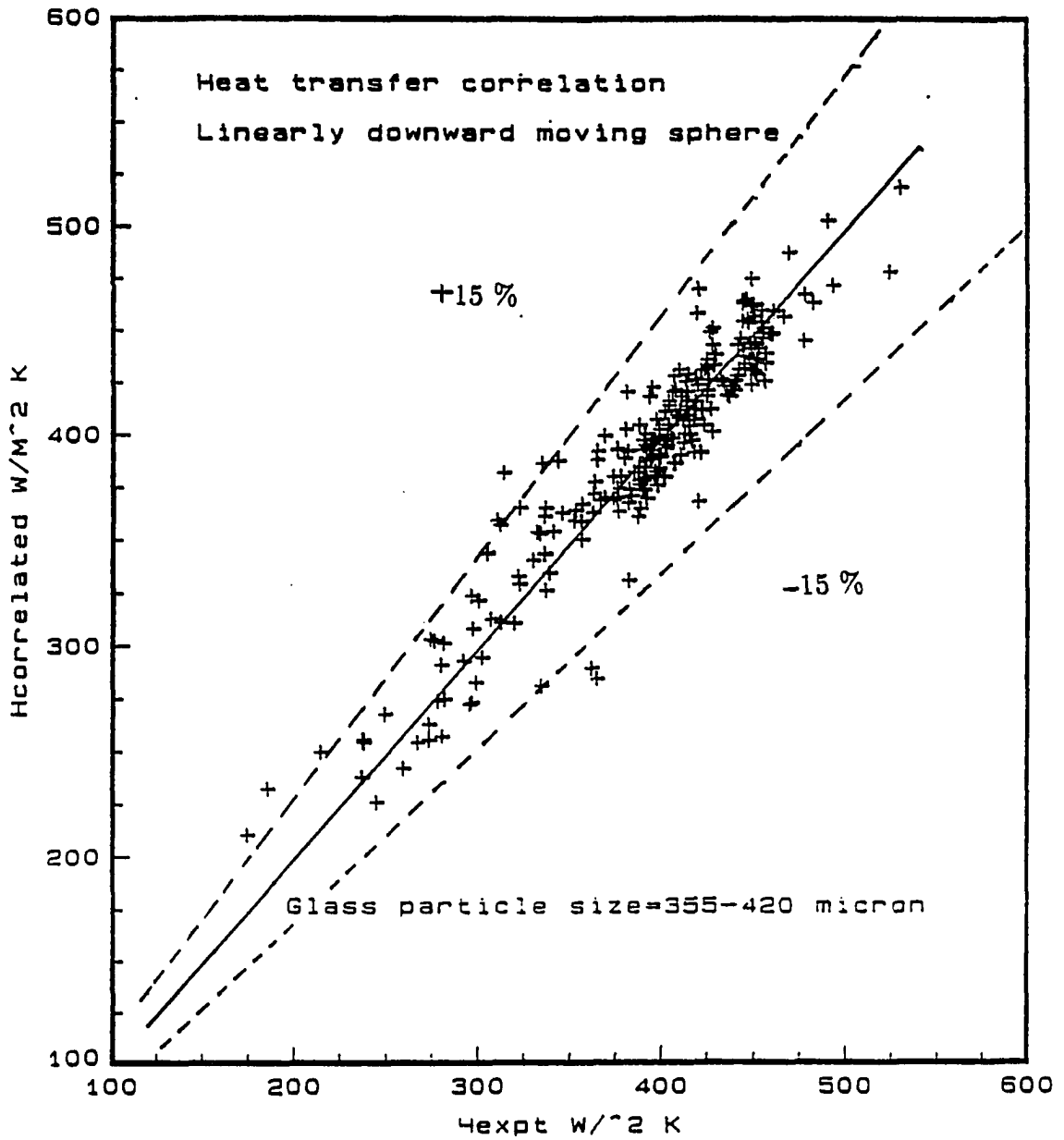

Figure 4.22: Predicted heat transfer coefficients (correlation III. equation 4.6) as a function of the experimental heat transfer coefficient for a fluidized bed of 355-420 μm glass particles

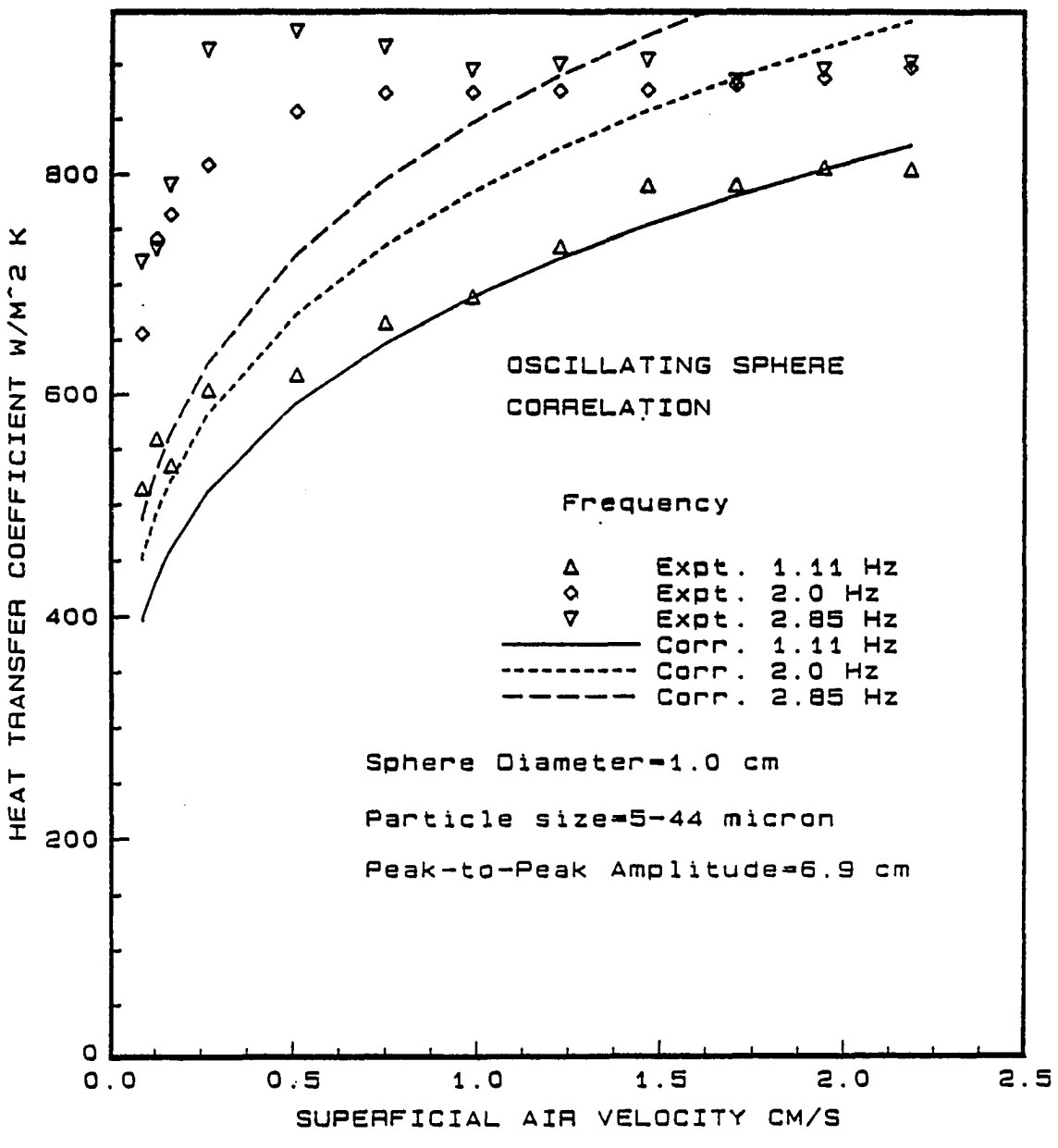

Figure 4.23: Experimental and predicted heat transfer coefficients as a function of superficial air velocity for an oscillating sphere in a fluidized bed of 5-44 μm glass particles

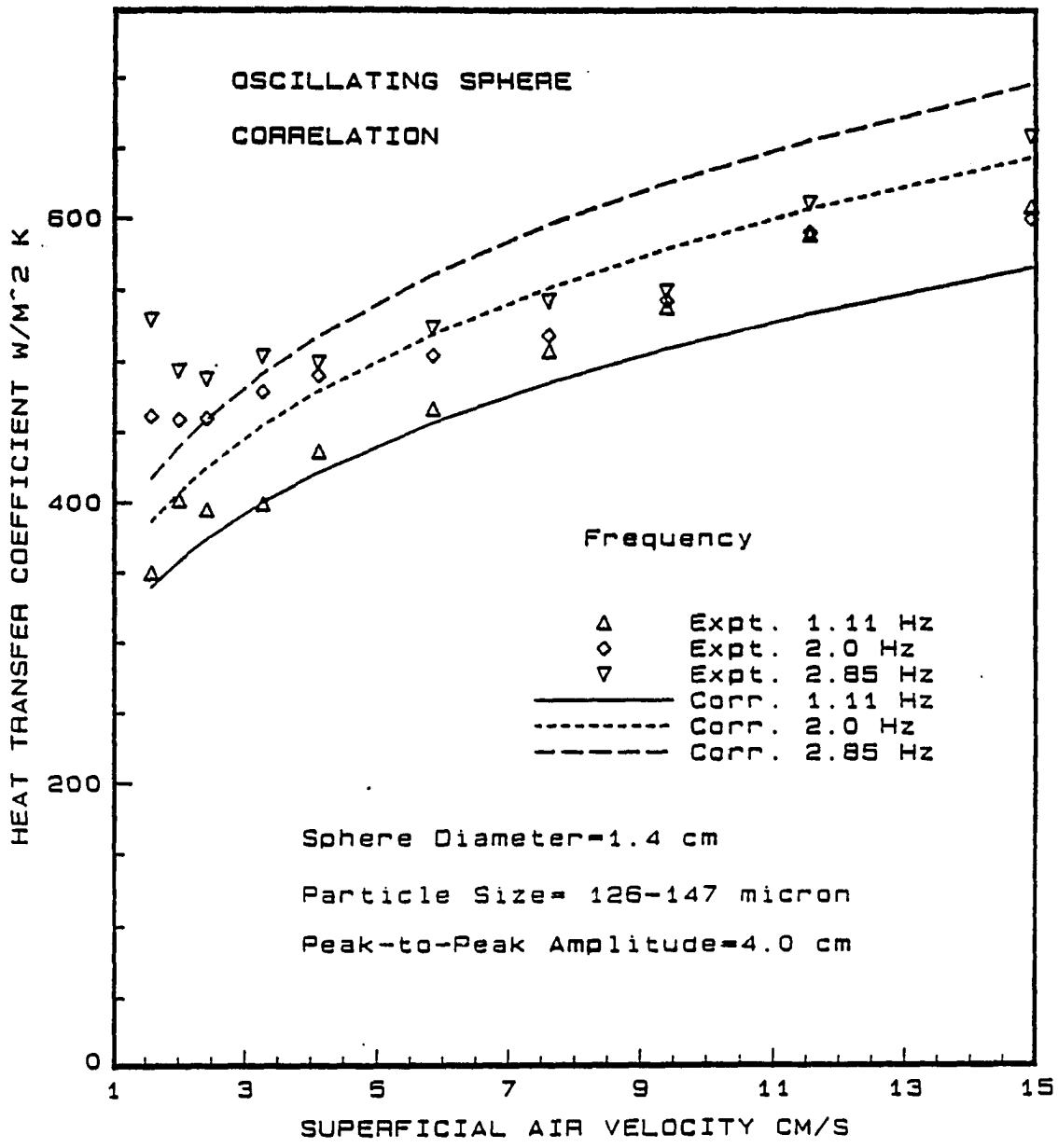

Figure 4.24: Experimental and predicted heat transfer coefficients as a function of superficial air velocity for an oscillating sphere in a fluidized bed of 126-147 μm glass particles

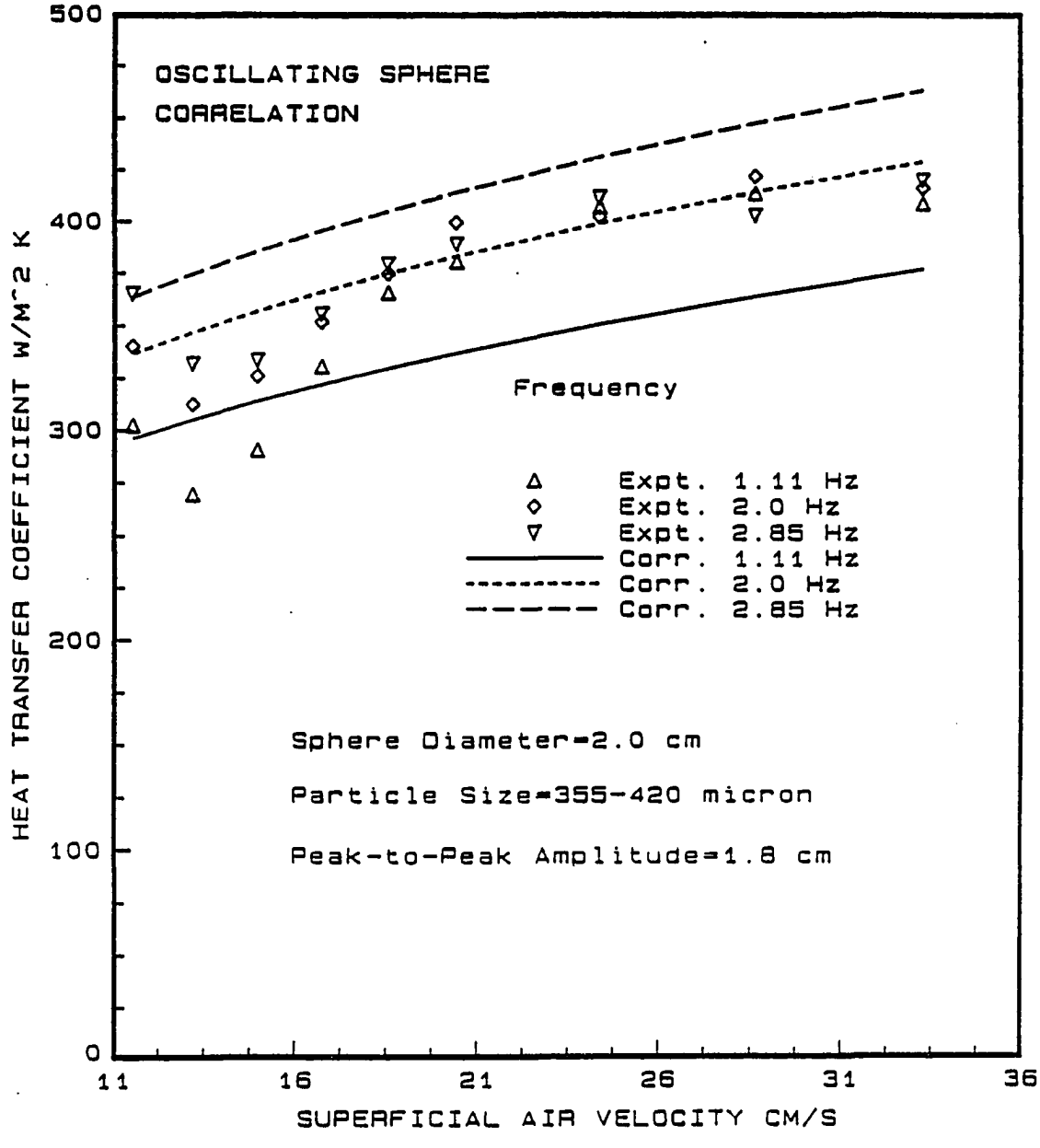

Figure 4.25: Experimental and predicted heat transfer coefficients as a function of superficial air velocity for an oscillating sphere in a fluidized bed of 355-420 μm glass particles

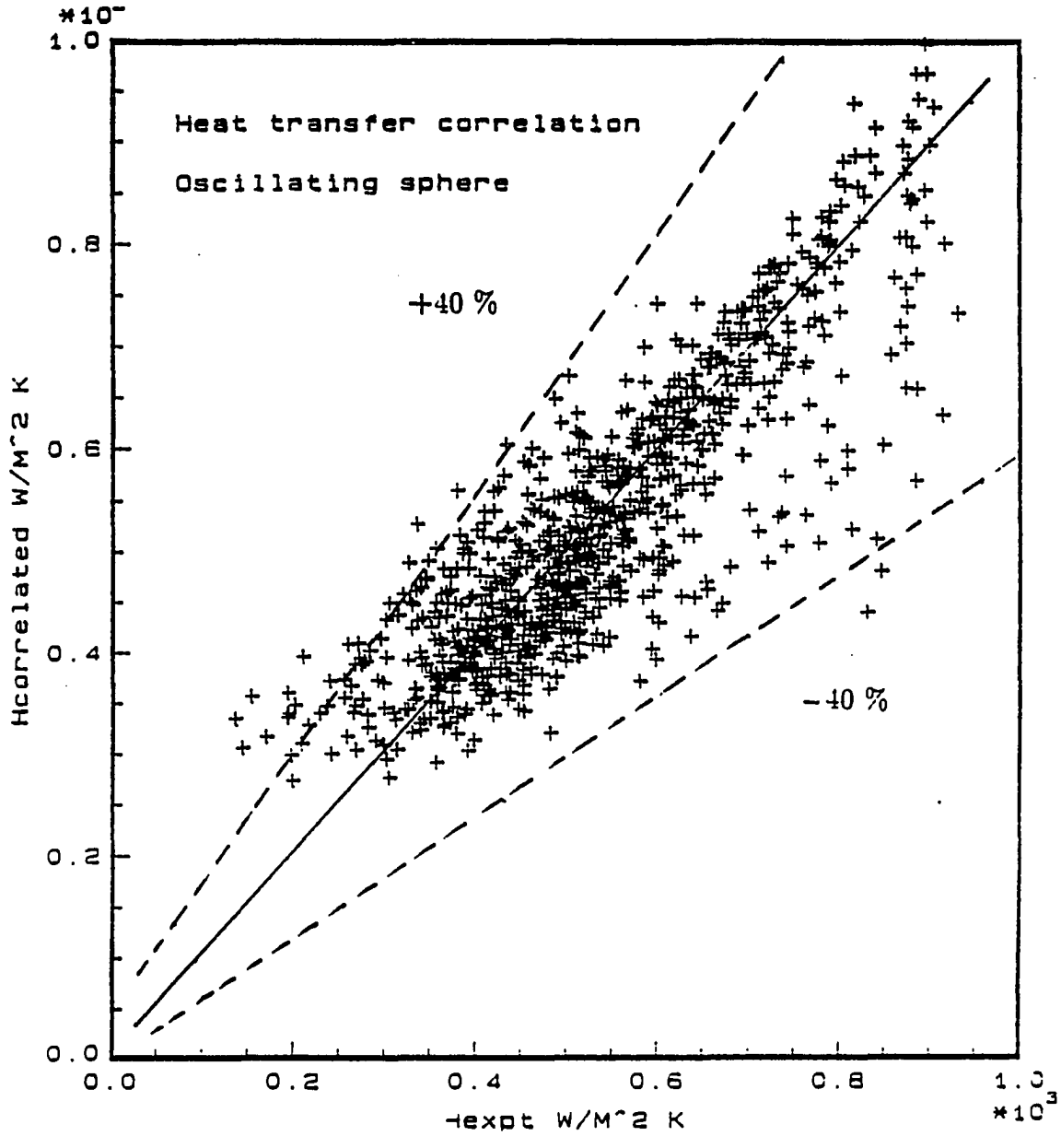

Figure 4.26: Predicted heat transfer coefficients as a function of the experimental heat transfer coefficient for an oscillating sphere in a fluidized bed

5 THEORETICAL HEAT TRANSFER MODEL

Many fundamental models have been proposed as described in chapter 1 to analyze the particle convective heat transfer process in a fluidized beds. A simple model containing the main features of the fluidized bed condition is the packet theory [Mickley and Fairbanks, 1955]. However, it predicts excessively high coefficients for very short particle residence times of a packet of emulsion adjacent to the heat transfer surface. To avoid this problem, a new model was postulated [Gelperin and Einstein, 1971]. At the instant t=0, the heat transfer surface, which is at temperature T_w, is approached by a packet of solid particles with the initial temperature equal to that of the bulk bed. In the zone adjacent to the wall, the voidage is different from that of the packet having a thermal resistance is R_w. However, the emulsion packet next to this zone is assumed to be homogeneous with a thermal resistance R_a. At the boundary of this zone the temperature drops from T_w to $\dot{T}$ as shown in Figure 5.1. The packet of the solid particles are being heated from the boundary (dotted line in Figure 5.1) of this zone, having an instantaneous thermal resistance,

$$R_a = \left(\frac{\pi \tau}{K_{eff} \rho_{mf} C_p} \right)^{1/2} \tag{5.1}$$

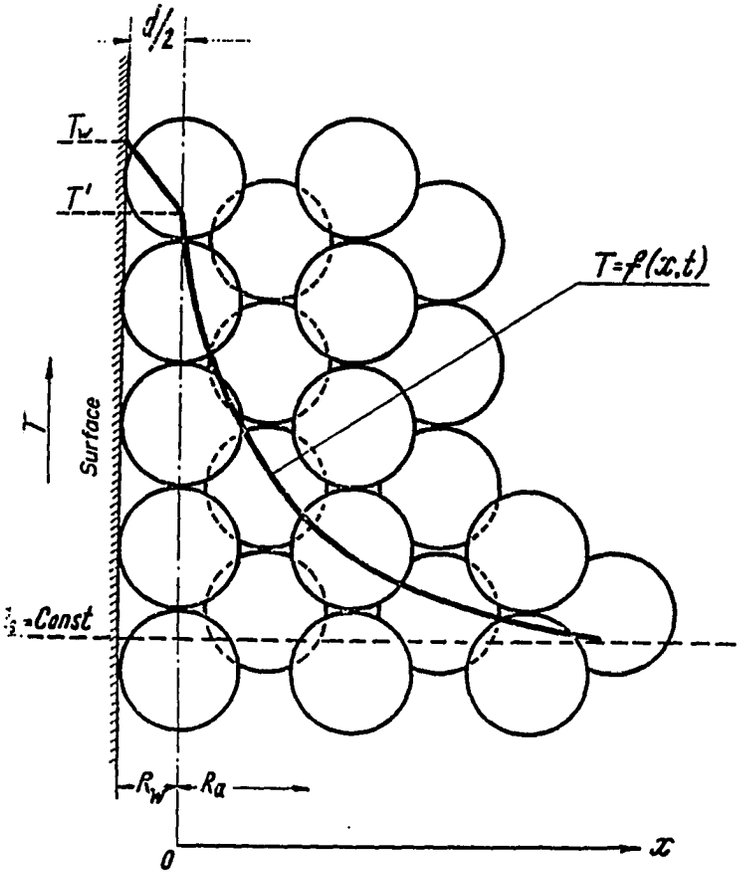

Figure 5.1: Schematic diagram to illustrate the mechanism of heat transfer from a surface to a fluidized bed

and an instantaneous heat transfer coefficient, assuming resistances in series,

$$h_i = \frac{1}{R_w + R_a} \tag{5.2}$$

Defining, the average heat transfer coefficient as;

$$h = \int_0^t h_i dt \tag{5.3}$$

The average heat transfer coefficient can be given by,

$$h = \frac{2}{R_a}\left[1 - \frac{R_w}{R_a}\ln(1 + \frac{R_a}{R_w})\right] \tag{5.4}$$

The wall resistance R_w, was assumed to be $d_p/10K_g$ [Geldart, 1986]. In a slightly different situation where, instead of the temperature of the boundary of the zone , $\acute{T}$, being constant, the temperature of the heat transfer remains constant. This condition is more typical of heat transfer in a fluidized bed. The average heat transfer coefficient obtained for this condition can be given as [Davidson and Harrison, 1971];

$$h = \frac{2}{R_a}\{1 - \frac{\pi R_w}{2R_a}[1 - \exp\left(\frac{R_a}{R_w\sqrt{\pi}}\right)^2 erfc\left(\frac{R_a}{R_w\sqrt{\pi}}\right)]\} \tag{5.5}$$

Instead of this strict solution, without large errors, an alternate simplified solution can be give as [Gelperin and Einstein, 1971],

$$h = \frac{1}{R_w + 0.5R_a} \tag{5.6}$$

the numerical difference between equations 5.3, 5.4 and 5.5 is negligible for most practical problems.

In order to estimate the average heat transfer coefficient using the above equations, for a fluidized bed system, the properties of the packet and the residence time of the emulsion packet should be known. The effective thermal conductivity of the packet K_{eff} can be given as a sum of two components, one responsible for the heat transfer mechanisms independent of fluid flow and the other representing the effect of the fluid flow [Xavier and Davidson, 1985];

$$\frac{K_{eff}}{K_g} = 1 + \frac{(1-\epsilon_{mf})(1-\frac{K_g}{K_p})}{0.28\epsilon^{0.63(\frac{K_p}{K_g})^{0.18}} + \frac{K_g}{K_p}} + 0.1\rho_g C_g d_p U_{mf} \qquad (5.7)$$

The following values of the properties were use,

$$\begin{aligned}
K_p &= 1.05 W/m^{\circ}K \\
C_{ps} &= 1133 J/Kg^{\circ}K \\
\rho_p &= 2500 Kg/m^3 \\
\rho_{mf} &= \rho_p(1-\epsilon_{mf}) \\
\epsilon_{mf} &= 0.52 \ for \ 5-44 \ \mu m \ glass \ particles \\
\epsilon_{mf} &= 0.44 \ for \ 126-147 \ \mu m \ glass \ particles \\
\epsilon_{mf} &= 0.42 \ for \ 355-420 \ \mu m \ glass \ particles
\end{aligned}$$

Furthermore, to use equation 5.3 or 5.4, the residence time of the emulsion packet needs to be evaluated. Baskakov et al. [1973] determined the residence time from the temperature fluctuation of a heat transfer surface immersed in a fluidized bed. Another method to estimate the residence time is to measure the solid velocity past the heat transfer surface [Colakyan and Levenspiel, 1984]. In the

present study such parameters were not measured. However, the residence time of the packet could be estimated. Ignoring the effect of particulate phase circulation near the minimum fluidizing condition, the residence time of the emulsion packet on the heated sphere can be given as;

$$t = \frac{L_h}{V_{sph}} \tag{5.8}$$

and the projected length of the heated sphere can be given by,

$$L_h = \frac{\pi D_{sph}}{2} \tag{5.9}$$

In Figures 5.2, 5.3 and 5.4 the heat transfer coefficient obtained by using equation 5.6 and the experimental values of the heat transfer coefficient are plotted against the residence time obtained using equations 5.7 and 5.8 for the various sphere diameters and sphere linear velocities. As seen in these Figures the agreement between the theoretical heat transfer coefficient and the experimental heat transfer coefficient for a linearly downward moving sphere at a minimum fluidization condition is good.

Two parameters play an important role in the transfer of heat from an immersed surface to the fluidized bed, namely the thermal time constant of the particles close to the heat transfer surface and the residence time of the emulsion packet. The thermal time constant of a single particle in the layer adjacent to the heat transfer surface, assuming the heat transfer coefficient to be $24K_g/d_p$ and neglecting the internal temperature gradients is given by,

$$TC = \frac{\rho_p C_p d_p^2}{144 K_g} \tag{5.10}$$

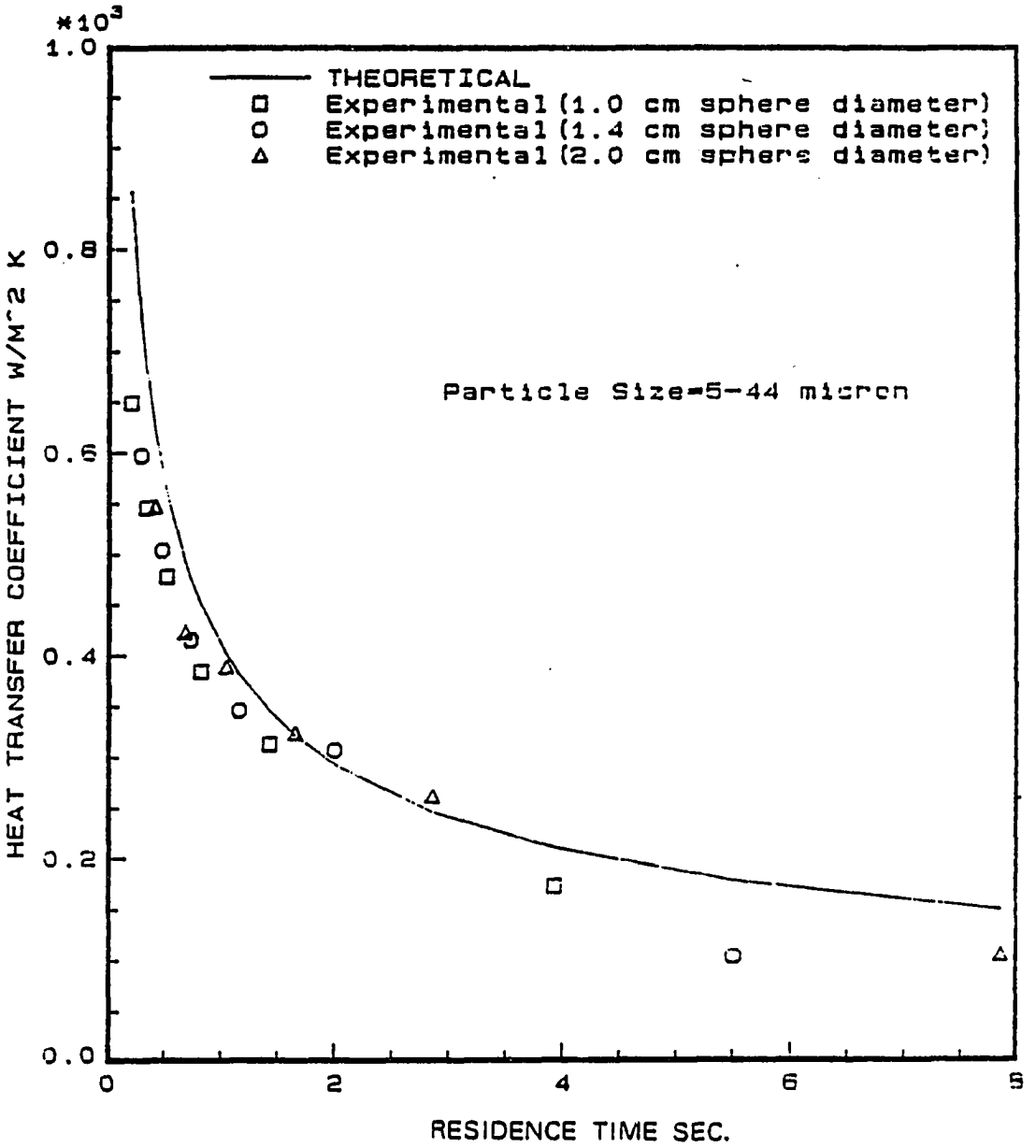

Figure 5.2: Experimental and theoretical (equation 5.6) heat transfer coefficient versus the residence time of the emulsion packet for 5-44 μm glass particle fluidized bed near minimum fluidization velocity

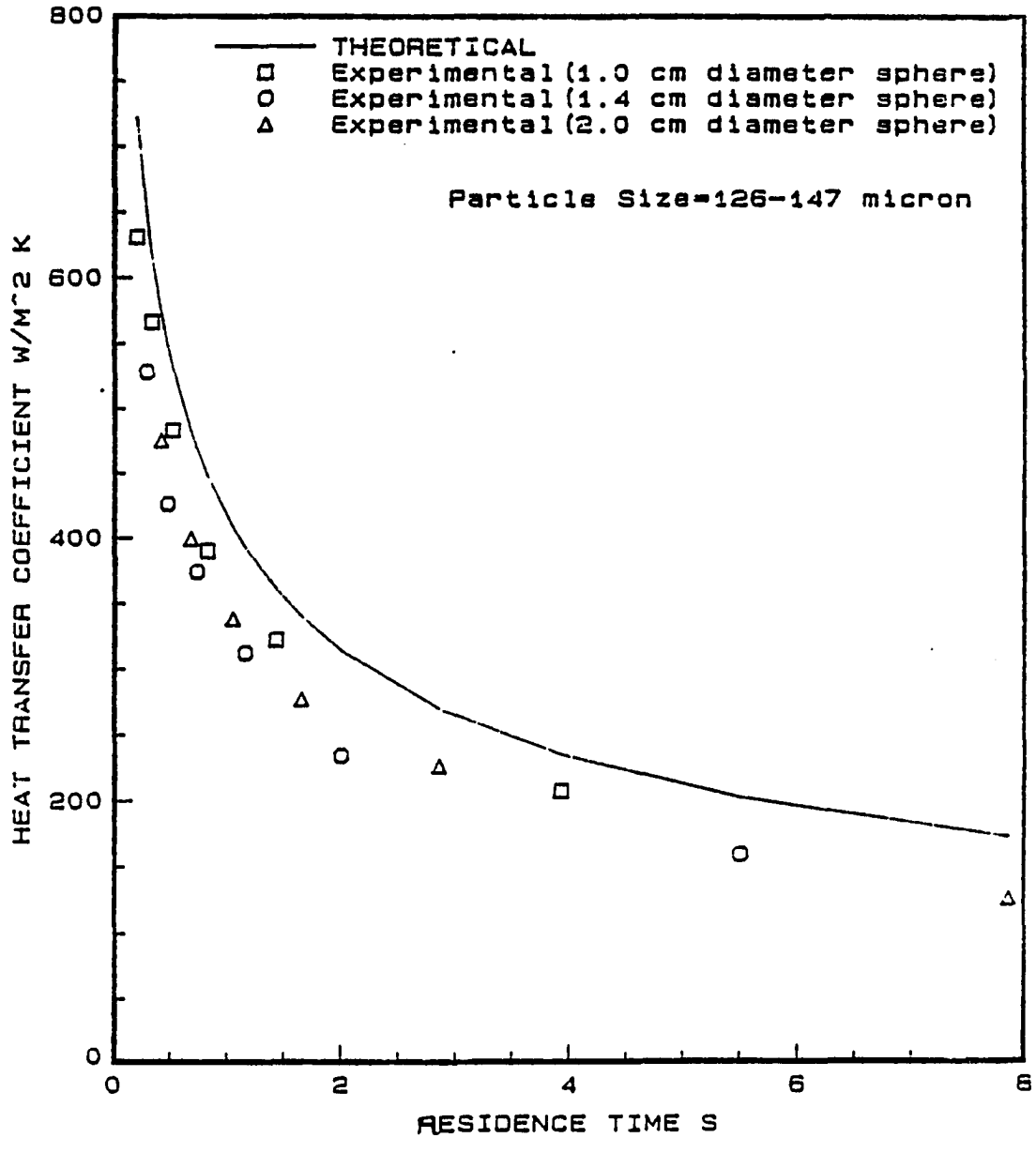

Figure 5.3: Experimental and theoretical (equation 5.6) heat transfer coefficient versus the residence time of the emulsion packet for 126-147μm glass particle fluidized bed near minimum fluidization velocity

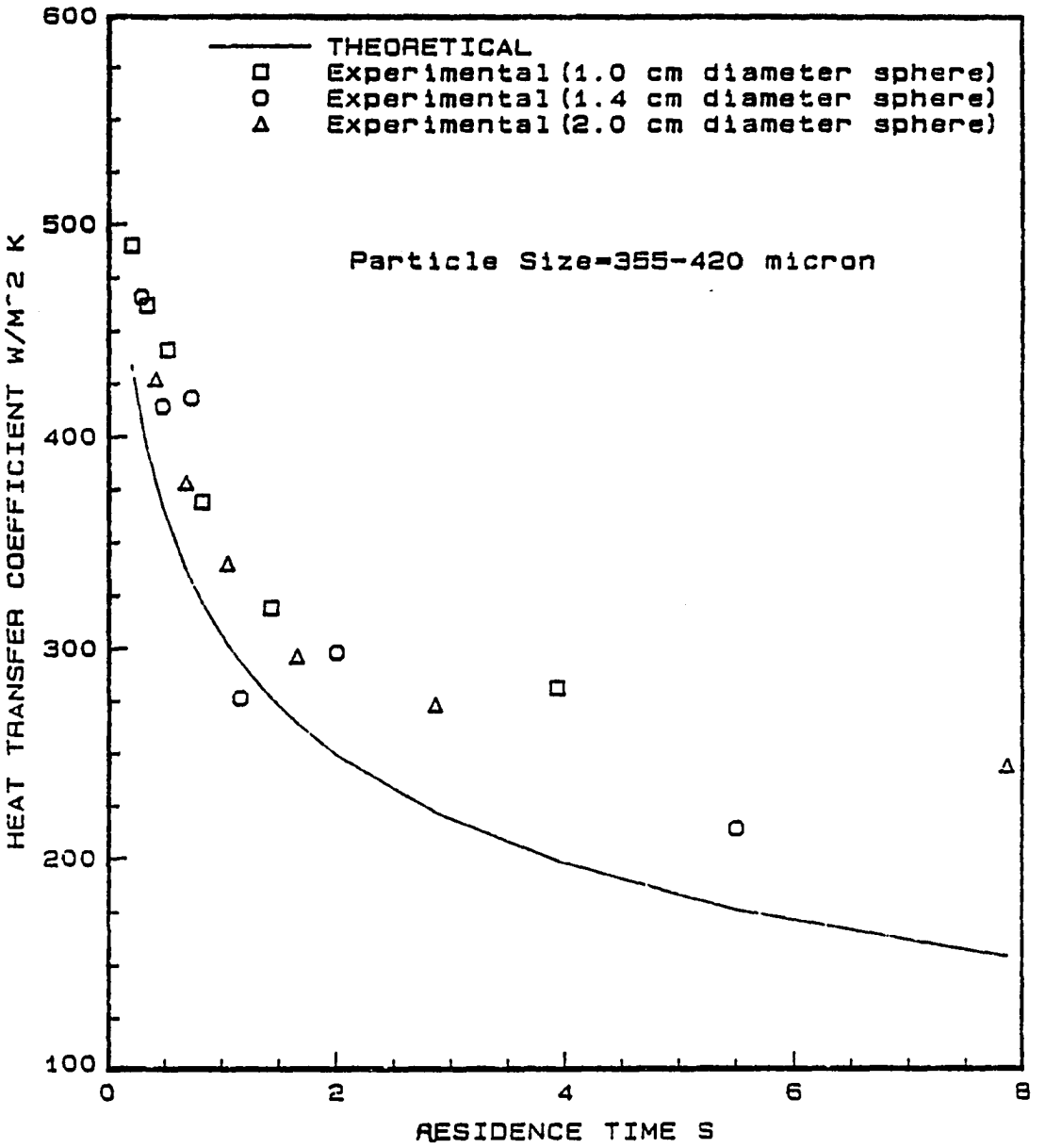

Figure 5.4: Experimental and theoretical (equation 5.6) heat transfer coefficient versus the residence time of the emulsion packet for 355-420μm glass particle fluidized bed near minimum fluidization velocity

typical values of the time constants for each glass particle size is as follows:

$$\begin{aligned} TC &= 0.0000452\ sec \quad for\ \ 5-44\ \mu m\ glass\ powder \\ &= 0.014 sec \quad for\ \ 126-147 \mu m\ glass\ powder \\ &= 0.113\ sec \quad for\ \ 355-420 \mu m\ glass\ powder \end{aligned}$$

The thermal time constant is an indication of how fast a single particle responds to the temperature of an adjacent heat transfer surface. Three regimes of packet thermal response can be classified;

1. For residence time much lower than the thermal time constant, only first layer of particles are affected and the resistance near the heat transfer wall R_w dominates.

2. When the residence time and the thermal time constant are of the same order of magnitude, additional layers of particles are affected and wall and packet resistance are significant.

3. If the residence time is much greater than the thermal time constant, first layer of particles approach the temperature of the heat transfer wall and the packet resistance R_a dominates.

Furthermore, the order of magnitude of the thermal penetration distance in to the emulsion packet can be estimated from the scale analysis of a one dimensional transient heat conduction equation. The thermal penetration distance can be given as;

$$x_{th} \sim \sqrt{\tau \frac{K_{eff}}{\rho_{mf} C_p}} \tag{5.11}$$

Using a nominal residence time of 1.0 second and the properties of the glass particle size of 355-420 μm, the thermal penetration depth was obtained as 175 μm. Thus, for small residence time the assumption of the emulsion packet being homogeneous fails. This may be the reason for very large difference in theoretical and experimental heat transfer coefficient at residence time lower than 0.5 second, in the case of 5-44 μm and 126-147 μm glass particles as shown in Figure 5.2 and 5.3. As at small residence time only the first layer of the particles are actively involved in the heat transfer process. In such case the single particle heat transfer models described in Chapter 1 should be used.

Figure 5.4 shows that the experimental heat transfer coefficients are consistently higher than the theoretical result. This may be explained as follow. For this size of the glass particle, the bubbling velocity and the minimum fluidization velocity are nearly equal. Thus, even at minimum fluidization condition some particulate circulation is present giving rise to a lower residence time and higher heat transfer coefficient.

5.1 Hydrodynamics of Fluidized Bed

Heat transfer in fluidized beds largely depend on the dynamics of gas-solid motion inside the bed. An attempt was made to study the motion of the particulate and the gas phase in the fluidized bed used for the present study. The main goal of this study was to estimate the particulate velocity close to an immersed sphere. This

velocity then, can be used to established the residence time of the particulate packet for the packet theory to predict the heat transfer coefficients at various superficial air velocities.

Hydrodynamic models of fluidization use the principles of conservation of mass, momentum and energy. The nonlinear coupled partial differential equations, written in a form suggested by Soo [1962] are modified by Gidaspow [1986] to account for the particle-to-particle friction. The continuity and separate phase momentum equations for transient two-phase flow in cylindrical coordinates are:

Gas Continuity

$$\frac{\partial \rho_g \epsilon}{\partial t} + \frac{1}{r}\frac{\partial \rho_g \epsilon r U_g}{\partial r} + \frac{\partial \rho_g \epsilon V_g}{\partial y} = 0 \tag{5.12}$$

Particle Continuity

$$\frac{\partial \rho_p (1-\epsilon)}{\partial t} + \frac{1}{r}\frac{\partial \rho_p (1-\epsilon) r U_p}{\partial r} + \frac{\partial \rho_p (1-\epsilon) V_p}{\partial y} = 0 \tag{5.13}$$

Gas Momentum Equation in r Direction

$$\frac{\partial \rho_g \epsilon U_g}{\partial t} + \frac{1}{r}\frac{\partial \rho_g \epsilon U_g^2}{\partial r} + \frac{\partial \rho_g \epsilon U_g V_g}{\partial y} = -\epsilon \frac{\partial P}{\partial r} + \beta_r (U_g - U_p) \tag{5.14}$$

Particle Momentum Equations in r Direction

$$\begin{aligned} &\frac{\partial [\rho_p (1-\epsilon) U_p]}{\partial t} + \frac{1}{r}\frac{\partial [\rho_p (1-\epsilon) U_p^2 r]}{\partial r} + \frac{\partial [\rho_p (1-\epsilon) U_p V_p]}{\partial y} \\ &= -(1-\epsilon)\frac{\partial P}{\partial r} + \beta_r (U_p - U_g) - \frac{\partial \tau_{rr}}{\partial r} \end{aligned} \tag{5.15}$$

where

$$\frac{\partial \tau_{rr}}{\partial r} = G(\epsilon)\frac{\partial \epsilon}{\partial r} \tag{5.16}$$

Gas Momentum Equation in y Direction

$$\frac{\partial \rho_g \epsilon U_g}{\partial t} + \frac{1}{r}\frac{\partial \rho_g \epsilon r U_g V_g}{\partial r} + \frac{\partial \rho_g \epsilon V_g^2}{\partial y} = -\epsilon \frac{\partial P}{\partial y} + \beta_y (V_g - V_p) - \rho_g \epsilon g \qquad (5.17)$$

Particle Momentum Equation in y Direction

$$\begin{aligned} &\frac{\partial [\rho_p (1-\epsilon) V_p]}{\partial t} + \frac{1}{r}\frac{\partial [\rho_p (1-\epsilon) V_p r U_p]}{\partial r} + \frac{\partial \rho_p (1-\epsilon) V_p^2}{\partial y} \\ = \; & -(1-\epsilon)\frac{\partial P}{\partial y} + \beta_y (V_p - V_g) - \frac{\partial \tau_{yy}}{\partial y} - \rho_p (1-\epsilon) g \end{aligned} \qquad (5.18)$$

where

$$\frac{\partial \tau_{yy}}{\partial y} = G(\epsilon)\frac{\partial \epsilon}{\partial y} \qquad (5.19)$$

In the equations of motion β_r and β_y are the friction coefficients between the gas and the solid particles [Kunii and Levenspiel, 1969]. The terms τ_{rr} and τ_{yy} are the normal components of the solid phase stress tensor. Gidaspow [1986] correlated these terms based on the experimental findings of Rietma and Mutsers [1974] employing a particle-to-particle interaction term G(ϵ). The K-FIX program [Gidaspow, 1986] was used to solve the set of nonlinear partial differential equations for U_p, U_g, V_p, V_g, ϵ, and P. The program employs the following boundary and initial conditions:

1. At y=0, prescribed gas mass flux through the distributor plate.

2. At y=bed height, P=atmospheric pressure.

3. At r=0, free slip condition for both the phases.

4. At r=bed radius, no slip condition for the gas phase and slip condition for the particulate phase.

5. At $t \leq 0$, the bed is at minimum fluidization condition. At t=0, superficial velocity is set to some value greater than that of the minimum fluidization condition.

The K-FIX code employes a staggered finite difference mesh system. Phase velocities are centered on cell boundaries, whereas all other quantities are centered at the center of the mesh. Mass and momentum fluxes across the cell boundaries are full donor cell differenced. The finite differenced equations can be solved semi-implicitly, by a combination of point relaxation, Newton's and secant methods.

Figure 5.5 shows the particulate velocity profile at 10 cm above the distributor plate, for 136-147 μm glass particle-fluidized bed system at 3 second after the superficial velocity was increased from 1.6 to 4.0 cm/s. For this case, 10 grids in the radial direction and 40 grids in the vertical direction were used. As it can be seen from the Figure 5.5, the particulate velocity is higher at the center of the bed. Even though the solution is not stable particulate circulation pattern is predicted in terms of negative particle velocity at the wall of the bed. For a stable solution, K-FIX program should be run on a fast computer till the particulate velocity achieves a steady state condition.

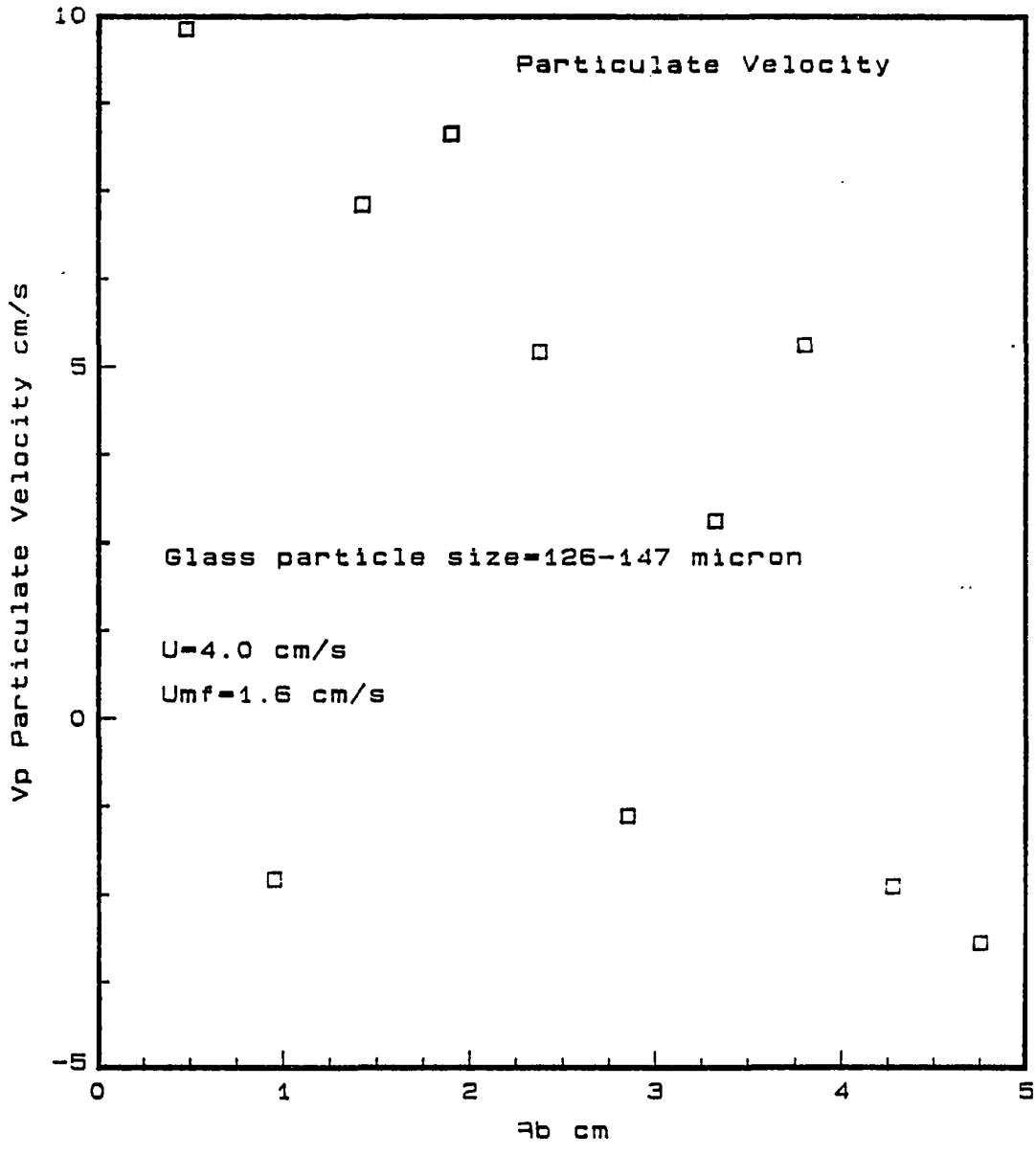

Figure 5.5: Plot of the radial distance in the bed versus the particulate velocity for 126-147 μm glass particle-fluidized bed system at 3 second

6 CONCLUSIONS AND RECOMMENDATIONS FOR FUTURE WORK

6.1 Conclusions

The heat transfer coefficients for a stationary, a linearly downward moving, and an oscillating copper sphere in an air fluidized bed-glass particle system were evaluated experimentally. The various parameters studied in this work were: the superficial air velocity, copper sphere diameter, glass particle diameter, linear downward sphere velocity, and the frequency and the amplitude of oscillation of the heated sphere. In addition the effect of the temperature of the sphere on the heat transfer coefficient was also studied. Important features of the results are summarized in this chapter.

6.1.1 Stationary sphere

The following heat transfer effects were observed for a small sphere held stationary in an air fluidized bed of glass particles.

1. The average heat transfer coefficient decreased slightly in the region where the superficial air velocity was less than that of the minimum fluidization velocity. However, in the fluidized bed region the average heat transfer coefficient

increased very rapidly followed by a levelling off with further increase in the superficial air velocity. This general trend in the heat transfer coefficient was not observed in the case of 5-44 μm glass particles where the heat transfer coefficients were low even at a superficial air velocity twice that of the minimum fluidization velocity.

2. The average heat transfer coefficient decreased with decreasing sphere diameter at superficial air velocities greater than that of the minimum fluidization velocity. At superficial velocities lower than that of the minimum fluidization velocity, the effect of the sphere diameter was found to be insignificant.

3. Decreasing the glass particle size was found to increase the heat transfer coefficient for all glass particle sizes and sphere diameters.

4. The contribution to sphere-bed heat transfer rate for a stationary submerged sphere was found as expected to be dominated by particle convective heat transfer in comparison to the gas convective part. At higher superficial air velocity the fraction of particle convective heat transport was observed to be about 92 to 98 % for the case of 5-44 and 126-147 μm glass particles. Whereas, for lower superficial air velocities and glass particle of 355-420 μm, the particle convective portion was found to be only 63 %.

5. It was found that in order to reliably detect an average heat transfer coefficient, using transient heat transfer theory, that the temperature step corresponding to the initial and final sphere temperature from which the average heat transfer coefficient is evaluated should be more than 20 $^{\circ}$ C. In general

the heat transfer coefficient was found to increase with increasing average sphere temperature. For the packed bed heat transfer, the heat transfer coefficient was also found to increase with increasing average sphere temperature. This was followed by a rapid drop in the heat transfer coefficient at the lower average sphere temperature.

6. The empirical correlation (equation 4.2) obtained agreed well with the experimental values within $\pm$ 25 %.

6.1.2 Linearly downward moving sphere

The following general conclusions can be drawn for the heat transfer study of a sphere moving linearly downward in an air fluidized bed.

1. At the lower superficial air velocity the average heat transfer coefficient increased continuously with the linear velocity of the sphere. However, the heat transfer coefficient leveled off at higher superficial air velocities.

2. The heat transfer coefficient increased by 4 to 13 times for a sphere moving at 7.5 cm/s near the minimum fluidizing condition as compared to the stationary sphere, depending on the glass particle size and the sphere diameter. However at higher superficial air velocities the difference between the heat transfer coefficient for a moving and a stationary sphere diminished.

3. The effect of the glass particle size on the heat transfer coefficient for a moving sphere was observed to be the same as in the case of a stationary sphere: increasing heat transfer coefficient with a decrease in the glass particle size.

4. A transitional value of a parameter (equation 4.4) was found to be equal to 191 μm below which all glass particle-sphere systems exhibited a similar trend in heat transfer coefficient; increasing or decreasing (Figure 5.1) trend with the superficial air velocity and above which the heat transfer coefficients were observed to be either leveling off or increased gradually.

5. The heat transfer correlations (equation 4.6) obtained for each glass particle size were found to give good agreement compared with the experimental data within ± 20 %.

6. A modified packet theory that included the contact resistance at the wall and the resistance in the emulsion packet was used to predict the theoretical heat transfer coefficient for the case of a sphere moving linearly in an air fluidized bed at a minimum fluidization condition. The predicted heat transfer coefficients compared favorably with the experimental values.

6.1.3 Oscillating sphere

The following important heat transfer results were observed for an oscillating sphere in an air fluidized bed.

1. The heat transfer coefficient increased 7.5 to 14 times for an oscillating sphere as compared to a stationary sphere at the same superficial air velocity. At lower peak-to-peak amplitude (1.8 cm) the heat transfer coefficient increased with an increase in the superficial air velocity. However, at higher peak-to-peak amplitude the heat transfer coefficient increased rapidly at lower su-

perficial air velocity followed by a gradual increase or leveling off at higher superficial air velocities.

2. For the case of 5-44 μm glass particles and a superficial air velocity of 0.087 cm/s, the average heat transfer coefficient increased more than three times as the average translational sphere velocity increased from 3.96 cm/s to 39.33 cm/s. Whereas, at an superficial air velocity of 1.95 cm/s, the heat transfer coefficient increased only by 20 % in the same range of the equivalent sphere velocity.

3. A different trend was observed for the case of 355-420 μm glass particles in which, the heat transfer coefficient decreased with an increase in equivalent sphere velocity.

4. The heat transfer coefficient for 5-44 μm glass particle system was observed to be about 260 % higher for the linearly downward moving sphere when compared to the oscillating sphere with the same average translational sphere velocity at low superficial air velocity. However for the case of the 355-420 μm glass particle system, the heat transfer coefficient was found to be only 40 % higher for a linearly moving sphere. At higher superficial air velocities the difference in the heat transfer coefficients for the oscillating and linearly moving sphere was found to be insignificant for all of the glass particles systems.

6.2 Recommendations for Future Work

Although the present study addresses many issues concerning heat transfer from an immersed sphere to an air fluidized bed, many more issues remain to be resolved. The following areas are recommended for further investigations:

1. Only three size ranges of the glass particles were available for the present (5-44, 126-147, and 355-420 μm). A more extensive and complete study would required many more glass particle size ranges. At least two to three glass powders should be used from each powder group (group A to group D) for better understanding of the effects of the particle size on the heat transfer coefficient.

2. The present study was conducted using only three sizes of relatively small diameter copper spheres (1.0, 1.4, and 2.0 cm). An industrially more useful study should include a complete heat transfer study involving the effects of size of the object (larger than used in the present study), orientation of the object, and shape of the object. Heat transfer in fluidized beds depends mainly on the hydrodynamics of the bed close to the object (e.g., the defluidized zone observed [Ginoux et al., 1974] is influenced by the size and the shape of the object).

3. This study indicated that the heat transfer coefficient could be a function of the average sphere temperature. In order to verify this result a different approach to this heat transfer study should be conducted. For example temperature fluctuation of an object with an internal heater can be used to study

the heat transfer coefficient as a function of the object temperature, the frequency of the bubbles passing by the immersed object, and the instantaneous heat transfer coefficient.

4. The residence time of the emulsion packet was estimated from the sphere diameter and sphere linear velocity for the minimum fluidization condition. In order to estimate the residence time for other values of the superficial air velocities, the computer program K-FIX (developed by Los Alamos and modified by IIT, Chicago) can be used to study the particulate flow around an immersed object. The later version of this software calculates the particulate slip velocity near the heat transfer surface. This slip velocity can be used to estimate the residence time of the particulate phase on the heat transfer surface for the various superficial air velocities.

5. A rigorous heat transfer study can be conducted using the K-FIX (with energy equation) program which can take the variable conductivity (due to variable voidage along the direction of heat transfer) of the particulate phase near the heat transfer surface into account and, thus, can calculate local heat transfer coefficient and an average heat transfer coefficient.

6. The sphere can be moved in upward direction inside the fluidized bed. In this case because of the absence of the defluidized region at the top portion of the sphere, it is expected that the heat transfer coefficient may be different (possibly being less) for this case compared to a sphere moving in downward direction.

7. The residence time of the emulsion packet can be measure experimentally for various superficial air velocities by recording the temperature fluctuation of a heated probe of a thin foil. The experimental value of the residence time can then be used to predict the heat transfer coefficient from the modified packet theory for the complete range of superficial air velocities.

8. Fluidized beds used in the industry are larger in size and have different behavior patterns in three major areas. (1) Properties of large gas distributors: the distributor plate used in the small scale fluidized beds is not practical due to its large pressure drop across the plate. Large fluidized beds employ multi-jet gas distributors of different design. (2) Bubble movement: bubble movement, bubble coalescence and bubble eruption are different in large fluidized beds. (3) Solids movement: multiple circulation patterns may be present along the radial direction of a large fluidized bed unlike in a small fluidized bed. These three factors are mainly responsible for different the heat transfer characteristics of a large fluidized bed. Thus, predictions of heat transfer behavior from testing of a small fluidized bed is often difficult and sometimes impossible. In order to generate useful information for application in industry, heat transfer study should be conducted on a large scale fluidized beds.

7 ACKNOWLEDGEMENTS

I wish to express my thanks to Professor Gerald M. Colver, under whose supervision this research was conducted. I am deeply appreciative of his confidence in my ability, respect for my opinion, and encouragement throughout the course of this research work. I am also grateful for the benefits I have received from his practical knowledge.

I am very grateful to my doctoral committee members; Professor G. H. Junkhan, Professor R. H. Pletcher, Professor George Burnet, Professor B. R. Munson, Professor A. Akers, and Professor Patrick Kavanagh, for their advice, support and encouragement.

The assistance and help of Mr. Hap Steed, Mr. Gaylord Scandrett, Mr. James Dautremont and Mr. Dave Louise of the Research Equipment Assistance Program is deeply appreciated. Thanks are also due to Professor George Burnet, of Chemical Engineering Department for lending the fluidized bed and to Professor T. D. Wheelock of Chemical Engineering Department for using his rotameter calibration rig. In addition I must thank my friend Se-Won Kim, for constant companionship during the long dreary nights of the graduate program.

The financial support of Engineering Research Institute and Mechanical Engineering Department of Iowa State University is greatly appreciated.

I am greatly in debt to my parents, family members, brothers, sister and in particular, my brother Professor Rasbihari Desai. Without their support, affection, faith and encouragement, I could not have pursued a graduate study program. I would also like to thank Atul and Hasu Amin for their friendship and love made our stay in Ames pleasurable. Finally, I wish to express deep appreciation to my wife Jignasa and daughter Shivani, whose patience, understanding and love has enabled me to sustain this effort.

8 BIBLIOGRAPHY

Abbi, Y. P., Benerji, M., Ghosh, M. K., Malliah, K. T. U., and Sharan, H. N. "Development of Fluidized Combustion Boilers for Indian Coal." Pp. 162-169 in C. Y. Wen, editor. *Fluidization: Application to Coal Conversion Process.* AIChE Symposium Series, 74, no. 176. New York: American Institute of Chemical Engineers, 1978.

Abuaf, N., and Gutfinger, C. " Experimental Coating and Heat Transfer Studies in a Vibrating Fluidized Bed." *International Journal of Multiphase Flow* 1 (1974):683-695.

Ainshtein, V. G., and Gelperin, N. I. " Heat Transfer between a Fluidized Bed and a Surface." *International Chemical Engineering* 6, no. 1 (1966):67-74.

Amundson, N. R., and Aris, R. " Heat Transfer in Fluidized and Moving Bed." Pp. 176-182 in P. A. Rottenburg and N. T. Shepherd, editors. *Proceedings of The Symposium on The Interaction between Fluids and Particles.* 3rd Congress of European Federation of Chemical Engineering. London, U. K: Institution of Chemical Engineers, 1962.

Anderson, D. A., Tannehill, J. C., and Pletcher, R. H. *Computational Fluid Mechanics and Heat Transfer.* New York: McGraw-Hill Book Company, 1984.

Anderson, T. B., and Jackson R. " A Fluid Mechanical Description of Fluidized Beds." *Industrial and Engineering Chemistry Fundamentals* 6, no. 4 (1967) :527-539.

Aulisio, C. J., Ehrlich, S., Bryers, R. W., and Bazan, J. "Fluidized-Bed Performance with Internals; Heat Exchanger above the Slumped Bed." Pp. 484-490 in D. L. Keairns, editor. *Fluidization Technology. Volume II.* New York: Hemisphere Publishing Corporation, 1976.

Babu, S. P., Shah, B., and Talwarkar, A. "Fluidization Correlation for Coal Gasification Materials, Minimum Fluidization Velocity and Fluidized Bed Expansion Ration." Pp. 176-186 in C. Y. Wen, editor. *Fluidization: Application to Coal Conversion Process.* AIChE Symposium Series, 74, no. 176. New York: American Institute of Chemical Engineers, 1978.

Bachovchin, D. M., Archer, D. H., and Neale, D. H. "Heat Transfer in Fluidized Bed Solar Thermal Receiver." Pp. 27-36 in T. M. Knowlton, editor. *Fluidization and Fluid-Particle Systems: Theories and Application.* The American Institute of Chemical Engineering Symposium Series 79, no. 222. New York: American Institute of Chemical Engineers, 1983.

Barker, J. J. "Microelectronic Device for Measuring Heat Transfer Coefficients in Fluidized Beds." *Industrial and Engineering Chemistry Fundamentals* 6, no. 1 (1967) :139-142.

Bartel, W. J., and Genetti, W. E. "Heat Transfer form a Horizontal Bundle of Tubes." Pp. 85-93 in D. L.Keairns, C. Y. Wen, R. Grace, R. Clift, T. D. Wheelock, A. H. Pulsifer, and G. J. Vogel, editors. *Fluidized Bed Fundamentals and Application.* The American Institute of Chemical Engineering 69, no. 128. New York: American Institute of Chemical Engineers, 1973.

Bartel, W. J., Genetti, W. E., and Grimmett, E. S. "Heat Transfer from a Horizontal Discontinuous Finned Tube in a Fluidized Bed." Pp. 85-89 in H. Littman, R. Pfeffer, C. Y. Wen, O. Levenspiel, and D. L. Keairns, editors. *Fluidization: Fundamental Studies, Solid-Fluid Reactions, and Application.* The American Institute of Chemical Engineering Symposium Series 67, no. 116. New York: American Institute of Chemical Engineers, 1971.

Baskakov, A. P. " The Mechanism of Heat Transfer between a Fluidized Bed and a Surface." *International Chemical Engineering* 4, no. 2 (1964):320-324.

Baskakov, A. P., and Kondrat'ev, E. A. " Calculation of Heating and Cooling of Products Moving Longitudinally in a Fluidized Bed." *Journal of Engineering Physics* 29 (1975):1354-1359.

Baskakov, A. P., and Suprun, V. M. " The Determination of the Convective Component of the Coefficient of Heat transfer to a Gas in a Fluidized Bed." *International Chemical Engineering* 12, no. 1 (1972):53-55.

Baskakov, A. P., and Vershinina, V. S. "An investigation of Heat Transfer between a Packing and a Fluidized Bed Interstices." *International Chemical Engineering* 4, no. 1 (1964):119-123.

Baskakov, A. P., and Vitt, O. K. "Pulsation in coefficient of heat transfer from a surface submerged in a fluidized bed." *Theoretical Found. Chem. Eng. (English translation)* 7 (1973):812-820.

Baskakov, A. P., Berg, B. V., Vandantseveeniy, B., Zunduygiyn, T. S., and Galperin, L. A. " Local Heat Transfer for a Sphere in a Fluidized Bed." *Heat Transfer Soviet Research* 4, no. 2 (1972):127-131.

Baskakov, A. P., Berg, B. V., Vitt, O. K., Filippovsky, N. F., Kirakosyan, V. A., Goldobin, J. M., and Maskaev, V. K. " Heat Transfer to Object Immersed in Fluidized Bed." *Powder Technology* 8 (1973):273-282.

Basu, P. "*Bed – To – Wall* Heat Transfer in a Fluidized Bed Coal Combustor." Pp. 187-193 in C. Y. Wen, editor. *Fluidization: Application to Coal Conversion Process.* AIChE Symposium Series, 74, no. 176. New York: American Institute of Chemical Engineers, 1978.

Beasley, D. E., Figliola, R. S., Khan, J. A., and Chakravoty, M. "A Model for Particle Convection Heat Transfer in a Bubbling Fluidized Bed of Mixed Particle Sizes." Presented at National Heat Transfer Conference, Pittsburgh, August 1987.

Beckwith, T. G., Buck, N. L., and Marangoni, R. D. *Mechanical Measurements*, Reading, Massachusetts: Addison-Wesley Publishing Company, 1982.

Bejan, A. *Convection Heat Transfer.* New York: John Wiley and Sons, 1984.

Bird, R. B., Stewart, W. E., and Lightfoot, E. N. *Transport Phenomena.* New York: John Wiley and Sons, Inc., 1960.

Botterill, J. S. M. "Heat Transfer to Gas Fluidized Beds." *Powder Technology* 4 (1971):19-26.

Botterill, J. S. M. " Bed to Surface Heat Transfer." Pp. 26-27 in D. L. Keairns, C. Y. Wen, R. Grace, R. Clift, T. D. Wheelock, A. H. Pulsifer, and G. J. Vogel, editors. *Fluidized Bed Fundamentals and Application.* The American Institute of Chemical Engineering 69, no. 128. New York: American Institute of Chemical Engineers, 1973.

Botterill, J. S. M. *Fluidized Bed Heat Transfer.* London U. K: Academic Press, 1975.

Botterill, J. S. M. "Fluidized Bed Behavior." Pp.1-35 in J. R. Howard, editors. *Fluidized Bed Combustion and Application.* London U. K.: Applied Science Publishers, 1983.

Botterill, J. S. M. "Fluid Bed Heat transfer." Pp. 219-258 in D. Geldart, editor. *Gas Fluidization Technology.* New York: John Wiley and Sons, 1986.

Botterill, J. S. M., and Denloye, A. O. O. "A Theoretical Model of Heat Transfer to a Packed or Quiescent Fluidized Bed." *Chemical Engineering Science* 33 (1978a):509-515.

Botterill, J. S. M., and Denloye, A. O. O. "Gas Convective Heat Transfer to Packed and Fluidized Beds." Pp. 194-202 in C. Y. Wen, editor. *Fluidization: Application to Coal Conversion Process.* AIChE Symposium Series, 74, no. 176. New York: American Institute of Chemical Engineers, 1978b.

Botterill, J. S. M., and Denloye, A. O. O. "Gas Convective Heat Transfer to Packed and Fluidized Beds." *The American Institute of Chemical Engineers Symposium Series* 74, no. 176 (1978c):194-202.

Botterill, J. S. M., and Desai, M. "Pressurized Fluidized Beds." *Powder Technology 6* (1972):231-240.

Botterill, J. S. M., and Williams, J. R. " The Mechanism of Heat Transfer to Gas Fluidized Bed." *Transactions of Institution of Chemical Engineers* 41 (1963):217-230.

Botterill, J. S. M., Redish, K. A., Ross, D. K., and Williams, J. R. " The Mechanism of Heat Transfer to Fluidized Beds." Pp. 183-189 in P. A. Rottenburg and N. T. Shepherd, editors. *Proceedings of The Symposium on The Interaction between Fluids and Particles.* 3rd Congress of European Federation of Chemical Engineering. London, U. K.: Institution of Chemical Engineers, 1962.

Botterill, J. S. M., Teoman, Y., and Yuregis, K. R. " Temperature Effects on the Heat Transfer Behavior of Gas Fluidized Bed." *The American Institute of Chemical Engineers Symposium Series* 77, no. 208 (1981):330-340.

Botterill, J. S. M., Toeman, Y., and Yuregir, K. R. " Factors Effecting Heat Transfer between Glass Fluidized Bed and Immersed Surfaces." *Powder Technology* 39 (1984):177-189.

Bowers, T. G., and Reintjes, H. "A Review of Fluid-To-Particle Heat Transfer in Packed and Moving Beds." Pp. 69-74 in J. W. Westwater, editor. *Heat Transfer-Buffalo.* Chemical Engineering Progress Symposium Series 57, no. 32. New York: American Institute of Chemical Engineers, 1961.

Bruinzeel, C., Reman, G. H., and van der Laan, E. Th. "Eddy Diffusion in Particulate Fluidized Beds: Model Experiments for the Design of a Large Scale Unit." Pp. 120-126 in P. A. Rottenburg and N. T. Shepherd, editors. *Proceedings of The Symposium on The Interaction between Fluids and Particles.* 3rd Congress of European Federation of Chemical. London: London Institute of Chemical Engineers, 1962.

Byam, J., Pillai, K. K., and Roberts, A. G. "Heat Transfer to Cooling Coils in the Slash Zone of a Pressurized Fluidized Bed Combustor." *American Institute of Chemical Engineers Symposium Series* 77, no. 208 (1981):350-358.

Campbell, E. K., and Davidson, J. F. "Combustion of Coal in Fluidized Beds." Pp. 285-288 in D. L. Keairns, editor. *Fluidization Technology. Volume II.* New York: Hemisphere Publishing Corporation, 1976.

Carleton, A. J. " The Effect of Fluid Drag Forces on the Discharge of Free Flowing Solids from Hoppers." *Powder Technology* 6 (1972):91-96.

Catipovic, N. M., Jovanovic, G. N., and Fitzgerald, T. J. " A Model for Heat Transfer to Horizontal Tubes Immersed in a Fluidized Bed of Large Particles." Pp. 225-234 in J. R. Grace, and J. M. Matse, editors. *Fluidization.* New York: Plenum Press, 1980.

Chen, P., and Pei, D. C. T. " A Model of Heat Transfer between a Fluidized Beds and Immersed Surfaces." *International Journal of Heat and Mass Transfer* 28, no. 3 (1985):675-682.

Cheremisinoff, N. P., and Gupta, R. *Handbook of Fluids in Motion.* Ann Arbor: Ann Arbor Science, 1983.

Chilton, E. G., and Lundberg, R. E. "The Drag of Cylinder in Dust-Laden Gas Flow." Pp. 35-42 in N. J. Lipstein, editor. *Multi-Phase Flow Symposium.* Presented at Winter Annual Meeting of th ASME, Philadelphia, Pa. Nov. 17-22, 1963. New York: The American Society of Mechanical Engineers, 1964.

Colakyan, M., and Levenspiel, O. " Heat Transfer Between Moving Bed of Solids and Immersed Cylinders." *The American Institute of Chemical Engineers Symposium Series* 80, no.241 (1984):156-168.

Colver, G. M. "Some Observations on Bubble Shedding from Sinking Objects in a Gas Fluidized Bed." *Proceedings of Condensed Papers, 16th Annual Meeting, Fine Particle Society,* Miami, April 22-26, 1985.

Colver, G. M. " Bubble Control in Gas Fluidized Beds with Applied Electric Fields." Presented at the ASME-AIChE Heat Transfer Conference, ST. Louis, August 1976.

Couderc, J. P. " Incipient Fluidization of particulate Systems." Pp. 1-45 in Davidson, J .F., Clift, R., and Harrison, D., Editors. *Fluidization.* London, U. K: Academic Press, 1985.

Cranfield, R. D. "Solid Mixing in Fluidized Beds of Large Particles." Pp. 54-59 in Wen, C. Y., editor. *Fluidization: Application to Coal Conversion Process.* AIChE Symposium Series, 74, no. 176, 1978. New York: American Institute of Chemical Engineers, 1978.

Daniels, T. C. " Measurements of the Drag on Spheres Moving Through Gaseous Fluidized Beds." *Journal of Mechanical Engineering Science* 4, no. 1 (1962):103-110.

Davidson, J. F. "Differences Between Large and Small Fluidized Beds" Pp. 16-17 in Keairns, D. L., Wen, C. Y., Grace, R., Clift, R., Wheelock, T. D., Pulsifer, A. H., and Vogel, G. J., editors. *Fluidized Bed Fundamentals and Application,* The American Institute of Chemical Engineering 69, no. 128. New York: American Institute of Chemical Engineers, 1973.

Davidson, J. F., and Harrison, D. *Fluidization.* New York: Cambridge University Press, 1971.

Decker, N. A., and Glicksman, L. R. " Heat Transfer in Large Particle Fluidized Beds." *International Journal of Heat and Mass Transfer* 26, no. 9 (1983):1307-1320.

Decker, N. A., and Glicksman, L. R. " Conduction Heat Transfer at the Surface of Bodies Immersed in Gas Fluidized Beds of Spherical Particles." *The American Institute of Chemical Engineering* 77, no. 208 (1981):341-349.

Desai, C. J., and Colver, G. M. " Heat Transfer to a Stationary and Moving Sphere in a Gas Fluidized Bed." Presented at the National Heat Transfer Conference, Pittsburgh, Pennsylvania, August 9-12, 1987.

Donahoe, T. S., and Colver, G. M. " Bubble Rise Velocity in AC and DC Electrofluidized Beds." *IEEE Transactions on Industry Application* 20, no. 2 (1984):259-266.

Donsi, G., and Massimilla, L. "Particle to Particle Forces in Fluidizati on of Fine Powders" Pp. 41-52 in H. Angelino, J. P. Couderc, H. Gibert, and C. Laguerie, editors. *Fluidization and its Application.* Proceedings of the International Symposium, Toulouse, France, Oct 1-5, 1973. Paris: Soiete de Chiemie Industielle, 1974.

Dow, W. M., and Jacob, M. "Heat Transfer between a Vertical Tube and a Fluidized Air-Solid FLow." *Chemical Engineering Progress* 47 (1951):637-648.

Drinkenburg, A. A. H., Huige, N. J. J., and Rietma, K. " Heat Transfer in a Gas Fluidized Bed." Pp. 271-279 in *Proceedings of the 3rd International Heat Transfer Conference, August 7-12, Chicago.* New York: The American Institute of Chemical Engineering, 1966.

Dunsky, V. D., Zabrodsky, and Tamarin, A. I. " On Mechanism of Heat Transfer between a Surface and a Bed of Moving Particles." Pp. 293-297 in *Proceedings of the 3rd International Heat Transfer Conference, August 7-12, Chicago.* New York: The American Institute of Chemical Engineering, 1966.

Eckert, E. R. G., and Drake, R. M. *Analysis of Heat and Mass Transfer.* New York: McGraw-Hill Book Company, 1981.

Eckert, E. R. G., and Goldstein, A. J. *Measurements in Heat Transfer.* New York: McGraw-Hill Book Company, 1976.

Elmas, M. "Fluidized Bed Heat Transfer." Pp. 312-319 in H. Angelino, J. P. Couderc, H. Gibert, and C. Laguerie, editors. *Fluidization and its Application.* Proceedings of the International Symposium, Toulouse, France, Oct 1-5, 1973. Paris: Soiete de Chiemie Industielle, 1974.

Ergun, S. "Fluid Flow through Packed Columns." *Chemical Engineering Progress* 48, no. 2 (1952):89-94.

Ettehadieh, B., Gidaspow, D., and Lyczkowski, R. W. " Hydrodynamics of Fluidization in a Semicircular Bed with a Jet." *The American Institute of Chemical Engineers* 30, no. 4 (1984):529-53

Figliola, R. S., Suarez, E. G., and Pitts, D. R. " Mixed particle size Distribution Effects on Heat Transfer in a Fluidized Bed." *Journal of Heat Transfer* 108 (1986):913-915.

Gabor, J. D. " *Wall – To – Bed* Heat Transfer in Fluidized Beds." *The American Institute of Chemical Engineers Journal* 18, no. 1 (1972):249-250.

Gabor, J. D. "Heat Transfer to Particle Beds With Gas Flows Less Than or Equal to that Required for incipient Fluidization." *Chemical Engineering Science* 25 (1970):979-984.

Gabor, J. D. "Wall to Bed heat Transfer in Fluidized and Packed Beds." Pp. 76-86 in H. Littman, R. Pfeffer, J. Feinman, B. S. Lee, and N. Levitz, editors. *Fluidization Fundamentals and Application.* Chemical Engineering Progress Symposium Series 66, no. 105, 1970. New York: American Institute of Chemical Engineers, 1970.

Ganzha, V. L., Upadhyay, S. N., and Saxena, S. C. " A Mechanistic Theory for Heat Transfer between Fluidized Beds of Large Particles and Immersed Surfaces." *International Journal of Heat and Mass Transfer* 25, no. 10 (1982):1531-1540.

Geldart, D., editor. *Gas Fluidization Technology.* New York: John Wiley and Sons, 1986.

Gelperin, N. I., Einshtein, V. G., and Aronovich, F. D. " The Effect of Screening on Heat Transfer in a Fluidized Bed." *International Chemical Engineering* 3, no. 2 (1963):185-189.

Gelperin, N. I., and Einshtein, V. G. "Heat Transfer in Fluidized Beds." Pp. 471-540 in J. F. Davidson, D. Harrison, editors. *Fluidization.* New York: Academic Press, 1971.

Gerald F. C. *Applied Numerical Analysis.* Philippines: Addison-Wesley Publishing Company, Inc, 1978.

Gidaspow, D., Ettehadieh, B., Lin, C., and Lyczkowski, W. " Theoretical and Experimental Hydrodynamics of a Jet in a Fluidized Bed of Particles." Pp. 672-681 in K. Linoya, J. K. Beddow, and G. Jimbo, editors. *Powder Technology.* Papers presented at the International Symposium on Powder Technology, Kyoto, Japan. New York: Hemisphere Publishing Corporation, 1981.

Gidaspow, D. " Fluid-Particle Systems." Pp. 115-128 in Kakac, S., and Mayinger, F., editors. *Two Phase Flows and Heat Transfer, 1.* New York: Hemisphere Publishing Corporation, 1977.

Gidaspow, D. " Hydrodynamics of Fluidization and Heat Transfer: Supercomputer Modeling." *Applied Mechanics Reviews* 39, no. 1 (1986):1-23.

Gidaspow, D., Seo, Y. C., and Ettehadieh, B. " Hydrodynamics of Fluidization Effect of Pressure." *Particulate Science and Technology* 4 (1986):25-43.

Ginoux, J. J., De Geyter, F. M., and Kilkis, B. " Hydrodynamics of a Two Dimensional Fluidized Bed in the Vicinity of a Cylinder with Horizontal Axis." Pp. 274-283 in in H. Angelino, J. P. Couderc, H. Gibert, and C. Laguerie, editors. *Fluidization and its Application.* Proceedings of the International Symposium, Toulouse, France, Oct 1-5, 1973. Paris: Societe de Chiemie Industielle, 1974.

Glass, D. H., and Harrison, D. "Hydrodynamics of Two Dimensional Fluidized Beds." *Chemical Engineering Science*, 19 (1964):1001-1002.

Gloski, D., Glicksman, L., and Decker, N. " Thermal Resistance at a Surface in Contact with Fluidized Bed Particles." *International Journal of Heat and Mass Transfer* 27, no. 4 (1984):599-610.

Goossens, W. R. A. " A Boundary Layer Penetration Model for the Heat Transfer to the Vertical Wall in Gas Fluidized Bed." Pp. 119-129 in Van Swaaij, and J. L. Afgan, editors. *Heat and Mass transfer in Fixed and Fluidized Beds.* Washington D. C.: Hemisphere Publishing Corporation, 1986.

Goossens, W. R. A., and Hellinckx, L. " A Film Penetration Approach for the Heat Transfer Between a Glass Fluidized Bed and a Vertical Wall." Pp. 302-311 in H. Angelino, J. P. Couderc, H. Gibert, and C. Laguerie, editors. *Fluidization and its Application.* Proceedings of the International Symposium, Toulouse, France, Oct. 1-5, 1973. Paris: Soiete de Chiemie Industielle, 1974.

Grace, J. R., and Matsen, J. M. *Fluidization.* New York: Plenum Press, 1980.

Grewal, N. S., and Saxena, S. C. " Heat Transfer between a Horizontal Tube and a Gas Solid Fluidized Bed." *International Journal of Heat and Mass Transfer* 23 (1980):1505-1519.

Gutfinger, C., and Abuaf, N. " Heat Transfer in Fluidized Beds." Pp. 167-218 in Hartnelt, J. P., and Irvine, T. F., editors. *Advances in Heat Transfer* 10. New York: Academic Press, 1974.

Gutfinger, C., and Abuaf, N. "Aplication of Fluidized Beds to Coating Process." Pp. 577-600 in Keairns, D. L., editor. *Fluidization Technology. Volume II.* New York: Hemisphere Publishing Corporation, 1976.

Harrison, D., and Leung, L. S. "The Coalescence of Bubbles in Fluidised Beds." Pp. 127-134 in P. A. Rottenburg and N. T. Shepherd, editors. *Proceedings of The Symposium on The Interaction Between Fluids and Particles.* 3rd Congress of European Federation of Chemical. London: London Institute of Chemical Engineers, 1962.

Highley, J. and Kaye, W. G. "Fluidized Beds Industrial Boilers and Furnaces." In *Fluidized beds-Combustion and Applications.* J. R. Howard, editor. London: Applied Science Publishers, 1983.

Ho, C. P., and Wang, C. S. "Collection of Solid Particles on Single Cylinders by Particle Inertia and Electrical Forces." Pp. 109-121 in J. K. Beddow, editor. *Particulate Systems, Technology and Fundamentals.* New York: Hemisphere Publishing Corporation, 1983.

Hosny, N., and Grace, J. R. " Forces on a Tube Immersed within a Fluidized Bed." Pp. 111-121 in D. Kunii, and R. Toei, editors. *Proceedings of The 4th International Conference on Fluidization*, Kashikojima, Japan, 1983. Engineering Foundation Conferences Society of Chemical Engineers, Japan. New York: United Engineering Trustees Inc., 1984.

Hsu, Y. Y., Simon, F. F., and Graham, R. W. "Application of Hot-Wire Anemometry for Two-Phase Flow Measurements suck as Void Fraction and Slip Velocity." Pp. 26-34 in N. J. Lipstein, editor. *Multi-Phase Flow Symposium.* Presented at Winter Annual Meeting of the ASME, Philadelphia, Pa., Nov. 17-22, 1963. New York: The American Society of Mechanical Engineers, 1964.

Hughmark, G. A. " Heat Transfer in Fluidized Bed of Small Particles." *The American Institute of Chemical Engineering* 19, no. 3 (1973):658-659.

Hughmark, G. A. " Momentum, Heat and Mass Transfer for Fixed and Homogeneous Fluidized Bed." *The American Institute of Chemical Engineers Journal* 18, no. 5 (1972):1020-1024.

Incropera, F. P., and DeWitt, D. P. *Fundamental of Heat Transfer.* New York: John Wiley and Sons, 1981.

Jackob, A., and Osberg, L. "Effect of Gas Thermal Conductivity on local Heat Transfer in a Fluidized Bed." *Canadian Journal of Chemical Engineering*, 35, no. 1 (1957):5-9.

Jackson, R. " Hydrodynamic Stability of Fluid-Particle Systems." Pp. 47-70 in J. F. Davidson, R. Clift, and D. Harrison, editors. *Fluidization.* London. U. K: Academic Press, 1985.

Jackson R. "The Present Status of Fluid Mechanical Theories of Fluidization." Pp. 3-13 in H. Littman, R. Pfeffer, J. Feinman, editors. *Fluidization Fundamentals and Application*, Chemical Engineering Progress Symposium Series 66, no. 105, 1970. New York: American Institute of Chemical Engineers, 1970.

Jahnig, C. E., Campbell, D. L., and Martin, H. Z. "History of Fluidized Solids Development at Exxon." Pp. 3-24 in J. R. Grace, and J. M. Matse, editors. *Fluidization.* New York: Plenum Press, 1980.

Jain, S. C., and Chen, B. H. "Heat Transfer in a Screen-Packed Fluidized Bed" Pp. 97-105 in H. Littman, R. Pfeffer, C. Y. Wen, O. Levenspiel, and D. L. Keairns, editors. *Fluidization: Fundamental Studies, Solid-Fluid Reactions, and Application.* The American Institute of Chemical Engineering Symposium Series 67, no. 116. New York: American Institute of Chemical Engineers, 1971.

Kabanov, V. V., and Klubnikin, V. S. "Experimental Determination of Resistance of a Spherical Particle in an Argon Plasma Stream." *Inzhenerno-Fizicheshii Zhurnal* 48, no. 3 (1985):396-402.

Kao, D. T. Y. "Rheology of Suspension." Pp. 863-893 in N. P. Cheremisinoff, and R. Gupta, editors. *Handbook of Fluid in Motion.* Ann Arbor: Ann Arbor Science, 1985.

Kharchenko, N. V., and Makhorin, K. E. " The Rate of Heat Transfer Between a Fluidized Bed and an Immersed Body at High Temperatures." *International Chemical Engineering* 4, no. 4 (1964):650-654.

Kiang, K. D., Liu, K. T., Nack, H., and Oxley, J. H. "Heat Transfer in Fast Fluidized Beds" Pp. 471-485 in D. L. Keairns, editor. *Fluidization Technology. Volume II.* New York : Hemisphere Publishing Corporation, 1976.

Kim, S. D., Kang, Y., and Kwon, H. K. " Heat Transfer in Gas Solid Coal Slurry Fluidized Beds." A. Teoman, and T. V. Nejat, editors. *International Symposium Workshop on Particulate and Multiphase Proceedings of 16th Annual Meeting of Fine Particle Society*, April 22-26, 1985, Miami Beach, Florida.

King, D. F., Mitchell, F. R. G., and Harrison, D. "Dense Phase Viscosities of Fluidized Beds at Elevated Pressures." *Powder Technology* 28 (1981):55-58.

Kobayashi, M., Ramaswami, D., and Brazelton, W. T. "Heat Transfer from an Internal Surface to a Pulsed Bed." Pp. 58-67 in H. Littman, R. Pfeffer, J. Feinman, B. S. Lee, and N. Levitz, editors. *Fluidization Fundamentals and Application.* Chemical Engineering Progress Symposium Series 66, no. 105, 1970. New York: American Institute of Chemical Engineers, 1970.

Koppel, L. B., Patel, R. D., and Holmes, J. T. " Statistical Models for Surface Renewal in Heat and Mass Transfer: part I. Dependence of Average Transfer Coefficient on Age Distribution." *The American Institute of Chemical Engineering Journal* 12, no. 5 (1966):941-946.

Koppel, L. B., Patel, R. D., and Holmes, J. T. " Wall-to-Fluidized Bed Heat Transfer Coefficient" *The American Institute of Chemical Engineering Journal* 16, (1970):464-471.

Korolev, V. N., and Syronyatnikoe, N. I. " Heat Transfer from a Surface to a Fluidized Bed." *Heat Transfer Soviet Research* 3, no. 4 (1971):112-116.

Korolev, V. N., and Syronyatnikoe, N. I., and Tolmachev, E. M. " The Structure of Fixed and Fluidized Granular Beds near Immersed Walls." *Journal of Engineering Physics*, 21, no.6 (1971):973-982.

Kreith, F. *Principles of Heat Transfer.* New York: Harper and Row, Publishers, 1973.

Kubie, J., and Broughton, J. " A Model of Heat Transfer in Gas Fluidized Beds." *International Journal of Heat and Mass Transfer* 18 (1975):289-299.

Kunii Dazio, and Levenspiel Octave. *Fluidization Engineering.* New York: John Wiley and Sons, Inc., 1969.

Kunii, D., and Smith, J. M. "Heat Transfer Characteristics of Porous Rocks." *American Institute of Chemical Engineering Journal*, 6, no. 1 (1960):71-78.

Kunii, D., and Toei, R. *Fluidization.* New York: United Engineering Trustees Inc., 1984.

Kunio, K., and Wen C. Y. "Gas-Particle Heat Transfer in Fixed and Fluidized Beds." Pp. 100-108 in H. Littman, R. Pfeffer, J. Feinman, B. S. Lee, and N. Levitz, editors. *Fluidization Fundamentals and Application.* Chemical Engineering Progress Symposium Series 66, no. 105, 1970. New York: American Institute of Chemical Engineers, 1970.

LaNauze, R. D., and Davidson, J. F. "The Flow of Fluidized Solids." Pp. 113-124 in D. L. Keairns, editor. *Fluidization Technology. Volume II.* New York : Hemisphere Publishing Corporation, 1976.

Leva, M. *Fluidization.* New York: McGraw Hill, 1959.

Leva, Max. "The Use of Gas-Fluidised Systems for Blending Particulate Solids." Pp. 143-150 in P. A. Rottenburg and N. T. Shepherd, editors. *Proceedings of The Symposium on The Interaction Between Fluids and Particles.* 3rd Congress of European Federation of Chemical. London: London Institute of Chemical Engineers, 1962.

Levenspiel, O., and Walton, J. S. "Fluidized Bed Heat Transfer." *Chemical Engineering Progress 45* (1954):563-570.

Levich,V. G. *Physicochemical Hydrodynamics.* Englewood Cliffs, New Jersy: Prentice-Hall Inc., 1962.

Leung, L. S. "The Ups and Downs of Gas-Solid Flow - A Review." Pp. 25-68 in J.R. Grace, and J. M. Matse, editors. *Fluidization.* New York: Plenum Press, 1980.

Lu, Wei-Ming, Chen, Cheng-Ching and Chiu, C. S. " Heat Transfer Between a Single Sphere and a Vibrated Fluidized Bed." *Journal of Chinese Institute of Chemical Engineers* 7 (1976):83-94.

Lyozkowski, R. W., Bouillard, J. X., Berry, G. F., and Gidaspow, D. " Erosion Calculations in a Two Dimensional Fluidized Bed." Pp. 697-706 in J. P. Mustonen, editor. *International Conference on Fluidized Bed Combustion* 2. New York: The American Society of Mechanical Engineers, 1987.

Malhotra, K., and Mujumdar, A. S. "Immersed Surface Heat Transfer in a Vibrated Fluidized Bed." *Ind. Eng. Chem. Res.* 20 (1987):1983-1992.

Maskayev, V. K,. and Nosov, V. S. " Heat Transfer between a Bed of Spherical Particles and the Fluidizing Gas Suspension." *Heat Transfer Soviet Research*7, no. 1 (1975):28-49.

Masson, H. A., Rios, G. M., Dang, T. K., and Bourtinbourg, M. C. " Shape and Density Effects on the Behavior of a large Isolated Body Moving in a Gas Solid Fluid Bed." Pp. 185-193 in D. Kunii, and R. Toei, editors. *Proceedings of The 4th International Conference on Fluidization* Kashikojima Japan,1983. Engineering Foundation Conferences Society of Chemical Engineers, Japan. New York: United Engineering Trustees Inc., 1984.

Mathur, M. P., and Klinzing, G. E. "Measurement of Particle and Slip Velocities in Coal/Gas System." Pp. 60-65 in T. M. Knowlton, editor. *Fluidization and Fluid-Particle Systems: Theories and Application.* The American Institute of Chemical Engineering Symposium Series 79, no. 222. New York: American Institute of Chemical Engineers, 1983.

Mickley, H. S., and Fairbanks, D. F. "Mechanism of Heat Transfer to Fluidized Beds." *The American Institute of Chemical Engineering Journal* 1, no. 3 (1955):374-384.

Mickley, H. S., Fairbanks D. F., and Hawthorn, R. D. "The Relation Between the Transfer Coefficient and Thermal Fluctuations in Fluidized-Bed Heat Transfer." Pp. 51-60 in J. W. Westwater, editor. *Heat Transfer- Buffalo.* Chemical Engineering Progress Symposium Series 57, no. 32, 1961. New York: American Institute of Chemical Engineers, 1961.

Mickley, H. S., and Trilling, C. A. "Heat Transfer Characteristics of Fluidized Bed." *Industrial and Engineering Chemistry* 41, no. 6 (1949):1135-1147.

Mink, W. H. "Critical Velocity in Solids Transport." Pp. 157-174 in J. K. Beddow, editor. *Particulate Systems, Technology and Fundamentals.* New York: Hemisphere Publishing Corporation, 1983.

Mujumdar, A. S. *Advances in Drying. Volume 2.* Washington: Hemisphere Publishing Corporation, 1983.

Nazemi, A. "Heat Transfer in Fluidized Beds of Flour and Starch." Ph.D. Thesis, Iowa, State University, Ames, Iowa, 1960.

Nguyen, T. H., and Grace, J. R. " Forces on Objects Immersed in Fluidized Beds." *Powder Technology* 19 (1978):255-364.

O'Brien, J. E., Wade, M. L., and Terpolilli, A. M. " The Contribution of Gas Convection to Total Heat Transfer for a Horizontal Cylinder Submerged in a Fluidized Bed." *The AIChE Symposium Series* 81, no. 245 (1985):48-54.

Padhye, A. R., and O'Brien, T. J. " Computer Simulation of Westinghouse Fluidized Bed Cold-Flow Experiments." Pp. 77-85 in J. T. Jurewicz, editor. *Gas-solid Flows, Fluids Engineering Division* 10. Presented at Energy Sources Technical Conference, New Orleans, Louisiana, February 1984. New York: The American Society of Mechanical Engineering, 1984.

Patel, R. D. "A Theoretical Heat Tranasfer Model." *U. S. Atomic Energy Commission*, ANL-7353, 1967.

Peters, M. H., and Nadkarni, A. R. "The Motion of Gas and Solids around a Spherical Void in a Fluidized Bed." Pp. 25-36 in D. Kunii, and R. Toei, editors. *Proceedings of The 4th International Conference on Fluidization*, Kashikojima Japan,1983. Engineering Foundation Conferences Society of Chemical Engineers. New York: United Engineering Trustees Inc., 1984.

Peyman, M., and Lague'rie, C. "Heat Transfer between Solids and Gas in a Multistaged Fluidized Bed." Pp. 243-251 in J. R. Grace, and J. M. Matse, editors. *Fluidization.* New York: Plenum Press, 1980.

Pfafflin, J. R., Shridhar, M., and Jullien, G. A. " Heat and Mass Transfer in Fluidized Beds." Pp. 69-72 in D. L. Keairns, editor. *Fluidization and Fluid Particle System.* The American Institute of Chemical Engineering Symposium Series 70, no. 141. New York: American Institute of Chemical Engineers, 1974.

Pfeiff, C. F., and Hopfinger, E. J. " Drag on Cylinders Moving Through Suspensions with High Solid Concentration." *PhysicoChemical Hydrodynamics* 7, no. 2/3 (1986):101-109.

Pillai, K. K. " Heat Transfer to a Sphere Immersed in a Shallow Fluidized Bed." *Letters in Heat and Mass Transfer* 3 (1976):131-146.

Prins, W., Casteleijn, T. P., and Van Swaaij, W. P. M. "Mass Transfer form a Freely Moving Single Sphere to the Dense Phase of a Gas Fluidized Bed of inert Particles." *Chemical Engineering Science* 30, no. 3 (1985):481-497.

Prins, W., Draijer, W., and Van Swaaij, W. P. M. " Heat Transfer to Immersed Sphere Fixed or Freely Moving in a Gas-Fluidized Bed." Pp.317-331 in Van Swaaij, and J. L. Afgan, editors. *Heat and Mass Transfer in Fixed and Fluidized Beds.* Washington D. C.: Hemisphere Publishing Corporation, 19 .

Pritchett, J. W., Black, T. R., and Garg S. K. "A Numerical Model of Gas Fluidized Beds." Pp. 134-148 in C. Y. Wen, editor. *Fluidization: Application to Coal Conversion Process.* AIChE Symposium Series, 74, no. 176, 1978. New York: American Institute of Chemical Engineers, 1978.

Pruden, B. B., Crosbie, D., and Whallwy, B. J. P. "Circulation of Large Bodies in an Aggregatively Fluidized Bed" Pp. 65-86 in D. L. Keairns, editor. *Fluidization Technology, Volume II.* New York : Hemisphere Publishing Corporation, 1976.

Quassim, R.Y., and De Souza, R. " A General Particle Stress Equation for Fixed and Fluidized Beds." *Powder Technology* 38 (1984): 33-38.

Ranz, W. E., and Marshall, W. R. *Chemical Engineering Progress*, 48, no. 141 (1952):173-185.

Reed, T. M., and Fenske, M. R. " Effects of Agitation on Gas Fluidization of Solids." *Industrial and Engineering Chemistry* 47, no. 2 (1955):275-282.

Richardson, J. F., and Shakiri, K. J. " Heat Transfer between Gas Solid Fluidized Bed and a Small Immersed Surface." *Chemical Engineering Science* 34 (1979):1019-1029.

Richmound, S. B. *Statistical Analysis.* New York: The Ronald Press Company, 1964.

Rietema, K. " Powder, What Are They?" *Powder Technology* 37 (1984):5-23.

Rietema, K., and Mutsers, S. M. P. "The Effect of Interparticle Forces on the Expansion of a Homogeneous Gas-Fluidized Bed." Pp. 28-40 in H. Angelino, J. P. Couderc, H. Gibert, and C. Laguerie, editors. *Fluidization and its Application.* Proceedings of the International Symposium, Toulouse, France, Oct 1-5, 1973. Paris: Soiete de Chiemie Industielle, 1974.

Rios, G. M., and Gibert, H. " Heat Transfer Between Gas Fluidized Bed and Big Bodies; Analysis and Explanation of Big Body Mobility Effect." Pp. 363-370 in D. Kunii, and R. Toei, editors. *Proceedings of the 4th International Conference on Fluidization* Kashikojima, Japan, May 29-June 3 1983, Kashikojima, Japan. New York: United Engineering Trustees Inc., 1984.

Rooney, N. M., and Harrison, D. "Flow Patterns Near Horizontal Tubes in a Gas-Fluidized Bed." Pp. 3-6 in D. L. Keairns, editor. *Fluidization Technology. Volume II.* New York: Hemisphere Publishing Corporation, 1976.

Rowe, P. N., and Partridge, B. A. "Particle Movement Caused by Bubbles in a Fluidized Beds." Pp. 135-142 in P. A. Rottenburg and N. T. Shepherd, editors. *Proceedings of The Symposium on the Interaction between Fluids and Particles.* 3rd Congrss of European Federation of Chemical. London: London Institute of Chemical Engineers, 1962.

Samson, T. " Heat Transfer to Objects in Fluidized Beds." Pp.283-303 in H. Angelino, J. P. Couderc, H. Gibert, and C. Laguerie, editors. *Fluidization and its Application.* Proceedings of the International Symposium, Toulouse, France, Oct. 1-5, 1973. Paris: Soiete de Chiemie Industielle, 1974.

Saxena, S. C., and Ghanza, V. L. " Dependence of Heat Transfer Coefficient of Immersed Surfaces in a Gas Fluidized Bed on Pressure." *Powder Technology* 44 (1985):115-124.

Schlichting, H. *Boundary Layer Theory.* New York : McGraw-Hill Book Company, 1979.

Sha, W. T., and Soo, S. L. " On the Effect Of P"DEL"alfa Term in Multiphase Mechanics." *International Journal of Multiphase Flow* 5 (1979):153-158.

Shih, Y. T., Gidaspow, D., and Wasan, D. T. " Hydrodynamics of Electrofluidization Separation of Pyrites from Coal." *The American Institute of Chemical Engineers Journal* 33, no. 8 (1987):1322-1333.

Shih, Y. T., Gidaspow, D., and Wasan, D. T. " Sedimentation of Fine particles in Nonaqueous Media: Part I-Experimental, Part II-Modeling." *Colloids and Surfaces* 21 (1986):393-429.

Shih, Y. T., Gidaspow, D., and Wasan, D. T. " Hydrodynamics of Sedimentation of Multisized Particles." *Powder Technology* 50 (1987):201-215.

Shirai, T., Yoshitome, H., Shoji, Y., Tanaka, S., Hojo, K., and Yoshida, S. " Heat and Mass Transfer on the Surface of Solid Spheres Fixed within Fluidized Beds." *Kagake Kogake* 4, no. 1 (1966):162-165.

Soo, S. L. " Note On Motions of Phases in a Fluidized Bed." *Powder Technology* 45 (1986):169-172.

Soo, S. L. " Boundary Layer Motion of a Gas Solids Suspension." Pp. 50-63 in P. A. Rottenburg and N. T. Shepherd, editors. *Proceedings of The Symposium on The Interaction Between Fluids and Particles.* 3rd Congress of European Federation of Chemical. London: London Institute of Chemical Engineers, 1962.

Soo, S. L., and Dimick, R. C. "Experimental Study of Thermal Electrification of Gas-Solid System." Pp. 43-46 in N. J. Lipstein, editor. *Multi-Phase Flow Symposium.* Presented at Winter Annual Meeting of th ASME, Philadelphia, Pa., Nov. 17-22, 1963. New York: The American Society of Mechanical Engineers, 1964.

Stepanoff, A. J. *Gravity Flow of Bulk Solids and Transportation of Solids in Suspension.* New York: John Wiley and Sons Inc., 1969.

Syamlal, M., and Gidaspow, D. " Hydrodynamics of Fluidization:Prediction of Wall to Bed Heat Transfer Coefficients." *The American Institute of Chemical Engineers Journal* 31, no. 1 (1985):127-135.

Toomey, R. D., and Johnstone, H. F. " Heat Transfer Between Beds of Fluidized Solids and the Walls of the Container." *Chemical Engineering Progress Symposium Series* 49, no. 5 (1953):51-60.

Toor, H. L., and Marchello, J. M. "Fluidized Bed Heat transfer." *American Institute of Chemical Engineering Journal* 4 (1958):97-103.

Ushimaru, K., and Butler, G. W. " Numerical Simulation of Gas Solid Flow in an Electrostatic Precipitator." Pp. 87-96 in J. T. Jurewicz, editor. *Gas-Solid Flows, Fluids Engineering Division* 10. Presented at Energy Sources Technical Conference, New Orleans, Louisiana, February 1984. New York: The American Society of Mechanical Engineers, 1984.

Van Heerden, A. V., Nobel, A. P. P., and Van Krevelen, D. W. "Mechanism of Heat Transfer in Fluidized Beds." *Industrial and Engineering Chemistry* 45, no. 6 (1953):1237-1242.

Van Heerden, A. V., Nobel, A. P. P., and van Krevelen, D. W. "Studies on Fluidization. II- Heat Transfer." *Chemical Engineering Science* 1, No. 2 (1951):51-66.

Virr, M. J. " Fluidized Bed Heat Recovery Systems." Pp. 341-367 in Howerd, J. R., editor. *Fluidized Bed Combustion and Application.* London, U.K: Applied Science Publishers, 1983.

Vittal, B. V. R., and Tabakoff, W. " Effect of the Solid Particle Size in Two Phase Flow around a Plane Cylinder." Pp. 608-627 in W. G. Habashi, and Swansea, editors. *Computational Methods in Viscous Flows. Volume 3*, in the series, Recent Advances in Numerical Methods in Fluids. London, U. K.: Pineridge Press, 1984.

Vreedenberg, H. A. "Heat Transfer between Fluidized Beds and Vertically Inserted Tubes." *Journal of Applied Physics* 2 (1952):26-33.

Wace, P. F., and Burnett, S. J. " Flow Patterns in Gas Fluidized Beds." *Transaction of Institution of Chemical Engineers* 39 (1961):168-174.

Wen-Ching, Yang and Kearins, D. L. "Rate of Particle Separation in a Gas Fluidized Bed." *Industrial and Engineering Fundamentals* 21 (1982):228-235.

Wender, L., and Cooper, G. T. " Heat Transfer between Fluidized Solids Beds and Boundary Surfaces-Correlation of Data." *The American Institute of Chemical Engineering Journal* 4, no. 1 (1958):15-23.

Werther, J. "Influence of Bed Diameter on the Hydrodynamics of Gas Fluidized Bed." Pp. 53-62 in D. L. Keairns, editor. *Fluidization and Fluid Particle System.* The American Institute of Chemical Engineering Symposium Series 70, no. 141. New York: American Institute of Chemical Engineers, 1974.

White, F. M. *Fluid Mechanics.* Tokyo, Japan: McGraw-Hill Kogakusha, Ltd., 1979.

Wood, R. T., Kuwata, M., and Staub, F. W. "Heat Transfer to Horizontal Tube Banks in the Splash Zone of a Fluidized Bed of Large Particles." Pp. 235-242 in J. R. Grace, and J. M. Matse, editors. *Fluidization.* New York: Plenum Press, 1980.

Xavier, A. M., and Davidson, J. F. " Heat Transfer in Fluidized Beds: Convective Heat Transfer in Fluidized Beds." Pp. 437-463 in J. F. Davidson, R. Clift, and D. Harrison, editors. *Fluidization.* London, U. K: Academic Press, 1985.

Xavier, A. M., King, D. F., Davidson, J. F., and Harrison, D. " Surface-Bed Heat Transfer in a Fluidized Bed at High Pressure." Pp. 209-216 in J. R. Grace, and J. M. Matse, editors. *Fluidization.* New York: Plenum Press, 1980.

Yamazaki, R., Hong, G. H., and Jimbo, G. " The Behavior of Gas Solid Fluidized Bed at Elevated Temperatures." Pp. 121-128 in D. Kunii, and R. Toei, editors. *Proceedings of The 4th International Conference on Fluidization*, Kashikojima, Japan,1983. Engineering Foundation Conferences Society of Chemical Engineers, Japan. New York: United Engineering Trustees Inc., 1984.

Yamazaki, R., and Jimbo, G. "Heat Transfer between Fluidized Beds and Heated Surface." *Journal of Chemical Engineering of Japan*, 3, no.1 (1970):44-49.

Yang, Wen-Ching, and Kearins D. L. "Momentum Dissipation of and Gas Enterainment into a Gas-solid Two-Phase Jet in a Fluidized Bed." Pp. 305-314 in J. R. Grace, and J. M. Matse, editors. *Fluidization.* New York: Plenum Press, 1980.

Yang Wen-Ching and Keairns D. L. "Rate of Particle Separation in a Gas Fluidized Bed." *Ind. Eng. Chem. Fundam.* 21, (1982):228-235.

Yong, J., Zhiqing Yu, Li, Zhang, and Zhanwen, W. "A Study of Particle Movement in a Gas-Fluidized Bed." Pp. 365-372 in J. R. Grace, and J. M. Matse, editors. *Fluidization.* New York: Plenum Press, 1980.

Yoshida, K., Kunii, D., and Levenspiel, O. "Heat Transfer Mechanisms between Wall Surface and Fluidized Bed." *International Journal of Heat and Mass Transfer*, 12 (1969):529-536.

Yreedenbeg, H. A. " Heat Transfer Between Fluidized Bed in a Horizontal Tube." *Chemical Engineering Science* 9 (1958):52-60.

Yur'ev, M. " Influence of Particle on the Drag on Bodies in a Disperse Flow." *Fluid Dynamics* 17, no. 3 (1982):462-465.

Zabrodsky, S. S. *Hydrodynamics and Heat Transfer in Fluidized Beds.* London, England: M. I. T. Press, 1966.

Zabrodsky, S. S., Antonishin, N. V., and Parnas, A. L. " On Fluidized Bed to Surface Heat Transfer." *The Canadian Journal of Chemical Engineering* 54 (1976):52-58.

Zabrodsky, S. S., Epanov, Vu. G., Galershtein, D. M., Saxena, S. C., and Kolar, A. K. "Heat Transfer in Large Particle Fluidized Bed with Immersed in-Line and Staggered Bundles of Horizontal Smooth Tubes." *International Journal of Heat and Mass Transfer* 24 (1981):571-581.

Ziegler, E. N., and Brazelton, W. T. " Mechanism of Heat Transfer to a Fixed Surface in a Fluidized Bed." *Industrial and Engineering Chemistry 3*, no. 2 (1964):94-98.

Ziegler, E. N., Koppel, L. B., and Brazelton, W. T. " Effects of Solid Thermal Properties on Heat Transfer to Gas Fluidized Beds." *Industrial and Engineering Chemistry Fundamentals* 3, no. 4 (1964):325-328.

9 APPENDIX A: ERROR ANALYSIS

The uncertainty in experimental measurements occurs mainly because of three types of errors; illegitimate, systematic, and random. Illegitimate errors are caused by the error in reading instruments and performing calculation which can be reduced by using care and repetition of experiments and calculation. Systematic error occurs owing to improper calibration of instruments, which can be reduced by careful calibration of instruments. However, the random errors originate from a variety of causes such as fluctuating experimental conditions, or disturbances. Random errors can not be usually be avoided since these errors are inherently present in any measuring system. The total uncertainty in any experiment in any experiment can be estimated through the use of propagation of error analysis.

For a function Z,

$$Z = X_1^a X_2^b X_3^c \ldots\ldots\ldots\ldots X_n^m \tag{9.1}$$

where, the exponents a, b, c...m may be positive or negative. A simplified form of the propagation of error equation [Beckwith et al. 1982] for the above form can be given as;

$$\left(\frac{U_Z}{Z}\right)^2 = a^2\left(\frac{U_{X_1}}{X_1}\right)^2 + b^2\left(\frac{U_{X_2}}{X_2}\right)^2 + \ldots\ldots + m^2\left(\frac{U_{X_m}}{X_m}\right)^2 \tag{9.2}$$

Applying the above propagation of error equation to the heat transfer correla-

tion(equation 4.5) which can be given in the following form,

$$Num = C_{m1}\left(\frac{U}{U_{mf}}\right)^{C_{m2}}\left(\frac{gd_p^3\rho g(\rho_p-\rho_g)}{\mu_g^2}\right)^{C_{m3}}\left(\frac{D_{sph}}{d_p}\right)^{C_{m4}}\left(\frac{V_{sph}}{U_{mf}}\right)^{C_{m5}} \tag{9.3}$$

From above equations A.2 and A.3 the uncertainty in the heat transfer coefficient can be given as;

$$\begin{aligned}\left(\frac{U_h}{h}\right)^2 = &\left(\frac{U_{D_{sph}}}{D_{sph}}\right)^2 + {C_{m2}}^2\left(\frac{U_U}{U}\right)^2 + {C_{m2}}^2\left(\frac{U_{U_{mf}}}{U_{mf}}\right)^2 \\ &+(3C_{m3})^2\left(\frac{U_{d_p}}{d_p}\right)^2 + {C_{m4}}^2\left(\frac{U_{D_{sph}}}{D_{sph}}\right)^2 + {C_{m4}}^2\left(\frac{U_{d_p}}{d_p}\right)^2 \\ &+{C_{m5}}^2\left(\frac{U_{V_{sph}}}{V_{sph}}\right)^2 + {C_{m5}}^2\left(\frac{U_{U_{mf}}}{U_{mf}}\right)^2\end{aligned} \tag{9.4}$$

Using the following values of the above parameters;

$$\begin{aligned} D_{sph} &= 1.0\ cm & U_{D_{sph}} &= \pm 0.1\ cm \\ U &= 10.0\ cm/s & U_U &= \pm 1.0\ cm/s \\ U_{mf} &= 1.6\ cm/s & U_U &= \pm 0.20\ cm/s \\ d_p &= 136.5\ \mu m & U_{d_p} &= \pm 10.0\ \mu m \\ V_{sph} &= 4.6\ cm/s & U_{V_{sph}} &= \pm 0.3\ cm/s \end{aligned}$$

the uncertainty in the heat transfer coefficient can be evaluated;

$$\left(\frac{U_h}{h}\right)^2 = 0.0001 + 0.001797 + 0.0028 + 0.010044$$

$$+0.000002079 + 0.00285 + 0.00019844 + 0.000729$$

$$= 0.01856$$

hence, the uncertainty in the heat transfer coefficient is about ± 13.6 %. The uncertainty is seem to be mainly due to the uncertainty in measuring the mean diameter of the glass particle, d_p.

10 APPENDIX B: FLOWMETERS

The volumetric flow rate of a variable area flowmeters like rotameters used in this experiment can be given as follows.

$$Q_r = A_w C_d \left(\frac{2gV_f(\rho_f - \rho_g)}{A_f \rho_g} \right)^{\frac{1}{2}} \tag{10.1}$$

The float density ρ_f is much larger than the gas density ρ_g (usually, $\frac{\rho_g}{\rho_f} \sim 10^{-3}$). So the above rotameter equation can be approximated as,

$$Q_r = A_w C_d \left(\frac{2gV_f \rho_f}{A_f \rho_g} \right)^{\frac{1}{2}} \tag{10.2}$$

The relationship between the rotameter flowrate at calibrating condition and at the standard conditions at the same rotameter reading is given by the following expression:

$$\frac{Q_{rc}}{Q_{rs}} = \left[\frac{\rho_{std}}{\rho_{rc}} \right]^{\frac{1}{2}} \tag{10.3}$$

In the calibration setup, the outlet of a rotameter was connected to the inlet of a wet test meter. Hence from the continuity equation

$$Q_{rc} = \frac{\rho_{wm}}{\rho_{rc}} Q_{wm} \tag{10.4}$$

During the calibration condition, the temperature of the air at rotameter and at wet test meter remained the same. Using the ideal gas law and equations A.3 and A.4,

$$Q_{rs} = \left(\frac{P_s}{T_s}\frac{T_{rc}}{P_{rc}}\right)\left(\frac{P_{wm}}{P_{rc}}\right)Q_{mw} \tag{10.5}$$

For each position of the steel float of the rotameter, the above equation was used to obtained a calibration curve for air flow rate at the standard condition. The following wet test meters and airmeter were used to calibrate all the rotameters:

1. Precision Scientific, Chicago, ISU-313167, 0.1 f^3/rev, maximum capacity= 24 f^3/hr, minimum capacity = 2 f^3/hr.
2. Precision Wet test meter, GCA Corporation, Chicago, ISU-335369, 1.0 f^3/rev, maximum capacity= 110 f^3/hr, minimum capacity = 10 f^3/hr.
3. Airmeter, Dresser Measurement, model-1.5M.

Table A.1 lists all rotameters, the range of their applicability, and the calibration equation. Under the operating condition, when air is passed through a rotameter first and then through the fluidized bed, the flow rate at the operating condition can be given by,

$$Q_{ro} = Q_{rs}\left(\frac{\rho_{std}}{\rho_o}\right) \tag{10.6}$$

From the ideal gas law,

$$Q_{ro} = Q_{rs}\left(\frac{P_s}{T_s}\frac{T_o}{P_o}\right)^{\frac{1}{2}} \tag{10.7}$$

Moreover, from the continuity equation, the air flow rate at the fluidized bed can be expressed as,

$$Q_b = \left(\frac{\rho_o}{\rho_b}\right)Q_{ro} \tag{10.8}$$

This equation can be rewritten using ideal gas relation, and considering constant temperature for rotameter section and fluidized bed section,

$$Q_b = \left(\frac{P_o}{P_b}\right) Q_{ro} \tag{10.9}$$

Table 10.1: List of rotameters used in the experiment

Rotameter type	Range in cc/s	Calibration equation cc/s
Lab Crest Div. F and P Co., Meter Tube Cat. no. 450-700	10 to 230	$Q_s = 1.5929R - 13.9910$
Devco Tube, Cat. no. 250-8	33 to 694	$Q_s = 27.9390R - 6.9009$
Brooks Instruments, Division of Emerson Co., Model no. 1114-08H2G1A	137 to 998	$Q_s = 9.6269R + 23.4293$
Brooks Instruments, Division of Emerson Co. Model no. 1110-01A1B1A	1.35 to 13.5	$Q_s = 8.10R/60$
Brooks Instrument Division of Emerson Electric Model no. 7710H42053 Co., Tube Size R7M25-1	80 to 713	$Q_S = 7.1395R - 4.0646$
Schtte and Koerting Co.	750 to 2794	$Q_s = 9.7284R + 440.9542$

11 APPENDIX C: THERMOCOUPLE CONDUCTION LOSSES

The heat loss through the thermocouple wires may introduce some error in calculation of overall heat transfer coefficient for the fluidized bed system. Heat conduction through the thermocouple wire can be treated as conduction through a thin long fin. In this case the governing equation becomes:

$$\frac{d^2T}{dx^2} - \frac{h_{eq}C}{(KA)_{eq}}(T_{tb} - T_b) = 0 \tag{11.1}$$

The conduction heat loss through a very long fin can be given as follows:

$$q_{cl} = \sqrt{h_{eq}C(KA)_{eq}}(T_{tb} - T_b) \tag{11.2}$$

where, h_{eq} and C are equivalent heat transfer coefficient for the convection losses along the fin surface and perimeter of the outer surface. The thermocouple wire along with the insulation and the equivalent radii are shown in Figures B.1a and B.1b. The equivalent radii and the thermal conductivity of the thermocouple wires are defined by Eckert and Goldstein [1976] as follows:

$$r_1 = \sqrt{2}r_w, \tag{11.3}$$

$$r_2 = \frac{L_1 + L_2}{4} \tag{11.4}$$

$$(KA)_{eq} = (K_{cu} + K_{cn})\pi r_w^2 \tag{11.5}$$

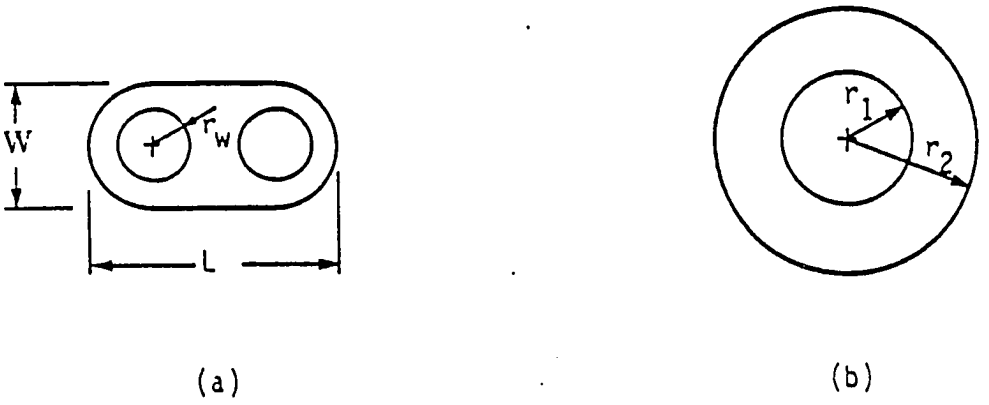

Figure 11.1: Thermocouple wire with the insulation (a) Thermocouple wires with insulation (b) equivalent radii

The thermocouple wire was passed through a hollow steel tube (O.D= 2.0828 mm, I.D=1.5748 mm). This provided a relatively thick air gap between the outer boundary of the teflon insulation and the inside surface of the steel tube. This arrangement is shown in Figure B.2. From the thermal resistance circuit, the equivalent heat transfer coefficient for the transverse conduction from the wire to the outer surface of the steel tube can be expressed as:

$$h_{eq} = \frac{1}{r_4\left(\frac{\ln(\frac{r_4}{r_3})}{K_{steel}} + \frac{\ln(\frac{r_3}{r_2})}{K_{air}} + \frac{\ln(\frac{r_2}{r_1})}{K_{ins}}\right) + \frac{1}{h_1}} \tag{11.6}$$

As a numerical example for the 30 gauge copper-constantan thermocouple wire,

$r_1 = 0.1796mm, \quad r_2 = 0.3229mm, \quad r_3 = 0.7874mm, \quad r_4 = 1.0414mm$

$K_{steel} = 50\ \mathrm{W}/m^{\circ}K, \qquad K_{ins} = 0.35\ \mathrm{W}/m^{\circ}K,$

$K_{air} = 0.026\ \mathrm{W}/m^{\circ}K, \qquad K_{cu} = 386.0\ \mathrm{W}/m^{\circ}K,$

$K_{cn} = 22.7\ \mathrm{W}/m^{\circ}K, \qquad h_1 = 100.0\ \mathrm{W}/m^{2\circ}K$

$C = 2\pi r_4 \qquad = 0.006543\ \mathrm{m}$

$Ch_{eq} = 0.1457\frac{w}{m^{\circ}k}$

$(KA)_{eq} = 2.07091 \times 10^{-5}\frac{w}{m^{\circ}k}$

For $T_{tb} - T_{fb} = 100^{\circ}K$,

$q_{cl} = 0.1736W$

Considering a typical value of heat transfer coefficient as 300 $\mathrm{W}/m^{2\circ}k$ for 1.0 cm copper sphere immersed in a fluidized bed with the temperature difference between the bed and the sphere of 100 $^{\circ}K$,

$$q_{conv} = hA_{sph}(T_{sph} - T_{fb}) = 9.425W. \tag{11.7}$$

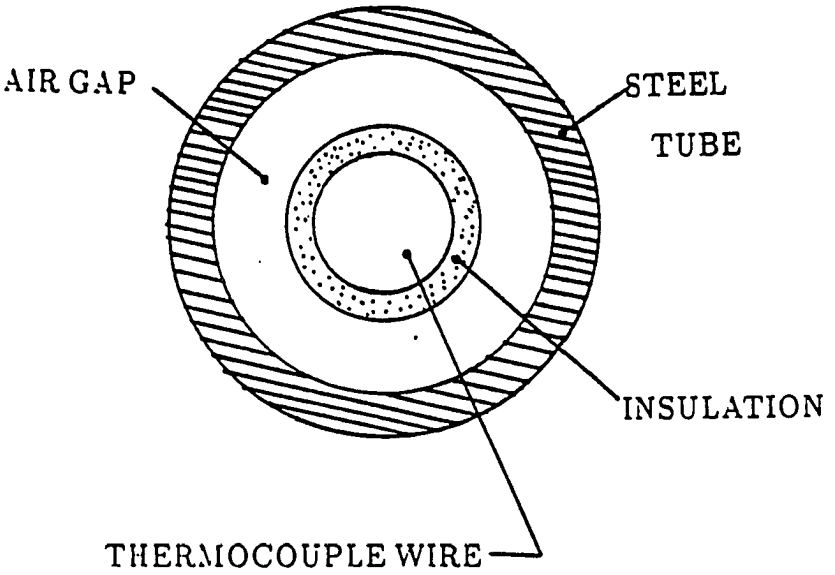

Figure 11.2: Thermocouple wires with equivalent radii inside a hollow steel tube

Hence, the thermocouple conduction heat loss is about 1.8 % of the total heat transfer from the sphere. This loss was considered to be negligible.

12 APPENDIX D: COMPUTER PROGRAMS

```
C*************************************************************
C       THIS DATA ACQUISITION PROGRAM CONNECTS IEEE AND HP
C       DIGITAL VOLTMETER
C
        DIMENSION DELTA(600),TEMPK(10)
        CHARACTER*50 CHVOLT,COMM(5)
        INTEGER*2 ISTAT(2)
        REAL VOLTS(600),TIME(600)
        CHARACTER*25 FNAME
        OPEN(UNIT=2,NAME='FOR002.DAT',STATUS='OLD')
C-------------------------------------------------------------
C       INITIALIZATION ROUTINE
C       ISTAT=STATUS CODE
C       ISYSC=1 > PC380 IS THE CONTROLLER
C       IADR   TAKEN AS DEFAULT
C       IADR1  TAKEN AS DEFAULT
C
C       IEFN=2 > STD EVENT FLAG
C       MODE=1 > SYNCHRONOUS I/O (WAIT UNTILL THIS SUBROUTINE
C                                 IS COMPLETED)
C-------------------------------------------------------------
C
        CALL IBINIT(ISTAT,1,,,2,1)
C
C-------------------------------------------------------------
C       WAIT FOR STD EVENT FLAG(=2)
C-------------------------------------------------------------
C
        CALL WAITFR(2)
C
```

```
      PRINT *,' ISTAT=',ISTAT
C-----------------------------------------------------------------
C     CALL SUBROUTINE TO CLEAR THE INTERFACE
C-----------------------------------------------------------------
C
      CALL IBIFC(ISTAT,2,1)
C-----------------------------------------------------------------
C
C     WAIT FOR EVENT FLAG(=2)
C-----------------------------------------------------------------
C
      CALL WAITFR(2)
      PRINT *,' ISTAT INTERFACE CLEAR=',ISTAT
C-----------------------------------------------------------------
C     CALL SUBROUTINE TO ENABLE REMOTE
C-----------------------------------------------------------------
C
      CALL IBREN(ISTAT,2,1)
C
C     WAIT FOR EVENT FLAG(=2)
      CALL WAITFR(2)
      PRINT *,' ISTAT ENABLE REMOTE=',ISTAT
C
C     CALL SUBROUTINE TO CLEAR THE DEVICE
C
      CALL IBDCL(ISTAT,2,1+2)
C
C     WAIT FOR EVENT FLAG(=2)
      CALL WAITFR(2)
      PRINT *,' ISTAT CLEAR DEVICE=',ISTAT
C
C     SET UP THE HP-DIGITAL VOLTMETER
C
      READ(2,42,END=31)ND
      READ(2,21,END=31)ENDTIM
      READ(2,42,END=31)MDIR
      READ(2,21,END=31)VSPH
      READ(2,21,END=31)FBH
 21   FORMAT(20X,G10.4)
```

```
42      FORMAT(20X,I4)
31      WRITE(6,22) ND,ENDTIM,MDIR,VSPH,FBH
22      FORMAT(' ND,ENDTIM,MDIR,VSPH,FBH'
     *  ,I4,1X,F10.4,1X,I4,2(1X,F10.4))
        TYPE 311
311     FORMAT(' ENTER THE BED TEMPERATURE IN C>',$)
        READ(5,*) TFC
        TYPE 32
32      FORMAT(' ENTER THE PRESSURE DROP ACROSS THE BED IN CMS>',$)
        READ(5,*) PD
        TYPE 33
33      FORMAT(' ENTER THE PRESSURE OUTSIDE THE RATAMETER>',$)
        READ(5,*) RPOUT
        TYPE 34
34      FORMAT(' ENTER RUN NUMBER>',$)
        READ(5,*) RUNNO
        TYPE 35
35      FORMAT(' ENTER ROTAMETER NO.(1 TO 6 )>',$)
        READ(5,*) ROTMNO
        TYPE 36
36      FORMAT(' DO YOU WANT TO START
     *  DATA ACQUISITION?(1-YES,0-NO)>',$)
        READ(5,*) ISTART
        IF(ISTART.EQ.0) GO TO 37
        COMM(1)='F1 R2 T2 Z0 FLO'
        ICOUNT=15
C
C       CALL SUBROUTINE TO SEND DATA FROM USER BUFFER TO
C       SPECIFIC LISTENER
C
        CALL IBSEND(ISTAT,COMM(1),ICOUNT,2,1+2+8,,,18)
        CALL WAITFR(2)
        T1=SECNDS(0.0)
C
C       CODE TO BE TIMED
```

```
C
      PRINT *,' ISTAT SEND=',ISTAT
      DO 100 I=1,ND
C
C     CALL SUBROUTINE IBGET TO EXECUTE TRIGGER
C
      CALL IBGET(ISTAT,2,1+2,,18)
      CALL WAITFR(2)
C
C     CALL SUBROUTINE IBRECV TO RECEIVE DATA
C
      DELTA(I)=SECNDS(T1)
      CALL IBRECV(ISTAT,CHVOLT,14,5,1+2,,,18)
      CALL WAITFR(5)
C
C     CONVERT CHARACTER VOLTS IN TO REAL NUMBER
C
      READ(CHVOLT,200) VOLTS(I)
      TIMEO=DELTA(1)
      TIME(I)=DELTA(I)-TIMEO
      WRITE(6,*) I,TIME(I),VOLTS(I)
      IF(TIME(I).GE.ENDTIM) GO TO 110
 100  CONTINUE
 200  FORMAT(E12.9)
 110  ND=I
      TIMEO=DELTA(1)
      TYPE 411
 411  FORMAT(' ENTER THE FILENAME>',$)
      READ(5,315) FNAME
 315  FORMAT(A15)
C
C
      OPEN(UNIT=1,TYPE='NEW',NAME=FNAME,ERR=312)
C
      WRITE(1,336) FBH,PD,RPOUT,RUNNO,ROTMNO,TFC,MDIR,VSPH
 336  FORMAT(F10.6/F10.6/F10.6/F10.6/F10.6/F10.6/I4/F10.6)
      DO 400 I=1,ND-1
      TIMEO=DELTA(1)
```

```
      TIME(I)=DELTA(I)-TIME0
      WRITE(1,300) TIME(I),VOLTS(I)
300   FORMAT(F10.6,2X,F12.9)
400   CONTINUE
312   TYPE 314
314   FORMAT(' ERROR WHILE WRITING IN THE FILE')
      I=1
306   CALL MVTEMP(VOLTS(I),TEMPK(I))
      IF(I.EQ.ND) GO TO 307
      I=ND
      GO TO 306
307   ND1=ND-1
      WRITE(6,402) N,TEMPK(1),TEMPK(ND)
402   FORMAT(' N,TINITIAL,TEND IN K',I3,3X,F10.4,3X,F10.4)
37    STOP
      END
C
C
      SUBROUTINE MVTEMP(E,TEMPK)
      X1=0.1008609
      X2=25727.94369
      X3=-767345.8295
      X4=78025595.81
      X5=-9247486589.0
      X6=697688000000.
      X7=-2.66192E+13
      X8=3.94078E+14
      TEMP1=X1+X2*E+X3*(E**2)
      TEMP2=X4*(E**3)+X5*(E**4)
      TEMP3=X6*(E**5)+X7*(E**6)+X8*(E**7)
      TEMP=TEMP1+TEMP2+TEMP3
      TEMPK=TEMP+273.2
      RETURN
      END
```

```
C*****************************************************************
C       THIS PROGRAM CALCULATES THE HEAT TRANSFER COEFFICIENT
C       FROM THE MILLIVOLTS READING OBTAINED BY THE DATA
C       ACQUISITION SYSTEM.
C
C-----------------------------------------------------------------
C
C       VARIABLES
C
C       Name    Type
C
C        AINPT  R*4    INTERCEPT OF REGRESSION LINE
C        AKAIR  R*4    CONDUCTIVITY OF AIR (W/M K)
C                      AIR AT NORMAL TEMPERATURE.
C        ANUEXP R*4    EXPERIMENTAL NUSSELT NO. BASED ON
C                      SPHERE DIAMETER AND GAS PROPERTIES
C        AREA   R*4    SURFACE AREA OF THE SPHERE
C        ATMP   R*4    ATMOSPHERIC PRESSURE
C        AVGHR  R*4    AVERAGE RADIATION HEAT TRANSFER COEFFICIENT
C        BOLTZ  R*4    BOLTZMAN'S CONSTANT
C        BSH    R*4    PACKED BED HEIGHT
C        CA     R*4    CONSTANT FOR THE EQUATION FOR THE SPECIFIC
C                      HEAT AS A FUNCTION OF TEMPERATURE
C        CB     R*4    CONSTANT FOR THE EQUATION FOR THE SPECIFIC
C                      HEAT AS A FUNCTION OF TEMPERATURE
C        DELTA  R*4    ALLOWABLE RANGE FOR THE INITIAL SPHERE
C                      TEMPERATURE
C        DIA    R*4    DIAMETER OF SPHERE
C        EMIS   R*4    EMISSIVITY OF THE SPHERE
C        EMIV   R*4    APPLIED VOLTAGE TO THE ELECTRIC MOTOR
C        FBDIA  R*4    FLUIDIZED BED INSIDE DIAMETER
C        FBH    R*4    FLUIDIZED BED HEIGHT
C        HCONV  R*4    CONVECTIVE HEAT TRANSFER COEFFICIENT
C        HT     R*4    TOTAL HEAT TRANSFER COEFFICIENT
C        MDIR   I*3    DIRECTION OF SPHERE MOTION IN THE FLUIDIZED BED
C                      0-MOVING DOWN,1-MOVING UP
```

```
C       PDIA    R*4   DIAMETER OF THE PULLEY
C       PD      R*4   PRESSURE DROP ACROSS THE BED
C       PLATNO  R*4   DISTRIBUTOR PLATE NUMBER
C       POUT    R*4   PRESSURE AT THE OUTLET OF ROTAMETER IN CMS OF
C                     Hg
C       PSTD    R*4   STANDARD PRESSURE
C       QRS     R*4   VOLUME FLOW RATE AT STD CONDITION
C       QOP     R*4   VOLUME FLOW RATE AT THE OPERATING CONDITION
C       QBED    R*4   VOLUME FLOW RATE IN SIDE THE BED
C       R       R*4   COEFFICIENT OF CORRELATION.
C       RHOS    R*4   DENSITY OF SOLID SPHERE
C       RMTEMP  R*4   ROOM TEMPERATURE
C       ROTM    R*4   ROTAMETER READING
C       ROTMNO  R*4   ROTAMETER CATALOG NUMBER
C       RPOUT   R*4   PRESSURE AT THE OUTLET OF THE ROTAMETER
C                     IN CM OF WATER
C       RSQ     R*4   SQUARE OF COEFFICIENT OF CORRELATION
C       RUNNO   R*4   RUN NUMBER
C       SETTI   R*4   SET INITIAL TEMPERATURE
C       SIZENO  R*4   PARTICLE SIZE NUMBER REPRESENTING
C                     THE SIZE RANGE
C       SIZE1   R*4   UPPER SIZE RANGE OF THE PARTICLES IN MICRONS
C       SIZE2   R*4   LOWER SIZE RANGE OF THE PARTICLES IN MICRONS
C       SLOP    R*4   SLOP OF THE COOLING CURVE ON A LOG-LOG
C                     BASES
C       SPHEAT  R*4   SPECIFIC HEAT OF THE SPHERE
C       S1      R*4   SPHERE MATERIAL IDENTIFICATION KEY(S1=
C       S2      R*4   SPHERE SIZE IDENTIFICATION KEY
C       TAO     R*4   TIME CONSTANT (SEC)
C       TAO1    R*4
C       TAVG    R*4   AVERAGE TEMPERATURE
C       TFLUID  R*4   BED TEMPERATURE IN K
C       TINI    R*4   INITIAL TEMPERATURRE OF THE SPHERE
C       TSTD    R*4   STANDARD TEMPERATURE
C       TTIME   R*4   TOTAL TIME
C       VOL     R*4   VOLUME OF THE SPHERE
C       VSPH    R*4   LONGITUDINAL SPHERE VELOCITY INSIDE
```

```
C                       THE FLUIDIZED BED
C        VSPH1  R*4
C        VSUF   R*4   SUPERFICIAL VELOCITY OF THE FLUIDIZING GAS
C
C
C        ARRAYS
C
C        Name   Type
C
C        E      R*4   THERMOCOUPLE READING IN MILIVOLTS.
C        TEMP   R*4   TEMPERATURE OF THE SPHERE IN C
C        TEMPK  R*4   TEMPERATURE OF THE SPHERE IN K
C        TIME   R*4   TIME IN SECS.
C
C
C*****************************************************************
C
        DIMENSION TIME(300),TEMP(300),E(300),TEMPK(300)
        DIMENSION TR(300),TRL(300)
        DIMENSION TRL1(300)
        CHARACTER*40 RA,RB
        INTEGER S1,S2,SIZE1,SIZE2,MDIR
        OPEN(UNIT=1,FILE='FOR001.DAT',STATUS='OLD')
        OPEN(UNIT=4,FILE='FOR004.DAT',STATUS='OLD')
        OPEN(UNIT=12,FILE='FOR012.DAT',STATUS='OLD')
        OPEN(UNIT=8,FILE='FOR008.DAT',STATUS='OLD')
        PI=3.1415926
        READ(8,100,END=130) S1
        READ(8,100,END=130) S2
        READ(8,110,END=130) SIZENO
        READ(8,110,END=130) FBH
        READ(8,110,END=130) BSH
        READ(8,110,END=130) TFC
        READ(8,110,END=130) PD
        READ(8,110,END=130) RMTEMP
        READ(8,110,END=130) ATMP
        READ(8,110,END=130) RPOUT
        READ(8,120,END=130) RUNNO
        READ(8,120,END=130) EMIS
```

```
      READ(8,120,END=130) SETTI
      READ(8,120,END=130) DELTA
      READ(8,120,END=130) TDIF
      READ(8,120,END=130) CA
      READ(8,120,END=130) CB
      READ(8,120,END=130) ROTM
      READ(8,120,END=130) PLATNO
      READ(8,120,END=130) ROTMNO
      READ(8,120,END=130) PSTD
      READ(8,120,END=130) TSTD
      READ(8,120,END=130) FBDIA
      READ(8,120,END=130) EMIV
      READ(8,120,END=130) PDIA
      READ(8,120,END=130) VSPH1
      READ(8,120,END=130) HG
      READ(8,120,END=130) AMPL
      READ(8,120,END=130) SPFREQ
100   FORMAT(42X,I4)
110   FORMAT(42X,G10.4)
120   FORMAT(42X,G10.4)
130   WRITE(6,140)
140   FORMAT(' FOLLOWING ARE THE INPUT PARAMETERS')
      WRITE(6,150) S1,SIZENO
150   FORMAT(' S1=1 FOR BRONZ AND 0 FOR COPPER-',I4/,
     *  ' SIZE NO. OF THE GLASS BEADS -',F10.4)
      WRITE(6,160) FBH,BSH,TFC,S2,PD,RMTEMP,ATMP,RPOUT
     *  ,RUNNO,EMIS,SETTI,DELTA,TDIF,ROTM
160   FORMAT(' BED HEIGHT IN FLUIDIZED STATE(CM)-',F10.4/,
     2  ' PACKED BED HEIGHT(CM)-',F10.4/,
     3  ' BED TEMPERATURE (K)-',F10.4/,
     4  ' SPHERE NUMBER-',I4/,
     5  ' PRESSURE DROP ACROSS THE BED (CM OF WATER)-',F10.4/,
     6  ' ROOM TEMPERATURE (C)-',F10.4/,
     7  ' ATMOSPHERIC PRESSURE (CM OF Hg)-',F10.4/,
     8  ' ROTAMETER OUTLET PRESSURE(CM OF WATER)-',F10.4)
     9  ' RUN NUMBER-',F10.4/,
```

```
     1  ' EMISSIVITY-',F10.4/,
     2  ' SET INITIAL TEMP.-',F10.4/,
     3  ' DELTA-',F10.4/,
     4  ' TDIF TEMP. DIFF. BET. A STEP-',F10.4/,
     5  ' ROTAMETER READING-',F10.4)
        WRITE(6,170) PSTD,TSTD,FBDIA,EMIV,PDIA
170      FORMAT(' STD PRESSURE IN CM OF Hg-',F10.4/,
     1  ' STD TEMPERATURE K-',F10.4/,
     2  ' INSIDE DIAMETER OF BED CM-',F10.4/,
     3  ' INPUT VOLTS TO THE MOTOR-',F10.4/,
     3  ' PULLEY DIAMETER CM-',F10.4)
        IF(PLATNO.EQ.1.) GO TO 171
        GO TO 190
171     WRITE(6,200)
200     FORMAT(' ORIGINAL DISTRIBUTOR PLATE USED')
190     WRITE(6,*)S1,S2
        TYPE 210
210     FORMAT(' DO YOU NEED THE HEADING?,YES=1,NO=0',$)
        READ(5,*) N1
        TYPE 220
220     FORMAT(' ENTER THE ROTAMETER READINGS>',$)
        READ(5,*)ROTM
        TYPE 230
230     FORMAT(' ENTER SETTI IN K>',$)
        READ(5,*)SETTI
        TYPE 240
240     FORMAT(' ENTER TDIF IN K>',$)
        READ(5,*)TDIF
C
C-------------------------------------------------------------
C       READ TIME AND THERMOCOUPLE VOLTAGE DATA FROM DATA FILE
C
C-------------------------------------------------------------
C
        READ(1,246)FBH,PD,RPOUT,RUNNO,ROTMNO,TFC
```

```
 246    FORMAT(F10.6/F10.6/F10.6/F10.6/F10.6/F10.6)
        WRITE(6,247)ROTMNO,TFC,MDIR,VSPH1
 247    FORMAT(' ROTMNO,TFC,MDIR,VSPH1',2F10.4,I4,F10.4)
        DO 250 K1=1,9999
        READ(1,260,END=270) TIME(K1),E(K1)
 250    CONTINUE
 260    FORMAT(F10.6,2X,F12.9)
 270    N=K1-1
        N3=1
        WRITE(6,271) FBH,PD,RPOUT,RUNNO,ROTMNO,MDIR,VSPH1
 271    FORMAT(F10.6/F10.6/F10.6/F10.6/F10.6/I3/F10.6)
C
C---------------------------------------------------------------
C       IF N1 IS EQUAL TO 1 OPEN A NEW OUTPUT FILE
C
C---------------------------------------------------------------
C
        IF (N1.EQ.1) GO TO 280
C
C---------------------------------------------------------------
C
C       IF N1 EQUAL TO 0 NO HEADING REQUIRED AND WRITE THE OUTPUT
C       DATA AT THE END OF THE OUTPUT FILE FOR001.DAT
C---------------------------------------------------------------
C
 300    READ(4,290,END=310) RA
        GO TO 300
 310    CONTINUE
 301    READ(12,290,END=302) RB
        GO TO 301
 302    CONTINUE
 290    FORMAT(A30)
 280    WRITE(6,*) SIZE
C
C---------------------------------------------------------------
C       THE KEY S1 SELECTS THE MATERIAL OF THE SPHERE. FOR BRONZE
C       SPHERE S1=1
C       AND FOR COPPER SPHERE S1=2
```

```
C
C-----------------------------------------------------------------
C
        IF (S1.EQ.1) GO TO 320
        RHOS=8954.0
        SPHEAT=383.1
        GO TO 330
 320    RHOS=8666.0
        SPHEAT=343.0
C
C-----------------------------------------------------------------
C       THE KEY S2 SELECTS THE SIZE OF THE SPHERE
C
C-----------------------------------------------------------------
C
 330    GO TO (340,350,360,370) S2
 340    DIA=0.0095
        CDIA=0.00
        GO TO 380
 350    DIA=0.01
        CDIA=0.0
        GO TO 380
 360    DIA=0.014
        CDIA=0.0
        GO TO 380
 370    DIA=0.02
        CDIA=0.0
C
C       CALCULATE THE SURFACE AREA AND VOLUME OF THE SPHERE
C
C
 380    VOL=4.0*PI*((DIA/2.)**3)/3.
```

```
C
C
C
        AREA=4*PI*((DIA/2.)**2)-PI*((CDIA/2.)**2)
        BOLTZC=5.6700E-08
        KEY1=0
C-----------------------------------------------------------------------
C       SELECT THE INITIAL TEMPERATURE RANGE
C-----------------------------------------------------------------------
        TFLUID=TFC+273.2
        SETTI1=SETTI+DELTA
        TIPD=SETTI-DELTA
C
C-----------------------------------------------------------------------
C       CONVERT THE THERMOCOUPLE VOLTAGE INTO TEMPERATURE IN K
C-----------------------------------------------------------------------
C
        DO 390 I=1,N
        CALL MVTEMP(E(I),TEMPK(I))
 390    CONTINUE
C
C-----------------------------------------------------------------------
C       SELECT THE INITIAL INDEX I FROM THE INITIAL TEMPERATURE RANGE
C
C-----------------------------------------------------------------------
C
 421    DO 400 I= 1,N
        IF((TEMPK(I).LE.SETTI1).AND.(TEMPK(I).GE.TIPD)) GO TO 410
 400    CONTINUE
 410    N3=I
C
```

```
C-------------------------------------------------------------
C       CALCULATE THE TEMPERATURE RANGE FOR WHICH THE HEAT TRANSFER
C       COEFFICIENT HAS TO BE CALCULATED
C-------------------------------------------------------------
C
 420    TSTEP=TEMPK(N3)-TDIF
        TSTEPH=TSTEP+DELTA
        TSTEPL=TSETP-DELTA
C
C
        WRITE(6,430) N3,TEMPK(N3)
 430    FORMAT(' *****N3,T(N3)',I3,F10.4)
C
C-------------------------------------------------------------
C       SELECT THE FINAL INDEX N4, FROM THE TEMPERATURE STEP
C-------------------------------------------------------------
C
        DO 440 I=N3,N
        IF((TEMPK(I).LE.TSTEPH).AND.(TEMPK(I).GE.TSTEPL)) GO TO 450
 440    CONTINUE
 450    N4=I
C
C-------------------------------------------------------------
C       IF FINAL INDEX IS GREATER THEN NUMBER OF DATA POINTS TAKEN
C       THEN SET N4 EQUAL TO THE NUMBER OF DATA POINTS
C-------------------------------------------------------------
C
C
        IF(KEY3.EQ.1) N4=N
        IF(N4.GE.N) N4=N
C
C-------------------------------------------------------------
C
C       INITIALIZE PARAMETERS USED FOR CALCULATING THE SLOP
C
C-------------------------------------------------------------
```

```
      SIGXY=0.0
      SIGXSQ=0.0
      SIGX=0.0
      SIGY=0.0
      SIGYSQ=0.0
      SIGXYC=0.0
      SIGXSC=0.0
      SIGXC=0.0
      SIGYC=0.0
      SIGYSC=0.0
      WRITE(6,*)N3,N4
C
C-----------------------------------------------------------------
C
C       CALCULATE TIME FROM THE DATA
C       (USE THIS WHEN ADM DATA ACQUISITION PROGRAM IS USED)
C-----------------------------------------------------------------
C
C       DUTIME=TIME(N3)
C       DO 460 I3=N3,N4
C        WRITE(4,470) I3,DUTIME,TIME(I3),TIME(N3)
C 470   FORMAT(' I3,DUTIME,TIME(I3),TIME(N3)',I3,1X,3(2X,F10.4))
C        TIME(I3)=TIME(I3)-DUTIME
C       WRITE(4,480) I3,N3,N4,TIME(I3)
C 480   FORMAT(' I3,N3,N4,TIME(I3)',I3,1X,I3,1X,I3,1X,F10.4,2X,F10.4)
C 460    CONTINUE
C
C-----------------------------------------------------------------
C
C       CALCULATE THE NECESSARY VARIABLES NEEDED FOR
C       LINEAR REGRESSION
C
C-----------------------------------------------------------------
C
      DO 490 I=N3,N4
      TR(I)=(TFLUID-TEMPK(I))/(TFLUID-TEMPK(N3))
```

```
C
C       IF I=N3 THEN TR=0.0 SO AVOID LOG OF 0.0
C
        IF(I.EQ.N3) GO TO 500
        GO TO 510
 500    TRL(N3)=0.0
        TRL1(N3)=0.0
        GO TO 520
C
C-----------------------------------------------------------------
C       FOR VARIABLE SPECIFIC HEAT OF THE COPPER SPHERE
C       CB IS NOT EQUAL TO ZERO
C-----------------------------------------------------------------
C
 510    IF(CB.EQ.0.0) GO TO 530
        TRL(I)=LOG(TR(I))*(CA+CB*TFLUID)+CB*(TEMPK(I)-TEMPK(N3))
        TRL1(I)=LOG(TR(I))
        GO TO 520
 530    TRL(I)=LOG(TR(I))
 520    E(I)=E(I)*1000.
        TIME1=TIME(I)-TIME(N3)
C
C
        SIGXY=SIGXY+TIME(I)*TRL(I)
        SIGXSQ=SIGXSQ+TIME(I)*TIME(I)
        SIGX=SIGX+TIME(I)
        SIGY=SIGY+TRL(I)
        SIGYSQ=SIGYSQ+TRL(I)*TRL(I)
C-----------------------------------------------------------------
C       REGRESSION ANALYSIS FOR THE CONSTANT SPECIFIC HEAT OF COPPER
C       SPHERE
C-----------------------------------------------------------------
C
        SIGXYC=SIGXYC+TIME(I)*TRL1(I)
        SIGXSC=SIGXSC+TIME(I)*TIME(I)
        SIGXC=SIGXC+TIME(I)
        SIGYC=SIGYC+TRL1(I)
        SIGYSC=SIGYSC+TRL1(I)*TRL1(I)
 490    CONTINUE
```

```
C
C-----------------------------------------------------------------
C
C       CALCULATE SLOP AND INTERCEPT
C
C-----------------------------------------------------------------
C
        NN=N4-N3+1.0
        DENO=NN*SIGXSQ-SIGX*SIGX
        DENO1=SQRT(DENO*(NN*SIGYSQ-SIGY*SIGY))
        SLOP1=SIGXY/SIGXSQ
        SLOP=(NN*SIGXY-SIGX*SIGY)/DENO
        WRITE(6,491)SLOP1,SLOP
 491    FORMAT(' SLOP1,SLOP',2(1X,F10.4))
        AINPT=(SIGY*SIGXSQ-SIGX*SIGXY)/DENO
C-----------------------------------------------------------------
C       CALCULATE SLOP AND INTERCEPT FOR THE CONSTANT SPECIFIC
C       HEAT OF THE COPPER SPHERE
C-----------------------------------------------------------------
C
        DENOC=NN*SIGXSC-SIGXC*SIGXC
        DENOC1=SQRT(DENOC*(NN*SIGYSC-SIGYC*SIGYC))
        SLOPC=(NN*SIGXYC-SIGXC*SIGYC)/DENOC
        AINPTC=(SIGYC*SIGXSC-SIGXC*SIGXYC)/DENOC
C
C-----------------------------------------------------------------
C       CALCULATE COEFFICIENT OF REGRESSION AND TIME CONSTANT
C
C-----------------------------------------------------------------
C
        R=(NN*SIGXY-SIGX*SIGY)/DENO1
        RC=(NN*SIGXYC-SIGXC*SIGYC)/DENOC1
        RSQ=R*R
        TAO=1./(ABS(SLOP))
        TAO1=1.0/(ABS(SLOP1))
```

```
      TAOC=1.0/(ABS(SLOPC))
C
C-----------------------------------------------------------------
C       CALCULATE HEAT TRANSFER COEFFICIENT DUE TO RADIATION
C
C-----------------------------------------------------------------
C
      TTIME=TIME(N4)-TIME(N3)
      TINI=TEMPK(N3)
      X1=0.5*TAO*(TFLUID*TFLUID-2.*TFLUID*TINI+TINI*TINI)
     *  *(EXP(-2.*TTIME/TAO))
      X2=2.*TFLUID*TFLUID-2.*TFLUID*TAO*(TFLUID-TINI)
     *  *(EXP(-TTIME/TAO))
      X3=2.*TFLUID+TAO*(TFLUID-TINI)*(EXP(-TTIME/TAO))
      X4=0.5*TAO*(TFLUID*TFLUID-2.*TFLUID*TINI+TINI*TINI)
      X5=2.*TFLUID*TFLUID-2.*TFLUID*TAO*(TFLUID-TINI)
      X6=2.*TFLUID+TAO*(TFLUID-TINI)
C      AVGHR=BOLTZC*EMIS*(((X2-X1)*(X3))-((X5-X4)*(X6)))/TTIME
      AVGHR=BOLTZC*EMIS*(TEMPK(N3)*TEMPK(N3)+TFLUID*TFLUID)
     *  *(TEMPK(N3)+TFLUID)
C
C       TOTAL HEAT TRANSFER COEFFICIENT FOR VARIABLE SPECIFIC HEAT
C       OF THE COPPER SPHERE
      HT=RHOS*VOL/(TAO*AREA)
      HT1=RHOS*VOL/(TAO1*AREA)
      HTC=RHOS*SPHEAT*VOL/(TAOC*AREA)
C
C       TOTAL HEAT TRANSFER FOR CONSTANT SPECIFIC HEAT
C       OF THE COPPER SPHERE
      IF(CB.LE.0.0) HT=RHOS*SPHEAT*VOL/(TAO*AREA)
      IF(CB.LE.0.0) HT1=RHOS*SPHEAT*VOL/(TAO1*AREA)
C
C-----------------------------------------------------------------
C       CALCULATE THE CONVECTION PART OF THE HEAT TRANSFER
C       COEFFICIENT
C
C-----------------------------------------------------------------
C
```

```
        HCONV=HT-AVGHR
        HCONVC=HTC-AVGHR
        TFILM=(TEMPK(N3)+TFLUID)/2.0
C
C-----------------------------------------------------------------
C       CALCULATE THE CONDUCTIVITY OF THE AIR FROM THE FILM
C       TEMPERATURE
C
C-----------------------------------------------------------------
C
        CALL AIRPRO(TFILM,AKAIR)
        ANUEXP=HCONV*DIA/AKAIR
        TAVG=(TEMPK(N3)+TEMPK(N4))/2.0
        DENOL=LOG((TEMPK(N4)-TFLUID)/(TEMPK(N3)-TFLUID))
        TLMTD=(TEMPK(N4)-TEMPK(N3))/DENOL
        TLMTD1=TLMTD+TFLUID
        ALTMLT=LOG(TLMTD1)
        TOF=TINI-TFLUID
        ALHC=LOG(HT)
        ALHM=LOG(HT1)
        WRITE(6,650) AVGHR,HT,HT1,HCONV
 650    FORMAT(' AVGHR,HT,HT1,HCONV',4(2X,F10.4))
C
C-----------------------------------------------------------------
C       CALCULATE THE SUPERFICIAL VELOCITY OF FLUIDIZING GAS
C
C-----------------------------------------------------------------
C
        CALL VSUP(ROTMNO,ROTM,PSTD,RMTEMP,TSTD,ATMP,RPOUT,FBDIA
     *  ,VSUF,PD,HG)
C
C-----------------------------------------------------------------
C       CALCULATE THE SPHERE VELOCITY FOR THE CASE OF A MOVING SPHERE
C
C-----------------------------------------------------------------
```

```
C
      IF(EMIV.GT.0.0) CALL SPHVEL(EMIV,PDIA,VSPH)
C
C-----------------------------------------------------------------
C
C     IF N1=1 WRITE THE TITLE IN THE OUTPUT DATA FILE
C     IF N1=0 SKIP THE TITLE
C-----------------------------------------------------------------
      IF(N1.NE.1) GO TO 670
      IF(KEY1.EQ.1) GO TO 670
      IF(KEY3.EQ.1) GO TO 670
C
C     WRITE AN APPROPRIATE HEADING FOR A STATIONARY SPHERE
C
      IF(EMIV.LE.0.0) GO TO 680
C
C     WRITE AN APPROPRIATE HEADING FOR COPPER/BRONZE SPHERE
C
C
      IF(S1.EQ.1) GO TO 690
      WRITE(4,700)
 700  FORMAT(6X,' HEAT TRANSFER OF A OSCILLATING COPPER SPHERE',/)
      GO TO 710
 690  WRITE(4,720)
 720  FORMAT(6X,' HEAT TRANSFER OF A MOVING BRONZE SPHERE',/)
 710  WRITE(4,730) AMPL
 730  FORMAT(6X,' AMPLITUDE OF OSCILLATION OF SPHERE (CM)=',F10.4)
      WRITE(4,731) SPFREQ
 731  FORMAT(6X, ' FREQUENCY OF THE SPHERE (C/S)=',F10.4)
      GO TO 740
 680  IF(S1.EQ.1) GO TO 750
      WRITE(4,760)
 760  FORMAT(6X,' HEAT TRANSFER OF A STATIONARY COPPER SPHERE')
      GO TO 740
 750  WRITE(4,770)
```

```
 770    FORMAT(6X,' HEAT TRANSFER OF A STATIONARY BRONZE SPHERE')
 740    IF(PLATNO.EQ.1.) GO TO 780
        WRITE(4,790)
 790    FORMAT(6X,' DISTRIBUTOR PLATE USED# A3420141'/
     *  6X,' STD PERMEABILITY=50,AVG PORE SIZE=100 MICRONS')
        GO TO 800
 780    WRITE(4,810)
 810    FORMAT(6X,' ORIGINAL DISTRIBUTOR PLATE USED')
 800    WRITE(4,820) FBDIA
 820    FORMAT(6X,' INSIDE DIAMETER OF THE BED(CM)=',F10.4)
C
C-----------------------------------------------------------------
C       SELECT THE PARTICLE RANGE FROM THE VALUE OF SIZENO
C-----------------------------------------------------------------
        GO TO (830,840,850,860,865) SIZENO
 830    SIZE1=147
        SIZE2=126
        GO TO 870
 840    SIZE1=44
        SIZE2=0
        GO TO 870
 850    SIZE1=450
        SIZE2=355
        GO TO 870
 860    SIZE1=2
        SIZE2=2
        GO TO 870
 865    SIZE1=2
        SIZE2=2
 870    WRITE(4,880) SIZENO,SIZE1,SIZE2
 880    FORMAT(6X,' SIZENO#',F3.1,3X,' GLASS BEADS OF
     *  SIZE =',I4,'-',I4 ,2X,' MICRONS')
        GO TO (900,901,902,903,904,905,906) ROTMNO
 900    WRITE(4,910)
 910    FORMAT(6X,' ROTAMETER CATALOGE#450-700,CREST DIV.')
        GO TO 920
 901    WRITE(4,930)
 930    FORMAT(6X,' ROTAMETER CATALOGE# 250-8,DEVCO TUBE')
        GO TO 920
```

```
902     WRITE(4,931)
931     FORMAT(6X,' ROTAMETER BROOKS INSTRUMENT DIV.')
        GO TO 920
903     WRITE(4,932)
932     FORMAT(6X,' ROTAMETER F&P CO. PRECISION BORE FLOWMETER')
        GO TO 920
904     WRITE(4,933)
933     FORMAT(6X,' BROOKS ROTAMETER -TUBE SIZE-R7M25-1')
        GO TO 920
905     WRITE(4,934)
934     FORMAT(6X,' SCHUTTLE & KOERTING CO. ROTAMETER')
906     WRITE(4,907)
907     FORMAT(6X,' BROOK INSTRUMENT DIV.,(%*8.10CC/MIN))')
920     WRITE(4,940) S2
940     FORMAT(6X,' SPHERE NUMBER#=',I4)
        WRITE(4,950) RMTEMP
950     FORMAT(6X,' ROOM TEMPERATURE (C)=',F10.4)
        WRITE(4,960) ATMP
960     FORMAT(6X,' ATMOSPHERIC PRESSURE(CM OF Hg)=',F10.4)
        WRITE(4,970) PSTD
970     FORMAT(6X,' STD PRESSURE IN CM OF Hg=',F10.4)
        WRITE(4,980) TSTD
980     FORMAT(6X,' STD TEMPERATURE K=',F10.4)
        WRITE(4,990) RHOS
990     FORMAT(6X,' DENSITY OF THE SPHERE MATERIAL(Kg/M3)=',F10.4)
        WRITE(4,1000) SPHEAT
1000    FORMAT(6X,' SPECIFIC HEAT OF THE SPHERE MATERIAL()=',F10.4)
        WRITE(4,1010) EMIS
1010    FORMAT(6X,' EMISSIVITY OF SPHERE=',F10.4)
        WRITE(4,1020) DIA
1020    FORMAT(6X,' DIAMETER OF SPHERE(MTS)=',F10.4)
        WRITE(4,1030) BSH
1030    FORMAT(6X,' PACKED BED HEIGHT (CMS)=',F10.4)
        WRITE(4,1040)TFLUID
1040    FORMAT(6X,' BED TEMPERATURE(K)= ',F10.4)
        WRITE(4,1050)CA,CB
1050    FORMAT(6X,' CA=',F10.4,3X,'CB=',F10.4//)
        WRITE(4,1060)
```

```
1060    FORMAT(5X,'ROTAMETER',2X,'VSUF',3X,'N3',2X,'N4',6X,
     *  'TIME',9X,'R',6X,'TINITIAL',3X,'TEND')
        WRITE(4,1070)
1070    FORMAT(5X,'READING',3X,'HCONV',6X,'AVGHR',6X,'HT',7X,'NUCON'
     *   ,4X,'HT1'//5X,'RUNNO',5X,'TAVG',7X,
     *  'TLMTD',5X,'ALTLMT',4X,'ALHC',5X,'ALMH'/15X,'PD',9X,'RPOUT'
     *   ,5X,'FBH',5X,'ROTMNO',3X,'HCONVC',3X,'RC',3X'MDIR')
 670    WRITE(4,1080) ROTM,VSUF,N3,N4,TTIME,R,TEMPK(N3),TEMPK(N4),
     *   HCONV,AVGHR,HT,ANUEXP,HT1,RUNNO,TAVG,TLMTD,ALTMLT,ALHC,ALHM
     *  ,PD,RPOUT,FBH,ROTMNO,HCONVC,RC,MDIR
 1080    FORMAT(5X,F6.2,4X,F6.2,1X,I3,2X,I3,3X,F8.4,3(2X,F8.4)
     *   /,5X,7X,F8.3,2X,F8.3,3X,F8.3,3X,F8.3,3X,F8.3/
     *   ,7X,F3.1,3X,F8.3,3X,F8.3,3X,F8.3,3X,F8.3,3X,F8.3/
     *   10X,F8.3,3X,F8.3,3X,F8.3,3X,F8.3,3X,F8.3,3X,F8.3,3X,I3/)
        IF(KEY3.EQ.1) GO TO 1110
        IF(N4.GE.N) GO TO 1100
        N3=N4
        KEY1=1
        GO TO 420
1100    KEY3=1
        GO TO 421
1110    WRITE(4,1090)
1090    FORMAT(6X,' ------------------------------------------')
        WRITE(12,640) VSUF,HCONV
 640    FORMAT(F10.4,1X,F10.4)
        CLOSE(UNIT=4)
        CLOSE(UNIT=12)
        CLOSE(UNIT=3)
        CLOSE(UNIT=8)
        CLOSE(UNIT=1)
        END
C
C
        SUBROUTINE MVTEMP(E,TEMPK)
        X1=0.1008609
        X2=25727.94369
        X3=-767345.8295
```

```
      X4=78025595.81
      X5=-9247486589.0
      X6=697688000000.
      X7=-2.66192E+13
      X8=3.94078E+14
      TEMP1=X1+X2*E+X3*(E**2)
      TEMP2=X4*(E**3)+X5*(E**4)
      TEMP3=X6*(E**5)+X7*(E**6)+X8*(E**7)
      TEMP=TEMP1+TEMP2+TEMP3
      TEMPK=TEMP+273.2
      RETURN
      END
C
      SUBROUTINE AIRPRO(TFILM,AKAIR)
      B=7402.0E-08
      A=3945.0E-06
      AKAIR=B*TFILM+A
      RETURN
      END
      SUBROUTINE VSUP(ROTMNO,ROTM,PSTD,RMTEMP,TSTD,ATMP,RPOUT,FBDIA
     *  ,VSUF,PD,HG)
      PI=3.1415926
      IF (HG.EQ.1.0) GO TO 100
      POUT=ATMP+0.074*RPOUT
      GO TO 110
 100  POUT=ATMP+RPOUT
 110  FBAREA=(PI/4.0)*(FBDIA*FBDIA)
      GO TO (10,20,30,40,50,60,80) ROTMNO
 10   QRS=1.5929*ROTM-13.9910
      GO TO 70
C 20  IF(ROTM.GT.3.0) GO TO 200
C      QRS=-2.4760*ROTM*ROTM+34.5873*ROTM+0.4431
C      GO TO 70
 20   QRS=27.9390*ROTM-6.9009
      GO TO 70
 30   QRS=9.6269*ROTM+23.4293
      GO TO 70
```

```
 40     QRS=22.9046*ROTM+68.6256
        GO TO 70
 50     QRS=7.1395*ROTM-4.0646
        GO TO 70
 60     QRS=9.7284*ROTM+440.9562
        GO TO 70
 80     QRS=8.10*ROTM/60.00
        QROP=((PSTD/POUT)*(273.2+RMTEMP)/(294.1))*QRS
        GO TO 90
C-----------------------------------------------------------------------
C       QROP-OPERATION CONDITION ROTAMETER FLOW RATE CC/SEC
C
C-----------------------------------------------------------------------
C
 70     QROP=(((PSTD/TSTD)*(273.2+RMTEMP)/(POUT))**0.5)*QRS
 90     PBED=(PD*0.074+ATMP+ATMP)*.5
        QBED=(POUT/PBED)*QROP
        VSUF=QBED/FBAREA
        RETURN
        END
C
C       USE THIS ONLY FOR RUBBER PULLEY DRIVEN SPHERE
C       (OLD ARRANGEMENT)
C
        SUBROUTINE SPHVEL(EMIV,PDIA,VSPH)
        PI=3.1415926
        RPM=6.037*EMIV-1.1515
        RPS=RPM/60.0
        VSPH=PI*PDIA*RPS
        RETURN
        END
```

```
C*****************************************************************
C     PROGRAM IADM
C     LANGUAGE: FORTRAN-77
C
C     Interactive Analog Data Module (IADM) program.
C
C
C     FUNCTION:
C       This program allows the user to interactively acquire
C       analog data using the PRTIL ADM subroutines.
C
C     ALGORITHMS USED:
C       This program uses the voltage-level external trigger
C       mode to start analog data acquisition. The user is
C       prompted for the appropriate channel to receive
c       the trigger.
C
C     ERROR CONDITIONS:
C       Most error conditions are handled internally.
C
C
C     SUBROUTINES REFERENCED:
C       FUNCTIONS YES,GETTIM
C       SUBROUTINES GETFRQ,GETCHN
C       SUBROUTINE WAIT (from P/OS system library);
C       ADM SUBROUTINES AIN,AINIT,CLKFRQ,CNVDIF,ERASE,PLOT,PLOTM.
C
C
C*****************************************************************
C
C Declare and define all constants:
C
        INTEGER*2 MAXPTS        !Declare the maximum number of data.
        PARAMETER (MAXPTS=2000)!Maximum number of data points= 2000.
        INTEGER*2 IEFN          !Declare default event flag number.
        PARAMETER (IEFN=10)     !Define  default event flag number.
```

```
        INTEGER*2 MDSYN       !Declare synchronous I/O mode constant.
        PARAMETER (MDSYN=1)   !Define  synchronous I/O mode constant.
        INTEGER*2 IFORM       !Declare constant, analog data format.
        PARAMETER (IFORM=2)   !Define double-word analog data format.
        INTEGER*2 ITRIG       !Declare constant, analog trigger type.
        PARAMETER (ITRIG=0)    !Define software trigger type.
        INTEGER*2 ITIME                !Define timeout parameter.
        PARAMETER (ITIME=0)            !Declare no timeout value.
        INTEGER*2 SBNOP                !Declare SBNOP status code.
        PARAMETER (SBNOP="40000)       !Define  SBNOP status code.
        INTEGER*2 SBTR1              !Declare SBTRIG1COM status code.
        PARAMETER (SBTR1="40040)     !Define  SBTRIG1COM status code.
C
C*********************************************************************
C Declare external functions
C*********************************************************************
C
        EXTERNAL YES                 !Declare name of external routine.
        LOGICAL*2 YES                !Declare type of external routine.
C
C*********************************************************************
C Declare variable storage locations:
C*********************************************************************
C
        BYTE FNAME(40)           !Declare storage for disk file name.
        INTEGER*2 ISTAT(2)       !Declare PRTIL status buffer holder.
        INTEGER*4 JDATA(MAXPTS)!Declare storage, double integer data.
        INTEGER*2 ICOUNT        !Declare storage, acquired data count.
        INTEGER*2 ICHAN(8)   !Declare desired channel array for AIN.
        INTEGER*2 ICOLOR(8)  !Declare storage for color descriptors.
        INTEGER*2 ICONV       !Declare storage for conversion format.
        INTEGER*2 LENGTH      !Declare storage for file name length.
        INTEGER*2 NUMCHN     !Declare storage, total # active chans.
        INTEGER*2 TRGCHN     !Declare storage for trigger channel #.
        INTEGER*2 MARRAY(4)    !Declare storage for plotting modes.
        INTEGER*2 IPLCHN(8) !Declare storage for desired plot chans.
        INTEGER*2 NUMPCH    !Declare storage  total # plotted chans.
        INTEGER*2 PTSPCH    !Declare storage  # points per channel.
        INTEGER*2 CHNPLT    !Declare storage plotted channel count.
```

```
      INTEGER*2 NPTS     !Declare storage number of data values.
      REAL*4 XDELTA     !Declare storage for plot x axis increme
      REAL*4 YORG        !Declare storage for plot y axis origin.
      REAL*4 YDELTA      !Declare storage for plot y axis increme
      REAL*4 RDATA(MAXPTS)!Declare storage for real numbered data.
      REAL*4 XPLOT(2)     !Declare storage for temp plot buffer.
      REAL*4 YPLOT(2)     !Declare storage for temp plot buffer.
      REAL*4 CFREQ        !Declare storage for desired frequency.
      REAL*4 TFREQ        !Declare storage for true frequency.
      REAL*4 TINC         !Declare storage for time increment.
      REAL*4 SECET       !Declare storage for total elapsed time.
      INTEGER*2 I,J,KO,K1          !Declare index variables
C Let JDATA and RDATA share the same spac
      EQUIVALENCE(RDATA,JDATA)
C
C*********************************************************************
C The next section begins the executable portion of the program.
C First identify the program:
C*********************************************************************
C
1       TYPE 9000
9000    FORMAT(//,16X,'General Purpose Real-Time Data Acquisition
     1Program',//)
C
C*********************************************************************
C Prompt the user for sampling frequency, conversion format, channel
C selection and total test time:
C*********************************************************************
C
C       Get desired, true frequency from user.
        CALL GETFRQ(CFREQ,TFREQ)
C

        TYPE 9010
9010    FORMAT(/' Enable autoranging ?')
        IF(YES())
     1    THEN
            ICONV=5                        !Enable autoranging.
          ELSE
```

```
          ICONV=0                        !Disable autoranging.
        ENDIF
C
        CALL GETCHN(ICHAN,NUMCHN)    !Get desired channel selection.
C
C       Get desired sample count.
        CALL GETTIM(TFREQ,NUMCHN,MAXPTS,ICOUNT,SECET)
        XDELTA=SECET/5.0
        YDELTA=2.0
        YORG= -5.0
C*****************************************************************
C Perform the data acquisition; initialize using event
c  flag number 10:
C*****************************************************************
        CALL AINIT(ISTAT,IEFN)  !Initialize analog conversion system.
        TYPE 9020                 !Print status identification.
9020    FORMAT(/' AINIT status was: ')
        TYPE 9030,ISTAT(1),ISTAT(2)     !Print two-word status array.
9030    FORMAT(' ISTAT(1) (octal) = ',O6/,
     *  ' ISTAT(2) (decimal) = ',I6)
        IF(ISTAT(1) .NE. SBNOP)GO TO 32767
        IF(NUMCHN.GT.1)
     1    THEN
            TRGCHN=0
          ELSE
            DO 10 I=1,8       !Loop to find the only single channel.
              IF(ICHAN(I).EQ.0) GO TO 10
              TRGCHN=I-1
10          CONTINUE           !Bottom of loop to find only channel.
        ENDIF
C
        TYPE 9040,TRGCHN                !Inform user about trigger.
9040    FORMAT(/' Hit return when ready ',I1,' when ready.')
C
        CALL AIN(ISTAT,            !Specify standard status buffer.
     2  JDATA,               !Specify double-word integer data buff.
     3  ICOUNT,               !Specify desired sampled data count.
     4  IEFN,                 !Specify desired event flag number.
```

```
     5  MDSYN,              !Specify synchronous mode, timeout off.
     6  ICHAN,              !Specify desired channel array.
     7  ICONV,              !Specify desired conversion format.
     8  IFORM,              !Specify double-word integer format.
     9  ITRIG,              !Specify software trigger.
     0  ITIME,              !Timeout based on data acquisition.
     1  CFREQ)              !Specify desired clock frequency.
        TYPE 9050               !Print status identification.
9050    FORMAT(/' AIN status was:')
        TYPE 9030,ISTAT(1),ISTAT(2)     !Print two-word status array.
        IF(ISTAT(1) .EQ. SBNOP .OR. ISTAT(1) .EQ. SBTR1) GO TO 15
        GO TO 32767                     !End prog due to error
15      NPTS=ISTAT(2)   !NPTS holds the no. of converted values.
C*********************************************************************
C Convert the raw acquired data from the double-integer
C format to standard floating-point format:
C*********************************************************************
        CALL CNVDIF(JDATA,RDATA,NPTS)
C
C
C
C
        TYPE 9060
9060    FORMAT(/' Do you want to plot any data ?')
        IF(.NOT.YES()) GO TO 40
        GO TO 17
C
C
5       TYPE 9063
9063    FORMAT(' Do you want to rescale the plot axes ?')
        IF(YES()) THEN
             GO TO 6
          ELSE
        ENDIF
        GO TO 17
6       TYPE 9064,XDELTA,YORG,YDELTA
9064    FORMAT('   The old values are :',/,' x axis delta value = ',
     1  1PE14.6,/,' y axis origin value = ',1PE14.6,/,
```

```
     2  ' y axis delta value = ',1PE14.6,/)
        TYPE 9065
9065    FORMAT(' Enter a new x axis delta value,
     1  y axis origin value,',/,
     2  '$and y axis delta value : ')
        ACCEPT *,XDELTA,YORG,YDELTA
17      NUMPCH=0
        DO 25 I=1,8
          IPLCHN(I)=0
          IF(ICHAN(I).EQ.0) GO TO 25
          TYPE 9070,I-1
9070      FORMAT(' Do you want to plot channel ',I1,' ? ')
          IF(YES())
     1      THEN
              IPLCHN(I)=1
              NUMPCH=NUMPCH+1
20            TYPE 9080
9080          FORMAT('$Enter Color number (1 to 7) from manual : ')
              ACCEPT *,ICOLOR(I)
              IF(ICOLOR(I) .GT. 0 .AND. ICOLOR(I) .LE. 7)GO TO 25
              TYPE 9090,7
9090          FORMAT(A1,' Improper input .. try again !!!')
              GO TO 20
            ELSE
          ENDIF
25      CONTINUE
        IF(NUMPCH.EQ.0) GO TO 40
        TYPE 9100                          !Inform user.
9100    FORMAT(/' After the plot is complete you
     1  will have 20 seconds'
     2  /' to press the PRINT SCREEN key on the PRO... After'
     3  /' 20 seconds the screen will be erased and you will'
     4  /' be prompted for further plotting.',//,
     5  ' PRESS THE RETURN KEY TO CONTINUE ')
C
C
        ACCEPT 9012,I,K                    !Get a dummy character
9012    FORMAT(Q,A1)                       !Dummy input
```

```
C
C
C*********************************************************************
C Draw and label the grid for plotting:
C*********************************************************************
C
        TINC=1.0/TFREQ
        MARRAY(1)=2                !explicit values for x axis.
        MARRAY(2)=7                     !Select white plotting color.
        MARRAY(3)=1                     !Select solid line drawing.
        MARRAY(4)=7                   !Select white plot grid lines.
        PTSPCH=NPTS/NUMCHN         !Compute data points per channel.
C
        CALL PLOT(ISTAT !Re-use old status holder for plot stat
     2  MARRAY,                           !Specify plot mode array.
     3  0.0,                              !Specify dummy x value.
     4  0.0,                              !Specify dummy y value.
     5  0,                                !Specify no data plotted yet.
     6  0.0,                              !X-axis start label.
     7  XDELTA,             !Specify increment per X-axis tick mark
     8  YORG,                             !Y-axis start label.
     9  YDELTA,                        !Increment per Y axis tick mark.
     1  '   TIME (SECONDS)   ',           !X axis label.
     2  '       VOLTS        ')           !Y axis label.
C
C
        IF(ISTAT(1) .EQ. 0)GO TO 30
        TYPE 9105,ISTAT(1)
        GO TO 32767                       !and leave the program
C*********************************************************************
C Plot the data one channel at a time:
C*********************************************************************
C
30      CHNPLT=0                  !Initialize channels plotted counter.
        DO 35 I=1,8                 !Loop for all available channels.
          IF(IPLCHN(I).EQ.0) GO TO 35
          CHNPLT=CHNPLT+1         !Increment channels plotted counter.
```

```
          MARRAY(2)=ICOLOR(I)           !Transfer color descriptor.
          XPLOT(2)=0.0                  !Initialize x axis values
            DO 32 J=1,PTSPCH-1     !Loop for all points per channel.
            XPLOT(1)=XPLOT(2)           !Use old value
            XPLOT(2)=XPLOT(1)+TINC      !Increment the next value
            KO=(J-1)*NUMCHN+CHNPLT      !Calculate index
            K1=J*NUMCHN+CHNPLT          !Calculate index
            YPLOT(1)=RDATA(KO)          !Get first point in segment
            YPLOT(2)=RDATA(K1)          !Get second point in segment
            CALL PLOTM(ISTAT,
     2      MARRAY(2),             !Specify plot mode array subset.
     3      XPLOT,                !Specify x axis explicit values
     4      YPLOT,           !Specify floating point data to plot.
     5      2)                        !Specify 2 points to plot.
            IF(ISTAT(1).EQ.0) GO TO 32
            TYPE 9105,ISTAT(1)
9105        FORMAT(' ISTAT(1) (decimal) = ',I8)
            GO TO 32767                 !And leave loop
32          CONTINUE
35      CONTINUE
C Provide a 20-second wait before prompting for more plotting:
        CALL WAIT(20,                   !Specify wait of 20 seconds
     2  2,
     3  ISTAT)
        IF(ISTAT(1).NE.1) GO TO 32767   !Exit on fatal errors.
C
        CALL ERASE
        TYPE 9110
9110    FORMAT(/' Do you want to replot any data ?')
        IF(YES()) GO TO 5               !Go back to plot more data.
C*****************************************************************
C Allow the user to optionally store the data in a file:
C*****************************************************************
40      TYPE 9120
9120    FORMAT(/' Do you want to store the data on disk ?')
        IF(.NOT.YES()) GO TO 70 !No disk storage, check for re-start.
```

```
45      TYPE 9130
9130    FORMAT('$Enter filename (up to 40 characters): ')
        ACCEPT 8000,LENGTH,FNAME
8000    FORMAT(Q,40A1)
        DO 50 I=LENGTH+1,40
        FNAME(I)=0          !Clear unused locations in name string.
50      CONTINUE
C                               !Open file for ASCII data storage.
        OPEN(UNIT=1,TYPE='NEW',NAME=FNAME,ERR=60)
        WRITE(1,9140) TFREQ       !Actual true clock frequency used.
9140    FORMAT(1X,1PE16.7)
        WRITE(1,9140) FLOAT(NUMCHN)
        DO 55 I=1,NPTS
        WRITE(1,9140)RDATA(I)           !All acquired data to disk.
55      CONTINUE
        CLOSE(UNIT=1)                   !Close the file.
        GO TO 70
60      TYPE 9150
9150    FORMAT(' Improper disk attribute .. try again !!!')
        GO TO 45
70      TYPE 9160
9160    FORMAT(/' Do you want to start again ?')
        IF(YES()) GO TO 1               !Go back to start again.
32767   STOP    ' End of program IADM.'
        END
```

13 APPENDIX E: EXPERIMENTAL DATA

Table 13.1: Heat transfer coefficient for stationary spheres immersed in a fluidized bed of $355 - 420\mu$m glass particle

superficial air velocity cm/s	D_{sph} =1.0 cm	D_{sph} =1.4 cm	D_{sph} =2.0 cm	Bed Height cm
1.7000	70.00	50.00	50.00	23.40
5.3000	65.00	48.00	48.00	23.40
8.5000	69.00	43.00	43.00	23.40
11.5582	79.70	58.65	63.00	23.40
13.1700	101.7	75.30	58.00	23.40
14.9443	189.9	221.8	204.0	23.40
16.6835	294.3	286.6	246.0	23.70
18.5214	351.7	287.8	258.0	24.40
20.4428	391.9	334.1	309.0	25.10
22.4324	413.8	372.0	332.0	25.70
24.2129	430.1	400.1	355.0	26.50
26.6532	437.1	423.2	375.0	27.30
28.4243	451.4	431.1	374.0	27.90
31.0736	461.7	432.8	389.0	28.20
33.4283	466.4	433.8	389.0	28.90
35.8354	472.7	429.5	391.0	30.00

Table 13.2: Heat transfer coefficient for stationary spheres immersed in a fluidized bed of $126 - 147\mu$m glass particle

super-ficial air velocity cm/s	D_{sph} =1.0 cm	D_{sph} =1.4 cm	D_{sph} =2.0 cm	Bed Height cm
0.4887	60.50	—-	—-	23.60
0.8993	58.50	—-	44.5	23.60
1.2344	58.50	—-	43.9	23.60
1.5828	67.60	49.60	41.9	23.60
01.9993	221.0	147.0	157.0	23.60
02.4187	258.0	230.0	217.0	24.00
02.8400	317.0	264.0	248.0	24.40
03.2676	349.0	312.0	315.0	24.80
04.1158	415.0	350.0	343.0	24.90
05.8416	483.0	394.0	389.0	25.20
07.5986	550.0	455.0	453.0	25.90
08.4921	583.0	501.0	481.0	26.20
10.3138	658.0	529.0	536.0	26.80
11.5421	679.0	585.0	556.0	27.70
13.1837	682.0	607.0	603.0	28.20
14.9100	694.0	612.0	602.0	28.50
16.7094	703.0	624.0	594.0	29.40
18.5297	721.0	636.0	615.0	30.20

Table 13.3: Heat transfer coefficient for stationary spheres immersed in a fluidized bed of $5 - 44\mu$m glass particle

superficial air velocity cm/s	D_{sph} =1.0 cm	D_{sph} =1.4 cm	D_{sph} =2.0 cm	Bed Height cm
0.0278	43.00	—	—	24.20
0.0415	46.60	77.30	42.6	24.20
0.0869	48.90	58.4	58.4	24.20
00.1245	46.20	101.0	65.0	24.20
00.1521	55.00	171.0	145.0	24.60
00.1857	63.00	154.0	96.0	24.70
00.2687	179.0	195.0	194.0	25.70
00.5082	249.0	260.0	241.0	26.00
00.7478	401.0	395.0	263.0	26.20
00.9874	501.0	474.0	395.0	26.00
01.2269	596.0	590.0	443.0	25.90
01.4665	636.0	595.0	518.0	26.40
01.7060	653.0	627.0	559.0	26.50
01.9456	714.0	671.0	600.0	26.60
02.1851	774.0	726.0	646.0	26.70

Table 13.4: Heat transfer coefficient for linearly downward moving 1.0 cm diameter sphere immersed in a fluidized bed of 355 – 420μm glass particle

superficial air velocity cm/s	V_{sph} =0.4 cm/s	V_{sph} =1.1 cm/s	V_{sph} =1.9 cm/s	V_{sph} =3.0 cm/s	V_{sph} =4.6 cm/s	V_{sph} =7.5 cm/s
11.5582	237.4	361.8	418.6	477.5	524.1	529.9
13.1700	281.4	319.6	369.1	441.9	482.3	490.3
14.9443	302.1	321.8	343.6	393.3	426.4	469.3
16.6835	306.8	332.0	363.8	397.2	444.5	448.8
18.5214	382.2	376.2	420.1	416.7	432.9	443.9
20.4428	422.3	413.9	435.8	439.3	434.4	456.0
22.4324	437.1	438.2	439.8	441.2	450.4	425.1
24.2129	448.7	451.5	445.4	445.0	450.4	429.8
26.6532	448.7	451.9	456.7	452.8	450.8	442.8
28.4243	447.5	448.9	448.0	454.8	460.2	428.0
31.0736	441.4	459.0	455.3	447.1	446.7	419.4
33.4283	453.5	454.3	450.3	460.8	448.3	443.9
35.8354	444.0	454.6	449.6	445.8	477.8	420.2

Table 13.5: Heat transfer coefficient for linearly downward moving 1.4 cm diameter sphere immersed in a fluidized bed of 355 – 420μm glass particle

superficial air velocity cm/s	V_{sph} =0.4 cm/s	V_{sph} =1.1 cm/s	V_{sph} =1.9 cm/s	V_{sph} =3.0 cm/s	V_{sph} =4.6 cm/s	V_{sph} =7.5 cm/s
11.5382	185.5	273.1	334.4	415.4	456.5	493.1
13.1700	214.5	298.8	276.0	418.1	414.3	466.4
14.9443	249.0	274.0	296.0	374.0	409.0	428.0
16.6835	364.9	300.0	305.0	376.0	390.0	424.0
18.5214	281.0	330.0	353.0	387.0	392.0	381.0
20.4428	314.0	335.0	380.0	399.0	390.0	391.0
22.4324	364.9	376.0	403.0	401.5	399.0	428.0
24.2129	376.0	395.0	413.0	399.0	388.0	412.0
26.6532	403.0	404.0	418.0	408.0	402.0	414.0
28.4243	423.4	415.0	410.0	404.0	404.0	425.0
31.0736	402.0	418.8	411.0	406.0	395.0	434.0
33.4283	414.0	425.0	420.0	426.0	407.0	422.0
35.8354	407.7	419.0	415.0	410.0	429.0	425.0

Table 13.6: Heat transfer coefficient for linearly downward moving 2.0 cm diameter sphere immersed in a fluidized bed of 355 – 420μm glass particle

superficial air velocity cm/s	V_{sph} =0.4 cm/s	V_{sph} =1.1 cm/s	V_{sph} =1.9 cm/s	V_{sph} =3.0 cm/s	V_{sph} =4.6 cm/s	V_{sph} =7.5 cm/s
11.5582	174.4	236.9	266.9	322.5	381.8	413.5
13.1700	244.5	273.2	296.3	340.9	378.1	427.1
14.9443	259.2	277.8	291.9	336.2	366.8	415.5
16.6835	280.2	279.7	312.3	338.9	352.3	399.7
18.5214	295.1	296.9	322.5	336.8	356.5	401.9
20.4428	333.7	311.8	310.2	336.0	362.6	388.5
22.4324	356.3	345.6	336.5	356.6	373.9	383.7
24.2129	376.3	381.9	369.2	363.0	390.3	397.9
26.6532	391.9	382.8	388.3	387.7	396.9	385.4
28.4243	389.6	390.5	396.4	397.0	390.6	406.8
31.0736	392.0	399.0	407.6	394.0	410.7	394.4
33.4283	387.8	391.5	421.6	402.7	394.1	396.5
35.8354	395.2	392.0	412.4	406.2	391.2	380.5

Table 13.7: Heat transfer coefficient for linearly downward moving 1.0 cm diameter sphere immersed in a fluidized bed of 126 – 147μm glass particle

superficial air velocity cm/s	V_{sph} =0.4 cm/s	V_{sph} =1.1 cm/s	V_{sph} =1.9 cm/s	V_{sph} =3.0 cm/s	V_{sph} =4.6 cm/s	V_{sph} =7.5 cm/s
1.58280	207.0	322.1	390.4	483.2	566.7	631.9
01.9993	300.0	298.0	414.0	434.0	539.0	571.0
02.4187	310.0	309.0	366.0	438.0	500.0	562.0
02.8400	348.0	302.0	327.0	430.0	457.0	545.0
03.2676	388.0	337.0	367.0	412.0	467.0	503.0
04.1158	466.0	393.0	402.0	428.0	470.0	501.0
05.8416	554.0	496.0	502.0	507.0	505.0	500.0
07.5986	610.0	550.0	570.0	572.0	586.0	502.0
08.4921	602.0	556.0	583.0	595.0	613.0	618.0
10.3138	626.0	612.0	625.0	639.0	659.0	646.0
11.5421	638.0	632.0	661.0	688.0	713.0	668.0
13.1837	646.0	642.0	678.0	690.0	697.0	674.0
14.9100	660.0	653.0	696.0	725.0	718.0	677.0
16.7094	690.0	661.0	700.0	727.0	732.0	690.0
18.5297	698.0	682.0	690.0	712.0	752.0	728.0

Table 13.8: Heat transfer coefficient for linearly downward moving 1.4 cm diameter sphere immersed in a fluidized bed of $126 - 147\mu m$ glass particle

superficial air velocity cm/s	V_{sph} =0.4 cm/s	V_{sph} =1.1 cm/s	V_{sph} =1.9 cm/s	V_{sph} =3.0 cm/s	V_{sph} =4.6 cm/s	V_{sph} =7.5 cm/s
1.5828	159.8	234.2	311.9	374.2	426.5	528.8
01.9993	279.0	334.0	332.0	415.0	447.0	524.0
02.4187	270.0	313.0	338.0	393.0	436.0	514.0
02.8400	280.0	325.0	329.0	383.0	433.0	493.0
03.2676	336.0	343.0	359.0	404.0	441.0	487.0
04.1158	392.0	362.0	370.0	399.0	454.0	443.0
05.8416	437.0	434.0	452.0	452.0	470.0	501.0
07.5986	495.0	506.0	509.0	535.0	517.0	530.0
08.4921	515.0	524.0	518.0	514.0	550.0	549.0
10.3138	522.0	578.0	552.0	562.0	583.0	579.0
11.5421	553.0	617.0	599.0	595.0	602.0	623.0
13.1837	610.0	636.0	628.0	651.0	632.0	639.0
14.9100	606.0	630.0	612.0	664.0	634.0	654.0
16.7094	613.0	638.0	647.0	657.0	637.0	694.0
18.5297	608.0	639.0	621.0	678.0	653.0	665.0

Table 13.9: Heat transfer coefficient for linearly downward moving 2.0 cm diameter sphere immersed in a fluidized bed of 126 – 147μm glass particle

superficial air velocity cm/s	V_{sph} =0.4 cm/s	V_{sph} =1.1 cm/s	V_{sph} =1.9 cm/s	V_{sph} =3.0 cm/s	V_{sph} =4.6 cm/s	V_{sph} =7.5 cm/s
1.58280	126.8	226.9	277.9	338.2	399.7	475.1
01.9993	271.0	337.0	349.0	389.0	432.0	495.0
02.4187	310.0	324.0	367.0	392.0	411.0	466.0
02.8400	304.0	313.0	356.0	378.0	397.0	450.0
03.2676	345.0	347.0	361.0	398.0	355.0	451.0
04.1158	364.0	379.0	371.0	401.0	407.0	456.0
05.8416	440.0	445.0	440.0	460.0	457.0	522.0
07.5986	493.0	488.0	523.0	514.0	492.0	574.0
08.4921	501.0	502.0	539.0	538.0	528.0	558.0
10.3138	525.0	551.0	570.0	582.0	561.0	546.0
11.5421	576.0	585.0	594.0	608.0	611.0	580.0
13.1837	585.0	617.0	607.0	610.0	628.0	584.0
14.9100	598.0	621.0	603.0	644.0	643.0	624.0
16.7094	609.0	635.0	635.0	625.0	624.0	619.0
18.5297	592.0	631.0	644.0	643.0	632.0	636.0

Table 13.10: Heat transfer coefficient for linearly downward moving 1.0 cm diameter sphere immersed in a fluidized bed of $5 - 44\mu$m glass particle

superficial air velocity cm/s	V_{sph} =0.4 cm/s	V_{sph} =1.1 cm/s	V_{sph} =1.9 cm/s	V_{sph} =3.0 cm/s	V_{sph} =4.6 cm/s	V_{sph} =7.5 cm/s
0.04150	173.4	313.3	384.4	478.7	546.3	649.5
0.08690	162.3	283.6	363.9	464.2	563.2	680.7
00.1245	151.0	316.0	365.0	438.0	453.0	670.0
00.1521	147.0	399.0	363.0	401.0	469.0	672.0
00.1857	147.0	306.0	350.0	421.0	458.0	650.0
00.2687	209.6	303.0	361.0	434.0	516.0	614.0
00.5082	294.0	314.0	315.0	373.0	459.0	527.0
00.7478	394.0	411.0	400.0	540.0	429.0	537.0
00.9874	553.0	561.0	548.0	607.0	605.0	618.0
01.2269	574.0	602.0	609.0	654.0	633.0	673.0
01.4665	627.0	692.0	662.0	710.0	734.0	698.0
01.7060	675.0	685.0	682.0	750.0	713.0	700.0
01.9456	664.0	702.0	674.0	694.0	785.0	738.0
02.1851	700.0	744.0	699.0	768.0	776.0	732.0

Table 13.11: Heat transfer coefficient for linearly downward moving 1.4 cm diameter sphere immersed in a fluidized bed of $5 - 44\mu$m glass particle

superficial air velocity cm/s	V_{sph} =0.4 cm/s	V_{sph} =1.1 cm/s	V_{sph} =1.9 cm/s	V_{sph} =3.0 cm/s	V_{sph} =4.6 cm/s	V_{sph} =7.5 cm/s
0.04150	104.4	307.3	346.9	415.8	504.3	597.5
0.08690	130.2	255.1	304.2	391.4	454.4	589.3
00.1245	130.0	291.0	277.0	356.0	480.0	662.0
00.1521	226.0	334.0	328.0	333.0	489.0	612.0
00.1857	171.0	376.0	330.0	359.0	481.0	624.0
00.2687	218.0	356.0	315.0	375.0	441.0	529.0
00.5082	256.0	376.0	410.0	404.0	448.0	553.0
00.7478	330.0	403.0	440.0	469.0	479.0	539.0
00.9874	575.0	562.0	550.0	592.0	601.0	620.0
01.2269	601.0	582.0	638.0	643.0	667.0	655.0
01.4665	625.0	653.0	691.0	673.0	712.0	681.0
01.7060	665.0	695.0	700.0	698.0	763.0	754.0
01.9456	672.0	713.0	744.0	723.0	767.0	808.0
02.1851	725.0	739.0	754.0	772.0	786.0	753.0

Table 13.12: Heat transfer coefficient for linearly downward moving 2.0 cm diameter sphere immersed in a fluidized bed of $5 - 44\mu$m glass particle

superficial air velocity cm/s	V_{sph} =0.4 cm/s	V_{sph} =1.1 cm/s	V_{sph} =1.9 cm/s	V_{sph} =3.0 cm/s	V_{sph} =4.6 cm/s	V_{sph} =7.5 cm/s
0.04150	106.7	262.7	324.5	389.5	423.6	547.6
0.08690	102.5	237.7	312.3	365.4	457.9	615.6
00.1245	151.0	241.0	294.0	372.0	429.0	578.0
00.1521	177.0	231.0	286.0	361.0	477.0	625.0
00.1857	190.0	221.0	303.0	357.0	485.0	590.0
00.2687	210.0	284.0	309.0	335.0	423.0	510.0
00.5082	320.0	310.0	322.0	321.0	435.0	492.0
00.7478	346.0	395.0	330.0	320.0	481.0	480.0
00.9874	483.0	467.0	474.0	474.0	511.0	493.0
01.2269	496.0	504.0	528.0	518.0	581.0	584.0
01.4665	555.0	553.0	535.0	590.0	626.0	600.0
01.7060	607.0	611.0	562.0	643.0	632.0	645.0
01.9456	602.0	660.0	672.0	707.0	660.0	653.0
02.1851	629.0	661.0	687.0	703.0	696.0	700.0

Table 13.13: Heat transfer coefficient for a copper sphere of 1.0 cm diameter, oscillating at constant peak-to-peak amplitude of 6.9 cm immersed in a fluidized bed of $5 - 44\mu$m glass particle

superficial air velocity cm/s	Frequency =1.11 Hz	Frequency =2.0 Hz	Frequency =2.85 Hz
0.0869	514.4596	655.0499	720.5953
0.1284	559.3044	741.0068	732.4918
0.1660	535.0045	763.1222	790.5498
0.2687	603.9405	808.4612	913.5311
0.5082	618.4099	856.7175	930.6714
0.7478	665.9142	873.4390	915.9703
0.9874	689.6120	874.1792	894.9048
1.2269	734.7418	875.6706	900.0388
1.4665	790.1766	876.5748	904.2752
1.7060	790.5606	881.3821	885.2902
1.9456	806.5665	887.6987	895.5869
2.1851	804.7311	897.0795	901.8790

Table 13.14: Heat transfer coefficient for a copper sphere of 1.0 cm diameter, oscillating at constant peak-to-peak amplitude of 4.0 cm immersed in a fluidized bed of $5 - 44\mu$m glass particle

superficial air velocity cm/s	Frequency =1.11 Hz	Frequency =2.0 Hz	Frequency =2.85 Hz
0.0869	394.1188	411.5658	671.6633
0.1284	396.7986	417.2717	616.6715
0.1660	406.7061	462.3411	710.0500
0.2687	445.5711	585.0626	808.9167
0.5082	527.3751	669.3301	801.7182
0.7478	593.8859	722.7284	800.4366
0.9874	638.6718	710.5384	800.3757
1.2269	706.7823	724.5542	789.3616
1.4665	693.9657	748.2843	821.4891
1.7060	731.2654	802.4001	834.7662
1.9456	767.2799	797.3808	840.1908
2.1851	780.4034	818.2127	816.3910
2.1851	780.4034	818.2127	816.3910

Table 13.15: Heat transfer coefficient for a copper sphere of 1.0 cm diameter, oscillating at constant peak-to-peak amplitude of 1.8 cm immersed in a fluidized bed of $5 - 44\mu$m glass particle.

superficial air velocity cm/s	Frequency =1.11 Hz	Frequency =2.0 Hz	Freqency =2.85 Hz
0.0869	229.2517	256.5021	341.0941
0.1284	240.0000	260.4054	336.4384
0.1660	273.0000	301.5412	362.3761
0.2687	355.0000	392.1918	443.4507
0.5082	390.0000	419.9237	474.8703
0.7478	457.0000	518.6845	597.4842
0.9874	590.0000	639.7214	670.2366
1.2269	640.0000	674.6279	673.5601
1.4665	672.0000	698.3148	710.7664
1.7060	675.0736	732.7658	743.8232
1.9456	738.3281	753.6589	776.7448
2.1851	783.4354	776.2154	780.6853

Table 13.16: Heat transfer coefficient for a copper sphere of 1.4 cm diameter, oscillating at constant peak-to-peak amplitude of 6.9 cm immersed in a fluidized bed of $5 - 44\mu$m glass particle

superficial air velocity cm/s	Frequency =1.11 Hz	Frequency =2.0 Hz	Frequency =2.85 Hz
0.0869	357.4700	636.7740	830.4295
0.1284	391.8060	641.0248	846.0692
0.1698	435.5582	680.1333	840.4732
0.2687	492.8869	736.3742	884.2593
0.5082	560.2501	786.5329	885.5651
0.7478	609.9991	760.3361	867.4367
0.9874	632.5657	781.3655	860.4662
1.2269	657.5005	795.7372	866.3934
1.4665	692.7724	813.7851	878.5820
1.7060	704.7387	822.1988	871.5027
1.9456	711.3650	828.0059	870.4899
2.1851	758.3270	840.2349	876.8582

Table 13.17: Heat transfer coefficient for a copper sphere of 1.4 cm diameter, oscillating at constant peak-to-peak amplitude of 4.0 cm immersed in a fluidized bed of $5 - 44\mu$m glass particle

superficial air velocity cm/s	Frequency =1.11 Hz	Frequency =2.0 Hz	Frequency =2.85 Hz
0.0869	268.2250	397.4128	593.6165
0.1284	351.8700	472.7295	665.6287
0.1698	378.6941	417.7922	653.2668
0.2687	356.8204	580.0168	813.3058
0.5082	432.6386	663.0964	847.9194
0.7478	544.1761	671.9865	872.9606
0.9874	579.3666	716.8525	873.6107
1.2269	625.7407	744.3026	875.0320
1.4665	677.7407	773.2654	885.3720
1.7060	701.4246	773.9287	880.4123
1.9456	690.7949	775.0499	896.4689
2.1851	712.6481	787.8332	880.4872

Table 13.18: Heat transfer coefficient for a copper sphere of 1.4 cm diameter, oscillating at constant peak-to-peak amplitude of 1.8 cm immersed in a fluidized bed of 5 – 44μm glass particle

superficial air velocity cm/s	Frequency =1.11 Hz	Frequency =2.0 Hz	Frequency =2.85 Hz
0.0869	144.3341	193.5692	256.5276
0.1284	136.5742	263.7477	275.9617
0.1698	153.7656	279.0484	295.8008
0.2687	210.9183	341.6526	367.9117
0.5082	320.0533	479.2215	485.8322
0.7478	491.2842	507.2061	580.1722
0.9874	525.7399	599.8036	630.2029
1.2269	625.7399	651.9561	650.9789
1.4665	644.7976	680.6917	736.4868
1.7060	663.2095	701.9520	681.8760
1.9456	699.1044	741.9878	742.6876
2.1851	710.3185	726.3648	728.2708

Table 13.19: Heat transfer coefficient for a copper sphere of 2.0 cm diameter, oscillating at constant peak-to-peak amplitude of 6.9 cm immersed in a fluidized bed of $5 - 44\mu$m glass particle

superficial air velocity cm/s	Frequency =1.11 Hz	Frequency =2.0 Hz	Frequency =2.85 Hz
0.0869	282.0000	580.5807	598.3300
0.1284	299.0000	540.5372	601.1257
0.1660	326.0000	487.0000	626.3359
0.2687	443.0000	570.4689	776.7490
0.5082	520.0000	653.6499	778.7289
0.7478	522.0000	644.0000	766.2819
0.9874	540.0000	681.5457	763.5927
1.2269	578.0000	692.1516	766.4329
1.4665	619.0000	710.0049	765.0714
1.7060	624.0000	717.2117	783.5569
1.9456	660.0000	720.2118	789.0593
2.1851	680.0000	722.1711	787.8743

Table 13.20: Heat transfer coefficient for a copper sphere of 2.0 cm diameter, oscillating at constant peak-to-peak amplitude of 4.0 cm immersed in a fluidized bed of $5 - 44\mu$m glass particle

superficial air velocity cm/s	Frequency =1.11 Hz	Frequency =2.0 Hz	Frequency =2.85 Hz
0.0869	209.1245	266.3235	433.4469
0.1284	194.2661	292.7989	485.1748
0.1660	193.5900	301.9961	511.2347
0.2687	284.2946	453.7225	499.8829
0.5082	339.7625	495.7662	542.0618
0.7478	447.9677	506.0973	557.3153
0.9874	464.2229	544.9890	592.1638
1.2269	556.6276	602.5355	642.4529
1.4665	534.0499	626.1793	648.5664
1.7060	627.9160	641.3028	667.5709
1.9456	608.6111	660.8315	674.8677
2.1851	650.4551	679.2175	716.5475

Table 13.21: Heat transfer coefficient for a copper sphere of 2.0 cm diameter, oscillating at constant peak-to-peak amplitude of 1.8 cm immersed in a fluidized bed of $5 - 44\mu$m glass particle

superficial air velocity cm/s	Frequency =1.11 Hz	Frequency =2.0 Hz	Frequency =2.85 Hz
0.0869	198.8894	241.8445	259.1021
0.1284	197.3252	216.8550	236.9686
0.1660	170.2106	201.7633	398.7040
0.2687	276.6682	268.4213	376.9923
0.5082	271.7534	304.9999	372.6108
0.7478	330.3211	347.7815	478.4136
0.9874	442.5559	435.6250	509.2136
1.2269	459.0000	570.3256	556.0613
1.4665	562.2364	583.3150	628.2855
1.7060	532.1682	605.6290	657.2958
1.9456	620.5880	606.1562	663.2410
2.1851	663.3030	633.0000	687.7365

Table 13.22: Heat transfer coefficient for a copper sphere of 1.0 cm diameter, oscillating at constant peak-to-peak amplitude of 6.9 cm immersed in a fluidized bed of 126 – 147μm glass particle

superficial air velocity cm/s	Frequency =1.11 Hz	Frequency =2.0 Hz	Frequency =2.85 Hz
1.5874	432.8799	546.6160	595.0358
1.9993	490.3516	513.8480	564.4389
2.4189	510.7740	534.6830	551.2775
3.2684	540.2994	569.9932	562.8593
4.1191	547.5786	570.3464	576.4047
5.8416	565.6009	583.2188	585.7821
7.5986	608.1260	618.7598	620.7714
9.3812	634.7286	639.4818	643.8718
11.5352	694.6512	695.8054	723.7652
14.8663	718.5732	728.5683	748.2288

Table 13.23: Heat transfer coefficient for a copper sphere of 1.0 cm diameter, oscillating at constant peak-to-peak amplitude of 4.0 cm immersed in a fluidized bed of 126 – 147μm glass particle

superficial air velocity cm/s	Frequency =1.11 Hz	Frequency =2.0 Hz	Frequency =2.85 Hz
1.5874	363.8278	439.4518	548.0328
1.9993	470.5147	509.6842	530.1421
2.4189	469.9268	516.2597	523.4219
3.2684	493.2931	561.7344	553.1145
4.1191	485.3305	563.5726	544.3648
5.8416	528.0762	561.5693	573.1008
7.5986	582.0762	615.4228	611.9221
9.3812	631.8159	661.7305	655.7387
11.5352	661.0369	695.3758	713.8058
14.8663	722.3005	743.7704	759.8920

Table 13.24: Heat transfer coefficient for a copper sphere of 1.0 cm diameter, oscillating at constant peak-to-peak amplitude of 1.8 cm immersed in a fluidized bed of 126 – 147μm glass particle

superficial air velocity cm/s	Frequency =1.11 Hz	Frequency =2.0 Hz	Frequency =2.85 Hz
1.5874	322.4174	373.6217	419.9831
1.9993	357.1472	449.7755	498.8911
2.4189	370.1042	474.1751	520.5796
3.2684	390.3265	471.1307	547.1454
4.1191	453.5492	502.5933	511.0402
5.8416	513.1451	548.0512	541.5055
7.5986	584.6529	562.9846	604.1107
9.3812	628.9300	639.6538	646.8693
11.5352	700.9064	693.5953	720.6553
14.8663	740.2498	741.2589	728.0034

Table 13.25: Heat transfer coefficient for a copper sphere of 1.4 cm diameter, oscillating at constant peak-to-peak amplitude of 6.9 cm immersed in a fluidized bed of 126 – 147μm glass particle

superficial air velocity cm/s	Frequency =1.11 Hz	Frequency =2.0 Hz	Frequency =2.85 Hz
1.5828	452.4903	477.7684	535.7787
1.9993	419.8135	493.5888	518.0382
2.4189	434.2409	497.0533	500.7810
3.2676	447.5967	506.6443	501.3821
4.1158	469.5173	518.4468	491.3632
5.8416	491.0444	557.1800	513.4672
7.5986	519.8400	574.6252	560.2620
9.3812	554.6663	594.7679	564.8611
11.5421	572.1490	612.7990	585.6038
14.9100	566.8116	626.1194	599.7634

Table 13.26: Heat transfer coefficient for a copper sphere of 1.4 cm diameter, oscillating at constant peak-to-peak amplitude of 4.0 cm immersed in a fluidized bed of 126 – 147μm glass particle

superficial air velocity cm/s	Frequency =1.11 Hz	Frequency =2.0 Hz	Frequency =2.85 Hz
1.5828	349.9455	460.9557	528.9337
1.9993	401.7349	458.6565	493.1604
2.4189	394.7468	459.5720	487.4160
3.2676	399.0468	478.6515	503.4030
4.1158	436.5608	490.4023	499.2046
5.8416	466.7350	504.5494	523.9044
7.5986	507.5731	518.2263	542.4863
9.3812	538.1652	542.8348	549.1708
11.5421	588.7981	590.3061	610.8052
14.9100	608.3952	599.8104	658.4618

Table 13.27: Heat transfer coefficient for a copper sphere of 1.4 cm diameter, oscillating at constant peak-to-peak amplitude of 1.8 cm immersed in a fluidized bed of $126 - 147\mu$m glass particle

superficial air velocity cm/s	Frequency =1.11 Hz	Frequency =2.0 Hz	Frequency =2.85 Hz
1.5828	299.0000	388.0000	452.1715
1.9993	281.9824	410.0000	473.3952
2.4189	309.7790	376.0000	455.2050
3.2676	357.9516	430.0000	494.6694
4.1158	417.3647	435.0000	478.6626
5.8416	465.0342	499.0000	489.7147
7.5986	499.3081	562.0000	522.4219
9.3812	535.6374	568.0000	574.5334
11.5421	606.3313	611.0000	625.5114
14.9100	639.7513	652.0000	650.0000

Table 13.28: Heat transfer coefficient for a copper sphere of 2.0 cm diameter, oscillating at constant peak-to-peak amplitude of 6.9 cm immersed in a fluidized bed of 126 – 147μm glass particle

superficial air velocity cm/s	Frequency =1.11 Hz	Frequency =2.0 Hz	Frequency =2.85 Hz
1.5828	453.1765	489.1227	511.6750
1.9993	438.0023	447.3324	493.9404
2.4189	427.1035	439.3440	477.6663
3.2676	459.2631	473.6894	474.9110
4.1158	476.9562	483.5100	487.5620
5.8416	494.7196	510.0179	510.0463
7.5986	535.4172	564.6907	539.7104
9.3812	558.8442	588.9620	603.1642
11.5421	589.8986	614.9872	630.0836
14.8663	602.3911	634.7756	638.7728

Table 13.29: Heat transfer coefficient for a copper sphere of 2.0 cm diameter, oscillating at constant peak-to-peak amplitude of 4.0 cm immersed in a fluidized bed of $126 - 147\mu$m glass particle

superficial air velocity cm/s	Frequency =1.11 Hz	Frequency =2.0 Hz	Frequency =2.85 Hz
1.5828	398.3637	447.2465	480.2260
1.9993	372.4565	400.4663	427.9585
2.4189	375.3829	434.7338	446.4659
3.2676	401.0657	459.1664	461.7180
4.1158	433.4277	461.3169	479.3409
5.8416	460.0218	488.5369	510.1329
7.5986	506.5017	523.7593	562.3281
9.3812	556.6818	561.3531	605.8672
11.5421	601.6987	580.6741	612.3115
14.8663	599.0187	617.8776	596.5348

Table 13.30: Heat transfer coefficient for a copper sphere of 2.0 cm diameter, oscillating at constant peak-to-peak amplitude of 1.8 cm immersed in a fluidized bed of 126 – 147μm glass particle

superficial air velocity cm/s	Frequency =1.11 Hz	Frequency =2.0 Hz	Frequency =2.85 Hz
1.5828	305.0277	391.5472	482.1596
1.9993	356.9357	379.2957	419.4676
2.4189	313.6333	342.9973	435.3418
3.2676	364.4860	416.5632	461.9252
4.1158	389.8284	413.5845	464.7759
5.8416	447.4284	451.7624	484.2151
7.5986	514.0577	518.9587	557.9658
9.3812	546.9561	583.8841	601.0128
11.5421	594.5064	600.6319	606.7147
14.8663	595.6278	603.8683	621.8720

Table 13.31: Heat transfer coefficient for a copper sphere of 1.0 cm diameter, oscillating at constant peak-to-peak amplitude of 6.9 cm immersed in a fluidized bed of $355 - 420\mu$m glass particle

superficial air velocity cm/s	Frequency =1.11 Hz	Frequency =2.0 Hz	Frequency =2.85 Hz
11.5403	393.0269	385.8647	335.5363
13.1960	429.3480	408.2615	535.3809
14.9766	437.7420	452.0262	379.7535
16.7374	523.4191	460.7054	431.1239
18.5453	526.3788	499.3461	452.8656
20.4246	536.2875	518.4488	461.6630
24.3764	525.1136	524.9075	493.0783
28.6316	511.9312	514.3947	486.4287
33.2488	510.1959	511.1244	502.3367

Table 13.32: Heat transfer coefficient for a copper sphere of 1.0 cm diameter, oscillating at constant peak-to-peak amplitude of 4.0 cm immersed in a fluidized bed of $355 - 420\mu$m glass particle

superficial air velocity cm/s	Frequency =1.11 Hz	Frequency =2.0 Hz	Frequency =2.85 Hz
11.5403	413.4594	410.7693	379.2700
13.1960	467.5523	422.4897	392.6254
14.9766	473.1195	455.8149	423.6037
16.7374	531.7742	475.4564	455.5452
18.5453	548.0058	514.5535	471.1240
20.4246	550.5437	512.6252	520.0195
24.3764	545.7437	539.8389	523.0612
28.6316	568.1077	547.1213	501.7117
33.2488	555.0024	525.0731	510.3907

Table 13.33: Heat transfer coefficient for a copper sphere of 1.0 cm diameter, oscillating at constant peak-to-peak amplitude of 1.8 cm immersed in a fluidized bed of $355 - 420\mu$m glass particle

superficial air velocity cm/s	Frequency =1.11 Hz	Frequency =2.0 Hz	Frequency =2.85 Hz
11.5403	355.8453	383.9637	414.0868
13.1960	437.9387	428.8649	444.6026
14.9766	445.9387	452.5867	469.3852
16.7374	489.0344	483.9915	503.7747
18.5453	512.6482	504.0905	514.6215
20.4246	532.9640	521.4975	520.8694
24.3764	529.3197	531.9842	497.0974
28.6316	558.5978	527.2308	540.9140
33.2488	547.8993	520.1747	526.7585

Table 13.34: Heat transfer coefficient for a copper sphere of 1.4 cm diameter, oscillating at constant peak-to-peak amplitude of 6.9 cm immersed in a fluidized bed of $355 - 420\mu$m glass particle

superficial air velocity cm/s	Frequency =1.11 Hz	Frequency =2.0 Hz	Frequency =2.85 Hz
11.5403	363.8154	369.2535	345.2952
13.1960	374.6036	372.5057	325.9158
14.9766	390.0226	405.0291	356.1190
16.7374	429.2713	430.0128	382.2882
18.5453	446.7863	450.7631	409.5555
20.4246	465.2669	469.6840	420.4525
24.3764	480.1001	485.3599	424.9525
28.6316	477.9667	472.3776	458.5812
33.2488	481.4926	470.5656	433.4055

Table 13.35: Heat transfer coefficient for a copper sphere of 1.4 cm diameter, oscillating at constant peak-to-peak amplitude of 4.0 cm immersed in a fluidized bed of $355 - 420\mu$m glass particle

superficial air velocity cm/s	Frequency =1.11 Hz	Frequency =2.0 Hz	Frequency =2.85 Hz
11.5403	361.7518	399.5459	359.9795
13.1960	388.4713	429.8352	377.9000
14.9766	380.6206	432.5376	414.9760
16.7374	437.4813	485.2713	437.4052
18.5453	452.6284	471.9525	447.7991
20.4246	472.0667	485.0882	462.7209
24.3764	493.9400	500.2713	474.5576
28.6316	489.6657	481.8553	479.8180
33.2488	491.7166	503.5739	486.6116

Table 13.36: Heat transfer coefficient for a copper sphere of 1.4 cm diameter, oscillating at constant peak-to-peak amplitude of 1.8 cm immersed in a fluidized bed of 355 – 420μm glass particle

superficial air velocity cm/s	Frequency =1.11 Hz	Frequency =2.0 Hz	Frequency =2.85 Hz
11.5403	339.0155	357.3980	395.5992
13.1960	363.2838	378.5270	386.3303
14.9766	358.1369	382.7383	411.7512
16.7374	415.3810	421.4320	466.5674
18.5453	452.3858	455.5369	472.5960
20.4246	488.9534	476.7601	486.1807
24.3764	499.2858	508.1780	497.3738
28.6316	496.6038	510.3413	482.8270
33.2488	504.5633	494.9860	501.4396

Table 13.37: Heat transfer coefficient for a copper sphere of 2.0 cm diameter, oscillating at constant peak-to-peak amplitude of 6.9 cm immersed in a fluidized bed of $355 - 420\mu$m glass particle

superficial air velocity cm/s	Frequency =1.11 Hz	Frequency =2.0 Hz	Frequency =2.85 Hz
11.5403	359.7212	397.3535	329.6180
13.1960	350.6171	360.7378	314.8083
14.9766	341.7200	351.2399	327.9600
16.7374	360.2961	368.4415	334.7017
18.5453	381.7827	383.9271	345.6426
20.4246	398.0002	396.1328	364.3485
24.3764	410.3565	420.1016	386.6181
28.6316	417.4318	413.4468	401.3488
33.2488	411.9253	424.2980	410.0000

Table 13.38: Heat transfer coefficient for a copper sphere of 2.0 cm diameter, oscillating at constant peak-to-peak amplitude of 4.0 cm immersed in a fluidized bed of $355 - 420\mu$m glass particle

superficial air velocity cm/s	Frequency =1.11 Hz	Frequency =2.0 Hz	Frequency =2.85 Hz
11.5403	350.7212	409.3535	345.6180
13.1960	299.6171	365.7378	338.8083
14.9766	334.7200	373.2399	354.9600
16.7374	334.2961	395.4415	380.7017
18.5453	381.7827	408.9271	405.6426
20.4246	401.0002	432.1328	428.3485
24.3764	399.3565	447.1016	438.6181
28.6316	411.4318	432.4468	438.3488
33.2488	422.9253	433.2980	443.0000

Table 13.39: Heat transfer coefficient for a copper sphere of 2.0 cm diameter, oscillating at constant peak-to-peak amplitude of 1.8 cm immersed in a fluidized bed of $355 - 420\mu$m glass particle

superficial air velocity cm/s	Frequency =1.11 Hz	Frequency =2.0 Hz	Frequency =2.85 Hz
11.5403	302.1776	339.9240	364.8348
13.1960	269.2965	312.1685	331.6301
14.9766	290.2898	325.9255	333.2096
16.7374	330.4717	351.6662	355.3993
18.5453	365.5963	374.5651	379.1163
20.4246	380.3336	399.3242	388.7432
24.3764	406.7972	402.0280	411.2264
28.6316	413.2539	421.3217	402.4093
33.2488	408.0000	415.4194	419.1076